THESIS

Active Congestion Quantification and Reliability Improvement Considering Aging Failure in Modern Distribution Networks

Jinping Zhao

Supervised by

A/Prof. Ali Arefi, Prof. Alberto Borghetti and A/Prof. GM Shafiullah

This thesis is presented in fulfilment of the requirements for the degree of

Doctor of Philosophy

Discipline of Engineering and Energy, Murdoch University, Australia

October 2022

Declaration

I, ***Jinping Zhao***, verify that in submitting this thesis:

the thesis is my own account of the research conducted by me, except where other sources are fully acknowledged in the appropriate format,

the extent to which the work of others has been used is documented by a percent allocation of work and signed by myself and my Principal Supervisor,

the thesis contains as its main content work which has not been previously submitted for a degree at any university,

the University supplied plagiarism software has been used to ensure the work is of the appropriate standard to send for examination,

any editing and proof-reading by professional editors comply with the standards set out on the Graduate Research School website, and

that all necessary ethics and safety approvals were obtained, including their relevant approval or permit numbers, as appropriate.

Jinping Zhao

October 2022

Acknowledgments

I would like to express my deepest gratitude to my principal supervisor, Associate Professor Ali Arefi, for his unlimited support and guidance on topic selection, methodologies, programming, and thesis writing. His kind encouragement and great friendship sustained me this far and helped me overcome various difficulties during this PhD journey.

I would also like to sincerely thank Professor Alberto Borghetti for his continuous help and endless support through all the stages of this project. I am extremely grateful for your assistance, brilliant comments, and suggestions on each chapter of this thesis.

I would also like to give my special thanks to Professor Gerard Ledwich for sharing his insights and comments on each chapter. I would also like to thank Dr GM Shafiullah for his outstanding support and friendship. Thanks to all my lovely friends, especially Kethaki, for their pure friendship and company.

Finally, I would like to thank my most beloved family members for giving me selfless love and unconditional support on this life journey.

The bits and pieces of the four years are all the precious experiences and treasures in my life.

List of Publications

Journal articles

I. **J. Zhao**, A. Arefi, A. Borghetti, and G. Ledwich, "Indices of Congested Areas and Contributions of Customers to Congestions in Radial Distribution Networks," in Journal of Modern Power Systems and Clean Energy, vol. 10, no. 3, pp. 656-666, May 2022, doi: 10.35833/MPCE.2020.000640.

II. **J. Zhao**, A. Arefi, A. Borghetti, G. Ledwich, R. Dabare, and S. M. Muyeen, "End-of-life Failure Probability and Reliability Evaluation in Distribution Networks Integrated with Large Penetration of Electric Vehicles," under review in IET Generation, Transmission & Distribution.

III. **J. Zhao**, A. Arefi, A. Borghetti, and G. Ledwich, "An Optimization Model for Reliability Improvement and Cost Reduction Assessment Achievable through EV Smart Charging," under preparation for submission.

Conference papers

I. **J. Zhao**, A. Arefi, A. Borghetti, J. M. Delarestaghi, and G. Shafiullah, "Characterization of Congestion in Distribution Network Considering High Penetration of PV Generation and EVs," in 2019 IEEE Power & Energy Society General Meeting (PESGM), 2019, pp. 1-5, doi: 10.1109/PESGM40551.2019.8973859.

II. **J. Zhao**, A. Arefi, and A. Borghetti, "End-of-life Failure Probability Assessment Considering Electric Vehicle Integration," in 31st Australasian Universities Power Engineering Conference (AUPEC), 2021, pp. 1-6, doi: 10.1109/AUPEC52110.2021.9597834.

Statement of Acknowledgement

This thesis is in the format of a standard dissertation. Chapter 3, chapter 4 and chapter 5 have been published in scientific conferences and journal. Chapters 6 and 7 are under review in scientific journals. The authors' contributions to each paper are shown below.

J. Zhao, A. Arefi, A. Borghetti, J. M. Delarestaghi, and G. Shafiullah, "Characterization of Congestion in Distribution Network Considering High Penetration of PV Generation and EVs," in 2019 IEEE Power & Energy Society General Meeting (PESGM), 2019, pp. 1-5.

Author's Name	Contribution	Overall
Jinping Zhao	Conceptualization, Methodology, Resources, Simulation, Validation, Data Analysis and Visualization, Original Draft, Revision	70%
Other co-authors	Validation, Resources, Supervision, Review, Proofreading, Editing	30%

J. Zhao, A. Arefi, A. Borghetti, and G. Ledwich, "Indices of Congested Areas and Contributions of Customers to Congestions in Radial Distribution Networks," in Journal of Modern Power Systems and Clean Energy, vol. 10, no. 3, pp. 656-666, May 2022.

Author's Name	Contribution	Overall
Jinping Zhao	Conceptualization, Methodology, Resources, Simulation, Validation, Data Analysis and Visualization, Original Draft, Revision	70%

Other co-authors	Validation, Resources, Supervision, Review, Proofreading, Editing	30%

J. Zhao, A. Arefi, and A. Borghetti, "End-of-life Failure Probability Assessment Considering Electric Vehicle Integration," in 31st Australasian Universities Power Engineering Conference (AUPEC), 2021, pp. 1-6.

Author's Name	Contribution	Overall
Jinping Zhao	Conceptualization, Methodology, Resources, Simulation, Validation, Data Analysis and Visualization, Original Draft, Revision	70%
Other co-authors	Validation, Resources, Supervision, Review, Proofreading, Editing	30%

J. Zhao, A. Arefi, A. Borghetti, G. Ledwich, R. Dabare, and S. M. Muyeen, "End-of-life Failure Probability and Reliability Evaluation in Distribution Networks Integrated with Large Penetration of Electric Vehicles" under review in IET Generation, Transmission & Distribution.

Author's Name	Contribution	Overall
Jinping Zhao	Conceptualization, Methodology, Resources, Simulation, Validation, Data Analysis and Visualization, Original Draft, Revision	70%
Other co-authors	EV load ML model training, Validation, Resources, Supervision, Review, Proofreading, Editing	30%

J. Zhao, A. Arefi, A. Borghetti, and G. Ledwich, "An Optimization Model for Reliability Improvement and Cost Reduction Assessment Achievable through EV Smart Charging," under preparation for submission.

Author's Name	Contribution	Overall
Jinping Zhao	Conceptualization, Methodology, Resources, Simulation, Validation, Data Analysis and Visualization, Original Draft, Revision	70%
Other co-authors	Validation, Resources, Supervision, Review, Proofreading, Editing	30%

By signing this document, the Candidate and Principal Supervisor acknowledge that the above information is accurate and has been agreed upon by all other authors.

Jinping Zhao June 2022	Ali Arefi June 2022

Abstract

The enormous concerns of climate change and traditional resource crises lead to the increased use of distributed generations (DGs) and electric vehicles (EVs) in distribution networks. This leads to significant challenges in maintaining safe and reliable network operations due to the complexity and uncertainties in active distribution networks, e.g., congestion and reliability problems. Effective congestion management (CM) policies require appropriate indices to quantify the seriousness and customer contributions to congested areas. Developing an accurate model to identify the residual life of aged equipment is also essential in long-term CM procedures. The assessment of network reliability and equipment end-of-life failure also plays a critical role in network planning and regulation.

The main contributions of this thesis include a) outlining the specific characteristics of congestion events and introducing the typical metrics to assess the effectiveness of CM approaches; b) proposing spatial, temporal and aggregate indices for rapidly recognizing the seriousness of congestion in terms of thermal and voltage violations, and proposing indices for quantifying the customer contributions to congested areas; c) proposing an improved method to estimate the end-of-life failure probabilities of transformers and cables lines taking real-time relative aging speed and loss-of-life into consideration; d) quantifying the impact of different levels of EV penetration on the network reliability considering end-of-life failure on equipment and post-fault network reconfiguration; and e) proposing an EV smart charging optimization model to improve network reliability and reduce the cost of customers and power utilities.

Simulation results illustrate the feasibility of the proposed indices in rapidly recognizing the congestion level, geographic location, and customer contributions in balanced and unbalanced systems. Voltage congestion can be significantly relieved by network reconfiguration and the utilization of the proposed indices by utility operators in CM procedures is also explained. The numerical studies also verify that the improved Arrhenius-Weibull can better indicate the aging process and demonstrate the

superior accuracy of the proposed method in identifying residual lives and end-of-life failure probabilities of transformers and conductors. The integration of EV has a great impact on equipment aging failure probability and loss-of-life, thus resulting in lower network reliability and higher cost for managing aging failure. Finally, the proposed piecewise linear optimization model of the EV smart charging framework can significantly improve network reliability by 90% and reduce the total cost by 83.8% for customers and power utilities.

Table of Contents

List of Figures

List of Tables

List of Abbreviations

AEMO	Australia Energy Management Operator
AENS	Average Energy Not Served
AFR	Aging Failure Rate
ASAI	Average System Availability Index
ASUI	Average System Unavailability Index
BBO	Biogeography Based Optimization
BCBV	Branch Current to Bus Voltage
BIBC	Bus Injection to Branch Current
BF-NM	Bacterial Foraging with Nelder-Mean
CAIDI	Customer Average Interruption Duration Index
CAIFI	Customer Average Interruption Frequency Index
CC	Charging Cost
CDF	Cumulative Distribution Function
CIF	Customer Interruption Frequency
CID	Customer Interruption Duration
CL	Customer Loss
CM	Congestion Management
CSA	Clonal Selection Algorithm
DER	Distributed Energy Resource
DG	Distributed Generators
DR	Demand Response
DSO	Distribution System Operator
DT	Distribution Transformer
ECOST	Expected Customer Interruption Cost
ECOI	Expected Cost of Interruption
EENS	Expected Energy Not Served
EDNS	Expected Demand Not Served
EMS	Energy Management System

ENS	Energy Not Supplied
ESS	Energy Storage System
FA	Firefly Algorithm
FACTS	Flexible AC Transmission System
GA	Genetic Algorithm
GAMS	General Algebraic Modelling Systems
G2V	Grid-to-Vehicle
HV	High Voltage
LA	Lion Algorithm
IDE	Differential Evolution Algorithm
ILP	Integer Linear Programming
LMP	Locational Margin Price
LOLE	Loss of Load Expectation
LOEE	Loss of Energy Expectation
LPIF	Load Point Interruption Frequency
LPID	Load Point Interruption Duration
LPENS	Load point Energy Not Served
LV	Low Voltage
MAE	Mean Absolute Error
MCS	Monte-Carlo Simulation
MILP	Mix-Integer Linear Programming
MIQCP	Mix-Integer Quadratically-Constrained Programming
ML	Machine Learning
MLP	Multi-Layer Perceptron
MMP	Multi-objective Mathematic Programming
MSE	Mean Squared Error
MTTF	Mean Time to Failure
MTTR	Mean Time to Repair
MV	Medium Voltage
NSGA-II	Non-dominated Sorting Genetic Algorithm II
OPF	Optimal Power Flow
PL	Power Loss
PSO	Particle Swarm Optimization

PV	Photovoltaic
RA	Reliability Assessment
RE	Reliability Enhancement
RI	Reliability Index
SAIFI	System Average Interruption Frequency Index
SAIDI	System Average Interruption Duration Index
SAMCSA	Self-Adaptive Modified Crow Search Algorithm
SCOPE	Security Constrained Optimal Power Flow
SFLA	Shuffled Frog-Leaping Algorithm
SoC	State-of-Charge
SSSC	Static Synchronous Series Compensator
ST	Substation Transformer
SVC	Static Var Compensator
TCSC	Thyristor Controlled Series Compensation
TLBO	Teaching Learning Based Optimization
UC	Utility Cost
UPFC	Unified Power Flow Controller
V2G	Vehicle-to-Grid
VCR	Value of Customer Reliability
WOA	Whale Optimization Approach

Chapter 1 Introduction

This chapter is devoted to the background and research motivation. The primary research objectives and contributions are presented. The structure and the organization of this thesis are outlined.

1.1 Background

Electric vehicles (EVs) and distributed energy resources (DERs) are popular globally due to environmental concerns and the crisis of traditional fossil resources [1][2]. However, ever-increasing load (e.g., led by the integration of EVs) and increasing penetration of DERs have posed significant challenges to the planning and operation of active distribution networks [3][4]. Heavier power flow led by increased load demand results in higher aging failures on equipment and a higher possibility of violating the thermal limit of transformers and lines, leading to frequent congestion in active distribution networks. Appropriate management of flexibility associated with DERs and the introduction of vehicle-to-grid (V2G) technology can improve network reliability and congestion level by effectively balancing system demand and supply [5][6].

Generally, congestion occurs when insufficient electrical energy is transmitted to customers due to network capacity limit and equipment failure [7]. The existing network has a specific capacity limit due to the thermal tolerance levels of lines and transformers. Moreover, the topology of the network is often radial. Once the power flow is higher than the limit, load demand cannot be accommodated fully due to safety considerations. Especially in an aging network, thermal stress tolerances of transformers and cable lines are deteriorated due to long-term operation.

Congestion management (CM) methods can be classified as short-term and long-term methods. Typical short-term CM strategies include network reconfiguration, DERs et

al. Short-term schemes should flexibly guarantee enough energy for congested areas and keep voltage quality stable. Replacing aged devices and installing low-voltage compensation devices are typical long-term CM methods. Identifying the aging status of transformers and cables is vital in determining the device that needs to be updated. Meanwhile, high aging speed on equipment results in higher aging failure (end-of-life failure), which leads to low reliability, significant customer loss and power utility costs. Proper grid planning and investment can significantly improve network reliability and congestion.

In the market environment, new opportunities have been brought since consumers who own distribution generations (DGs) can play a role in relieving the burden of congested lines or transformers by injecting their energy in the network and also by providing to other neighbouring customers. Responsive consumers who can control their electrical consumption flexibly by demand response (DR) can also help power utilities mitigate congestion. The optimal allocation of EV charging stations is an effective method to relieve the maximum power flow, reduce the probability of congestion, and improve network reliability. In distribution networks, smart charging/discharging of EVs is also an efficient method to accommodate part of the energy shortage during congestions.

1.2 Motivation

Congestion evaluation and reliability assessment are vital for safe operation, efficient investment, and planning of power networks. Power utilities should provide sufficient energy for customers in a reliable manner. Moreover, congestion and reliability are not independent, and low reliability due to aging failure on equipment is one of the main reasons for the congestion in distribution networks. To fully explore the potential of power networks, it is essential to develop a framework using the flexibilities (e.g., EV) in active distribution networks to manage congestion and improve reliability. Large-scale EV integration affects the reliability of the network [8] as non-regulated charging of large numbers of EVs intensifies the load demand. The growing load demand leads to severe congestion due to the increased energy supply shortage. The ever-increasing power flow led by growing load demand results in higher thermal pressure and aging rate on equipment, which leads to lower reliability and a high possibility of congestion. EVs also play a vital role in managing congestion and improving reliability. With daily

regulation, EV charging load can be coordinated to shave the peak load and relieve aging. EVs can work as storage and recover electricity for customers suffering from energy blackouts during congestions and contingencies.

The traditional congestion definition only considers the energy shortage due to the network capacity limitation. However, this definition cannot indicate the complexity of congestion in modern distribution networks. Besides the energy quantity that cannot be transmitted, voltage issues and current limit violations also need to be considered to indicate the congestion level. Furthermore, probabilistic identification of congested areas helps power utilities to recognize vulnerable areas and make better network planning and investment decisions in a distribution network. It is crucial to characterize the congestion events and propose effective indices to reveal the level and seriousness of a congestion event for better managing congestion in active distribution networks. A fair electricity market is useful to encourage the customers' participation in improving the network operation, relieving congestion, and enhancing network reliability.

Identifying the aged transformers and lines is important for the long-term CM scheme and network reliability. As the aging processes of transformers and lines are related to the thermal stress due to flowing power, the vulnerable transformers and cables are identified by the accurate modelling of aging processes, considering the growing penetration of EVs. Meanwhile, when the aging failure happens, tripping devices respond and take action to isolate the damaged component. Therefore, considering post-fault reconfiguration and aging failure, the network reliability assessment is also essential for power utilities to make correct investment plans and proper CM procedures.

1.3 Research Objectives

Considering the background and the research motivation, the primary objectives of this thesis are to:

- Analyze the characteristics of congestion in active distribution networks integrated with EVs and PV generation.
- Develop procedures to quantify the seriousness of network congestion and incorporate the congestion quantification in CM strategies.

- Investigate the aging process and formulate accurate calculations of aging failure probability and loss-of-life on transformers and cable lines.
- Design a framework to estimate the EV's impacts on network reliability and power utility cost due to end-of-life failure on equipment.
- Improve grid reliability and minimize the costs from customer and utility costs due to end-of-life failure and EV charging in active distribution networks.

1.4 Research Contributions

Considering the research objectives, the specific contributions of this thesis include:

- Characterization of the congestion events in active distribution networks as thermal violation and voltage violation considering integration of EVs and PV units.
- Spatial and temporal indices are developed to reveal the level and seriousness of congested areas in terms of thermal violation and voltage violation in active distribution networks.
- Indices are proposed to quantify the contribution from customers at each bus to thermal or voltage congestion to identify the leading cause and flexibilities that may perform effectively in relieving congestion.
- Procedures for assessing end-of-life failure probabilities on transformers and cable lines based on Arrhenius-Weibull distribution, considering relative aging speed due to loading variations.
- An accurate model to predict the EV load based on a machine learning algorithm considering the EV owner's driving behaviour.
- Quantify the EVs' impact on reliability cost due to end-of-life failure on equipment and power utility cost due to equipment replacement.
- A mix-integer quadratically-constrained programming (MIQCP) model by piece-wise linearization of end-of-life failure model to minimize the customer reliability cost and power utility cost due to end-of-life failure and EV charging payment.

1.5 Thesis Structure

The structure of this thesis is shown in Figure 1.1. Chapter 3 characterizes congestion events in active distribution networks as thermal and voltage violations in the presence

of PV generation units and EVs. Chapter 4 explains the proposed indices to quantify the severity and level of a congestion event in terms of spatial violation and temporal continuity. The indices of customer contributions to congested areas provide useful information for making fair electricity policies during a congestion event.

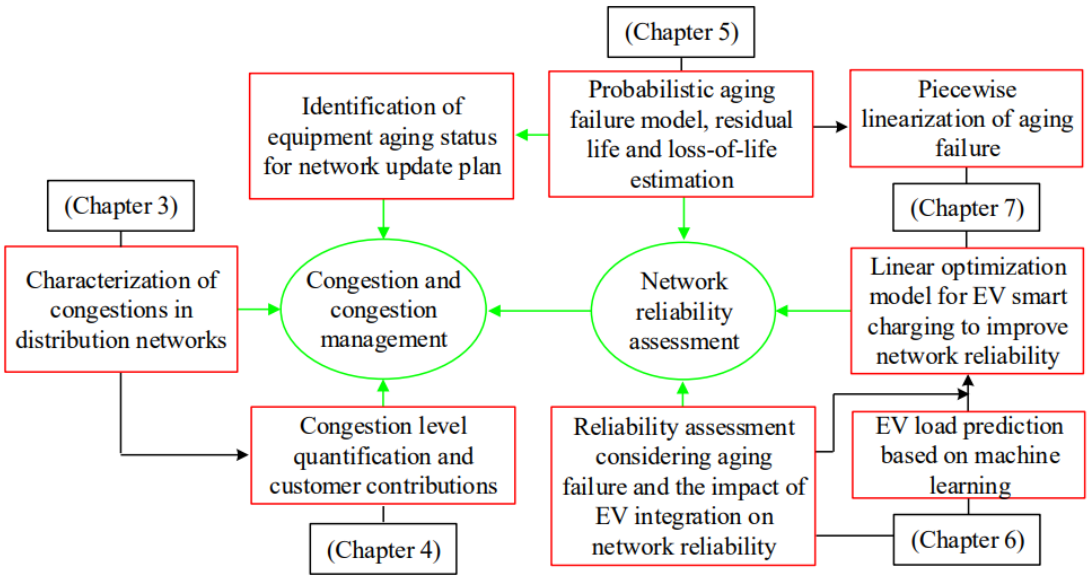

Fig. 1.1 Thesis structure

As an efficient long-term CM strategy, the reasonable decision on updating the aged equipment is made by power utilities after identifying the equipment aging status, which brings the need to develop an accurate aging failure model to reveal the actual aging process in equipment. Therefore, Chapter 5 develops the probabilistic models of aging failures on transformers and cables based on Arrhenius-Weibull distribution considering loading variations. The impact of EV penetration on the residual lives of transformers and lines is assessed.

Network reliability is influenced by the equipment aging failure probability. Proper procedures to explore the impacts of different penetration of EVs on equipment aging failure and network reliability are essential for network operation and planning. Chapter 6 evaluates the EV's impact on network reliability regarding node unavailability, expected energy not supplied (ENS), and customer loss due to end-of-life failure on equipment. An accurate EV charging load prediction model using machine learning (ML) is developed.

The highly non-linear characteristic of aging failure calculation brings difficulties in direct utilization in optimizing network reliability by commercial solvers. Chapter 7

introduces a MIQCP model to optimize EV charging load for minimizing the customer reliability cost due to aging failure and utility cost for replacing damaged equipment and payments to the wholesale electricity market. Aging failure probability is linearized by using the piecewise linearization technique. Chapter 8 concludes and summarizes the whole thesis.

1.6 Thesis Outline

Chapter 2 reviews the most recent literature on congestion, congestion management, and reliability studies in distribution networks. **Chapter 3** characterizes the congestion in distribution networks considering a high penetration of PV generation units and EVs. In **Chapter 4**, indices of congested areas and contributions of customers to congestions in radial distribution networks are introduced. **Chapter 5** develops the procedures for assessing end-of-life failure probabilities of transformers and cable lines considering EV integration. In **Chapter 6**, EV charging load prediction based on machine learning is developed, and the impact of EVs on end-of-life failure probability and reliability is quantified. **Chapter 7** proposes an optimization model for improving reliability and cost in radial distribution networks.

Chapter 2 Literature review

This chapter reviews recent studies on congestion issues and network reliability problems in modern distribution networks and the corresponding solutions for solving those problems. Studies on congestion and CM methods are reviewed. Reliability issues and improvement methods are explained. Finally, the optimization algorithms utilized in solving the nonlinear CM optimization and reliability improvement problems are listed.

2.1 Introduction

Congestion refers to a condition in which insufficient energy is provided by power utilities to consumers due to the physical limitations of networks, such as the thermal limitations of wires/cables or transformers [9]. Insufficient infrastructure investment, ineffective resource scheduling or equipment failure are the most common reasons for congestion [10]. Consequently, congestion leads to electricity shortages, high electricity prices, and violations to reliability and stability of system operation [11]. CM indicates the scheme of alleviating network congestion considering the safety, reliability, and stability requirements. The primary task of CM is to provide adequate energy for congested areas (or customers) by utilizing resources in the network or curtailing part of the load in case of the occurrence of instability or faults.

Up to date, this definition of congestion mainly focuses on the shortage of energy due to overcurrent caused by emergencies of generation or network. It neglects other factors such as voltage quality and satisfaction of consumers. The primary task of a CM method indeed is to provide additional power to customers while satisfying the network and load constraints. CM procedures should also have the ability to guarantee the continuity of supply without a decrease in reliability and security levels, especially for important customers in congested areas, such as train stations and hospitals.

Moreover, the fundamental task of a power system is to supply power to the customers economically and reliably even though modern power systems are facing various faults, problems, and challenges. Power system reliability is defined from the perspectives of adequacy and security. Adequacy refers to the capability of supplying adequate electricity to customers even facing the risk of failures and outages in the network, while security is the ability to withstand sudden disturbances without major interruptions [12]. In active distribution networks, the uncertainties from renewable generation and load fluctuations need to be considered in reliability estimation, and new coordination control algorithms of flexibilities provide great opportunities to improve network reliability. Fig. 2.1 shows the structure of this chapter.

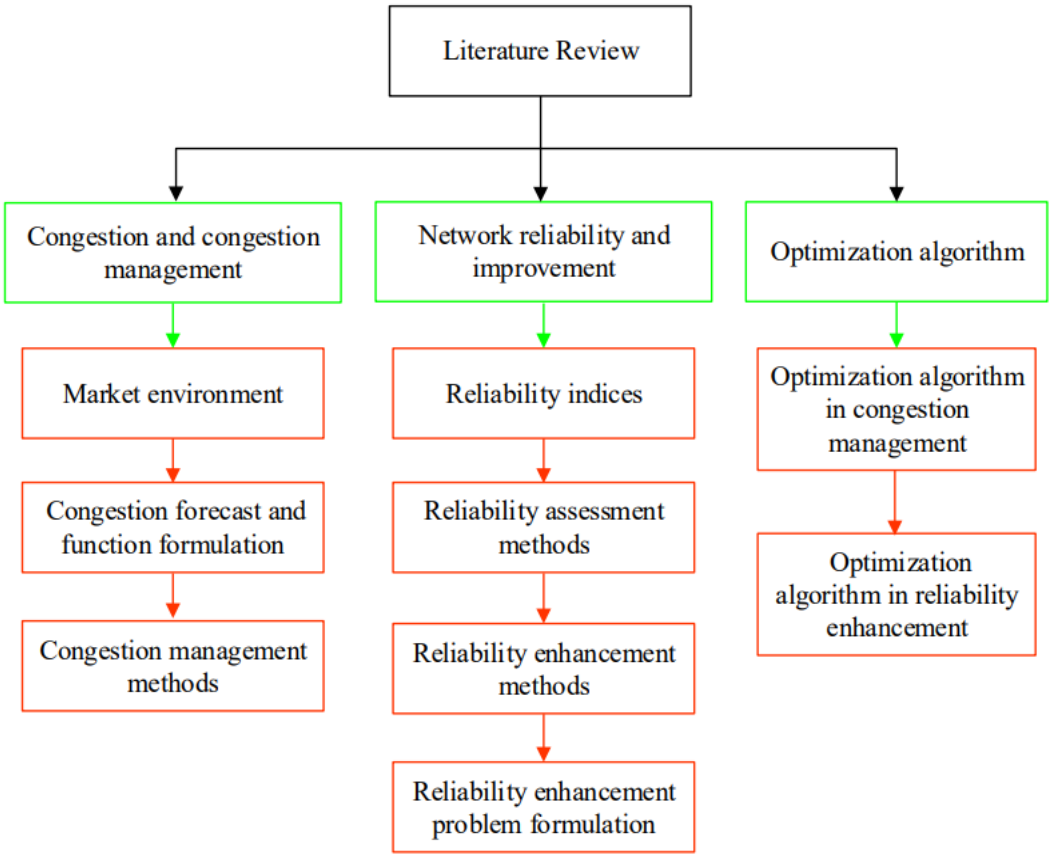

Fig. 2.1 Structure of Chapter 2.

2.2 Congestion and Congestion Management

With the increasing penetration of DG and the advent of new loads, such as EVs, the frequency of congestion increases in transmission and distribution networks. CM is

important to guarantee the safe, stable, and efficient operation of power systems.

Generally, CM is becoming more difficult because of the complexity and uncertainties of power networks. DERs have been proven as a useful participants in the operations of networks in [13][14][15][16] by providing voltage support and enhancing the system's stability. DR or load management [17][18] is another important tool that can decrease load variation by peak shaving and valley filling. More active demand-side participation would make electricity markets more efficient and competitive [9].

Up-to-date, limited works have been done on CM in distribution networks and most of the work mainly focuses on tackling congestion due to the limit of network transmission capacity. The direct implementation of traditional methods, such as generation re-dispatching and Flexible AC Transmission System (FACTS) devices, is ineffective in distribution networks. Moreover, CM methods should be able to address both voltage and overloading issues by using all the resources provided by DG control, DR mechanisms, and the presence of transformers equipped with on-load tap changers and other control devices. The uncertainties of flexibilities in the distribution network should be considered.

2.2.1 Market Environment

Congestion can be eliminated by generation rescheduling, load curtailment, FACTS devices, etc. There are both possibilities and challenges for consumers and power utilities in mitigating congestion in the market environment. Proactive customers who own distribution DGs and smart loads can decrease congestion levels and increase reliability by assisting in load shaving and providing the local power supply. In the meantime, they will gain more benefits because the spot price of electricity is related to congestion and the amount of power demand [19]. Power utility can save extra investment on new equipment and the performance of system operation is improved to a great extent by employing the flexibilities effectively.

By knowing the opportunities, power utility should realize the importance of coordinate control of all the flexibilities, especially with large penetration of DGs and intelligent load, e.g., EVs. Meanwhile, this is a challenging task due to the increased uncertainties in power systems, and Ref [20] discussed the uncertainties from supply planning, load changes, and power flow under the electricity market environment.

Reference [21] studied the local flexibility markets in Germany, the Netherlands, the United Kingdom and France. In this article, the type and depth of a congestion event, the organization and governance of network operators, the current congestion management approach, and the need to develop additional flexibility sources are compared. The authors concluded that the local flexibility market needs to be well designed after characterizing and understanding the local context. The motivations for regional differences in the development of local flexibility markets are highlighted in this research.

2.2.2 Congestion Forecast and Function Formulation

1. Congestion forecast

The increasing uncertainties and complexity in distribution networks make it more challenging to forecast loads and congestion precisely due to the change of traditional structure to modern configuration with extensive penetration of DGs combined with increasing electricity consumption and controllable load level. Nevertheless, from the perspective of governing congestion, the importance of forecast is getting higher and higher.

A short-term congestion forecast method within wholesale power markets is proposed in [22] to provide useful information on congestion, help power system participants know price behaviours and facilitate their decision-making without taking the influence of DGs and DR into account. Comparatively, in [23] a model to estimate the probability emergency of congestion is proposed with both mathematical and simulation procedures considering the uncertainties of DGs. Monte-Carlo simulation is implemented in [24][25] to simulate the uncertainties from wind power integration and load in short-term congestion forecasting. In [26], a visualization tool is presented to forecast network congestions with extensive penetration of renewables for distribution system operators (DSOs) based on the probabilistic power flow. Different errors in power forecast based on actual wind farm data in [27] provide a reference for evaluating the accuracy of forecasting methods in distribution networks connected with flexibilities.

2. Function formulation

The function of CM is an optimization problem with the goal of optimal power flow (OPF) [28][29][30] or optimum economic benefits (in the market environment) considering the equality and inequality constraints. Equality constraints refer to an equilibrium between generation and demand in terms of active power and reactive power taking loss into account. In contrast, inequality constraints suggest CM should guarantee power networks free from unacceptable capacity violations, thermal, voltage magnitude, stability, and reliability. By simplifying the requirements mentioned above, a simple but straightforward function of CM is described in [31], shown as follows:

$$P_G^* = arg \min_{P_{Gi}} \sum_{i=1}^{ng} b_i(P_G) \tag{2.1}$$

$$\sum_{i=1}^{ng} P_{Gi} = \sum_{j=1}^{nd} P_{Lj} \tag{2.2}$$

$$|F_l| \leq F_l^{max} \tag{2.3}$$

where P_{Gi} is the output of generator i; ng is the number of generators in the power system; P_{Lj} is the demand of load j; nd is the number of loads in the system; $b_i(P_G)$ is the supply bids; F_l is the power flow of line l for the given injection; F_l^{max} is the maximum power flow allowed for line l [31].

Load bus voltage constraints and transformer taps constraints are also considered in some studies, e.g., [32]. A more competitive model is introduced in [33], using active and reactive power control for congestion elimination coordinately. Besides congestion alleviation, minimizing the voltage disturbance is one of the objectives of this article. CM schemes provide economic benefits for customers and power utilities in the market environment. Therefore, the model proposed in [34] is attractive as it maximizes social gains by rescheduling bilateral and multilateral contracts.

Ref [35] formulated a flexible economic modelling framework for relieving congestion in the long term. Another effective CM model is developed in [36] with three objectives: less CM cost, higher voltage stability, and transient stability. Indeed, responses from active customers and employment of flexibility have increased the complexity of modelling the CM schemes.

3. Index in CM

FACTS, DGs and generation re-dispatching are typical CM methods, and certain

indices are employed to determine the optimal investment and locations of FACTS, energy dispatching plan of DG and generator in relieving congestion. For instance, Power Flow Contribution Factor (PFCF), Generator Sensitivity Factor (GFS) and Load Sensitivity Factors (LFS) are used in [37][38][39][40] to select the participating generators for rescheduling. Line Loading Index (LLI) and Congestion Distribution Factors (CDF) [41] have been utilized separately to indicate the congestion level of a wire/cable in distribution networks. Moreover, the performance index of DG placement based on generation cost is proposed in [42] to find the optimal size of DG. In terms of voltage stability, the values between 0 and 1 are utilized to indicate the system condition (voltage stability limit) in [43] and Load Margin (LM) is used as a criterion for assessing voltage stability in [44].

Additionally, the sensitivity index (SI) is proposed in [45] to indicate the optimal location and number of Thyristor Controlled Series Compensation (TCSC). Similarly, SI and sensitivity factor (SF) are utilized to identify the optimal siting and sizing of DG in [46]. Remarkably, the congestion indicator factor (CIF) is proposed to quantify the tendency of the distribution network towards congestion situations in [47]. Power transfer distribution factor (PTDF), topological generation and load distribution factor (TGDF, TLDF) are utilized to indicate the relation between generator/load/aggregator and line power in a market environment to relieve congestion in [48]. Bus sensitivity factor (BSF) is utilized in [49] to find the optimal location for solar PV in CM. The indices presented above could provide useful information for finding the optimal sizing and location of flexibilities in congestion management in distribution networks.

2.2.3 CM Methods

1. CM method classification

There are two major categories of CM: technical methods and non-technical methods [50], as shown in Fig. 2.2. Technique methods include outage of congested lines, transformer tap changers and operation of FACTS devices. Non-technical methods include two categories depending on the effect of the market. Typical market-based methods are auctioning, market splitting, generation re-dispatching, load curtailment and pricing. CM schemes can also be classified into two broader categories: cost-free methods, where generation and distribution companies are not involved, and non-cost-

free methods, where generation rescheduling and demand response are considered [11] shown in Fig. 2.3.

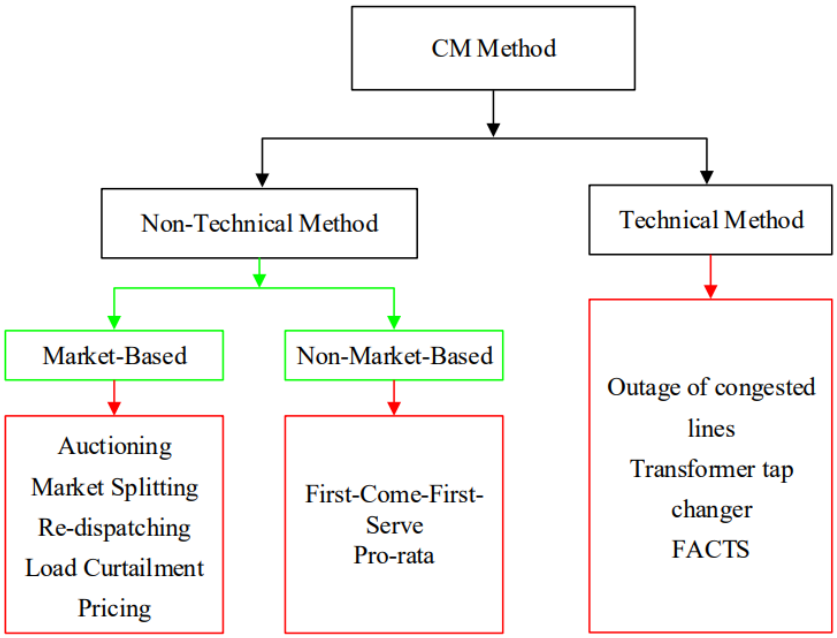

Fig. 2.2 Congestion management methods classification in [50].

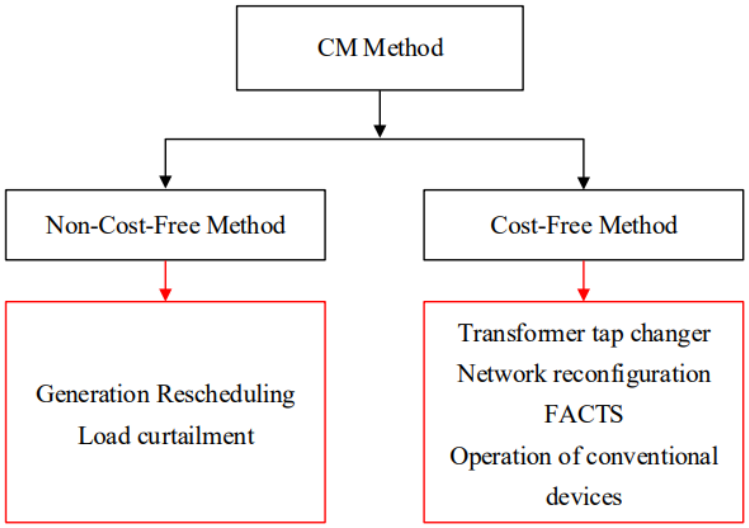

Fig. 2.3 Congestion management methods classification in [11].

Typical cost-free methods are reconfiguring feeders, changing transformer taps, implementing traditional compensation and FACTS devices, etc. Non-cost-free methods are generation re-dispatching and load curtailment. CM approaches can be classified based on the application side, e.g., generation, transmission, and end-user [11][51]. The optimal location of DG and generation rescheduling are CM methods from the generation side. OPF and optimal placement of FACTS are two typical CM

methods from the transmission side. CM methods from the end-user side include DR, zonal and nodal pricing, load curtailment, etc.

2. Technical methods

(1) Transformer

Changing or updating the settings of transformers can assist in relieving congestion. For example, optimal phase-shifting transformers (PSTs) are discussed in [52] to minimize the overall risk of congestion on power system lines. A novel method for real-time congestion management is proposed in [53] to resolve the congestion problem at the MV/LV transformer. Additionally, a smart transformer is introduced in [54] to improve the voltage profile and mitigate current in CM, interfacing small generation units by exchanging information. Those methods can mitigate congestion to some extent. However, when the system is seriously congested and voltage is violated critically, it is difficult to gain satisfying results merely relying on the transformer regulation.

(2) FACTS devices

Thyristor-Controlled Series Capacitor (TCSC), Unified Power Flow Controller (UPFC) and static synchronous series compensator (SSSC) are three typical FACTS devices. In [32][43][55][56][57][58][59], optimal position for installation of TCSC is calculated to remove the line congestion based on power flow reduction, additionally, the optimal location of Static Var Compensator (SVC) and SSSC is discussed separately in [43][57][60]. Likewise, the optimal setting of UPFC is discussed along with re-scheduling generation to mitigate congestion in [61]. Moreover, the performance and analysis of UPFC, TCSC and SSSC are provided for the enhancement of system transient stability when congestion happens in [62]. These examples show the validity of utilizing FACTS devices to alleviate congestion in transmission networks. However, the investment in FACTS brings about the possibility of higher electricity prices in distribution networks.

(3) Network configuration

Network reconfiguration is the change of the topological structure by closing usually opened switches and vice versa [63] to provide additional pathways for power flow to

congested customers. Based on CIF values, the researchers in [47] illustrate that reconfiguration of feeders is an effective method to relieve congestion and reduce extra investment. Similarly, a transmission network configuration method achieved by automatic control actions of switches is presented in [29] to mitigate congestion on regional transmission lines and tie lines in a multi-area network.

To sum up, technique methods can help the system to remove congestion. The competitive characteristic of the market environment urges new algorithms to bring optimal benefits for customers and power utility. Therefore, market-based schemes: employing DGs, DR, and pricing methods are becoming more popular in CM.

3. Market-based methods

Market-based methods can improve transparency and liquidity of the electricity market and have bright prospects to apply in the electric supply industry [16][48], including auction, pricing, generation re-dispatching, demand response and DG employment.

(1) Pricing

Modulating nodal price and zonal price are two typical pricing methods. Nodal price is the Location Margin Price (LMP) of one specific node related to the number of flexibilities and congestion level. For instance, stable LPM is considered a sign of congestion elimination in [64] and a distribution LMP method is introduced in [65] to achieve optimum energy plans for flexible demands. Nodal price methods are reasonable within the market environment but not appropriate for large-scale systems considering their time-consuming characteristic. Compared with nodal price methods criticized for their complexity and coordination in computation, the zonal price method bundles particular nodes into areas with one price [66]. Furthermore, increasing the price in the deficit area and decreasing the price in the surplus area are utilized in [67] to manage congestion. The capacity subscription tariff [68] is proposed and demonstrated to avoid transformer overloading in power networks in the presence of EVs.

(2) Generation re-dispatching

Generation rescheduling, which also raises the challenge of minimizing the rescheduling cost, is one important CM approach [69][70]. The most sensitive

generators that participated in the power rescheduling process are determined in [39] using GSF to relieve congestion. The researchers in [71] claimed that the number of generators needs to be minimized during generation rescheduling for security-oriented power system operation. In [72][73][74], the rescheduling cost is considered as the objective function in CM formulated as non-linear problems subject to generation capacity limit, power balance constraint, network transmission constraint, and voltage inequality constraint.

(3) DR

The flexibilities, e.g., EVs, storage and heat pumps, can help mitigate congestion by modifying the load profile. For example, the controllable load of consumers is shifted to reduce load peak and diminish congestion in [75]. An efficient control algorithm is proposed in [76] to change the load demand for peak shaving/congestion management in radial distribution systems. The potential benefits of demand-side management applied in congestion areas to improve voltage security are discussed in [77]. Customers' willingness in a flexible demand swap market is considered in the DR scheme proposed in [78]. Additionally, authors in [79] used the number of hours of loading violations and the number of houses experiencing under-voltage as metrics to assess the performance of DR strategies in congestion relief.

Recently, the authors of [80] introduced the typical processes in the approach of flexibility deployment in CM from the perspective of DSO: data acquisition, load forecasting, decision-making and flexibility mechanism interfacing. In [81], an incentive-based mechanism is proposed to facilitate flexibility engagement in CM in distribution networks. In [82], another flexibility aggregation method is described to aggregate flexibility from DER at a high voltage level.

The growing popularity of EVs results in a higher possibility of congestion in feeders. EVs also offer a potential solution by coordinating control of grid-to-vehicle (G2V) and vehicle-to-grid (V2G) schemes. G2V-V2G coordination strategy is formulated to avoid line congestion and minimize the charging cost after the prediction of the state-of-charge (SoC) level of EVs using the gradient boosting method [83] and random forest method [84]. In [85], the authors proposed an adaptive decentralized control algorithm to regulate the charging load from plug-in EVs (PEVs) according to the congestion signals from phasor measurement units and avoid transformer overloading

and voltage violations. Compared with the static smart charging strategy, a dynamic smart EV charging algorithm is proposed in [86] to avoid congestion in distribution networks. An aggregated EV scheduling framework based on the distributed LMP is developed in [87] to minimize the congestion in radial distribution networks.

A Mobility-on-Demand scheme-based EV regulation strategy is proposed in [88] to assign trips and loads to minimize congestion. Specifically, a distributed control strategy for charging large-scale EV fleets is proposed in [89] to avoid congestion and reduce the charging cost and battery degradation. The research results of these papers all prove that DR is a crucial method for shaving load and helping the network get rid of congestion. Besides, voltage violation can be decreased by a proper control strategy.

(4) DG engagement

DG is gaining popularity in CM [90] by reconstructing power networks. For instance, the optimal sizing and location of DG are formulated in [46] to relieve congestion. Additionally, the uncertainty of DGs has been considered when generating the candidate lines for installation of DGs and the priority list of buses for optimal location and sizing of DGs in [91][92]. In [93], a real-time controller of wind power and storage for congestion mitigation is proposed. In [94], DGs are utilized to reduce the locational marginal price (LMP) and avoid violating the maximum transmission capacity of lines. The optimal combination of investment in urban energy storage and incremental grid expansion, analyzed in [95] from the perspective of the network, provides a good reference for power utilities. A long-term method [96] and day-ahead congestion management [97] by scheduling flexibilities have been presented for distribution networks. DG engagement can reduce investment and provide extra energy for congested areas. However, environmental factors and customers' preferences should also be considered. Meanwhile, a reasonable reward strategy needs to be developed to facilitate the participation of customers.

4. Hybrid methods

The hybrid method uses two or more different CM methods simultaneously to achieve maximum benefit. For instance, in [98], an optimal combination of DR and FACTS devices is proposed considering the network constraints in a restructured market environment. Similarly, DR combined with SVC and TCSC has been discussed based

on optimal power flow in [99]. Additionally, different scenarios of congestion management by DR, auction, generation re-dispatch and generation accompanying demand re-dispatch are discussed in [100]. The test result shows generation and demand re-dispatch can considerably reduce congestion costs. Finally, an economical combination method of restructuring system buses and DG is presented in [101]. DR, re-scheduling, transmission expansion and DR are employed in [102] to manage AD/DC congestion in transmission networks. Generator settings, voltage settings, transformer tap settings and FACTS settings are optimized in [103] to guarantee the power flows within the capacities of lines and avoid congestion. Dynamic tariff and incentive-based flexibility services are coordinated in [104] to manage congestion a day ahead. Power distribution companies (PDC) owned DGs and DR are considered in the multi-objective model to mitigate congestion in transmission networks in [105]. Combining different CM strategies increases the flexibility and efficiency of CM procedures. Meanwhile, it brings higher requirements for the control algorithm due to the increased number of variables and complexity in coordination.

In the following sub-sections, challenges, and opportunities of the market environment for power utilities and customers in CM are first introduced. Then, congestion forecast methods, the generic function of CM, and commonly used indices in CM are explained. Finally, the CM method classification and typical CM methods are thoroughly reviewed.

2.3 Network Reliability and Enhancement

Generally, reliability assessment (RA) is categorized into three hierarchical levels: generation system level, transmission system level, and distribution system level [106]. Furthermore, the reliability analysis for distribution networks is different from generation and transmission networks in different aspects [107] due to network complexity and new opportunities due to the proliferation of DG and new loads, such as EVs. Meanwhile, the uncertainties of DG and low load forecast accuracy also bring challenges to RA [108]. This subsection explains the reliability indices (RI), RA methods and reliability enhancement (RE) strategies in active distribution networks.

2.3.1 Reliability Indices

Failure rate (λ, failure/year), annual unavailability (U, hour/year), annual outage time (r, hour/year) [106][109], mean times to failure (MTTF), mean times to repair (MTTR) [110][111], time to failure (TTF) and time to repair (TTR) [112] are the commonly used indices to represent the failure characteristics of devices. Aging failure rate (AFR) and loss of life (LoL) are considered to evaluate the reliability of transformers and cables in [113][114][115][116][117][118]. RI can be clustered into two groups from the perspectives of a single load point or the whole network.

1. Load point reliability indices

RIs include loss of load index function (LLIF), unsupplied load function (ULF), loss of load probability (LOLP), expected unsupplied load (EUL), loss of load expectation (LOLE) or loss of energy expectation (LOEE), load point interruption frequency (LPIF), load point interruption duration (LPID), load point energy not served (LPENS) or expected demand not served (EDNS) or expected energy not served (EENS) [121][122][123][124] from the load point of view.

2. System reliability indices

Indices that indicate the reliability performance of a power network include: system average interruption frequency index (SAIFI), system average interruption duration index (SAIDI), customer interruption frequency (CIF), customer interruption duration (CID), customer average interruption frequency index (CAIFI), customer average interruption duration index (CAIDI), average system availability index (ASAI), average system unavailability index (ASUI), and average energy not served (AENS) [125][126][127][128][129][130], expected customer interruption cost (ECOST) [127][131][132] or expected cost of interruptions (ECOI) [128].

2.3.2 Reliability Assessment Method

This section firstly explains the commonly used RA methods for bulk power systems. After that, RA methods that consider the uncertainties and opportunities of DGs and

EVs in active distribution networks are discussed.

1. RA method classification

RA methods are classified into deterministic, probabilistic, and intelligent methods [106]. The deterministic methods calculate the capacity reserve margin and loss of the larger unit. Probabilistic methods estimate certain RIs through analytical and simulation methods, such as Monte-Carlo simulation. The intelligent methods use intelligent techniques (e.g., GA) to predict or assess the reliability of distribution networks. Monte Carlo, MATLAB, ETAP, DigSILENT and NEPLAN are utilized to simulate the device failure rate under normal conditions and evaluate network performance during contingencies.

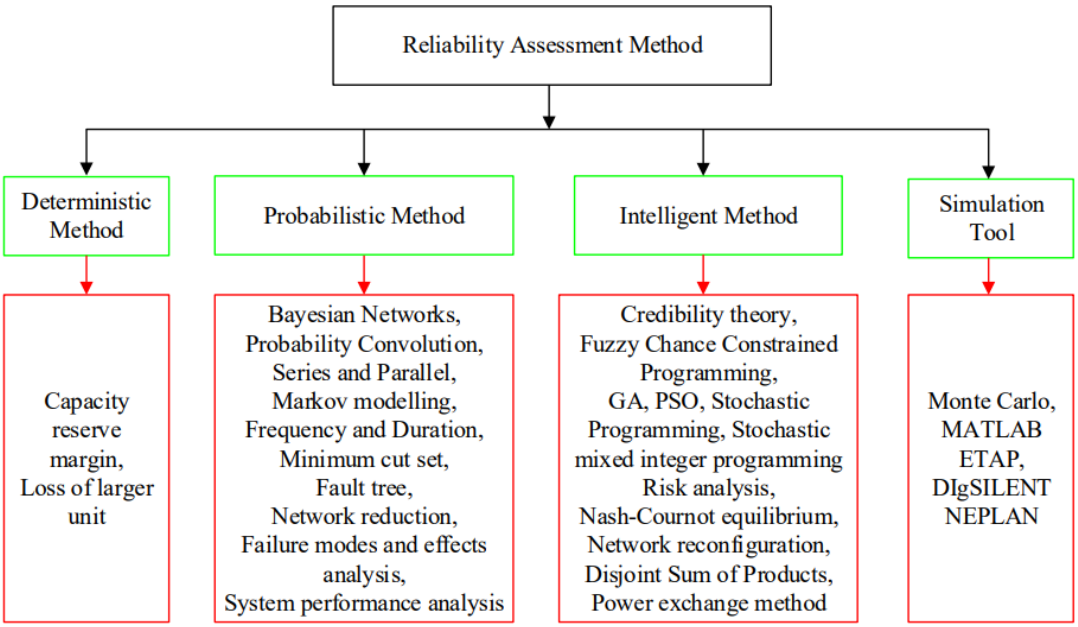

Fig. 2.4 RA methods in [106].

The methods shown in Fig. 2.4 accommodate the reliability evaluation techniques for generation, transmission, and distribution systems. In distribution networks including renewable energy, e.g., wind power, PV, battery energy storage systems (BESS), and extensive penetration of EVs, the reliability estimation and analysis needs to take the uncertainties from those components into consideration [133][134].

2. RA in active distribution networks

Compared with generation and transmission systems, RA in distribution networks has

its unique feature due to the proliferation of DGs and EVs. There are challenges and opportunities in controlling DGs and EVs to assess and enhance network reliability. The challenges brought by the uncertainties in distribution networks, such as the fluctuations in the generation output of DGs [135], the dynamics of charging load and charging time from uncontrolled EVs, and the randomness in incentive-based DR behaviours [133], lead to lower assessment accuracy. Meanwhile, DGs, DR and V2G technology can provide extra energy to supply to the customers during contingencies, thus improving network reliability. However, DGs, DR, and EVs' level of engagement depends on the electricity market and the benefits that owners will receive.

The reliability evaluation techniques of distribution systems are classified into two general groups: analytical methods [129][136][137][138][139] and simulation methods [112][121][140][141][142]. Analytical methods calculate the values of RIs by mathematical calculations based on traditional probability theory. Simulation methods use Monte-Carlo simulation (MCS) to imitate the actual process and random behaviour of faults. Three types of MCS methods named Sequential MCS [109][111][143], Pseudo-Sequential MCS, and Non-Sequential MCS are utilized in probabilistic analysis of network reliability [135].

3. RA considering DGs

The uncertainties in the output power from wind turbines and PVs are simulated by the MCS technique in the probabilistic reliability model in [144]. A comprehensive reliability evaluation framework for distribution systems considering the controls of microgrids and distributed energy resources (DERs) based on Sequential MCS is developed in [112]. Moreover, the power electronic converters reliability model is incorporated into the power system reliability analysis in [145]. Authors in [146] explored the benefits of employing the self-healing control and microgrid in improving distribution system reliability using time-sequential MCS. An analytical RA based on linear programming technique is established for radial distribution networks in [147]. The authors of [141] estimated the impacts of the integration of DG in the coupling relationship between power supply capacity and reliability of distribution systems. The network topology uncertainties and isolated operating probability of DG clusters are integrated with the RA formulation of active distribution networks in [127].

4. RA considering EVs

The proliferation of EVs increases the load demand and deteriorates the reliability of distribution networks. Therefore, establishing a method to determine the maximum permissible integration of EVs and keep the system reliability at a certain level is very important, such as the method proposed in [111] using Sequence MCS. Ref [122] assessed the impacts of load from different EV types (plug-in and full EV) and different charging strategies on system reliability. After evaluating the impact of EVs on power system reliability, the authors in [148] also prove that the system reliability can be improved by EVs deploying appropriate charging/discharging strategies. In [123], EVs are considered movable loads. A load model considering the randomness in charging times and locations of EVs is developed to evaluate the EVs' effects on system reliability.

Moreover, Ref [149] introduced a Monte Carlo method and Markov decision process (MDP) theory-based approach to predict the EVs load in evaluating RIs and voltage stability. Battery exchange (BE) mode or V2G mode of EVs can improve network reliability by providing electricity to customers during faults and contingencies. Therefore, the BE mode, V2G mode, and vehicle-to-home (V2H) mode are considered in the evaluation of network reliability in [136][150][151]. Reliability studies of distribution systems integrated with DGs and EVs under different scenarios are conducted in [110][142][152], demonstrating the feasibility of intelligent control of EVs in reliability enhancement.

5. Equipment failure on RA problem

Circuit breaker failure, feeder failure, and post-fault reconfiguration also play their roles in reliability evaluation. The sensitive analysis of failure rate and average repair time of feeder components on the reliability of EV-supported distribution network is carried out in [124]. Notably, a linear programming-based analytical RA model is proposed in [139] considering the post-fault reconfiguration, DG uncertainty and protection failures. Circuit breaker failure is modelled by an incidence matrix to evaluate the corresponding RIs in [153]. The impact of remote-controlled cut-off switches (not equipped or equipped at different locations) on SAIFI and SAIDI is simulated in [154]. The RIs of a test network under four different configurations are

tested given the failure date, switching and downtime data of all components in [155]. Using deep learning techniques, the authors in [156] also developed a PSO-based deep belief network (PSO-DBN) model to analyze the distribution network reliability. Moreover, EENS is evaluated and considered in [157] to support the decision-making process for network expansion and planning.

2.3.3 Reliability Enhancement Methods

According to the problem formulation, RE methods for active distribution networks can be divided into direct and indirect methods. The direct method, e.g., [152][158], tries explicitly to maximize the system performance in reliability. The objectives of the indirect methods, e.g., [159][160][161], are reducing power loss, enhancing voltage magnitude and balance degree, decreasing load deviation, and improving reliability simultaneously. The reliability enhancement methods can also be classified into three groups: cost-free method (flexibility-based method), non-cost-free (technical method) method, and hybrid method based on whether investment from power utilities is needed, shown in Fig. 2.5.

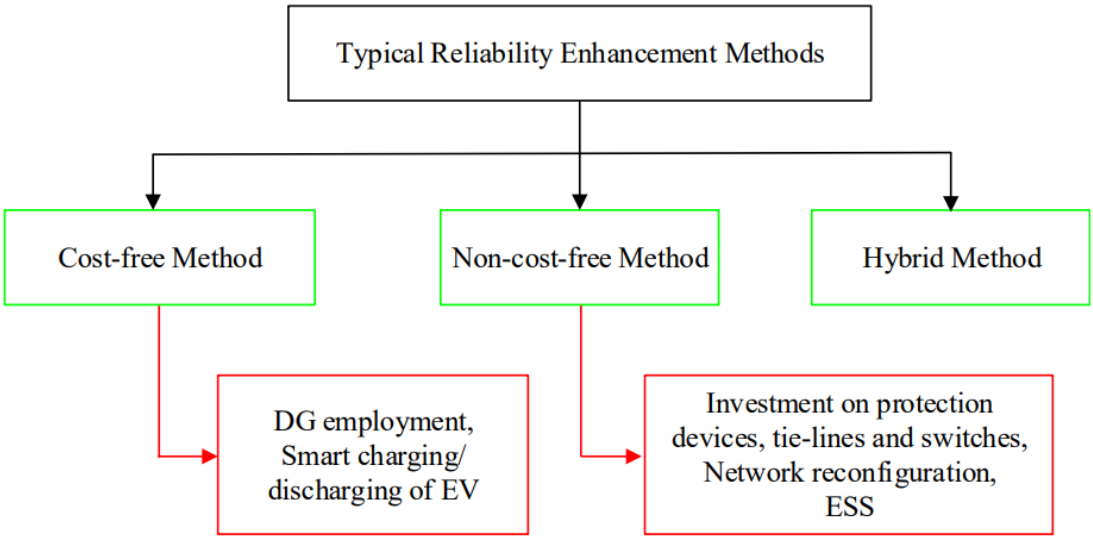

Fig. 2.5 Typical RE methods in distribution networks.

1. Cost-free methods

Typical cost-free methods are flexibility-based to balance the power supply and demand during faults or contingencies by scheduling load and supply, mainly

including distributed generations (DGs) and smart charging/discharging of EVs.

(1) DG Employment

DG plays an essential role in the energy restoration process during and after a system fault. Therefore, it is a valuable method to improve the network reliability as a backup electricity source. For example, DG units supply energy for the interrupted load points during system restoration processes after system faults in [162] to minimize customer interruption duration and system reliability in terms of SAIDI and SAIFI. A graph-theory-based clustering method to divide the distribution system into a cluster of multiple microgrids (MMGs) is proposed in [126] to improve the network performance in terms of energy efficiency and system reliability. Furtherly, an energy management system (EMS) for managing MMGs is developed in [128] to against emergencies and guarantee system reliability.

Meanwhile, in [132], optimal allocation of DGs and capacitors is proved to be an efficient method in RE. Interestingly, biomass-fueled gas engines are modelled and utilized to optimize overall system reliability in [163]. The study of DG re-dispatch after a contingency event in radial and meshed distribution networks furtherly in [129] illustrates the feasibility of RE by deploying DG.

(2) Smart charging/discharging of EV

The EV smart charging/discharging algorithm contributes to reliability enhancement from two aspects. First, smart charging of EVs can shave the load peak and thus reduce the fault probability of the network and improve the network reliability. For example, smart charging strategies are proposed to mitigate the aging failures on transformers in [115][118][164][165]. Secondly, the network reliability can be improved by discharging the power from EVs to support the interrupted customers through V2G techniques. For instance, EVs are utilized as transportable ESS in [131] to provide power for interrupted customers when faults occur in the distribution network. In [166], DR programs and smart charging/discharging of EVs are coordinated to improve reliability in radial distribution networks. Backup support from EV parking lots when power is insufficient due to component faults or supply shortages in [167] illustrates that EVs can be an efficient method of improving system reliability.

2. Non-cost-free methods

Non-cost-free methods involve purchasing operating devices (recloser, circuit breaker, fuse, switches, tie lines, DSTATCOM, energy storage systems) and network reconfiguration to enhance/expand or change the network topology.

(1) Protection devices, tie-lines and switches

Investment in the protection devices (circuit breaker and fuse), tie-lines, and switches (sectional switch and recloser) can reduce the number of customers influenced during a fault. For instance, the placement of reclosers is optimized to improve reliability in [125][168][169]. Furthermore, placements of switches and protective devices are optimized in [169][170][171][172][173][174][175] to maximize the reliability in distribution networks. Tie-lines can change the normal configuration of a network after a fault. In [173][176], tie lines are utilized to provide power from neighbouring feeders to the customers, and the optimal location of tie-lines is determined for maximum reliability. Moreover, the optimal placement and sizing of DSTATCOM are studied in [159] to improve the voltage profile and power loss. A distribution system planning strategy by replacing, adding or reinforcing the feeders and substations is proposed in [177] to enhance the network performance and reliability.

(2) Network reconfiguration

Network reconfiguration changes the topological structure and reroutes the power flow path in the presence of faults and contingencies by modifying the normal status (open or close) of the sectionalizing and tie switches. For example, optimal distribution feeder reconfiguration considering the composite customer damage function is conducted in [178] to improve the reliability of distribution networks. Similarly, a graph theory-based feeder reconfiguration strategy is proposed in [179] to optimize power loss and reliability. Specifically, reconfiguration for radial distribution systems on the improvement of RIs (SAIFI, SAIDI, AENS, CAIDI, ASAI) is discussed in [180][181]. Multiple objectives, including minimizing the power loss and operation costs, improving voltage stability and enhancing network reliability, have been realized by optimization of network reconfiguration in [157][182][183].

(3) Energy Storage Source

In distribution networks integrated with DGs, ESS can absorb energy from DGs and prevent overvoltage issues during normal conditions. ESS can also work as a backup

electricity source to provide energy for customers during power outages or network faults. For instance, the optimal placement and sizing of ESSs and the best location for battery ESS to enhance the reliability of radial distribution systems are studied in [184] and [185], respectively. Moreover, a management strategy of ESS and DGs is proposed in [186] to improve the network reliability considering the investment and operation cost. The size of movable energy resources is optimized in [143] to support power restoration and enhance reliability for customers.

3. Hybrid methods

Concerning the possibility of insufficient power from flexibilities and investments involved in technique methods, hybrid methods are developed by accommodating the benefits of both to enhance system reliability and reduce the cost. Hybrid methods employ two or more approaches from non-cost-free and cost-free methods. For example, DG, sectioning switches and tie switches are combined and optimized to minimize the utility liability while assuring the supply to the prioritized customers in [187]. Similarly, the optimization of switches placement and pre-positioning strategy of mobile generators are developed to enhance the distribution system reliability in [188]. DGs and network reconfiguration, DGs and cross-connections are optimally planned to improve system reliability and minimize power loss on lines in [161] and [189]. Network reconfiguration and V2G strategy are coordinated in [190] as a RE strategy. Finally, a comprehensive RE strategy is established in [158] by optimal allocation of protective devices, DGs and EV charging stations.

2.3.4 Formulation of RE Problem

RE strategies are formulated as optimization problems by regulating the flexibilities from DGs and EVs, network planning and network reconfiguration. Generally, the optimization problems are mixed-integer linear or nonlinear problems due to the complexity of active distribution networks. For example, optimal location and sizing of protection devices in [125][168][169][171][174], optimal clustering of MMGs in [191], utilization of DG, ESS and EV in [132][162][166][184][187] are formulated as nonlinear optimization and heuristic algorithms are utilized to find the optimal solutions for improving reliability. However, the results obtained by heuristic methods

are skeptical due to the inability to guarantee global optimality. Linear programming is getting more attention due to the availability of sophisticated commercial software, e.g., general algebraic modelling systems (GAMS), Gurobi, etc.

Distribution system planning is formulated as a MILP problem and solved by GAMS/CPLEX in [177] to improve network reliability. Network reconfiguration is also developed as a MILP problem and is solved by Dijkstra's shortest-path algorithm and lexicographic optimization in [179] and [180], respectively. Investment in protection devices, switches, and tie-lines can effectively improve network reliability by isolating the faulted area, reducing the faulted areas, and providing additional power flow paths to interrupted customers. To minimize the investment and optimize the reliability by finding the optimal locations and sizing of components are summarized as a MILP problem in [130][170][172][173][175][192]. Also, RE by finding the optimal augmentation of the distribution network in [176] is summarized as an integer linear programming (ILP) optimization problem.

Additionally, energy planning and generation re-dispatch during contingencies are formulated as a Newton-Lagrange problem in [129] for enhancing network reliability. Ref [157] develops a tri-level network expansion planning considering reliability constraints in active distribution networks. The first level is formulated as a MILP optimization problem to meet the EENS target and the third level is a nonlinear AC optimal power flow (AC-OPF) problem.

2.4 Optimization Algorithm in CM and RE

2.4.1 Optimization algorithm in CM

Genetic Algorithm (GA) [28][67] is the most commonly used method for finding solutions for single-objective or multi-objective optimization problems. In [55][193][194], GA is utilized to find optimal location of FACTS devices (TSCS, UPFC, SVC). GA is also used to find optimum DG placement and designated dispatched generation of DG units considering the system uncertainties in [195]. Furthermore, Non-dominated Sorting Genetic Algorithm II was adopted in [196] to minimize CM cost and maximize load margin.

In contrast, another frequently used method in CM problems is Particle Swarm Optimization (PSO). For instance, Ref [197] employed PSO to find the optimal allocation for FACTS devices to improve the transmission ability of lines and provide voltage support to minimize total generation cost. Moreover, PSO has been developed to find the best solution for the real-time CM problem in a specific time interval [198]. Interestingly, Ref [199] combined GA with PSO for finding the optimal location and sizing of DG on distributed systems to minimize network power loss and voltage regulation.

Besides GA and PSO, various evolutionary methods are implemented to solve optimization problems. For example, Firefly Algorithm (FA) [38] is used to minimize transmission congestion costs. By comparative analysis, the authors concluded that the performance of FA is much better than other optimization techniques, such as PSO and Artificial Bee Colony (ABC). Bacterial Foraging with the Nelder-Mead method (BF-NM) [200] is employed to determine the optimal location and size of TCSC to minimize costs of generation, emission, and TCSC. Lion Algorithm (LA) is engaged in [69] to solve the CM problem aiming at minimum rescheduling cost. A meta-heuristic technique Teaching learning-based optimization (TLBO) [70] was used to minimize rescheduling costs. Table 2.1 shows some recent research on optimization problems and algorithms to manage congestion directly or indirectly in transmission and distribution networks.

Table 2.1 Optimization algorithms utilized in CM

Reference	CM method	Optimization problem	Optimization algorithm
F. Shen et al. [104]	DR (EVs and HPs)	Minimize the energy cost for EVs and HPs without violating the line loading limit	PSO
S. T. Suganthi and D Devaraj [49]	Generation rescheduling	Minimizing the rescheduling cost	ITLBO
S. K. Behera and N. K. Mohanty [103]	Hybrid method (Generation re-scheduling and FACTS)	Minimizing the generation cost and power loss subject to congestion constraints	Improved Grey Wolf Optimization (IGWO)

H. Doagou-Mojarrad and et al. [102]	Hybrid method (Generation re-scheduling, network expansion, DR)	minimize the investment cost, demand response cost, generation cost, congestion cost, and power loss cost	NSGA-II
M. Dashtdar et al. [94]	DG	Minimize the operating and production costs and eliminate congestion by optimizing the location and size of DG	GA-Generating Scaling Factor
K. Paul et al. [39]	Generation rescheduling	Minimize congestion cost based on the actual power adjustment and bids of the generators	Modified Whale Optimization Approach (WOA)
S. T. Suganthi et al. [74]	Generation rescheduling	Minimize the congestion management cost based on the bids of generating units	ITLBO incorporates the self-motivated learning concept
S. Saravanabalaji and et al. [40]	Hybrid method (Generation re-scheduling and load curtailment)	Minimize congestion management cost considering GSF and LSF	IDE
M. UI Bashir et al. [73]	Generation rescheduling	Minimize the rescheduling cost according to the incremented and decremented price bids and active power generations	Hybrid TLBO-PSO
J. Srivastava and N. K. Yadav [72]	Generation rescheduling	Minimize the rescheduling cost and voltage violation	Hybrid LA with Moth-based Mutation
T. T. Nguyen and F. Mohammadi [59]	FACTS	Minimize the active power loss, congestion level on lines, and TCSC compensation rate	Multi-Objective GA
A. Bagheri et al. [60]	FACTS	Minimize the loading of transmission and sub-transmission lines and improve voltage profile	DIgSILENT-Based Discrete PSO
A. Vengadesan and et al. [32]	FACTS	Minimizing power violation, transmission loss, and voltage deviation	WOA

S. Sachan and M. H. Amini [201]	Allocation of EV parking lots and EV management	Minimize active and reactive power losses, line congestion	BBO
E. S. Rigas and K. S. Tsompanidis [88]	DR (EV in Mobility-on-Demand scheme)	Maximize the number of completed tasks of EV owners for CM	Equivalent Greedy Algorithm
A. Mohsenzadeh and et al. [202]	DR (EV and DR)	Minimize local consumption and power injection from EVs, and reduce power from DR	GA
S. Gope et al. [38]	Hybrid method (Generation rescheduling and storage technology)	Minimize the congestion cost of power rescheduling with incremental/detrimental price bids	FA
S. A. Hosseini and et al. [36]	Hybrid method (Generation rescheduling, DR, and load shedding)	Minimize the CM cost, including rescheduling cost, DR cost, load shedding cost, and value of loss load	MMP Approach
R. Hooshmand et al.[200]	FACTS	Minimize the cost of generation, cost of emission, and cost of TCSC	BF-NM
V. K. Prajapati and V. Mahajan [203]	Energy storage system (ESS)	Minimize the congestion and planning cost by optimal scheduling and planning of ESS	TLBO
S. Huang et al. [65]	Hybrid method (Pricing and DR)	Minimize the EV charging cost and HP energy cost within network constraints	General Algebraic Modelling System (GAMS) optimization software
H. Labrini and et al. [96]	DG	Minimize the total power loss considering operational constraints	Graph Theory

Both cost-free and non-cost-free methods are summarized as optimization problems with single or multiple objectives. Researchers have adopted different algorithms to find optimal solutions. GA and PSO are the two most popular strategies among all the algorithms implemented for searching for the optimal solution in CM. More studies still need to be done to illustrate their superior performance compared to the other methods.

2.4.2 Optimization algorithm in RE

As mentioned in Section 2.3.4, the formulation of RE problems is characterized as nonlinear optimization problems. Different heuristic algorithms are utilized to solve the nonlinear reliability-oriented optimization problems, such as GA, PSO, WOA, FA and hybrid GA-QPSO method, etc. This section summarizes the commonly used optimization algorithms to find the optimal location, sizing, operation status of components, and flexibilities in recent studies of RE in Table 2.2.

Table 2.2 Optimization algorithms in RE

Reference	RE Method	RI	Optimization algorithm	Year
A. Noori et al. [159]	DSTATCOM	ENS	WOA	2021
S. Biswal et al. [132]	DGs and Capacitors	SAIFI, AENS, ECOST	Modified Chaotic Cuckoo Search Algorithm (MCCSA)	2021
A. Alam et al. [125]	Optimal placement of Reclosers	SAIDI, SAIFI, CAIDI, ASUI, ASAI, AENS	GA	2021
V. Y. Lyubchenko and el al. [168]	Reclosers optimal allocation	SAIFI, SAIDI	GA	2021
S. Razavi et al. [182]	Reconfiguration	Network failure probability	Self-Adaptive Modified Crow Search Algorithm (SAMCSA)	2021
M. Naguib et al. [161]	Reconfiguration and DG allocation	Cost for ENS	FA	2021
F. M. Rodrigues and et al. [188]	Mobile Emergency Generator (MEG)	SAIFI, SAIDI	GA	2021
O. Kahouli et al. [183]	Configuration	ENS	GA and PSO	2021
H. Karimi et al. [174]	Cross-section Switches	SAIFI, SAIDI, CAIFI, CAIDI, EENS, AENS, etc.	GA	2021
A. Jafari et al. [191]	Optimal operation of MMGs	ENS	Wild Goats Algorithm (WGA)	2020

P. Lata and S. Vadhera [184]	Optimal placement and sizing of ESSs	Cost of energy not supplied (CENS)	TLBO, PSO, GA	2020
K. Zou et al. [162]	Reconfiguration and DG	SAIDI, SAIFI,	Tuning-parameter-free PSO	2020
A. Banerjee et al. [169]	Reclosers, Fuses, Switches	SAIFI, SAIDI	Hybrid GA-QPSO	2020
P. Srividhya et al. [181]	Reconfiguration	SAIFI, SAIDI, CAIDI, ASAI, ASUI	Binary PSO	2020
O. Sadeghian and et al. [166]	EV	LOLE, EENS	PSO	2019
A. Hariri et al.[158]	Optimal allocation of protective devices, DGs, and EV charging station	EENS	GA, PSO	2019
Y. Li et al. [204]	EV and Network Topology Optimization	LOLP, EENS	Evolution Strategy PSO (ESPSO)	2018
A. Azizivahed and et al. [186]	ESS	ENS	Hybrid Grey Wolf Optimizer-Particle Swarm Optimization (HGWO-PSO)	2018
J. R. Bezerra and et al. [171]	Optimal switch placement	ECOST	PSO	2015
A. Kavousi-Fard and et al. [190]	EV	AENS	Modified Symbiotic Organism Search (MSOS)	2015
F. J. Ruiz-Rodriguez and et al. [163]	DG	Network failure probability	Binary Shuffled Frog-Leaping Algorithm (BSFLA)	2014
S. Junlakarn and M. Ilić [187]	DGs and switches	EENS	GA	2014
A. Kavousi-Fard and T. Niknam [178]	Reconfiguration	SAIFI, SAIDI, AENS, ECOST	Clonal Selection Algorithm (CSA)	2014
I. Ziari et al. [189]	DGs and cross-connections	Demand Not Supplied (DNS)	Modified Discrete PSO	2012

This subsection lists and discusses the commonly used optimization methods in recent studies of CM and RE. It is necessary to mention that the heuristic methods listed in Table 2.1 and Table 2.2 only review the representatives of studies in CM and RE.

2.5 Summary

The growing consumption, integration of DGs, and new load (e.g., EV) have led to an increasing number of congestion and low reliability in distribution networks. Considering the rich flexibility resources and opportunities in the market environment, EVs and DGs are of great importance in CM and reliability improvement in modern distribution networks. Meanwhile, the uncertainties from renewable generation and lower accuracy in load forecast due to extensive EV integration have led to significant challenges and increased complexity for CM and RE in active distribution networks. This chapter thoroughly reviews the state-of-art studies of CM and RE from the perspectives of problem formulation and managing strategies. The objectives of different CM and RE methods can be formulated as optimization problems. GA and PSO are the two commonly used heuristic algorithms for finding the optimum solutions.

It is observed that the characterization of congestion events in active distribution networks and efficient indices to suggest the congestion levels for better management still need to be further studied. Usually, sudden equipment failure is one of the main reasons for network congestion and low reliability, and the influence of aging failure is rarely considered. For the long-term CM strategy and RE in modern distribution networks, it is important to discover the impacts of DERs and EVs on the aging process of equipment, thus furtherly suggesting their potential roles in managing aging failure and improving network performance. Moreover, considering the inherent weakness of heuristic methods, appropriate linear CM and RE models using the flexibilities in the market environment need further research.

Chapter 3 Characterization of Congestion in Distribution Networks Considering High Penetration of PV Generation and EVs[1]

Congestion management plays a key role in the safe and efficient operation of electric networks. Regarding the congestion in distribution systems, which tends to include a large number of photovoltaic (PV) systems and charging stations of electric vehicles (EVs), the identification of congestion characteristics should be taken into consideration for improved satisfaction of customers. This chapter first discusses the limitations of traditional congestion definition, then characterizes congestion and congestion management procedures in the distribution network. Besides, congestion metrics both in the short-term and long-term horizon are proposed. Simulation tests on the IEEE-33 bus distribution test system illustrate the impacts of the presence of PV generation and EV charging stations on violations of current and voltage limits that are the two main reasons for congestion. An effective control algorithm for PV units and EV charging stations can play an essential role in the mitigation of congestion.

3.1 Introduction

With the advent of distributed generation and new types of loads, such as electric vehicles (EVs), the frequency of congestion has generally increased in both transmission and distribution networks. In particular, the connection of solar

[1] This chapter is based on J. Zhao, A. Arefi, A. Borghetti, J. M. Delarestaghi and G. Shafiullah, "Characterization of Congestion in Distribution Network Considering High Penetration of PV Generation and EVs," presented at the 2019 IEEE Power & Energy Society General Meeting (PESGM), 2019, pp. 1-5.

photovoltaic (PV) units and EV charging stations has gained attention due to several reasons. Firstly, in distribution networks where wires are aging and the equipment is dated, the requirements are increasing more quickly than network upgrading. Secondly, forecasting the load share to be fed by the network and traditional generation is more difficult than in the past. Congestion management (CM) is an important guarantee for the safe, stable, and efficient operation of the whole system since congestion not only brings energy shortage which will lead to price fluctuation in the market environment, resulting in a higher possibility of equipment damage.

Traditionally, CM procedures are mainly used in transmission networks rather than in distribution networks. CM procedures in distribution networks have peculiar characteristics, due to the need to exploit the various flexibility resources provided by many participants. Therefore, addressing congestion in distribution networks, especially with a higher number of flexible participants is a very critical task. These flexibilities in the distribution network present some new challenges for CM, but also provide new opportunities for CM if managed appropriately.

CM procedures in transmission networks can be classified into technical methods and non-technical methods in [50]. Technical methods include outage of congested lines, transformer tap changers and operation of the flexible AC transmission system (FACTS) devices. Non-technical methods include two categories based on with or without consideration of the market environment. CM schemes can be classified into two broader categories including cost-free methods, where generation and distribution companies are not involved, and non-cost-free methods, where generation rescheduling and demand response are considered [7][98]. The typical cost-free methods are feeder reconfiguration, changing transformer tap, compensation equipment and FACTS devices, etc., while non-cost-free methods are generation re-dispatching and load curtailment [7]. Among those CM methods, generation re-dispatching, load shedding, market splitting, nodal pricing and DG deployment are well-known schemes in the market environment [205].

The direct implementation of these CM schemes in distribution networks is not effective. Up-to-date, limited works have been done on CM in distribution networks and most of the work mainly focuses on tackling congestion due to overcurrent. In [33] [54][206][207], CM methods have been proposed based on the control of active and reactive power flows, taking into account voltage security and voltage stability limits.

In [208], an agent-based CM algorithm combined with voltage control in distribution networks is proposed that considers both the influence of PV units and heat pumps. Although voltage stability has been taken into consideration in CM methods, most of the proposed approaches treat CM and voltage stability as two independent issues. However, in the presence of a large installation of PV units and EV charging stations, the control of PV active and reactive power outputs and demand response (DR) mechanisms play an important role in both CM procedures and voltage management [209][210].

3.2 Characterization of Congestion

Typically, congestion refers to a condition in which insufficient energy is provided by power utilities to consumers due to physical limitations of the network [211], such as the thermal limitation of conductors/cables or transformers. Insufficient infrastructure investment, ineffective resource scheduling, or equipment failure are the most common reasons for congestion [205]. Consequently, CM procedures generally indicate the schemes for alleviating congestion considering safety, reliability, and stability requirements. The basic task of a CM procedure is to provide additional power to congested areas (or customers) by utilizing new resources or to curtail part of the load while satisfying the network and load constraints. CM procedures should have the ability to guarantee the continuity of supply without a decrease in reliability and security levels, especially for important customers in congested areas, such as train stations and hospitals.

In general, if power utility fails to meet the expectations of their customers in terms of energy quantity or voltage quality, this could be considered as congestion. In particular, it is critical to consider voltage problems, since voltage violations are in general more frequent in distribution systems than in transmission networks [208], because of the higher impedance of distribution networks along with the increasing amount of distributed generation (DG) by the time. Based on the specific characteristics of congestions in distribution networks, CM methods should be able to address both voltage and overloading issues by using all the resources provided by DG control, DR mechanisms, and the presence of transformers equipped with on-load tap changers and other control devices.

A sequence of the typical objectives of CM methods in distribution networks is to:

- meet the requirements of voltage quality in terms of magnitude and balance degree.
- give priority to important customers, especially when the capacity of flexibilities is limited.
- generate optimal scheduling and network configuration in different circumstances to maximize the benefits for customers, power utility and network.
- propose backup schemes as a response to failures.

In [212], Kirby and Van Dyke suggest using some metrics for congestion events such as the values of congestion frequency and duration, energy curtailments, and congestion costs. CM procedure should include the evaluation of those metrics and take the reliability efficiency changes into account. Indeed, a congestion event should be alleviated with the minimum decrease in reliability and efficiency levels.

To address this topic for the case of CM in distribution networks, Fig. 3.1 reviews the metrics for both short-term and long-term horizons. Short-term metrics or metrics for daily operational congestion contain the congestion probability, duration, electricity price changes caused by congestion, and the congestion level. Section 3.4 will illustrate the use of congestion level and the calculation of congestion duration and frequency of that. These short-term metrics will build up long-term metrics. Long-term metrics (monthly, seasonally, or yearly calculated) refer to the total congestion frequency and duration, average congestion levels (both for current violations and voltage violations), congestion costs and the total required energy in congested areas.

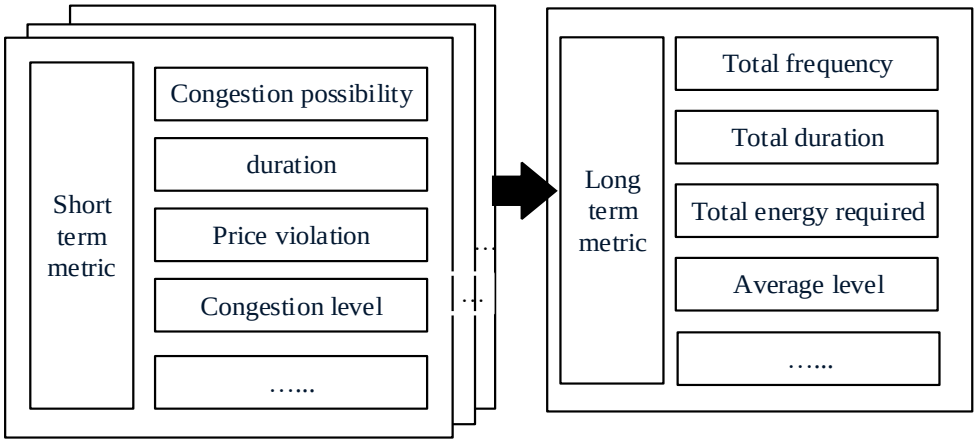

Fig. 3.1 Metrics for congestion.

3.3 Simulation Results for Identifying Characteristics of Congestion

The specific characteristics of congestion in distribution networks have been analyzed by using the IEEE-33 bus test system. Table 3.1 shows the original load level in a day without any PV, where PF represents the power factor.

Table 3.1 Scaling factor for each bus to generate the corresponding load level of that bus

Bus no.	**2**	**3**	**4**	**5**	**6**	**7**	**8**	**9**
Pmax(kW)	106.8	96.2	128.2	21.4	21.4	213.7	213.7	21.4
PF	0.89	0.94	0.87	0.62	0.77	0.92	0.92	0.77
Bus no.	**10**	**11**	**12**	**13**	**14**	**15**	**16**	**17**
Pmax(kW)	21.4	5.3	21.4	21.4	128.2	21.4	21.4	21.4
PF	0.77	0.20	0.57	0.57	0.87	0.92	0.77	0.77
Bus no.	**18**	**19**	**20**	**21**	**22**	**23**	**24**	**25**
Pmax(kW)	96.2	96.2	96.2	96.2	96.2	96.2	448.7	448.7
PF	0.94	0.94	0.94	0.94	0.94	0.91	0.93	0.93
Bus no.	**26**	**27**	**28**	**29**	**30**	**31**	**32**	**33**
Pmax(kW)	21.4	21.4	21.4	128.2	213.7	160.3	224.4	64.1
PF	0.69	0.69	0.77	0.90	0.37	0.93	0.93	0.87

Fig. 3.2 depicts aggregated load variation in terms of the ratio of hourly active power to rated active power at each bus. The adopted average EV charging profile taken from [213] is shown in Fig. 3.3. The capacity of each EV battery is assumed to be 24 kWh and the maximum production of each PV unit is 5 kW. For simplicity, all loading points (buses) are supposed to have PV generation units and EV charging stations. All the data are in per-unit (pu), and the bases for power and voltages are 1 MVA and 10 kV, respectively. Same PV capacity and EV charging stations with the same rated power. In this paper, four cases comprising the following loading condition are studied.

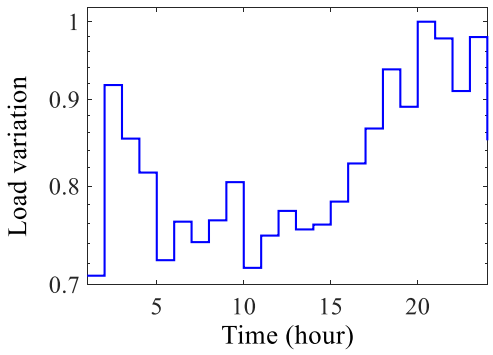

Fig. 3.2 Typical load profile of a day.

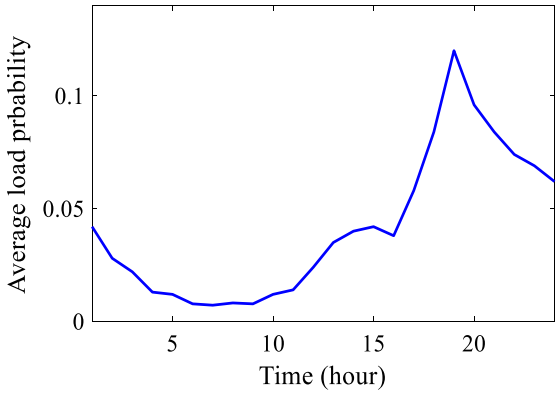

Fig. 3.3 Average electric vehicle charging profile from [213].

Fig. 3.4 shows the congested lines and nodes for the original loading condition of the test system at 16:00, in which one line is congested and four nodes are suffering from under-voltage. Congestion areas under original load conditions and considering different power injection levels from PV units are presented in Fig. 3.5 and Fig. 3.6.

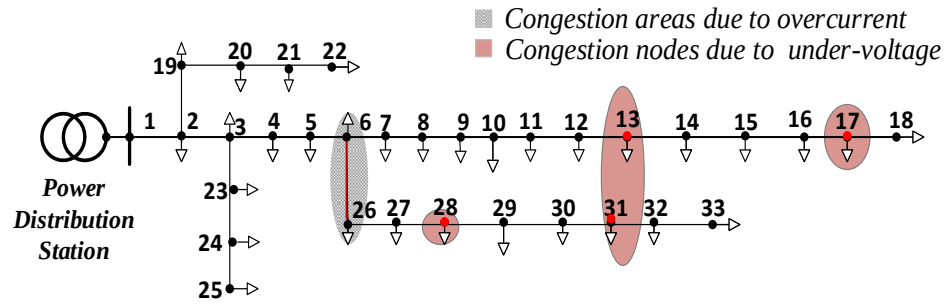

Fig. 3.4 Congested lines and nodes under original load (no PV or EV) at 16:00.

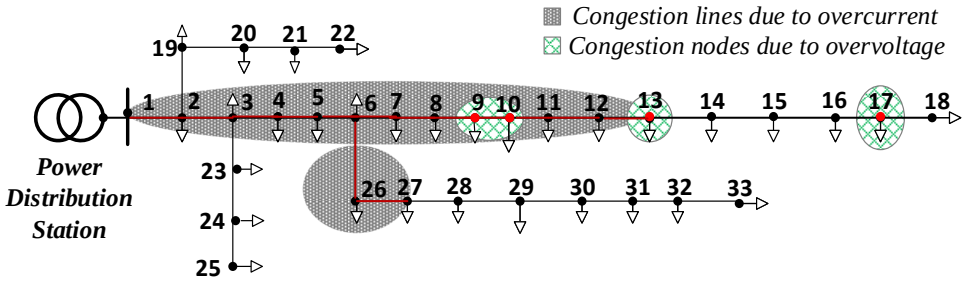

Fig. 3.5 Congested lines and nodes under original load + 50 PV units at 13:00.

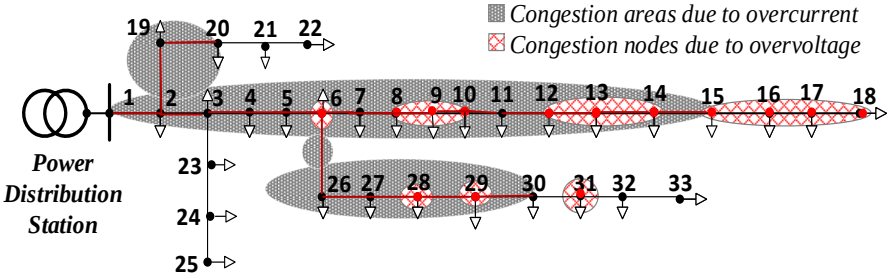

Fig. 3.6 Congested lines and nodes under original load + 100 PV units at 13:00.

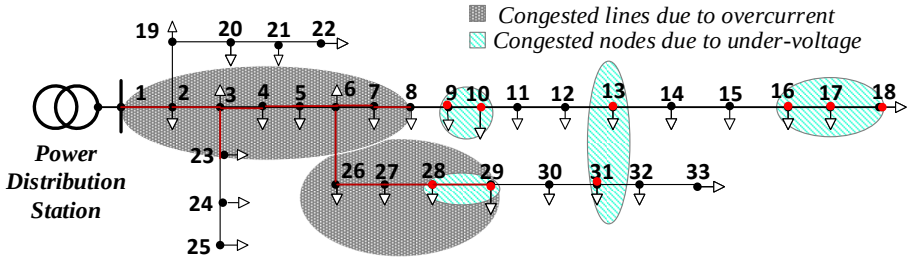

Fig. 3.7 Congested lines and nodes under original load + 50 EVs at 16:00.

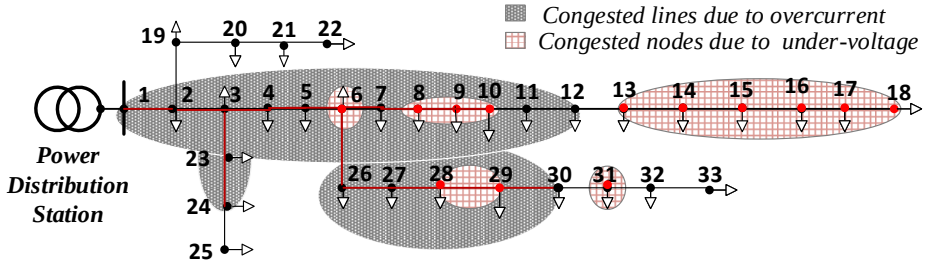

Fig. 3.8 Congested lines and nodes under original load + 100 EVs at 16:00.

Fig. 3.7 and Fig. 3.8 illustrate the congestion areas at 16:00 taking different numbers of EV charging stations into account. To sum up, in terms of congested lines, the congested areas significantly increase due to overcurrent due to the presence of PV units and EV charging stations. Similarly, also the number of nodes affected by voltage problems increases: overvoltage issues caused by PV production and under-voltage issues caused by the charging of EVs. As expected, the increase in the number of PV units and EV charging stations expands the affected lines and nodes. In this analysis, lines near the substation have a higher probability to suffer from congestion, and nodes 9, 10, 13, 17, 28, and 31 are more vulnerable to voltage problems than other nodes.

Table 3.2 and Table 3.3 show the type of congestion during a day for four cases including the case with the original load and the cases with the combination of only 50 PV units, only 50 EVs and 50 PVs+50 EVs at each bus. In this analysis, the congestions are categorized as: C1 is the congestion due to overcurrent, and C2 and C3 are used to describe the congestion due to under-voltage and overvoltage conditions, respectively; No. accounts for the total number of congested nodes or lines due to overvoltage, under-voltage and overcurrent; Ave (pu) is the average value of current violation at congested lines or voltage violations at congested nodes; Max (pu) is the maximum violation of current or voltage, which equals to:

(1) $I_{max} - I_{ref}$, I_{ref} is 4 pu for L12; 3 pu for L23; 2 pu for L34, L45 and L56; and 1 pu for the other lines, where L_{ij} represents the line that starts at i and ends at j;

(2) $U_{min} - 0.95$, when voltage is lower than 0.95 pu.

(3) $U_{max} - 1.05$, when voltage is greater than 1.05 pu.

Table 3.2 Information of congested lines under different conditions

Time	Original Load				Original Load + 50 PVs				Original Load + 50 EVs				Orig. Load + 50 PVs + 50 EVs			
	T	No.	Max (pu)	Ave (pu)	T	No.	Max (pu)	Ave (pu)	T	No.	Max (pu)	Ave (pu)	T	No.	Max (pu)	Ave (pu)
1:00	×	×	×	×	×	×	×	×	C1	11	0.809	0.364	C1	11	0.809	0.364
2:00	C1	5	0.115	0.083	C1	6	0.18	0.11	C1	13	1.129	0.447	C1	13	1.129	0.447
3:00	C1	3	0.061	0.034	C1	8	0.213	0.073	C1	11	0.701	0.288	C1	11	0.701	0.288
4:00	C1	1	0.011	0.011	C1	4	0.064	0.039	C1	8	0.282	0.121	C1	8	0.282	0.121
5:00	×	×	×	×	×	×	×	×	C1	1	0.008	0.008	C1	1	0.008	0.008
6:00	×	×	×	×	×	×	×	×	C1	1	0.003	0.003	×	×	×	×
7:00	×	×	×	×	×	×	×	×	×	×	×	×	×	×	×	×
8:00	×	×	×	×	×	×	×	×	C1	1	0.008	0.008	×	×	×	×
9:00	×	×	×	×	C1	4	0.126	0.076	C1	2	0.057	0.041	C1	3	0.051	0.036
10:00	×	×	×	×	C1	10	1.084	0.547	×	×	×	×	C1	8	0.837	0.502
11:00	×	×	×	×	C1	14	1.631	0.699	C1	1	0.034	0.034	C1	12	1.337	0.615
12:00	×	×	×	×	C1	14	1.895	0.864	C1	10	0.47	0.186	C1	12	1.358	0.628
13:00	×	×	×	×	C1	14	1.935	0.888	C1	10	0.75	0.354	C1	11	1.125	0.531
14:00	×	×	×	×	C1	14	1.667	0.722	C1	11	0.93	0.425	C1	8	0.739	0.443
15:00	×	×	×	×	C1	11	1.127	0.531	C1	12	1.084	0.469	C1	6	0.176	0.123
16:00	C1	1	0.024	0.024	C1	7	0.33	0.21	C1	12	1.107	0.477	×	×	×	×
17:00	C1	4	0.079	0.056	×	×	×	×	C1	16	1.918	0.703	×	×	×	×
18:00	C1	6	0.344	0.146	×	×	×	×	C1	19	3.084	1.067	C1	14	1.414	0.55
19:00	C1	7	0.174	0.082	C1	6	0.06	0.031	C1	20	4.385	1.495	C1	20	3.894	1.314
20:00	C1	11	0.576	0.226	C1	12	0.786	0.302	C1	19	3.844	1.348	C1	19	3.844	1.348
21:00	C1	10	0.493	0.2	C1	12	0.698	0.256	C1	19	3.248	1.127	C1	19	3.248	1.127
22:00	C1	8	0.244	0.106	C1	9	0.435	0.174	C1	18	2.633	0.927	C1	18	2.633	0.927
23:00	C1	10	0.499	0.204	C1	12	0.705	0.26	C1	18	2.722	0.956	C1	18	2.722	0.845
24:00	C1	6	0.476	0.105	C1	7	0.206	0.079	C1	15	2.002	0.794	C1	15	2.002	0.794

Table 3.3 Information of congested nodes under different conditions

Time	Original Load				Original Load + 50 PVs				Original Load + 50 EVs				Orig. Load + 50 PVs + 50 EVs			
	T	No.	Max (pu)	Ave (pu)	T	No.	Max (pu)	Ave (pu)	T	No.	Max (pu)	Ave (pu)	T	No.	Max (pu)	Ave (pu)
1:00	C2	1	-0.01	-0.01	C2	3	-0.022	-0.012	C2	8	-0.052	-0.02	C2	9	-0.052	-0.018
2:00	C2	5	-0.039	-0.018	C2	6	-0.043	-0.018	C2	8	-0.062	-0.026	C2	9	-0.062	-0.024
3:00	C2	4	-0.032	-0.017	C2	4	-0.037	-0.021	C2	7	-0.042	-0.021	C2	7	-0.042	-0.021
4:00	C2	4	-0.029	-0.014	C2	4	-0.033	-0.017	C2	5	-0.039	-0.019	C2	5	-0.039	-0.019
5:00	C2	3	-0.02	-0.01	C2	3	-0.023	-0.014	C2	4	-0.029	-0.015	C2	4	-0.029	-0.015
6:00	C2	3	-0.023	-0.014	C2	4	-0.027	-0.013	C2	4	-0.03	-0.015	C2	4	-0.029	-0.015
7:00	C2	3	-0.021	-0.012	C2	1	-0.006	-0.006	C2	4	-0.027	-0.013	C2	1	-0.085	-0.085
8:00	C2	3	-0.024	-0.014	×	×	×	×	C2	4	-0.03	-0.016	×	×	×	×
9:00	C2	4	-0.028	-0.013	×	×	×	×	C2	4	-0.034	-0.019	×	×	×	×
10:00	C2	3	-0.019	-0.01	C3	2	0.016	0.01	C2	4	-0.029	-0.014	C3	1	0.01	0.01
11:00	C2	3	-0.022	-0.013	C3	3	0.032	0.017	C2	4	-0.033	-0.018	C3	2	0.024	0.018
12:00	C2	3	-0.024	-0.015	C3	3	0.04	0.023	C2	6	-0.051	-0.019	C3	2	0.024	0.017
13:00	C2	3	-0.023	-0.013	C3	4	0.042	0.019	C2	8	-0.051	-0.019	C3	2	0.017	0.011
14:00	C2	3	-0.023	-0.014	C3	3	0.033	0.018	C2	9	-0.05	-0.02	C3	1	0.005	0.005
15:00	C2	3	-0.025	-0.016	C3	2	0.015	0.008	C2	9	-0.06	-0.023	×	×	×	×
16:00	C2	4	-0.03	-0.015	×	×	×	×	C2	9	-0.054	-0.023	×	×	×	×
17:00	C2	4	-0.034	-0.018	×	×	×	×	C2	11	-0.081	-0.032	C2	1	-0.106	-0.106
18:00	C2	5	-0.041	-0.02	C2	1	-0.005	-0.005	C2	13	-0.11	-0.045	C2	8	-0.069	-0.031
19:00	C2	4	-0.036	-0.02	C2	4	-0.031	-0.016	C2	15	-0.136	-0.054	C2	14	-0.127	-0.052
20:00	C2	7	-0.047	-0.018	C2	7	-0.052	-0.022	C2	14	-0.127	-0.052	C2	14	-0.125	-0.052
21:00	C2	7	-0.045	-0.016	C2	7	-0.05	-0.02	C2	13	-0.115	-0.047	C2	13	-0.115	-0.047
22:00	C2	4	-0.038	-0.022	C2	6	-0.043	-0.018	C2	13	-0.099	-0.038	C2	13	-0.095	-0.038
23:00	C2	7	-0.045	-0.017	C2	7	-0.043	-0.02	C2	9	-0.06	-0.023	×	×	×	×
24:00	C2	4	-0.032	-0.017	C2	4	-0.037	-0.021	C2	13	-0.102	-0.039	C2	13	-0.097	-0.039

C1: Congestion caused by overcurrent; C2: Congestion caused by under-voltage; C3: Congestion caused by overvoltage.

Table 3.2 shows the results for different congestion scenarios due to overcurrent. Congestion levels considering the congested lines and current violations are increasing to a great extent with the connection of PV units and EV charging stations. The effect due to EV charging stations is greater than that of PV units. Analogously, Table 3.3 presents the results for different congestion scenarios due to voltage violations. The power injection due to PV units can lead to a voltage increase, which, to some degree, will improve the voltage profile. Inversely, the voltage will decrease greatly due to EV charging which increases the under-voltage problems.

A more detailed comparison between the results obtained for the different operating conditions is shown in Figs. 3.9-3.12. Fig. 3.9 shows the number of congested lines in the four scenarios within a day. The figure shows that both PV production and EV charging intensify the severity of the congestion: PV production has a larger impact from 9:00 to 15:00 because the sunlight is strong at that time interval, while EV charging has more influence from 12:00 to 24:00 due to the travel habits of the people.

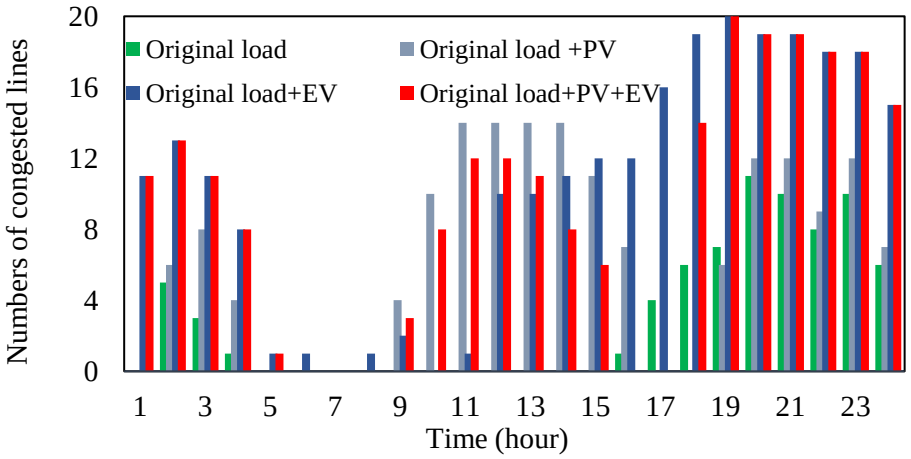

Fig. 3.9 Numbers of congested lines from 1:00 to 24:00.

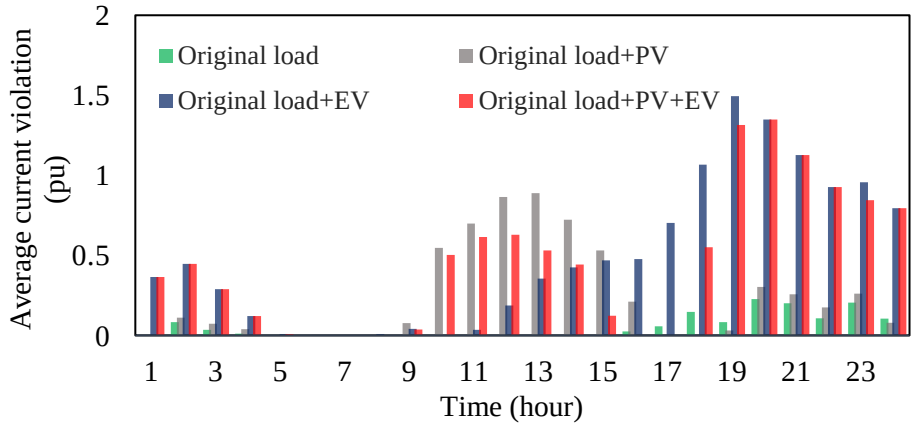

Fig. 3.10 Hourly average of current violations from 1:00 to 24:00.

The average current violation caused by PV units and EV charging stations is shown in Fig. 3.10. Fig. 3.11 shows the number of nodes affected by voltage issues. The figure shows that the number decreases when there is PV production. Fig. 3.12 shows the level of voltage deviations. Since the charging of EVs leads to under voltage conditions whilst PV production increases the voltage profile, a coordinated control action of PV units and EV charging stations may improve the operating conditions and could be the basis of a CM approach that alleviates congestions due to voltage violations.

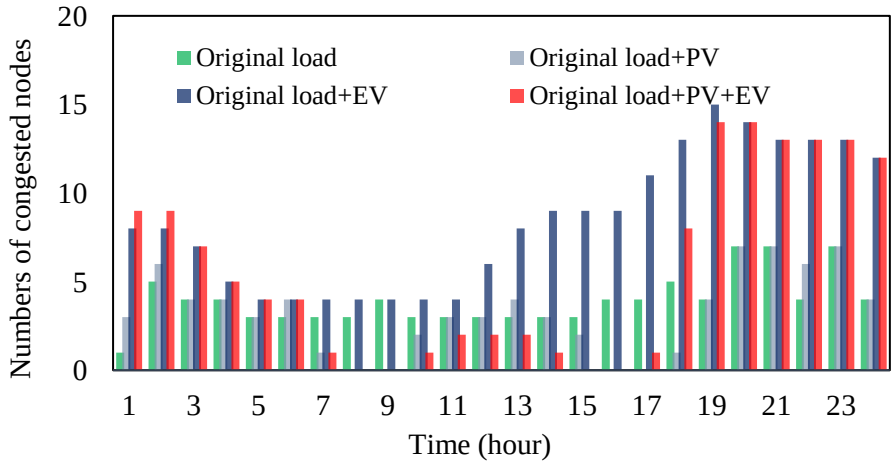

Fig. 3.11 Numbers of congested nodes from 1:00 to 24:00.

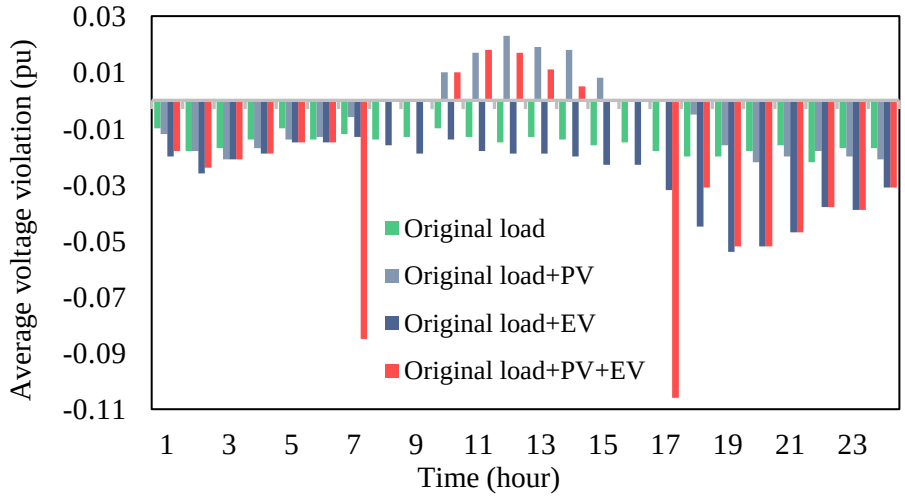

Fig. 3.12 Average voltage violation from 1:00 to 24:00.

3.4 Summary

This chapter outlines specific characteristics of congestion events and introduces the typical metrics to assess the adequacy of CM approaches in distribution networks. The simulation test illustrates the effects of different combinations of load, PV production,

and EV charging on congestion. The results suggest that congestion area increases to a great degree by also considering voltage violation in addition to overcurrent conditions. A coordinated control action of PV units and EV charging stations could effectively mitigate congestion levels due to voltage violations.

Chapter 4 Indices of Congested Areas and Contribution of Customers to Congestions in Radial Distribution Networks[2]

Congestions are becoming a significant issue with an increasing number of occurrences in distribution networks due to the growing penetration of distributed generation and the expected development of electric mobility. Fair congestion management (CM) policies and prices require proper indices of congested areas and customer contributions to congestions. This chapter presents a) spatial and temporal indices for rapidly recognizing the seriousness of congestions from the perspectives of both magnitude violation and duration, to prioritize the affected areas where CM procedures should be primarily activated, and b) indices that describe the contribution of aggregate customers to the congestions. Simulation tests on IEEE 123-bus and Australian 23-bus low voltage distribution test feeders illustrate the calculation and capabilities of the proposed indices in balanced and unbalanced systems.

4.1 Introduction

The operation and control of distribution networks are undergoing significant changes due to a large number of active customers and new types of loads, such as air conditioners, heat pumps, and electric vehicles (EVs) [19][214]. With the growing penetration of generation from renewable energy [215], e.g., photovoltaic (PV), and increasing load, there is a need for the development of improved congestion

[2] This chapter is based on J. Zhao, A. Arefi, A. Borghetti and G. Ledwich, "Indices of Congested Areas and Contributions of Customers to Congestions in Radial Distribution Networks," in Journal of Modern Power Systems and Clean Energy, vol. 10, no. 3, pp. 656-666, May 2022.

management (CM) procedures in distribution networks [216].

Traditionally, congestion happens when sufficient energy cannot be transmitted to customers due to aged equipment, ineffective network planning, faults, and the low accuracy of the load forecasts [205]. In distribution networks, congestions often occur due to the rapid increase in penetration of distributed generation (DG), sudden rise of load growth, the installation of EV charging stations without adequate planning [217][218], and the electrification of heating systems. Massive power injection from DGs will give rise to congestion with over-voltage issues, and specific control approaches are needed to relieve voltage violations [210][219]. The intermittency of DG output power and the randomness of the EV charging result in the durations and frequencies of congestion varying significantly in different periods. Flexibilities from active customers via a dedicated market [220] or active distribution management systems [221] are considered as essential components of CM procedures in distribution networks. In this context, improved monitoring of congestion is needed. Short-term (e.g., 24 hours) and long-term (e.g., a year) congestion estimation can provide useful information for adopting CM strategies in flexibility regulation, system planning, and investments.

Duration, extension, and levels of expected congestions need to be determined to assess the adequacy and performance of a CM procedure. The direction of power flow suggests the congestion scenario. If the power flows from the substation to end-users, the DG power output can help the system to relieve congestion in some areas, while if the direction is opposite, the output from DG is the main reason for the congestion. In some cases, the intervention of CM procedures is not required when there is slight congestion for a short time due to fluctuating load and growing uncertainties. Appropriate indices are needed to promptly recognize the seriousness of congestions. Moreover, they can be a reference for the design of fair CM policies [212].

Compared with the studies regarding CM in transmission networks, research on congestion prediction and management in distribution systems is still limited. So far, to the best of the authors' knowledge, overloading, and locational marginal prices (LMPs) are utilized to identify the seriousness of congestions in the wholesale power markets. In transmission networks, higher electricity prices appear in case of overloading of transmission lines [22]. The values of LMP can indicate the congestion level. The CM method proposed in [222] prevents line overloading by applying a

cost/curvature-constrained power flow optimization.

Similarly, load reduction and costs are the primary components to minimize the objective function considered in [223]. Power flow constraint violation and generation capacity limits are the two indicators considered in [29][31], whilst voltage and transient stability margins are included in [36]. For the CM based on bilateral contracts among participants combined with probabilistic optimal power flow (POPF) presented in [31], congestion distribution factors (CDF) are proposed to aggregate customers into different clusters by their impacts on constrained transmission lines. Congestion is also defined by explicitly considering the presence of renewable generation in [23].

In distribution networks, overloading and voltage violation are the two main concerns [224][225][226]. The percentage of time that power flow exceeds the constraint of a line is defined as the risk of congestion in [52]. Although related, the estimation of the congestion severity has some peculiarities with respect to probabilistic load flow analysis. While probabilistic load flow is concerned with estimating system states and short- or long-term planning [227], the assessment of congestion severity focuses on the level of thermal (current) limit violations and voltage violations that can cause equipment issues, unsatisfied load demand, and DG curtailment.

The improved implementation of all the flexibilities is required for fair and efficient CM procedures and markets intending to maximize the active participation of all the users. DG and demand response (DR) are expected to help in the CM of transmission networks, as described in [29][36][228][229][230]. Dynamic tariff subsidy and asymmetric block offer to the electricity market are proposed in [225][226] for the deployment of DR in CM. The role of storage units is also promising, as analyzed in [38][231]. For the implementation of these schemes, customer contributions to congestions and their solution need to be calculated. Moreover, improved market policy and regulation schemes can be achieved by considering long-term contribution indices.

The shortcomings in the literature mentioned above include:

a) although overloading (or power flow constraints violation), increased LMPs, and voltage violations are indicators for the occurrence of congestions in distribution systems, an additional analysis is needed for the definition of indices that can be utilized to estimate the severity of congestions both in the short-term and long-term.

b) long-term congestion estimation, network planning, and investment decisions require improved indices able to better capture the intermittent characteristic, frequency, and duration of congestions.
c) there is still a lack of aggregate indices, combining both temporal and spatial aspects, able to recognize and prioritize congested areas.

This chapter aims at presenting indices that better reveal the severity of congestion and monitor the specific contribution to congestion by the customers connected to each bus in the long-term horizon, e.g., a year. A clear indication of congestion severity and customer contributions to congested areas will help utility operators to recognize problems and activate a fair CM procedure promptly. The long-term estimation of congested areas and customer contribution can be derived from the clustering of power flow conditions. The analysis considers both the daily violations of the branch thermal limits and the voltage violations caused by excess power flow in feeders with significant impedance.

In this context, the specific contributions of this paper are:

a) definition of spatial and temporal indices to reveal the level and seriousness of congested areas in radial distribution networks in terms of both thermal limit violations and voltage violations.
b) definition of indices of the relationships between the customers at each bus and each thermal/voltage congestion considering the average contribution, to identify both customers who are the leading cause of the congestion and those whose flexibilities may perform effectively in relieving congestions.

4.2 Quantitative Indices for Congestion Level

The proposed quantitative indices for congestion level evaluation are shown in Fig. 4.1. Spatial indices indicate the violation of current and voltage limits at different branches and buses. Spatial indices for thermal violation include maximum, average and accumulative thermal violation (MCI, ACI, and ACCI). Spatial indices for voltage violations contain maximum, average, and accumulative voltage violations (MCV, ACV, and ACCV). Temporal indices reveal the seriousness of congestion in terms of frequency (CRI, CRV) and continuity (ConIci, ConIcv) for thermal violation and voltage violation, separately. Aggregate index of thermal violation (AICI) and voltage

violation (AICV) combined spatial and temporal indices are proposed to identify congested areas. For simplicity, all the described indices refer to a short-term horizon, typically a day. Long-term indices (e.g., for a month or a year) can be calculated by combining the clusters (typical days) with their probabilities.

Although we apply the proposed indices to three-phase networks in unbalanced conditions, the reference to a specific phase is avoided in the description for simplicity. If a phase conductor or the neutral of a branch is overloaded, we assume thermal congestion in that branch. The same applies to voltage violations at a bus, considering that both maximum and minimum limits cannot be violated at the same bus and period for different phase voltages. For illustrative purposes, Section 4.5 shows the evaluation of the indices for each phase of a low-voltage network (Case 2).

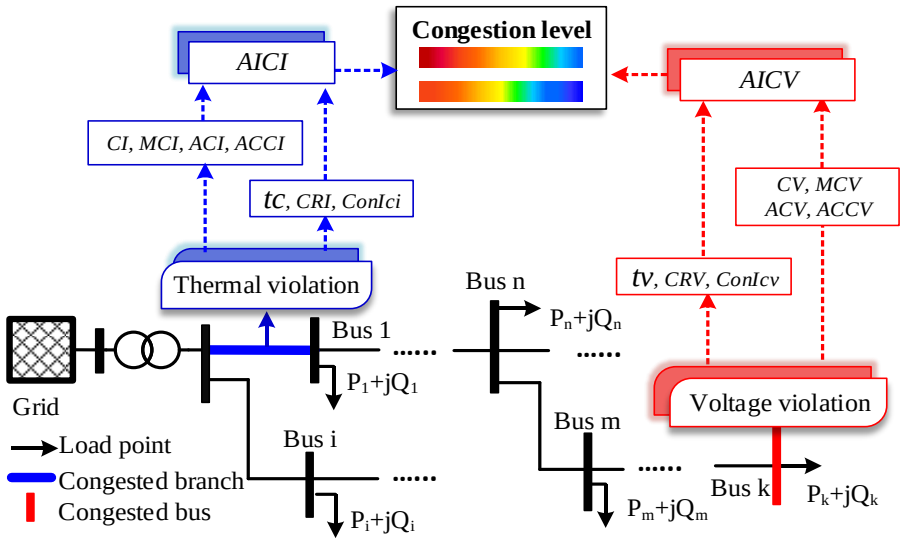

Fig. 4.1 Quantitative indices for the evaluation of congestion levels.

4.2.1 Spatial Indices

Typical indices able to quantify spatial congestion levels are the maximum, average, and cumulative violation values both for branch currents and bus voltages in a specific period. For a distribution network with N_{br} branches and N_{nd} buses, we define $\boldsymbol{B}$ as the $(N_{br} \times t_r)$ matrix of branch current rms values and $\boldsymbol{V}$ as the $(N_{nd} \times t_r)$ matrix of bus voltage rms values at each interval Δt ($\sum \Delta t = t_r$ where t_r is the time horizon). For any branch i and bus j, the duration of the congestion in the considered time horizon is indicated by $\boldsymbol{tc}(i)$ and $\boldsymbol{tv}(j)$. Spatial indexes are:

- $\boldsymbol{CI}$ is the ($N_{br} \times t_r$) matrix of thermal violations;
- $\boldsymbol{CV}$ is the ($N_{nd} \times t_r$) matrix of voltage violations;
- $\boldsymbol{MCI}$, $\boldsymbol{ACI}$, and $\boldsymbol{ACCI}$ are the maximum, average, and cumulative thermal violation vectors ($N_{br} \times 1$) in all the branches;
- $\boldsymbol{MCV}$, $\boldsymbol{ACV}$, and $\boldsymbol{ACCV}$ are the maximum, average, and cumulative voltage violation vectors ($N_{nd} \times 1$) at all the buses;
- $\boldsymbol{I_r}$ is the ($N_{br} \times 1$) vector of current rated values for all the branches;
- V_N is the rated voltage in per unit (1 pu);
- V_{max} and V_{min} are voltage upper and lower constraints, $V_{max} = 1.05$ pu, $V_{min} = 0.95$ pu;
- $\boldsymbol{tc}$ is the ($N_{br} \times 1$) vector of total thermal congestion durations on each branch;
- $\boldsymbol{tv}$ is the ($N_{nd} \times 1$) vector of the entire voltage congestion duration at each bus;
- Δt is interval time, 1 hour for Case 1 and 0.5 hour for Case 2.

The relevant definitions at *t*-th interval are:

$$\boldsymbol{CI}(i,t) = \begin{cases} \dfrac{\boldsymbol{B}(i,t) - \boldsymbol{I_r}(i)}{\boldsymbol{I_r}(i)} & \boldsymbol{B}(i,t) > \boldsymbol{I_r}(i) \\ 0 & \boldsymbol{B}(i,t) \leq \boldsymbol{I_r}(i) \end{cases} \tag{4.1}$$

$$\boldsymbol{CV}(j,t) = \begin{cases} \dfrac{\boldsymbol{V}(j,t) - V_{max}}{V_N} & \boldsymbol{V}(j,t) > V_{max} \\ \left|\dfrac{\boldsymbol{V}(j,t) - V_{min}}{V_N}\right| & \boldsymbol{V}(j,t) < V_{min} \\ 0 & Otherwise \end{cases} \tag{4.2}$$

$$\boldsymbol{MCI}(i) = max\left\{\boldsymbol{CI}_{\boldsymbol{row}^{(i)}}\right\} \tag{4.3}$$

$$\boldsymbol{ACI}(i) = \frac{\sum_{t=1}^{t_r} \boldsymbol{CI}(i,t)}{\boldsymbol{tc}(i)} \tag{4.4}$$

$$\boldsymbol{ACCI}(i) = \sum_{t=1}^{t_r} \boldsymbol{CI}(i,t) \cdot \Delta t \tag{4.5}$$

$\boldsymbol{MCV}$, $\boldsymbol{ACV}$ and $\boldsymbol{ACCV}$ are calculated with expressions analogous to (4.3)-(4.5). For example, in the simulation on the IEEE 123-bus system shown in Section 4.3, the values of ACCI, ACI, and MCI of branch 1 are 4.487, 0.299, and 0.65, the cumulative overloading is 4.487 p.u., whilst the average and the maximum overloading is 0.299 and 0.65 pu.

4.2.2 Temporal Indices

Temporal indices are proposed to quantify the congestion duration, frequency, and continuity. CRI and CRV are temporal indices that show the congestion duration in a specific time horizon:

- ***CRI*** is the ($N_{br} \times 1$) vector of the ratio between the thermal violation durations in the branches and the time horizon.
- ***CRV*** is the ($N_{nd} \times 1$) vector of the ratio between voltage violation durations at the buses and the time horizon.

The elements of these vectors are defined as

$$\boldsymbol{CRI}(i) = \frac{\boldsymbol{tc}(i)}{t_r} \times 100 \tag{4.6}$$

$$\boldsymbol{CRV}(j) = \frac{\boldsymbol{tv}(j)}{t_r} \times 100 \tag{4.7}$$

From the perspective of the CM procedure application, congestions that last longer than a predefined time interval should have priority. The following indices are specifically defined to reveal the degree of continuity of the congestion:

- ***ConIci***: the ($N_{br} \times 1$) vector of thermal violation continuity indices;
- ***ConIcv***: the ($N_{nd} \times 1$) vector of voltage violation continuity indices.

The values of these indices are obtained as described below. We define $\boldsymbol{S_{ci}}$ as the ($N_{br} \times t_r$) matrix in which $\boldsymbol{S_{ci}}(i,t) = sgn(\boldsymbol{CI}(i,t))$ (sgn is the sign function) and $\boldsymbol{S'_{ci}}$ as the shifted matrix of $\boldsymbol{S_{ci}}$ by l time intervals, i.e.

$$\boldsymbol{S'_{ci}}(i,t) = \begin{cases} \boldsymbol{S_{ci}}(i,t-l) & l < t \leq t_r \\ 0 & 0 \leq t \leq l \end{cases} \tag{4.8}$$

Then, $\boldsymbol{ConIci}$ is given by

$$\boldsymbol{ConIci}(i) = \frac{\boldsymbol{S_{ci,row^{(i)}}}(\boldsymbol{S'_{ci,row^{(i)}}})^T}{\boldsymbol{tc}(i)} \times 100 \tag{4.9}$$

where T is the transpose operation. The definition depends on the predefined value of l (equal to 1 for the simulations in Section IV). $\boldsymbol{S_{ci,row^{(i)}}}$ is the *i*-th row of $\boldsymbol{S_{ci}}$. ConIcv is defined analogously and includes the definition of $\boldsymbol{S_{cv}}$ as the ($N_{nd} \times t_r$) matrix with $\boldsymbol{S_{cv}}(j,t) = sgn(\boldsymbol{CV}(j,t))$, and of $\boldsymbol{S'_{cv}}$ as the shifted matrix of $\boldsymbol{S_{cv}}$ by l time

intervals. For example, in Case 1 of Section IV, the *CRI* and *ConIci* of branch 1 are 62.5% and 73.33%, representing the overloading frequency per day and the continuity of overloading periods, respectively.

4.2.3 Accumulative Overload Index

The accumulative indices of congestion level (AICI, AICV) integrate the spatial and temporal indices in terms of thermal violation and voltage violation, respectively, for short-term and long-term congestion estimation. These indices provide a clear vision of congestion scenarios and congested levels. The definitions are

$$\boldsymbol{AICI = ACI \circ tc \circ ConIci} \tag{4.10}$$

$$\boldsymbol{AICV = ACV \circ tv \circ ConIcv} \tag{4.11}$$

where $\circ$ indicates the element-by-element multiplication. For instance, in the simulations relevant to the Australian 23-bus system shown in Section IV, the AICI and AICI of branch 10 and bus 23 at phase C are 2.4497 pu and 0.2024 pu.

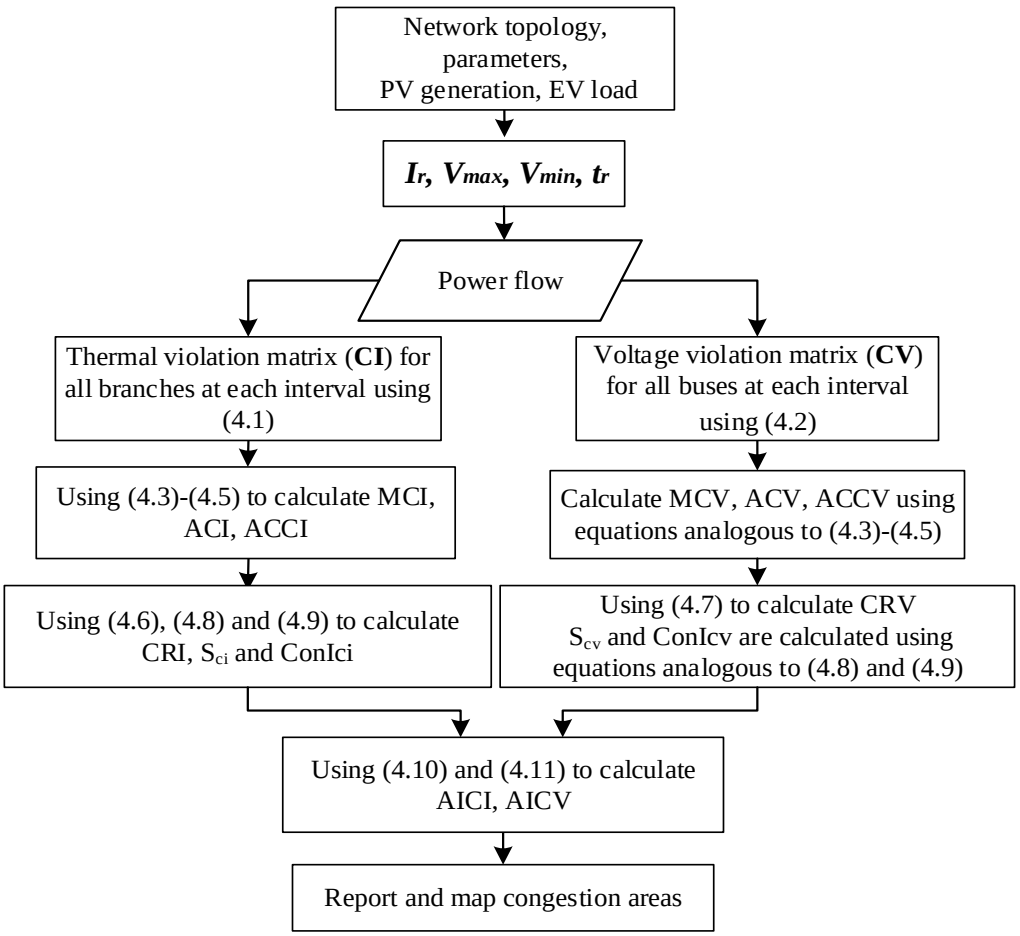

Fig. 4.2 Spatial and temporal indices calculation procedure.

The flow chart of the calculation procedure of the proposed spatial and temporal indices is shown in Fig. 4.2. At first, the data of a typical day is selected. Then, the power flow calculation is performed. If there are congestions, all the indices relevant to both thermal congestion and voltage congestion are calculated according to the equations shown in the previous subsections.

4.3 Indices of the Relationship Between Users and Congestions

In the case of thermal violations, in a radial distribution network, all the downstream nodes of one congested branch/bus would contribute to the congestion of this branch/bus. In the case of voltage violations, also the flexibility of customers connected upstream with respect to the affected area can be used by the CM procedure as they may be more effective than those in the other nodes. After identifying the congestion level, the assessment of the specific relationship between each customer and congestion has significant importance in building a fairer market by allocating the duty for congestion alleviation. In this framework, specific indices are proposed to identify these relationships that can be exploited by electricity policy for rewarding proactive consumers able to use local generation and DR mechanisms [93][97] [98][211].

The proposed customer contribution indices include maximum, average and standard deviation of contributions to thermal violation (max_{ci}, ave_{ci}, and Std_{ci}) and voltage violation (max_{cv}, ave_{cv}, and Std_{cv}), respectively. The aggregate contribution index (AGCI) is also proposed to present the aggregate contribution from one customer. The indices are illustrated in Fig. 4.3 and described in the following three subsections: subsection 4.3.1 is devoted to thermal violations, 4.3.2 to voltage violations, and 4.3.3 to the aggregate contribution.

Customers are aggregated at each bus due to two reasons. Firstly, in nodal price regulation, the knowledge of the aggregate contribution is more useful than the specific contribution from a single customer connected to the same bus. Secondly, the contribution from an individual customer can be calculated by multiplying the proportion of a single customer by the total load. The load from a single customer is obtained by an appropriate metering infrastructure.

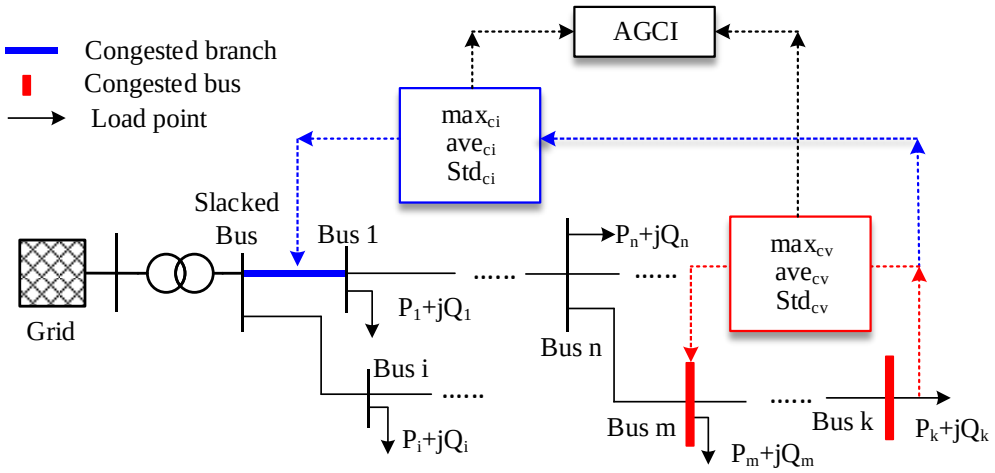

Fig. 4.3 Overview of the customer contribution indices.

4.3.1 Customer Contribution to Thermal Violation

To express the influence of bus currents on branch currents and voltage drops, the well-known matrices in the direct power flow approach: bus-injection to branch-current (**BIBC**) matrix and branch-current to bus-voltage (**BCBV**) matrix [232] are used.

We define the following spatial and temporal indices:

- $\boldsymbol{CTV_k}$ is the $(N_{br} \times t_r)$ matrix of the contribution of the customer at bus k to the thermal violation during t_r
- $\boldsymbol{M_{ci}}$ is a $(N_{nd} \times t_r)$ matrix of the number of congested branches influenced by the customers at each bus during t_r
- $\boldsymbol{t_{ci}}$ is the $(N_{nd} \times N_{br})$ matrix of the duration (in hours) of congestion in each branch due to the customers connected to each bus
- $\boldsymbol{max_{ci}}$, $\boldsymbol{ave_{ci}}$, and $\boldsymbol{Sd_{ci}}$ are the $(N_{nd} \times 1)$ vectors of maximum, average, and standard deviation values of the contributions from the aggregate customer at each bus to thermal violations.

Consider $\boldsymbol{I}$ as the $(N_{nd} \times t_r)$) matrix of the currents injected in the buses and $\boldsymbol{CTV'_k}$ as the $(N_{br} \times t_r)$ matrix of the ratios between the current in branch i due to the current injected at bus k and the total current in the same branch, i.e.

$$\boldsymbol{CTV'_k}(i,t) = \frac{\boldsymbol{BIBC}(i,k) \cdot \boldsymbol{I}(k,t)}{\boldsymbol{B}(i,t)} \tag{4.12}$$

$$\boldsymbol{CTV_k}(i,t) = \begin{cases} \boldsymbol{CTV'_k}(i,t)\ \dfrac{\boldsymbol{B}(i,t) - \boldsymbol{I_r}(i)}{\boldsymbol{I_r}(i)} & \boldsymbol{B}(i,t) > \boldsymbol{I_r}(i) \\ 0 & othewise \end{cases} \tag{4.13}$$

One aggregate customer may contribute to several congested branches. Also, the contribution from that customer varies according to the fluctuation of thermal violations. Therefore, the variation of contributions needs to be considered in evaluating the contribution in the short-term and long-term time horizon. We consider the $\boldsymbol{max_{ci}}$ and $\boldsymbol{ave_{ci}}$ are the mean values of maximum and average contributions to all the congested branches throughout the thermal congested periods.

For instance, to calculate $\boldsymbol{max_{ci}}$ from the aggregate customer at bus *k*, the maximum contributions to all congested branches contributed from this aggregate customer are calculated separately at each interval firstly. Then, add up all the maximum contributions and divide by the maximum congestion duration. The elements of $\boldsymbol{max_{ci}}$, $\boldsymbol{ave_{ci}}$, and $\boldsymbol{Std_{ci}}$ are calculated as

$$\boldsymbol{max_{ci}}(k) = \sum_{t=1}^{t_r} max\{\boldsymbol{CTV_{k,column^{(t)}}}\} / max\{\boldsymbol{t_{ci,row^{(k)}}}\} \tag{4.14}$$

$$\boldsymbol{ave_{ci}}(k) = \sum_{t=1}^{t_r} \frac{\sum \boldsymbol{CTV_k}(i,t)}{\boldsymbol{M_{ci}}(k,t)} / max\{\boldsymbol{t_{ci,row^{(k)}}}\} \tag{4.15}$$

$$\boldsymbol{Std_{ci}}(k) = \sum_{t=1}^{t_r} \frac{\sqrt{\sum_i (\boldsymbol{CTV_k}(i,t) - \overline{\boldsymbol{CTV_{k,row^{(i)}}}})^2}}{\boldsymbol{M_{ci}}(k,t)} \Big/ \boldsymbol{t_{ci,row^{(k)}}} \tag{4.16}$$

where $\overline{\boldsymbol{CTV_{k,row^{(i)}}}}$ is the mean of the elements of row *i* of the matrix $\boldsymbol{CTV_k}$. For example, in Case 1 of the simulations in Section V, the maximum and average contribution from customers on bus 48 with configuration 1 to overloading are 0.0495 pu and 0.0431pu, respectively.

4.3.2 Customer Contribution to Voltage Violation

Analogously to the relationship between customers and the thermal violations in the branches, we define the following indices for the contributions to the bus voltage violations:

- $\boldsymbol{CVV_k}$ is the ($N_{nd} \times t_r$) matrix of the contribution of the customer at bus *k* to the voltage violation during t_r
- $\boldsymbol{M_{cv}}$ is a ($N_{nd} \times t_r$) matrix of the number of congested buses caused by each bus current during t_r
- $\boldsymbol{t_{cv}}$ is the ($N_{nd} \times N_{br}$) matrix of the duration (in hours) of congestion at each bus caused by each bus current
- $\boldsymbol{max_{cv}}$, $\boldsymbol{ave_{cv}}$, and $\boldsymbol{Std_{cv}}$ are the ($N_{nd} \times 1$) vectors of maximum, average, and standard deviation values of the contributions from the aggregate customer at each bus to voltage violations.

The definition of $\boldsymbol{max_{cv}}$, $\boldsymbol{ave_{cv}}$, and $\boldsymbol{Std_{cv}}$ are analogous to (4.14)-(4.16). For the calculation of $\boldsymbol{CVV_k}$, we define at first $\boldsymbol{CVV'_k}$ as the ($N_{nd} \times t_r$)) matrix of the ratios between the voltage drop due to the current at bus *k* and the total voltage drop in the same bus, i.e.

$$\boldsymbol{CVV'_k}(j,t) = \frac{\boldsymbol{DLF}(j,k) \cdot \boldsymbol{I}(k,t)}{\Delta \boldsymbol{V}(j,t)} \tag{4.17}$$

where matrix ***DLF*** is equal to ***BCBV*** · ***BIBC***. Then,

$$\boldsymbol{CVV_k}(j,t) = \begin{cases} \boldsymbol{CVV'_k}(j,t) \cdot [\boldsymbol{V}(j,t) - V_{max}/V_N] & if\ \boldsymbol{V}(j,t) > V_{max} \\ \boldsymbol{CVV'_k}(j,t) \cdot |\boldsymbol{V}(j,t) - V_{min}/V_N| & if\ \boldsymbol{V}(j,t) < V_{min} \\ 0 & Otherwise \end{cases} \tag{4.18}$$

4.3.3 Aggregate Contribution Index

AGCI shows the contribution of the customer at each bus to the congested areas, considering both thermal and voltage violations. For its calculation, at first, the total contribution of the injected current at bus *k* to the congested branches and buses is evaluated for each time slot. Then, the two contributions are weighted by using the coefficients $\boldsymbol{C_1}$ and $\boldsymbol{C_2}$. Finally, $\boldsymbol{AGCI}(k)$ is calculated as the contribution over the total duration of congestions:

$$\boldsymbol{AGCI}(k) = \frac{\sum_{t=1}^{t_r} [\boldsymbol{C_1}(t) \sum \boldsymbol{CTV_k}(i,t) + \boldsymbol{C_2}(t) \sum \boldsymbol{CVV_k}(i,t)]}{\boldsymbol{N}(k)} \tag{4.19}$$

where $\boldsymbol{C_1}$ and $\boldsymbol{C_2}$ are the vector of coefficients that allow for weighting the contributions to thermal congestion and voltage congestion, respectively, which can

be decided by the customer damage function (CDF) or value of customer reliability (VCR). Since CDF or VCR is not in the scope of this chapter, $\boldsymbol{C_1}$ and $\boldsymbol{C_2}$ are considered equal to 0.5. $\boldsymbol{N}(k)$ is the total duration of congestions due to injected current at bus k, i.e., $\boldsymbol{N}(k) = max\{\boldsymbol{t_{ci,row^{(k)}}}, \boldsymbol{t_{cv,row^{(k)}}}\}$.

4.4 Illustrative Results of the Proposed Indices

Two test cases are considered: Case 1 uses the IEEE 123-bus test system [233] considering two different configurations in this paper. In Case 1 we assume a 100% penetration of EV and 40% penetration of PV generation (i.e., the ratio between the total EV or PV capacity and the peak load). Case 2 uses Australian 23-bus low voltage (LV) distribution network [234] considering 30% EV penetration. Regarding Case 1, Fig. 4.4 shows the spot load active power (P) and reactive power (Q) at each bus. The load at each interval is obtained by combining rated power and the daily load demand profile (per unit) from [231]. For simplicity, each node has the same daily profile. Analogously, Fig. 4.5 shows the spot power request at each phase of each bus for Case 2, considering the presence of PV generation. We have assumed the interval time Δt is 1 hour for Case 1 and Δt is 0.5 hour for Case 2.

In both cases, the load demand of EV charging has been obtained by using the profiles of weighted arrival time probability distribution from [235] and state-of-charge (SoC) difference from [236] due to the charging process. Although it is an effective method of relieving congestions, smart charging is not considered in this chapter.

We assume a constant voltage equal to the rated value at the MV side of the substation transformer due to the action of its automatic voltage regulator. The I_r for branch 1 (between nodes of 149 and 1), 4, 8, 11, 14, 37, 42, 44, 46, 49-54, 56, 59, 115 (between nodes 18 and 35), 117 (between nodes 13 and 52), and 119 (between nodes 54 and 94) is 200A; for branch 73, 78, 87, 89, 91, 93, 94, 102, 106, 109, 119 (between nodes 97 and197), 121 (between nodes 151 and 300) is 150A; and for the rest of branches is 100 A in Case 1. The I_r of branches 7, 9, 10, 15, 16, and 17 is 200 A, and 100 A for the rest of the branches in Case 2. Also, each branch is named by the number of its receiving node in Case 2.

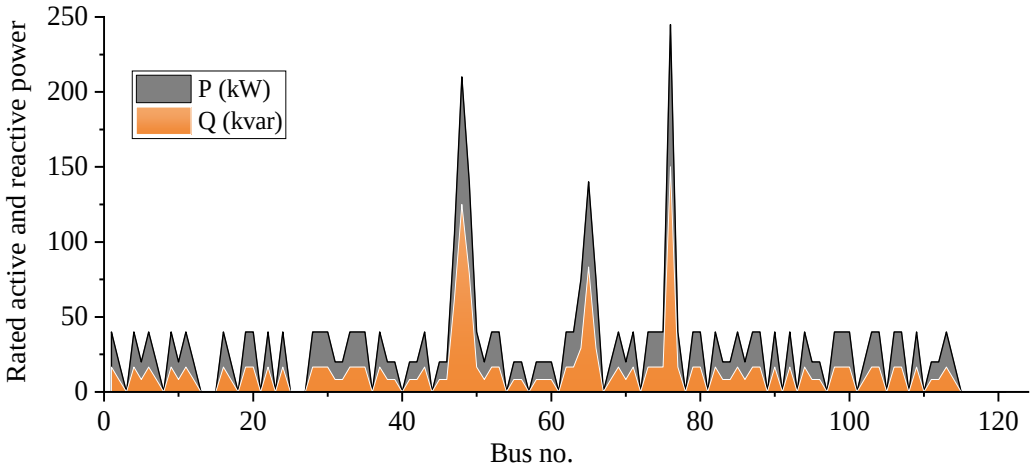

Fig. 4.4 Spot load at each bus of Case 1.

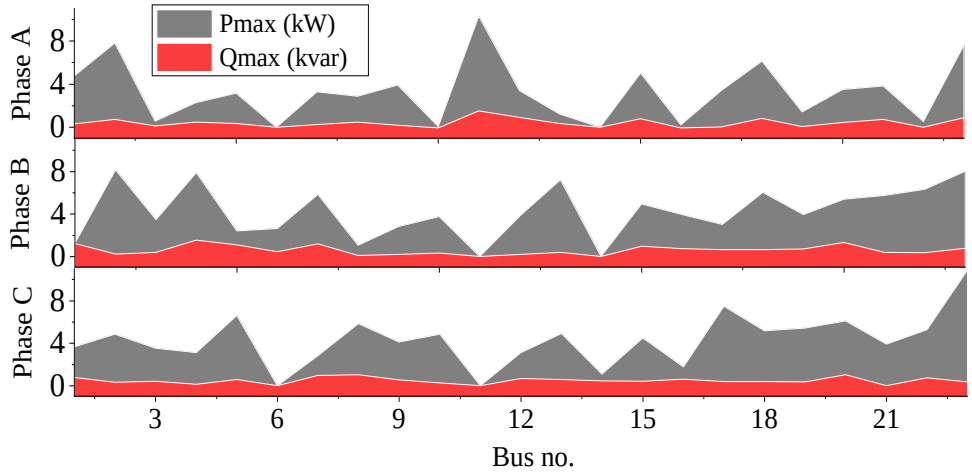

Fig. 4.5 Maximum active and reactive power of Case 2.

4.4.1 Case 1: IEEE 123-Bus Test Network

As mentioned, two different configurations of the IEEE 123-bus test distribution feeder are considered. In configuration 1, switches 1, 2, 3, 6, and 7 are closed, while switches 4 and 5 are open, as shown in Fig.4.10. The voltage regulator between bus 160 and bus 67 is operating within a 10% maximum range. In configuration 2, switches 1, 2, 3, 4, and 5 are closed, and switches 6 and 7 are open. The voltage regulator between bus 25 and bus 26 is in operation.

Figures 4.6 and 4.7 show the simulation results of the proposed spatial and temporal indices relevant to configuration 1. Branches 1, 4, 8, 11, 53, and 116 are congested due to thermal violations. Among those congested branches, branch 1 experienced the most

severe thermal violation. The values of ACCI, ACI, and MCI of branch 1 are 4.487, 0.299, and 0.65, respectively. Concerning congestion duration, 62.5% of a day is congested with the continuity index equal to 73%. Buses from 44 to 51 are congested due to voltage violations for one hour, with similar ACCV, ACV, and MCV, which are around 0.001-0.004.

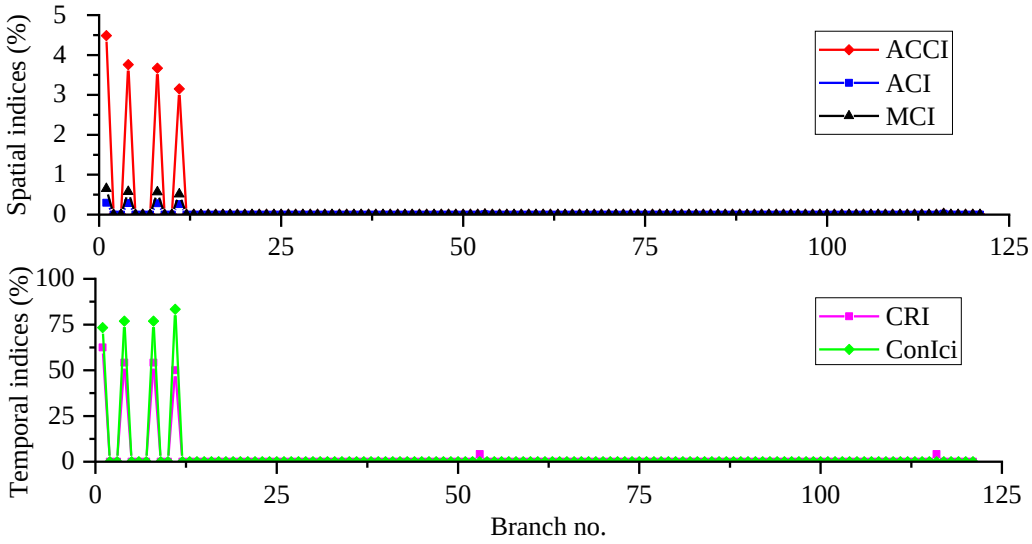

Fig. 4.6 Spatial and temporal indices of congested branches for configuration 1.

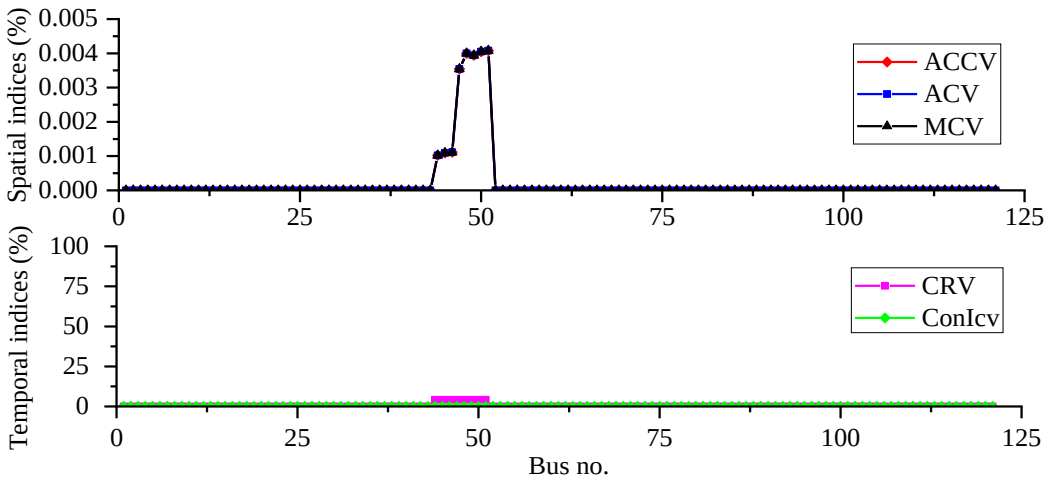

Fig. 4.7 Spatial and temporal indices of congested buses for configuration 1.

Figures 4.8 and 4.9 depict the simulation results of spatial and temporal indices relevant to configuration 2. As in the first configuration, branches 1, 4, 8, 11, 38, 95, 96, and 119 are suffering from thermal violation, but a larger number of buses are congested. Moreover, the congestion levels are higher than in configuration 1, from 0.0013 pu to 0.034 pu.

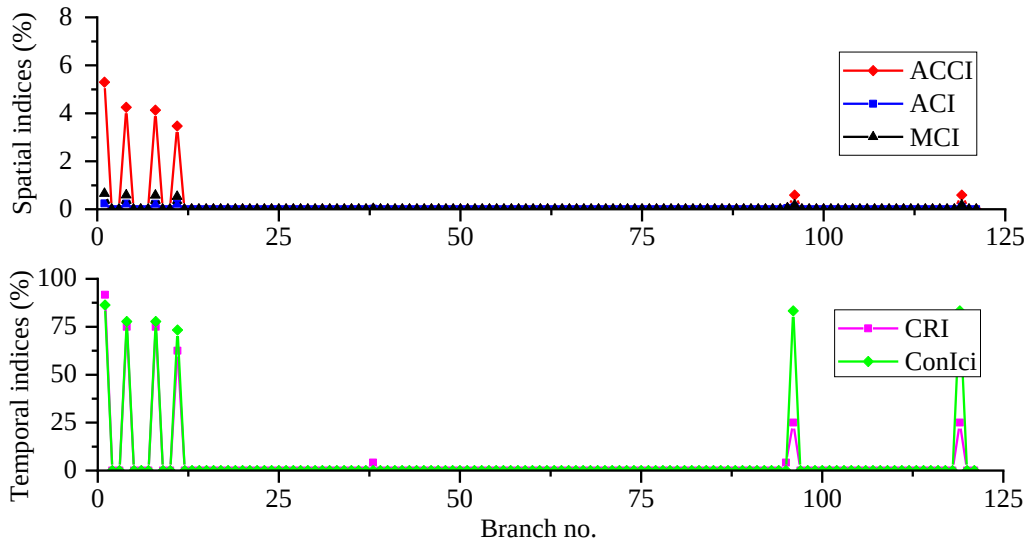

Fig. 4.8 Spatial and temporal indices of congested branches for configuration 2.

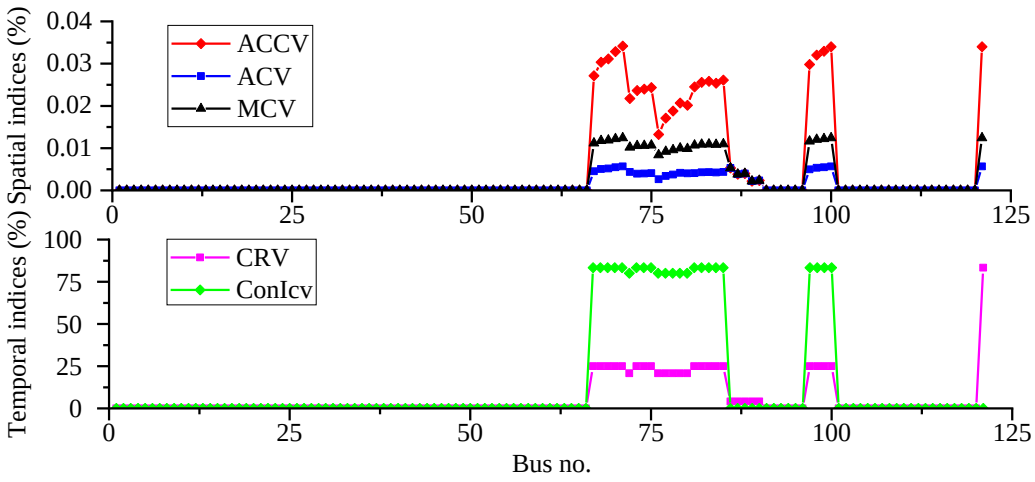

Fig. 4.9 Spatial and temporal indices of congested buses for configuration 2.

Fig. 4.10 shows the congestion map based on AICI and AICV values of configurations 1 and 2. Compared with configuration 1, the thermal congestion level of the second configuration is slightly lower with more congested branches. However, the increased number of congested buses shows that the chance of configuration substantially impacts voltage values in this case. It is worth noting that the congested buses of configuration 1 experience voltage violations for 1 hour. According to the definition (l = 1 hour for Case 1), AICV values of congested buses in configure 1 equal to 0 imply that the voltage issue can be ignored in this scenario. As for configuration 2, even though the AICV values of buses 67-85 and 97-100 are not as high as AICI, voltage violation cannot be neglected by power utilities. Furthermore, priority in the

application of the CM procedure should be considered according to the VCR.

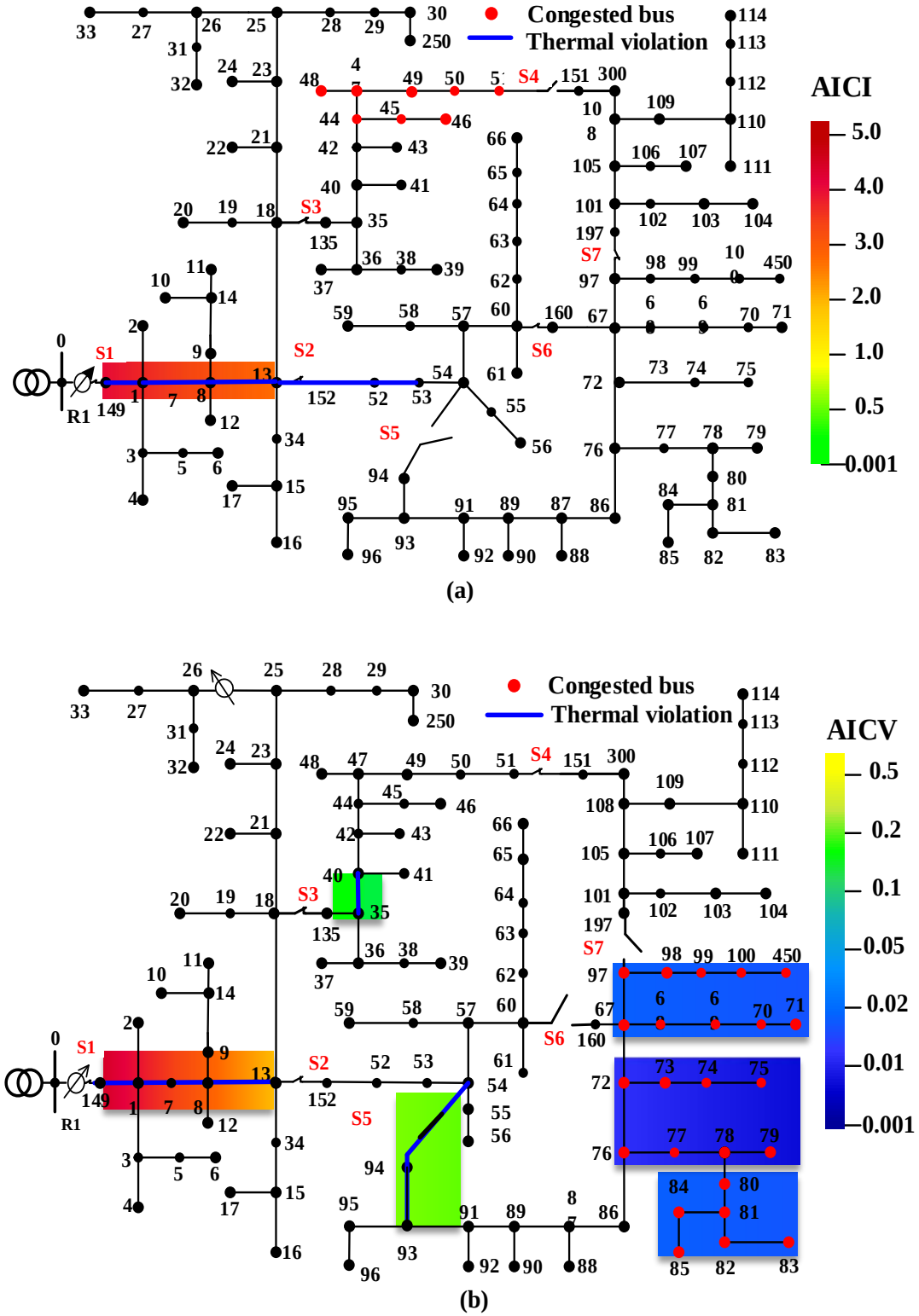

Fig. 4.10 Congestion map based on AICI and AICV (pu): (a) is the AICI of configuration 1; (b) is AICI and AICV of configuration 2.

4.4.2 Case 2: Australian 23-Bus LV Distribution Network

As mentioned, the Australian 23-bus LV distribution network, shown in Fig. 4.13, is characterized by unbalanced loads. Fig. 4.13 also shows the location of the PV installations connected to the different phases. The total PV installation is 30% of the MV/LV transformer capacity.

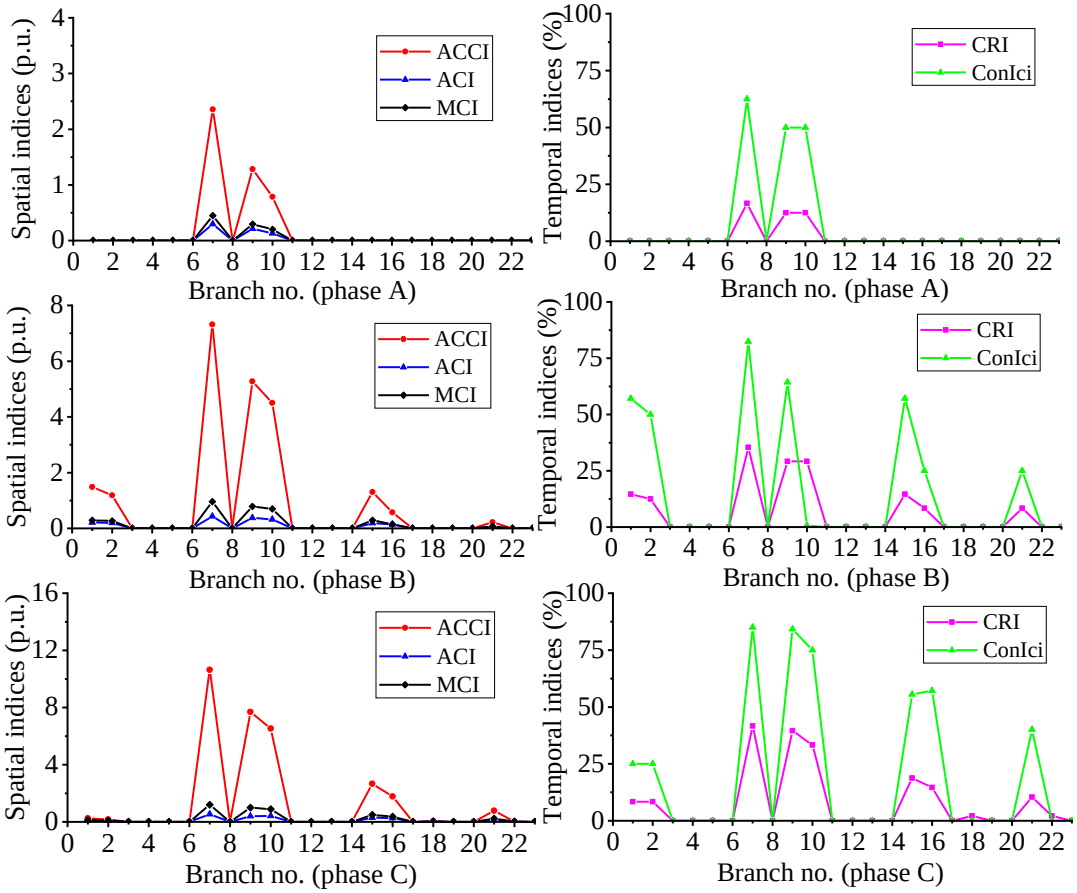

Fig. 4.11 Spatial and temporal indices of congested branches at each phase of Case 2.

According to Fig. 4.11, branches 7, 9 and 10 at phase A are suffering from thermal violations. Branches 1, 2, 7, 9, 10, 15, 16, and 21 at phases B and C experience thermal violations. The maximum ACI values of congested branches at phases A, B, and C are 0.29 p.u., 0.43 p.u., and 0.53 p.u., respectively. Branches 7, 9, and 10 are experiencing the most severe thermal violation since each phase is congested. Phases B and C suffer longer congestion, over 30% of the time horizon. In summary, phase C experiences the severest thermal violation compared with the other two phases. Also, no voltage congestion occurs in phase A.

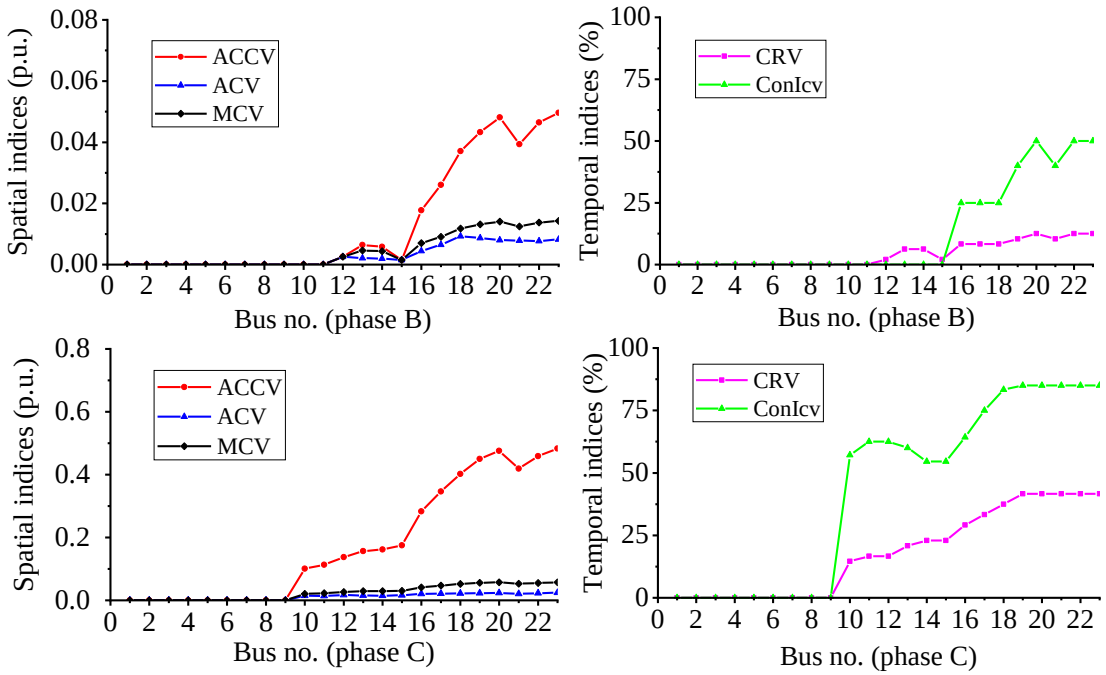

Fig. 4.12 Spatial and temporal indices of congested buses at each phase of Case 2.

Fig. 4.12 illustrates the voltage congestions in phases B and C. 41.67% of the time horizon at phase C and 12.5% of the time horizon at phase B are suffering from voltage violations. The maximum continuity of voltage congestion at phases B and C are 20% and 83.33%, separately. More nodes with higher voltage violations encounter voltage violations at phase C. Overall, phase C is more vulnerable than the other two phases in terms of thermal violation and voltage violation.

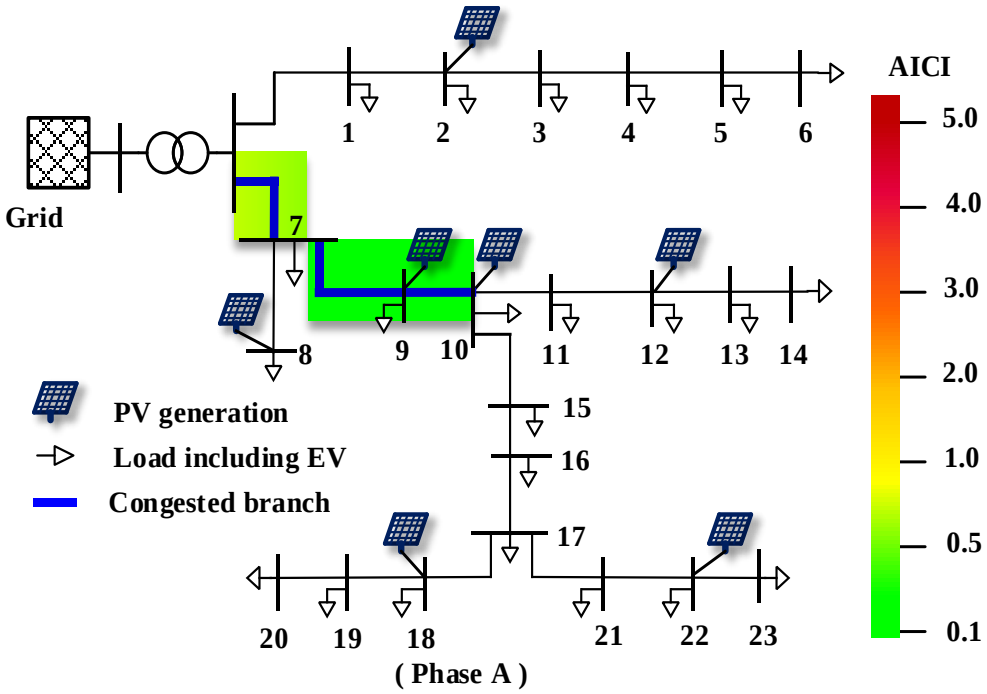

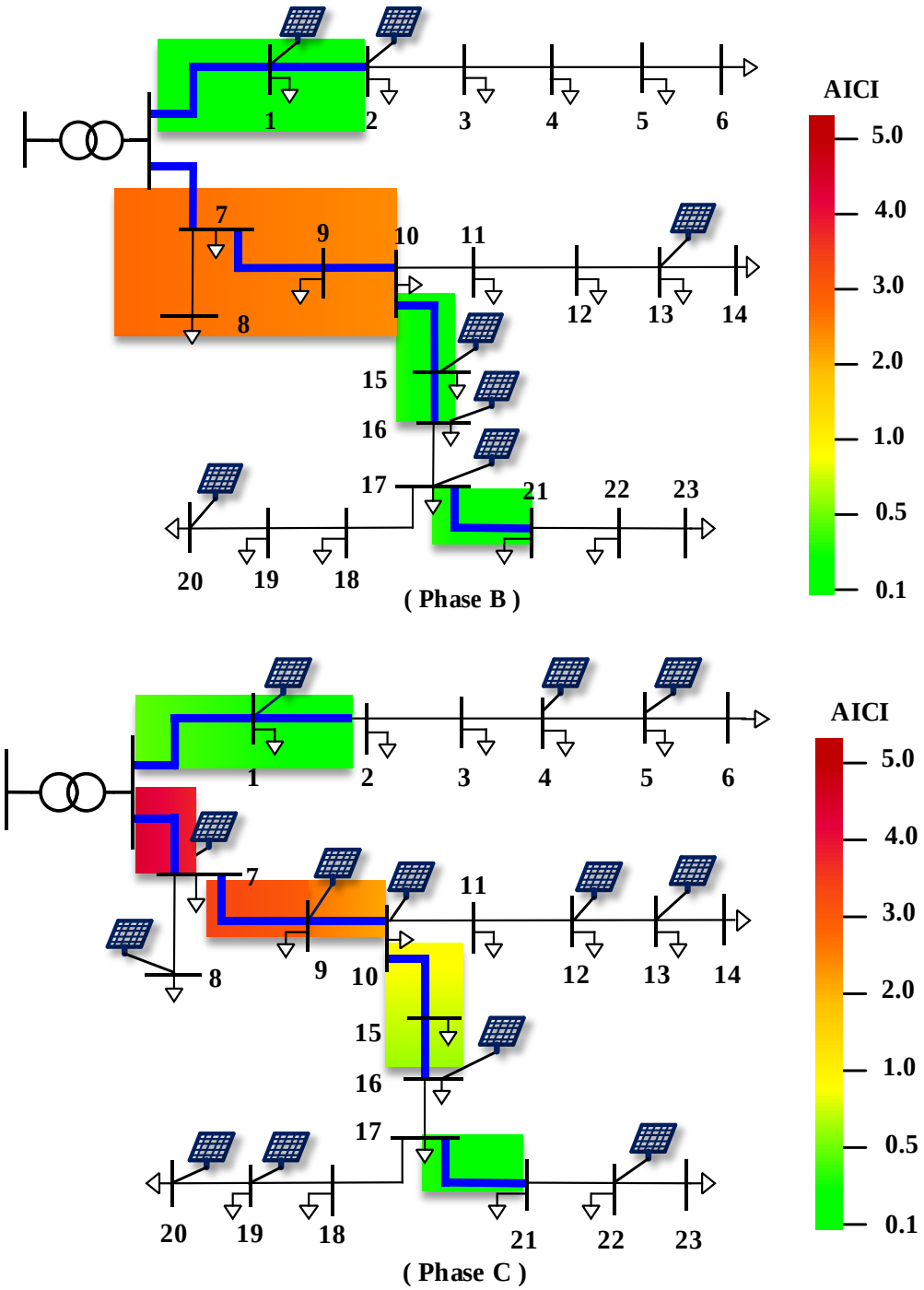

Fig. 4.13 Thermal congestion map at each phase based on AICI (pu) of Case 2.

Fig. 4.13 shows the congestion map at each phase according to index AICI. According to these maps, phase C suffers the most serious congestion compared with phases B and A in terms of thermal and voltage violations. Fig. 4.14 depicts the congestion map at each phase according to index AICV. Phase C suffers the most serious congestion in terms of the number of congested buses and AICV values. In summary, phase C experiences the most serious congestion issue among the three phases, in terms of

magnitude violation and duration.

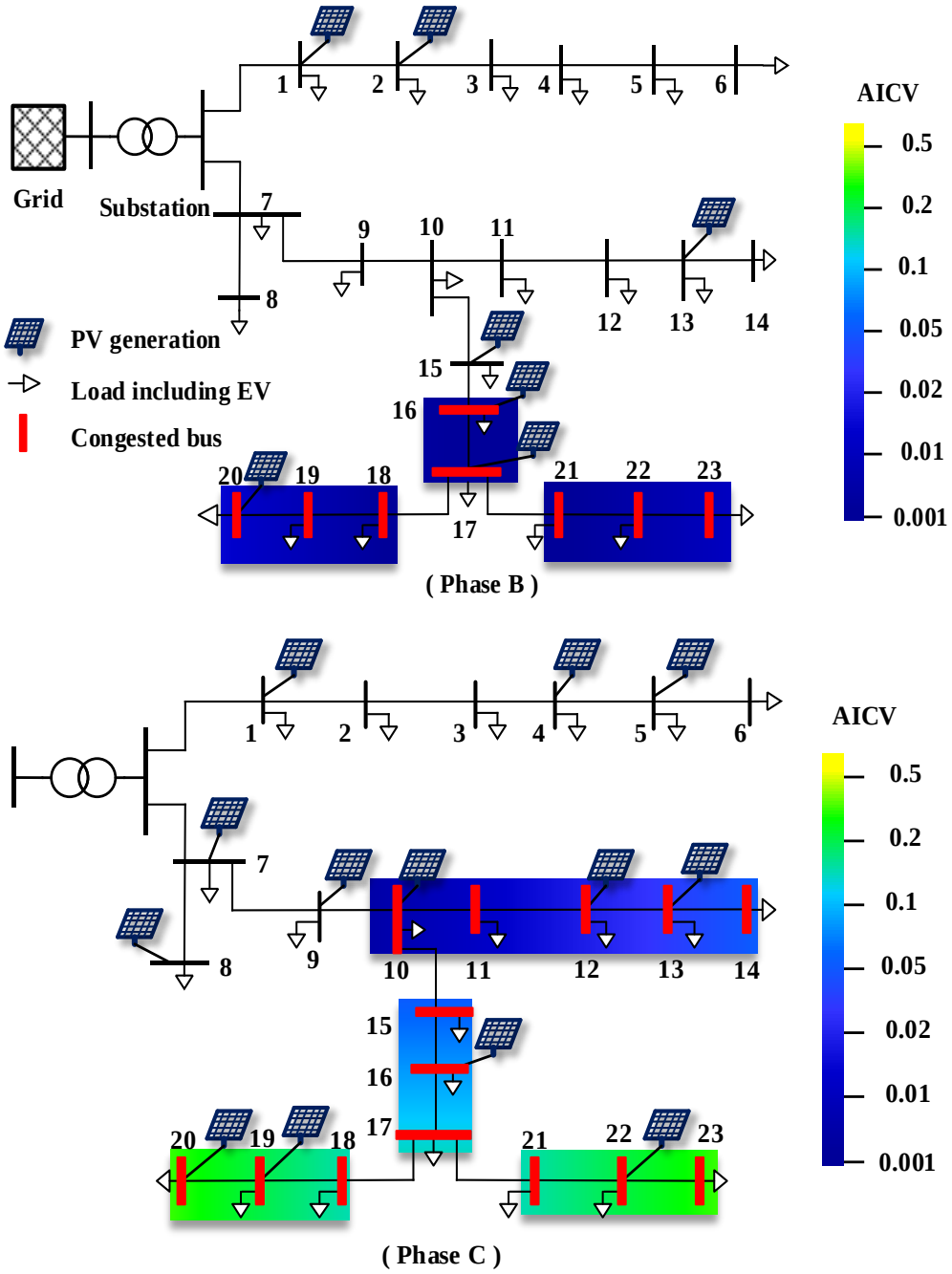

Fig. 4.14 Voltage congestion map at each phase based on AICV (pu) of Case 2.

4.5 Illustrative Results of Customer Contribution Indices

We again consider the same test cases already described in Section 4.4. As in that Section, we present the results relevant to Case 1 and Case 2, which use the IEEE 123-bus test system with two configurations, and the Australian 23-bus LV distribution

network for the horizon of a day, respectively. The contribution from aggregate customers will be analyzed in this Section.

4.5.1 Case 1: IEEE 123-Bus Test Network

Contributions of the aggregate customer at each bus to the thermal violation and voltage violation with configuration 1 are presented in Fig. 4.15. The customer on bus 48 contributes the most to the thermal violation in branches and the voltage violation at buses on averagely. Fig. 4.16 shows the contribution from aggregate customers to congested branches and buses with configuration 2. The most significant contribution is from the customer on bus 76, followed by the customer on bus 48. The customer on bus 48 contributes slightly more than the customer on bus 65.

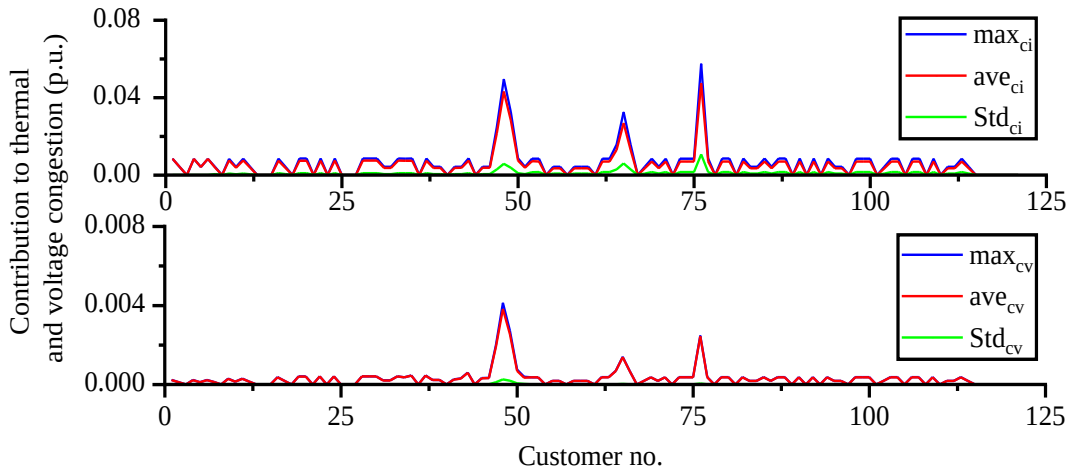

Fig. 4.15 Customer contribution to congestion with configuration 1.

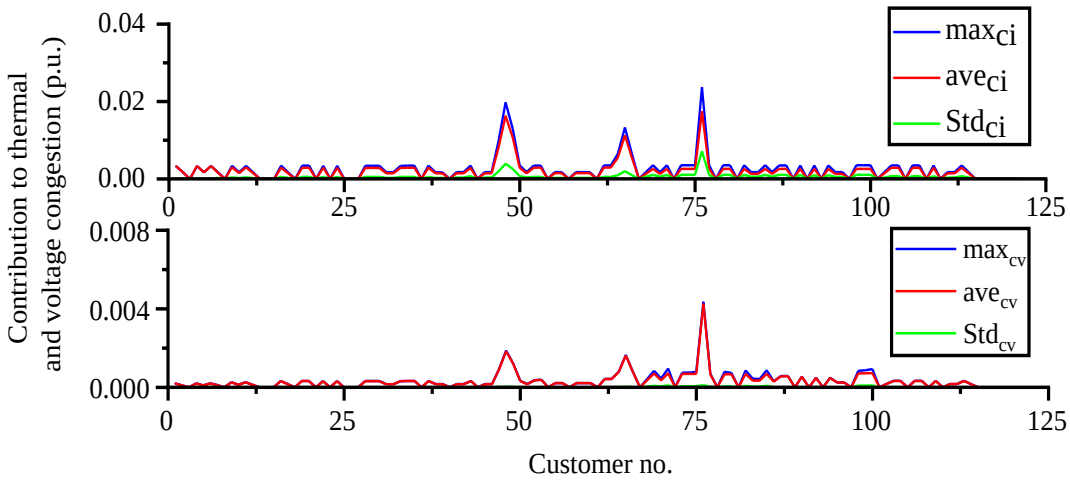

Fig. 4.16 Customer contribution to congestion with configuration 2.

Fig. 4.17 shows the values of AGCI of the customers at each bus for the two configurations. Considering the numbers of congested branches and buses influenced, the values of AGCI at buses 76, 48, and 67 are larger than other buses, showing that the average contributions from the aggregate customer at those buses to thermal and voltage violations are higher than other customers. Also, it suggests that regulating load consumption from those nodes will be more effective in CM.

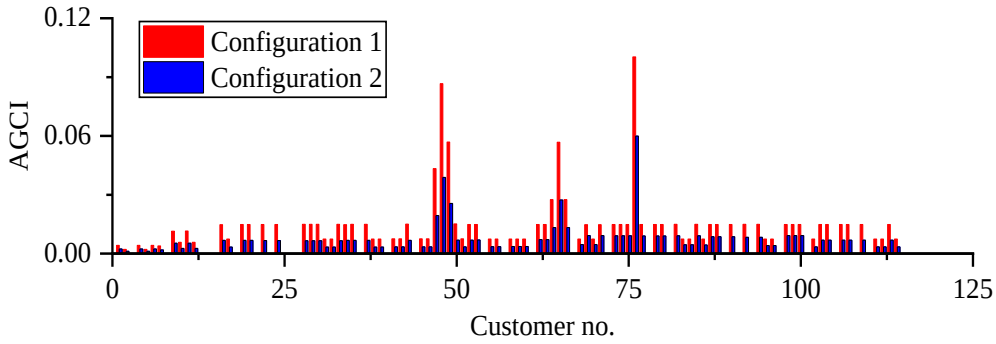

Fig. 4.17 AGCI of load at each bus.

4.5.2 Case 2: Australian 23-Bus LV Distribution Network

For Case 2, the average and maximum contributions of customers to thermal violations and voltage violations at three phases are shown in Fig. 4.18. Customers on bus 11, followed by customers on bus 23, contribute the most to congestion in phase A on averagely. Customers on buses 2, 4, 7, 13, 18, 22 and 23 contribute more than 0.05 p.u. to the thermal violation in phase B. Customers on buses 17, and 23 contribute more than 0.08 p.u. to the thermal violation in phase C. Similarly, customers, with the largest contributions to the thermal violation, also contribute most to voltage violation in phases B and C.

Fig. 4.19 presents the AGCI values for the customers at each bus and phase. Customers at phase C contribute the most to congestion compared with the customers connected at phases B and A in the system. Customers at buses from 1 to 6 have minimal contribution to congestions since there is no voltage violation with a trivial thermal violation at the corresponding branches and nodes. In total, the customer on bus 23 contributes the most to the congestion in the network, considering the number of congested branches and buses.

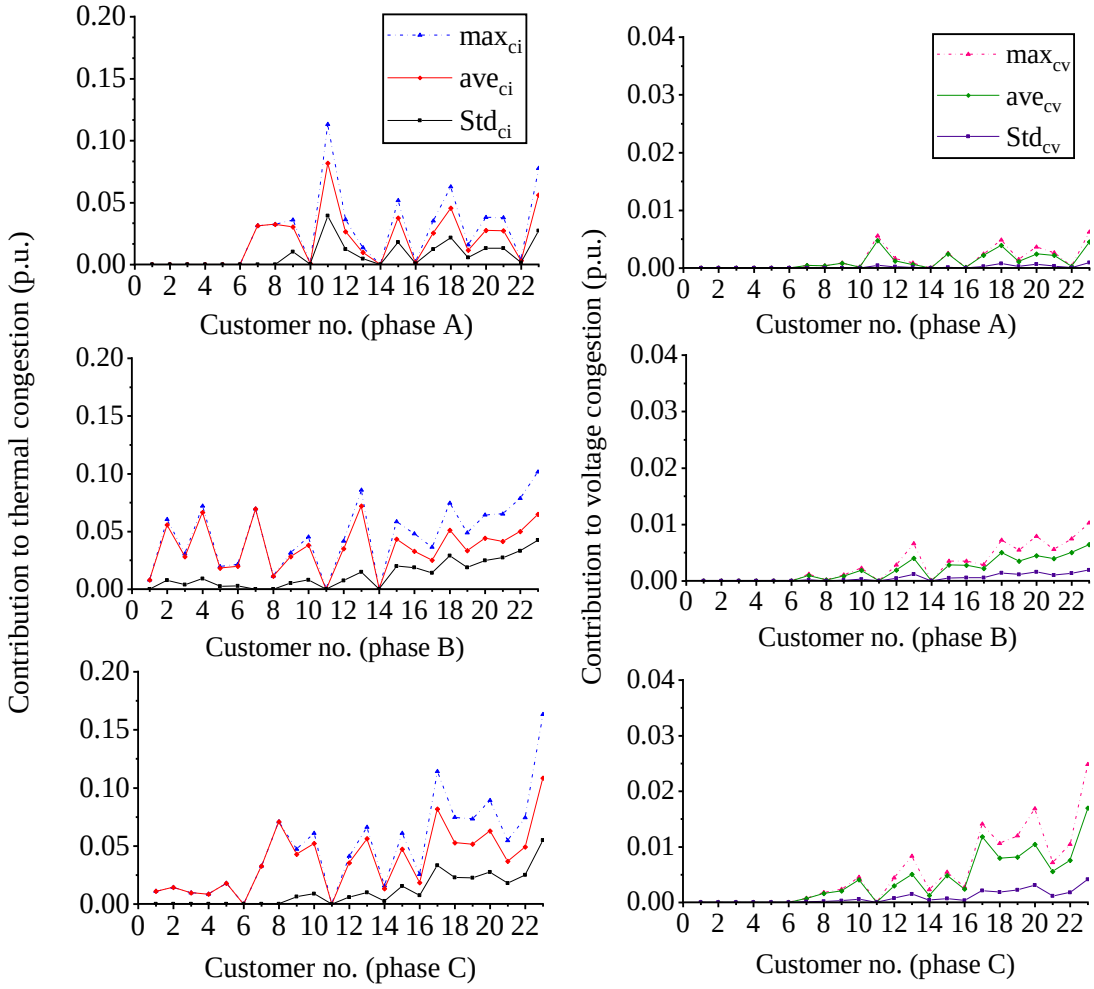

Fig. 4.18 Customer contribution to congestion at each bus for Case 2.

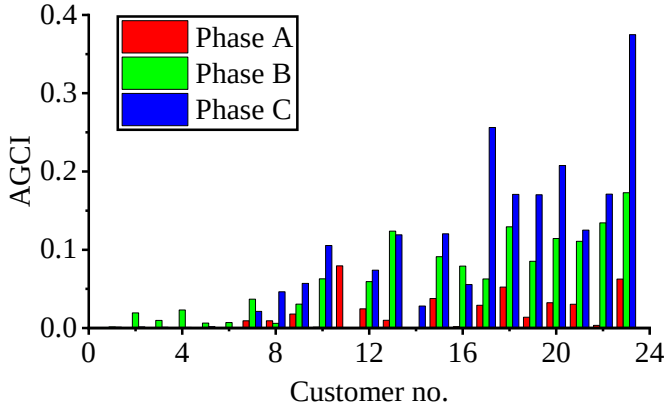

Fig. 4.19 AGCI of customers at each bus for Case 2.

As expected, the buses with higher injected currents show significant contributions to congestion. Customers, connected to the buses at the end of the feeder, exhibit larger contributions than those connected to buses near the substation, even though they have

similar loads. Moreover, different configurations may lead to different contributions, even though the loads are not changed. The number of congested branches and buses is another critical factor that influences the aggregative contribution index.

4.5.3 Application of Proposed Indices by Utility Operators

In the simulation, the time horizon is 24 hours (a day) with intervals of 1 hour and 0.5 hour for Case 1 and Case 2. Long-term (e.g., a year or 5 years) congestion estimation can be attained by clustering the load with probabilities and application of the same procedures as presented in this paper. Evaluation of proposed indices for congestion areas and customer contributions can help power utility to regulate proper CM procedures, make long-term investment plans, and build a fair market for active customers, especially when the flexibilities are limited.

For a short-term congestion estimation (e.g., 24 hours), vulnerable areas can be detected by calculating the proposed indices for thermal and voltage violations based on the load forecast for the next following 24 hours. The most vulnerable regions for thermal congestion and voltage congestion can be distinguished by checking the congestion severity map according to the AICI and AICV values. Spatial and temporal indices provide detailed information on congested branches and nodes in these vulnerable areas. With the thermal vulnerable area map and voltage vulnerable map, power utilities can prioritize the areas according to the seriousness of congestion and regulate short-term CM procedures.

Moreover, evaluating the proposed indices of customer contribution to congestions helps build fairer flexibility management and regulation of rewards for the customers contributing to congestion solutions. According to [237], the capability to discover the location where flexibility is needed is a necessity for an active distribution market. The proposed customer contribution indices can help power utilities to recognize the areas in which response from active customers to CM procedures has a better outcome than other areas. Following the electricity market scheme proposed in [238], the customers triggering volatility need to be appropriately penalized. However, the reward policy that encourages customers to participate in the CM is also important. For improving customer participation, customers can be classified into different clusters based on the values of contribution indices. Furthermore, the proposed indices both for quantifying

the seriousness of congestion and customer contribution can also be utilized for the evaluation of the effectiveness of specific CM strategies and adjustment of real-time spot price during congestion.

Investment planning referencing the long-term congestion estimation can help power utilities relieve congestion and improve system reliability. For instance, the deployment of the energy storage system (ESS) can shave load and absorb excessive renewable generation in a distribution network integrated with high penetration of DER [237]. Also, ESS is a suitable option for the long-term management of congestion. The drawback of the utilization of ESS is its high cost. Long-term estimation of congested areas is vital in determining an appropriate budget by finding the lowest cost and optimal location of ESS. As proposed in this paper, the correct understanding of the CM indices enhances the procedure of decision-making in long-term planning. Moreover, encouraging investment from customers in the areas in which congestion happens frequently, and customers have better performance over others in response to CM procedures can reduce power loss and better implementation of flexibilities in distribution networks.

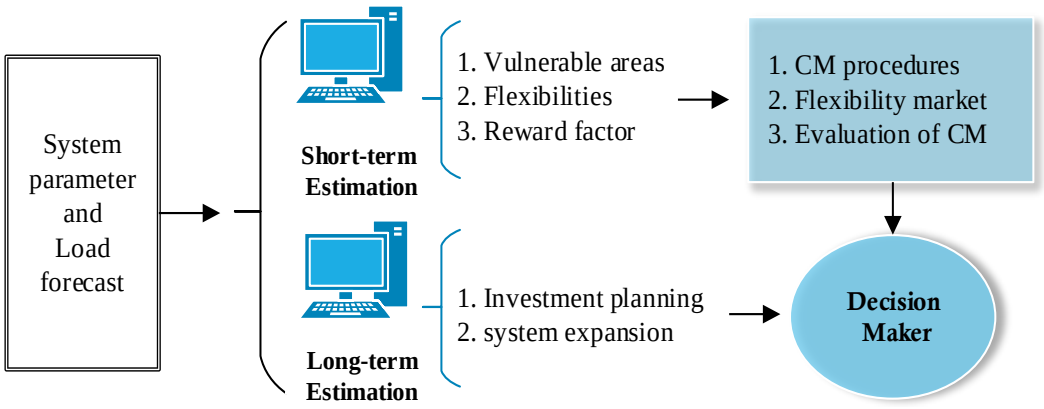

Fig. 4.20 Application of the proposed indices.

4.6 Summary

This chapter proposes spatial and temporal indices to quantify the seriousness of congestion in the distribution network regarding thermal and voltage violations. Spatial indices include maximum, average, and cumulative values of thermal and voltage magnitude violations. Temporal indices are congestion duration, congestion

rate, and continuity. Two aggregate congestion level indices are proposed to represent the congestion level thermal violations and voltage violations considering the frequencies and continuities in the long term. Also, the contribution indices from aggregate customers to thermal congestion and voltage congestion are represented in this chapter. Numerical results obtained using the IEEE 123-bus test feeder with two configurations and an Australian 23-bus LV distribution system confirm that the proposed indices can be utilized to quantify the seriousness of congestions from perspectives of amplitude violation and duration in a balanced system and an unbalanced system. For the considered cases, changing the system configuration impacts voltage congestion more than thermal congestion. Congestion may exacerbate the voltage unbalance issue. The proposed indices can prompt identify the severity of the congestion, the geographical location of concerned areas, and customer contribution. Moreover, suggestions on the deployment of the proposed indices for applying demand response or regulating electricity prices in the CM procedure are presented. Concerning traditional indices that only consider the magnitude of violation at a specific load point, the aggregated indices that consider duration and spatial will help make better decisions relevant to congestion management policy and strategies with limited flexibility resources.

Chapter 5 End-of-life Failure Probability Assessment Considering Electric Vehicle Integration[3]

This chapter proposes a method to estimate the end-of-life failure probabilities of transformers and cable lines in distribution networks considering electric vehicle charging processes. The estimation of the probabilities is obtained using a model based on the Arrhenius-Weibull distribution considering different aging speeds according to load variation. The EV penetration may significantly accelerate the aging speed and loss-of-life, thus adversely influencing failure probability and network reliability. The impacts of different penetration of electric vehicles (EVs) on the thermal aging of transformers and lines are estimated on a distribution test feeder. The simulation results illustrate the calculation and capabilities of the proposed method.

5.1 Introduction

Distribution network reliability estimation plays an essential role in system planning and investment. In the reliability theory, the bathtub failure rate is widely used. In this representation, the wear-out period mainly results from the aging process [239]. The extensive integration of electric vehicles (EVs) exacerbates the aging speed of insulation materials in transformers and cable lines, which leads to increased possibilities of aging failures and lower system reliability. Whilst, large penetration of renewable generations provides new opportunities for managing unreliability

[3] This chapter is based on J. Zhao, A. Arefi and A. Borghetti, "End-of-life Failure Probability Assessment Considering Electric Vehicle Integration," presented at the 2021 31st Australasian Universities Power Engineering Conference (AUPEC), 2021, pp. 1-6.

[240][241]. Therefore, this paper presents a method to reveal the aging processes and the most vulnerable components of the network. The results are useful to find solutions for mitigating aging speed and improving system reliability by better employing renewable generations and EVs.

Analytical methods for evaluating the end-of-life failure (aging or non-repairable failure) probability for a long-term period are not well developed. Transformer end-of-life failure refers to the deterioration of the insulation in which temperature is the leading factor of deterioration [242][243]. Similarly, end-of-life failure occurs on lines, especially under excessive loading conditions [116]. Weibull distribution is the most used distribution to describe the failure probability of devices. Nevertheless, the traditional Weibull distribution-based method needs to be extended to appropriately represent real-time loss-of-life (LoL) and aging speed due to loading variation [244]. An Arrhenius-Weibull failure model is adopted to represent the effect of thermal stress on the end-of-life failure of transformers in [120], without considering different aging speeds in the estimation period. The impact of EVs on the LoL of transformers is discussed in [245] considering the accelerated aging factor. The Arrhenius model of the thermal aging of insulating materials is utilized to estimate the life loss of low-voltage power cables in [116][117]. Even though the end-of-life failure at a single interval is more accurate considering real-time relative aging speed and LoL, precise long-term failure probability estimation still needs to be explored.

This chapter aims at analyzing the influence of EV integration on the end-of-life failure probability and reliability of transformers and cables. End-of-life failure probabilities of transformers and lines are estimated based on the Arrhenius-Weibull distribution, considering relative aging speed due to loading variations. Long-term end-of-life failure probability is derived based on the failure probability at each interval. In addition, the impact of EV penetration on the residual lives of transformers and cable lines is assessed.

5.2 End-of-life Failure Model

End-of-life failure is the conditional probability that failure will occur within a time interval after the device has survived for a specified time. It indicates the likelihood that a component transits from a survival state to a failure state [119].

5.2.1 Arrhenius-Weibull Model

Weibull distribution has been widely used in the modelling of failures [246]. Supposing the end-of-life failure follows Weibull distribution, then, failure rate λ, failure density function *f*, survivor function *R*, and cumulative failure distribution *CDF* are expressed by

$$\lambda(t) = \frac{\beta}{\alpha} \cdot \left(\frac{t}{\alpha}\right)^{\beta-1} \tag{5.1}$$

$$f(t) = \frac{\beta t^{\beta-1}}{\alpha^{\beta}} exp\left[-\left(\frac{t}{\alpha}\right)^{\beta}\right] \quad t \geq 0, \beta > 0, \alpha > 0 \tag{5.2}$$

$$R(t) = exp\left[-\left(\frac{t}{\alpha}\right)^{\beta}\right] \tag{5.3}$$

$$CDF(t) = 1 - R(t) = \int_0^t f(t)dt \tag{5.4}$$

where α is the scalar parameter, and β is the shape parameter. $\beta > 1$ represents an increasing hazard rate at the wear-out period, $\beta = 1$ represents a constant failure probability, and $\beta < 1$ represents a decreasing hazard rate or the debugging period. The appendix of [244] describes a method of calculating α and β from the mean and standard deviation of statistic data. Arrhenius-Weibull distribution, with α the Arrhenius lifespan *L*, is utilized in [247] and [243], for the aging modelling of cables and transformers, respectively. From (5.3) and (5.4), end-of-life failure *CDF* based on Arrhenius-Weibull distribution can be written as,

$$CDF(t) = 1 - exp\left[-\left(\frac{t}{L}\right)^{\beta}\right] \tag{5.5}$$

It is widely recognized that the life of a device mainly depends on the operating temperature. In this paper, the impacts of temperature fluctuation on the lifespan and aging speed are considered explicitly in the Arrhenius-Weibull distribution to achieve better aging failure probability evaluation considering extensive integration of EVs. The aging failure models of transformers and cable lines are obtained by integrating the relative aging rate with respect to the nominal lifespan at the rated temperature. Then, both the probability of end-of-life failure for each interval (e.g., 1 hour) and the probability of long-term aging failure (e.g., 1 year) are formulated.

5.2.2 Relative Aging Speed and Loss-of-life

The nominal lifespan of a transformer or a cable line is given under rated temperature. The real-time temperature (θ_t) is not generally equal to this rated temperature (θ_r) due to loading variations. Following [118], the relative aging speed (RAS) with respect to rated temperature is

$$RAS(t) = \frac{L(\theta_r)}{L(\theta_t)} \tag{5.6}$$

where $L(\theta_r)$ and $L(\theta_t)$ are lifespan when the hot-spot temperature is θ_r and θ_t, respectively. When $\theta_r > \theta_t$, $L(\theta_r) < L(\theta_t)$, and $RAS(t) < 1$, the LoL of 1 hour with θ_t is smaller than the LoL of 1 hour for θ_r, and vice versa. For continuous and discrete estimation, respectively, LoL over a certain period from T_0 to $T_0 + t$ is expressed as

$$LoL = \int_{T_0}^{T_0+t} RAS(t) \cdot dt \tag{5.7}$$

$$LoL = \sum_{j=1}^{n} RAS_j \cdot \Delta t \tag{5.8}$$

where T_0 is the hours of survival for the device, and n is the number of time periods in the $[T_0, T_0 + t]$ interval.

5.2.3 End-of-life Failure CDF of Transformers

The expected lifespan at the constant hot-spot temperature of the transformer varies according to Arrhenius law [120] and is defined by,

$$L(\theta_r^T) = A \cdot exp\left(\frac{B}{\theta_r^T + 273}\right) \tag{5.9}$$

where $L(\theta_r^T)$ is the lifespan of a transformer when the temperature is constant and equal to the rated temperature (θ_r^T). A and B are the empirical constants and are typically estimated from historical loading data. According to [164], the temperature of a transformer θ_t^T is calculated by

$$\theta_j^T = \theta_{A,j} + \Delta\theta_{TO,j} + \Delta\theta_j \tag{5.10}$$

$$\Delta\theta_{TO,j} = \Delta\theta_{TO,R} \times \left[\left(\frac{K_{u,j}^2 R + 1}{R + 1}\right)^p - \left(\frac{K_{i,j}^2 R + 1}{R + 1}\right)^p\right] \times \left[1 - exp\left(\frac{R(R+1)^{p-1}\left(K_{u,n}^2 - K_{i,n}^2\right)\Delta t}{\tau_{TO,R}\left[\left(K_{i,n}^2 R + 1\right)^p - \left(K_{u,n}^2 R + 1\right)^p\right]}\right)\right] \tag{5.11}$$

$$\Delta\theta_j = \Delta\theta_R \left\{ \left(K_{u,j}^{2m} - K_{i,j}^{2m} \right) \times \left(1 - exp\left(-\frac{\Delta t}{\tau_w} \right) \right) + K_{i,j}^{2m} \right\} \tag{5.12}$$

where, $\theta_{A,j}$, $\Delta\theta_{TO,j}$, $\Delta\theta_j$ are the ambient temperature, the top-oil temperature rise over ambient temperature, and the winding hot-spot temperature rise over top-oil temperature at the *j*-th interval in degree Celsius; $\Delta\theta_{TO,R}$ is the top-oil temperature rise over ambient temperature at rated load; $\Delta\theta_R$ is the rated value of hot-spot temperature rise over top-oil temperature; $K_{u,j}$ is the ratio of the load at the end of *the j*-th interval to the rated load; $K_{i,j}$ is the ratio of the load at the beginning of the *j*-th interval to the rated load. Constants p, m, τ_w, R , and $\tau_{TO,R}$ are determined by the configuration and load variation of transformers, and the detailed values of these constants are shown in section 5.4. Considering the LoL, the relative aging speed at *j*-th interval given by

$$RAS_j^T = exp\left(\frac{B\left(\theta_j^T - \theta_r^T\right)}{\left(\theta_r^T + 273\right) \cdot \left(\theta_j^T + 273\right)} \right) \tag{5.13}$$

the cumulative end-of-life failure of a transformer from T_0 to $T_0 + j\Delta t$ is expressed as

$$CDF_T(t) = 1 - exp\left[-\left(\frac{T_0 + \sum RAS_j^T}{A \cdot exp\left(\frac{B}{\theta_r^T + 273}\right)} \right)^{\beta_T} \right] \tag{5.14}$$

5.2.4 End-of-life Failure CDF of Cable Lines

According to [117], the rated lifespan of a cable line at actual temperature is given by

$$L(\theta_r^L) = 10^{\left(a + \frac{b}{\theta_r^L + 273}\right)} \tag{5.15}$$

$$\theta_j^L = \theta_a + (\theta_R^L - \theta_{a0}) \frac{I_j^2}{I_{Z0}{}^2} \left(1 - e^{\frac{-\Delta t}{k}}\right) + \left(\theta_{j-1}^L - \theta_{a0}\right) \frac{I_{j-1}^2}{I_{Z0}{}^2} e^{\frac{-\Delta t}{k}} \tag{5.16}$$

where $L(\theta_r^L)$ is the lifespan when the rated temperature is θ_r^L; a and b are constants given by manufacturers; θ_a is the ambient temperature; θ_{a0} is the reference ambient temperature; I_t and I_{Z0} are current-carrying capacity at the actual temperature in *j*-th interval and at the reference ambient temperature, respectively, and k is the thermal time constant. The relative aging speed at each interval and the cumulative end-of-life failure probability of lines, respectively, are expressed as

$$RAS_j^L = 10^{\left[\frac{b\left(\theta_j^L-\theta_r^L\right)}{\left(\theta_r^L+273\right)\cdot\left(\theta_j^L+273\right)}\right]} \tag{5.17}$$

$$CDF_L(t) = 1 - exp\left[-\left(\frac{T_0+\sum RAS_j^L}{10^{\left(a+\frac{b}{\theta_r^L+273}\right)}}\right)^{\beta_L}\right] \tag{5.18}$$

Compared with the Arrhenius-Weibull distribution adopted in [241] and [243], this approach allows a more accurate representation of the influence of the temperature on the relative aging speed.

5.2.5 Long-term End-of-life Failure Probability

According to the aging failure definition [119], the end-of-life failure probability *p* of a device in a specified period $(T_0, T_0 + t)$ is expressed as

$$p(t) = \frac{R(T_0)-R(T_0+t)}{R(T_0)} \tag{5.19}$$

From the definition, the failure probability at *j*-th interval means end-of-life failure happens at *j*-th interval on the condition that it survives before *j*-th interval. Combined with the improved cumulative failure probability of the Arrhenius-Weibull distribution, end-of-life failure probability at *j*-th interval and long-term failure probability are calculated as

$$p(j\Delta t) = \frac{exp\left[-\left(\frac{T_0+(j-1)\Delta t}{L(\theta_R)}\right)^{\beta}\right]-exp\left[-\left(\frac{T_0+j\Delta t}{L(\theta_R)}\right)^{\beta}\right]}{exp\left[-\left(\frac{T_0+(j-1)\Delta t}{L(\theta_R)}\right)^{\beta}\right]} \tag{5.20}$$

$$p = \sum_{j=1}^{n}\left(1 - exp\left[\left(\frac{T_0+(j-1)\Delta t}{L(\theta_R)}\right)^{\beta} - \left(\frac{T_0+j\Delta t}{L(\theta_R)}\right)^{\beta}\right]\right) \tag{5.21}$$

Using the scale and shape parameters and replacing the Δt with the LoL of transformers and cables at each interval with respect to the nominal lifespans, the long-term end-of-life failure probability for transformers (p_T) and cable lines (p_L) are calculated by using the corresponding loss-of-lives at each interval and shape parameters:

$$p_T = \sum_{j}^{n}\left(1 - exp\left[\left(\frac{T_0+LoL_{j-1}^T}{L(\theta_r^T)}\right)^{\beta_T} - \left(\frac{T_0+LoL_j^T}{L(\theta_r^T)}\right)^{\beta_T}\right]\right) \tag{5.22}$$

$$p_L = \sum_j^n \left(1 - exp\left[\left(\frac{T_0 + LoL_{j-1}^L}{L(\theta_r^L)}\right)^{\beta_T} - \left(\frac{T_0 + LoL_j^L}{L(\theta_r^L)}\right)^{\beta_T}\right]\right) \quad (5.23)$$

It should be noted that the overall health condition of a cable or transformer can be considered and converted to the survival hour (T_0) according to the historical operating date. For simplicity, we assume T_0 is 160,000 hours throughout the simulation. When the life of a transformer or a cable line is expired, the end-of-life failure probability is equal to 1. Therefore, the residual lives of a transformer and cable line can be estimated by calculating the reciprocals of failure probabilities. Clustering the yearly load into typical days, a common method used in system planning avoids calculating the failure probability at each interval throughout the year. The next sections present the failure probabilities of transformers and lines calculated for a typical day. The failure probability estimate for a whole year is obtained by carrying out this calculation for all typical days and combining the probabilities of these days.

5.3 Test Case and Simulation Results

5.3.1 Test Network and Parameters

The adopted test system topology is shown in Fig. 5.1, which includes a slack bus at the substation equipped with an HV/MV transformer, 5 nodes with MV/LV distribution transformers, and 5 cable branches. The voltage at the slack bus is 1 pu.

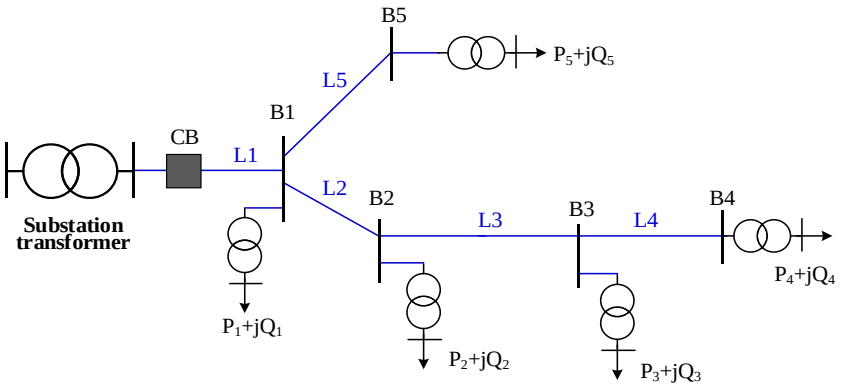

Fig. 5.1 Sample 5-bus network [241].

Table 5.1 reports the values of the resistance and reactance of each line. The rated active power (P) and reactive power (Q) of each node are shown in Table 5.2. Bus 3 has the highest load, and buses 4 and 5 have the smallest load. Table 5.3 and Table 5.4

reports the parameters and constants of transformers and lines adopted to calculate relative aging speed, CDF, and end-of-life failure probability. The designed lifespan for transformers is 180,000 hours for a rated temperature of 110 ºC, and the nominal lifespan for lines is 175,000 hours operating at the rated temperature of 80 ºC.

Table 5.1 Parameters of lines

Parameter	**Line 1**	**Line 2**	**Line 3**	**Line 4**	**Line 5**
Resistance (Ω)	0.092	0.493	0.493	0.366	0.819
Reactance (Ω)	0.047	0.251	0.186	0.194	0.707

Table 5.2 Parameters of each bus

Parameter	**Bus 1**	**Bus 2**	**Bus 3**	**Bus 4**	**Bus 5**
Rated P (kW)	100	90	120	20	20
Rated Q (kVar)	60	40	40	12	12

Table 5.3 Constants of transformers [117][243]

Parameter	$\Delta\theta_{TO,R}$	$\tau_{TO,R}$	R	p	$\Delta\theta_R$
33/11.5 kV (ST)	65.0 ºC	3.5 h	3.2	0.9	30.0 ºC
11/0.433Kv (DTs)	55.0 ºC	3.0 h	8	0.9	20.3 ºC
Parameter	m	τ_w	B	β_{ST}	β_T
33/11.5 kV (ST)	0.8	4.8 min	15000	6.0	-
11/0.433Kv (DTs)	0.8	10 min	15000	-	6.0

Table 5.4 Constants of lines

Lifespan	A	b	$\boldsymbol{\theta_r^L}$	$\boldsymbol{\theta_{a0}}$	$\boldsymbol{\beta_L}$
175000 hours	-10.403	5502	80 ºC	30 ºC	1.4

5.3.2 Load and EV Profiles

The load profile in the simulation is shown in Fig. 5.2. Multiplying this profile (for simplicity assumed equal for each node) by the rated power, a load demand for 24 hours with an interval of 1 hour is obtained.

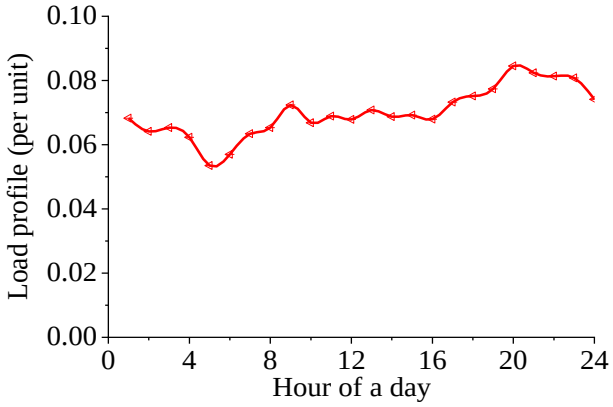

Fig. 5.2 Load profile in the simulation (adapted from [246]).

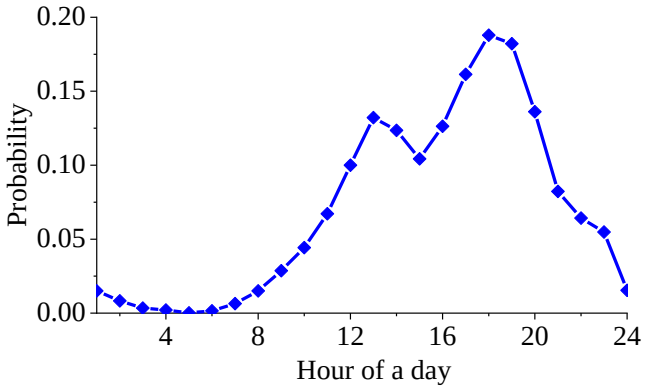

Fig. 5.3 Weighted arrival time probability distribution (adapted from [248]).

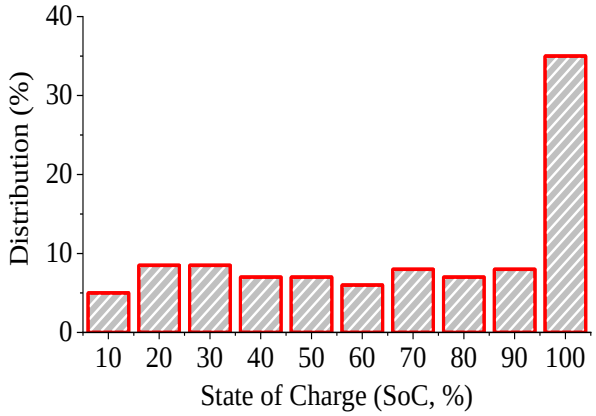

Fig. 5.4 Distribution of the SoC-level difference due to the charging process (from [236]).

Assuming EV owners start charging their vehicles when they arrive home, then the load demand from EV charging is generated by taking the EV penetration (ρ), the weighted probability distribution of arrival time, and the probability distribution of state-of-charge (SoC) level difference. Fig. 5.3 and Fig. 5.4 depict the probability distributions of arrival time and SoC-level difference, respectively, adopted in the

simulation section. ρ is defined as the ratio of total rated capacity (P_{ev}) of EV charging and the peak load (P_{max}), as

$$\rho = P_{ev}/P_{max} \tag{5.24}$$

The time horizon is 24 hours, and the annual probability of end-of-life failure can be estimated by integrating the simulation results of clustered daily load profiles and their probabilities.

5.3.3 Simulation Results

This section presents the simulation results of end-of-life failure probability for both transformers and lines in the test network. Assuming T_0 equal to 160,000 hours, failure probabilities at each interval are estimated for EV penetration percentages between 0% and 200%, with steps of 50%. The estimated failure probabilities of the most vulnerable equipment and residual lives are presented.

Fig. 5.5 shows the end-of-life failure probability of the substation transformer and distribution transformer under different percentages of EV penetrations during the day. The failure probability is minimal without EVs and increases when EV penetration increases. The maximum failure probability is at 8 pm with 200% EV penetration. The estimated failure probabilities on distribution transformers are relatively small due to lower loading, even considering EV charging load.

Figures 5.6 shows the end-of-life failure probabilities of lines 1-5 during the day. Line 1 has the highest failure probability due to the highest loading current. The failure probability of each line increases when the EV penetration increases. The results quantify the impact of EV penetration on the likelihood of aging failures for each line.

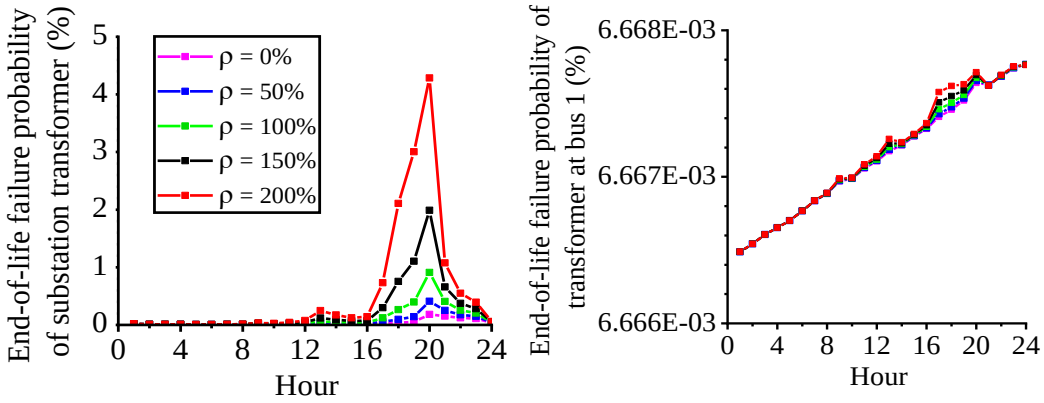

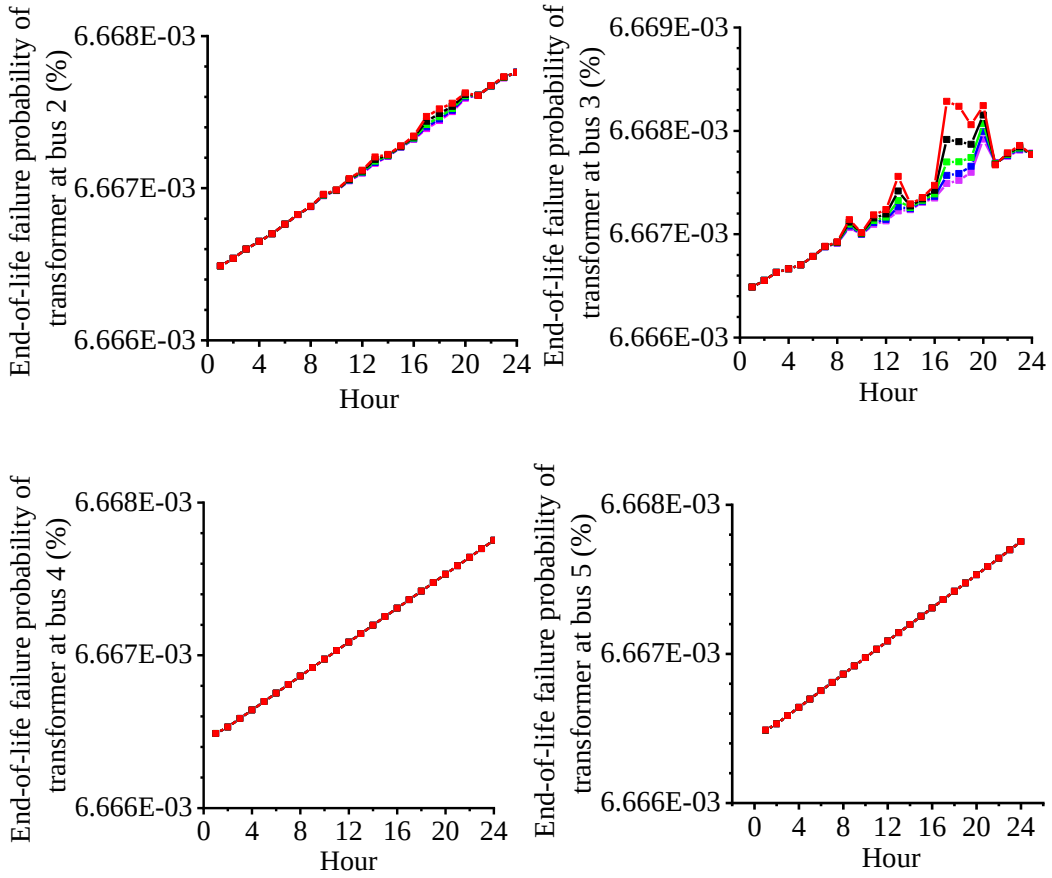

Fig. 5.5 End-of-life failure probability of transformers.

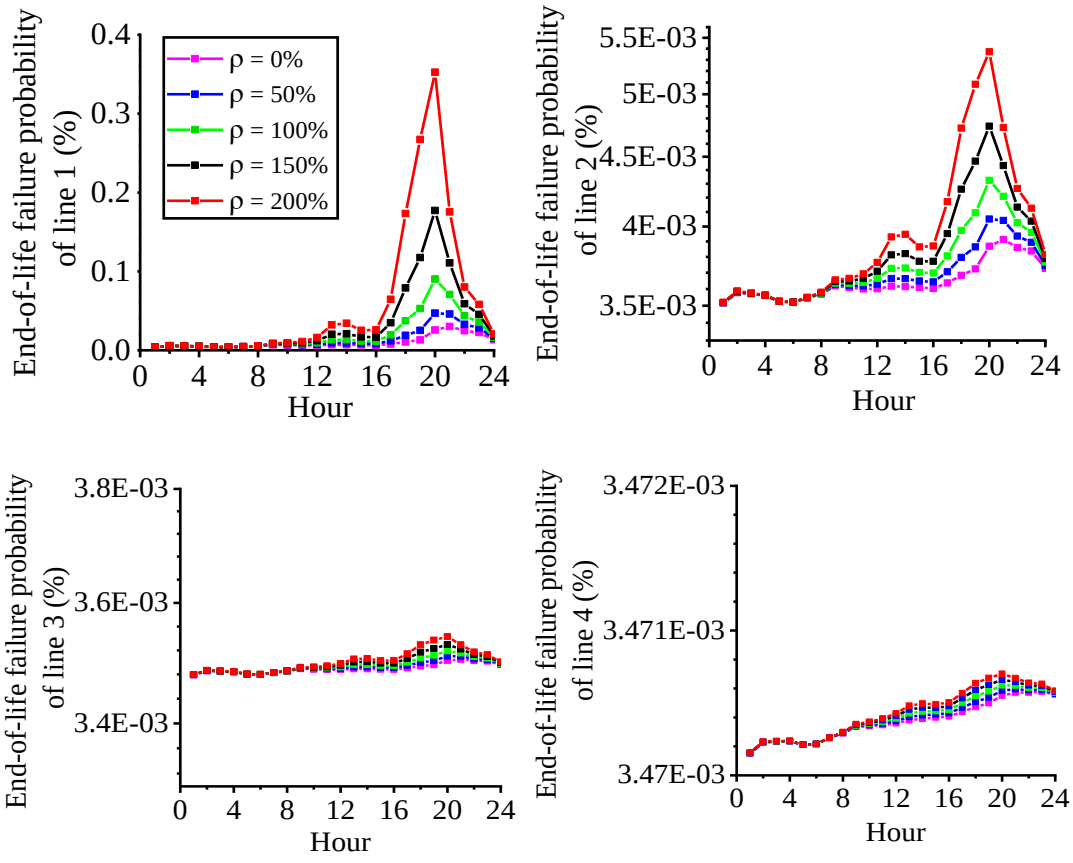

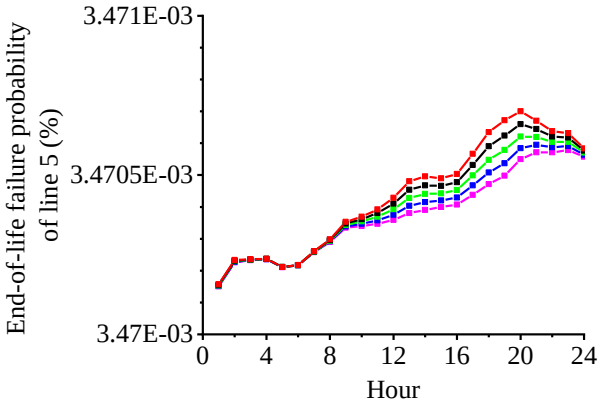

Fig. 5.6 End-of-life failure probability of lines 1-5.

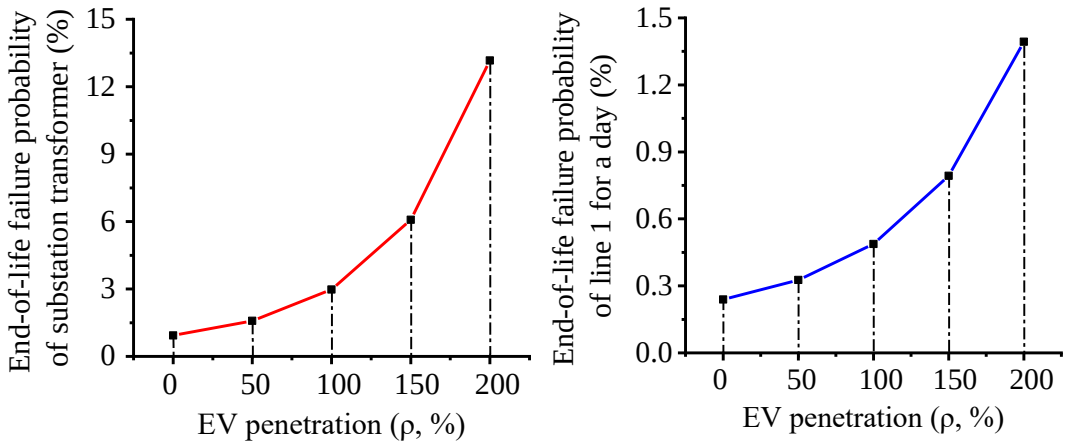

Fig. 5.7 End-of-life failure probability of substation transformer and line 1 for a day.

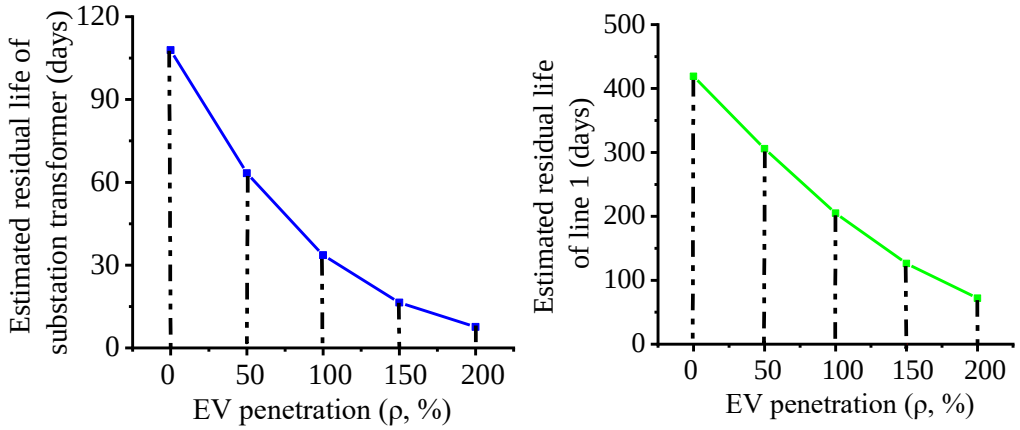

Fig. 5.8 Estimated residual life of substation transformer and line 1.

The results show that the substation transformer and line 1 are more vulnerable to end-of-life failure than other components. The total failure probability of the substation transformer and line 1 for the typical day considering EV penetrations are presented

in Fig. 5.7. With 200% EV penetration, the failure probabilities of the substation transformer and line 1 are 0.132 and 0.014, respectively.

The calculated residual life (in days) of the substation transformer and line 1 are shown in Fig. 5.8 Assuming the wear-out period starts at T_0, the residual life is estimated based on the failure probability of the considered typical day. Without EVs, the estimated residual lives of the substation transformer and line 1 are 419 days and 108 days. The residual lives reduce to only 72 days and 8 days with 200% EV penetration.

5.4 Summary

Arrhenius-Weibull distribution is utilized to formulate the end-of-life failure probability of transformers and lines considering the actual operating time and temperature in the various load conditions. The representation of the failure probability considers the different relative aging speeds when the loading varies at different intervals. The method analyzes the impact of different EV penetration on failure probabilities in a power test network. The results quantify the positive correlation between EV penetration and end-of-life failure probability. They also identify the vulnerability of specific transformers and cable lines. Since lower power flows will slow down the aging speed, the smart EV charging/discharging algorithm appears well justified for reducing network unavailability due to end-of-life failures.

Chapter 6 End-of-life Failure Probability and Reliability Evaluation in Distribution Networks Integrated with Large Penetration of Electric Vehicles[4]

Reliability assessment due to end-of-life failure of equipment plays an essential role in network planning and regulation with the increasing integration of electric vehicles (EVs), especially in aging networks. This chapter proposes a method to quantify the impact of different levels of EV penetration on the end-of-life failure of equipment in distribution networks. This quantification includes the cost of expected energy not supplied (ENS) for customers and the replacement cost for utility. The probabilistic models for estimating the end-of-life failure of transformers and cable lines based on Arrhenius-Weibull distribution are presented. Considering network topology and post-failure reconfiguration, reliability indices (i.e., node unavailability, ENS, and equipment loss-of-life) due to EV integration are derived. Moreover, the total cost, including customer loss and power utility costs, is calculated. An accurate prediction model based on machine learning (ML) is adopted for the load profiles of EV charging. The numerical simulations on a 5-bus network and the IEEE 123-bus distribution test feeder illustrate the capability of the proposed method and its expected superior accuracy compared with traditional methods in assessing end-of-life failure and network reliability in the presence of EVs.

[4] This chapter is based on the paper J. Zhao, A. Arefi, A. Borghetti, G. Ledwich, R. Dabare, and S. M. Muyeen, "End-of-life Failure Probability and Reliability Evaluation in Distribution Networks Integrated with Large Penetration of Electric Vehicles" submitted to IET Generation, Transmission & Distribution (under review).

6.1 Introduction

Reliability estimation of the distribution network is essential to provide customers with acceptable reliability, economic, and quality service [155]. The increasing electric vehicle (EV) penetration can further weaken distribution network reliability due to significant energy consumption by EVs [149]. According to the Australian Energy Market Operator (AEMO), demand from EV charging stations is predicted to reach over 1 terawatt hour (TWh) each year from the late 2020s and approach the level of total residential consumption by 2050 [249]. Voltage issues and congestion led by high penetration of EVs have been analyzed extensively in the literature [83][250]. However, the growing pressure on aging equipment from EV charging also poses a significant threat to reliable and safe network operation. Hence, the assessment of the reliability of distribution networks in the new scenario is a fundamental issue for planning and regulation decisions of power utilities.

Analytical methods for evaluating the reliability of distribution networks due to random failures are well developed. Reliability indices are calculated considering post-fault network reconfiguration of circuit breakers and switches in a complex distribution network [130][139][153][172]. Cross-connect operation and small-scale distribution generation (DG) are useful methods to improve the reliability of distribution networks [241]. However, usual methods only consider constant failure rates of branches without a specific representation of end-of-life failures due to aging [119].

According to the bathtub failure rate model, the wear-out period mainly results from the aging process of insulation materials [239][251]. Faster deterioration of insulation exacerbates end-of-life failures due to high load demand [116][242]. The Weibull distribution is the most used distribution able to describe the end-of-life failure probability. Nevertheless, the traditional Weibull distribution-based method needs to be improved to appropriately represent real-time loss-of-life (LoL) due to loading variations [244]. In [120], an Arrhenius-Weibull failure model is adopted to characterize the effect of thermal stress on the end-of-life failure of transformers without considering the different aging rates in the estimation period. Insights for the LoL improvements of low voltage transformers considering a high penetration of plug-in hybrid EVs are provided in [118]. Arrhenius models of the thermal aging of

insulating materials are utilized in [116][117] to represent the life loss of low-voltage power cables, without a specific analysis of the influence of EV charging station integration.

An accurate load demand model of EV charging is needed to analyze the negative influence on end-of-life failure probability. Drivers' travel pattern is one of the main factors that determine the EV charging demand [122][252]. The distribution functions of departure time, arrival time and travel distance represent the drivers' travel pattern [115][253][254][255]. Two general methodologies are used to predict EV charging demand: Monte Carlo methods and artificial intelligence approach based on the real EV charging data, transportation surveys or historically collected data. Monte Carlo methods are used in [149], [254], [256], and [257] considering the Markov decision processes, the dependence structure between the main variables (departure time, travel distance and the number of journeys), different EV types and different travel purposes, respectively. Deep learning [258], artificial neural network (ANN) [259] and fuzzy logic [260] are typical artificial intelligence strategies employed to predict the charging load of plug-in EVs.

The primary purpose of this chapter is to quantify the impact of a high EV penetration rate on the reliability of distribution networks and end-of-life equipment failures. The end-of-life failure probabilities of transformers and lines are calculated by using an estimation method based on the Arrhenius-Weibull distribution, considering the aging rate and the real-time LoL rates. Furthermore, the procedure calculates the reliability indices considering the post-failure network reconfiguration, the impacts of EV charging on the failure probability and the network reliability, the ENS and utility costs. The main contributions of this chapter are:

- A procedure is proposed able to evaluate node unavailability, expected energy not supplied (ENS), customer reliability cost based on the value of customer reliability (VCR) and power utility cost due to equipment replacement considering end-of-life failures and post-fault network reconfiguration.
- The analysis of EV charging impact on customer reliability and power utility costs is carried out by using the proposed procedure together with an accurate machine learning (ML)-based data-driven model of EV charging load which uses the multi-layer perceptron (MLP) method.

6.2 Methodology and Proposed Procedure

As illustrated in Fig. 6.1, the proposed procedure includes the probabilistic models of end-of-life failure for transformer and cable lines, the calculation of the system reliability indices, and the model of the load demand of EV charging. Subsection 6.2.1 describes the end-of-life failure models of both transformers and cable lines based on the Arrhenius-Weibull distribution and the calculation of end-of-life failure probabilities and LoL. Subsection 6.2.2 describes the calculation of the node unavailability, expected ENS, and economic losses of the customers and power utilities, considering varying load demand and long-term failure probability. Subsection 6.2.3 presents the developed ML model of EV charging load.

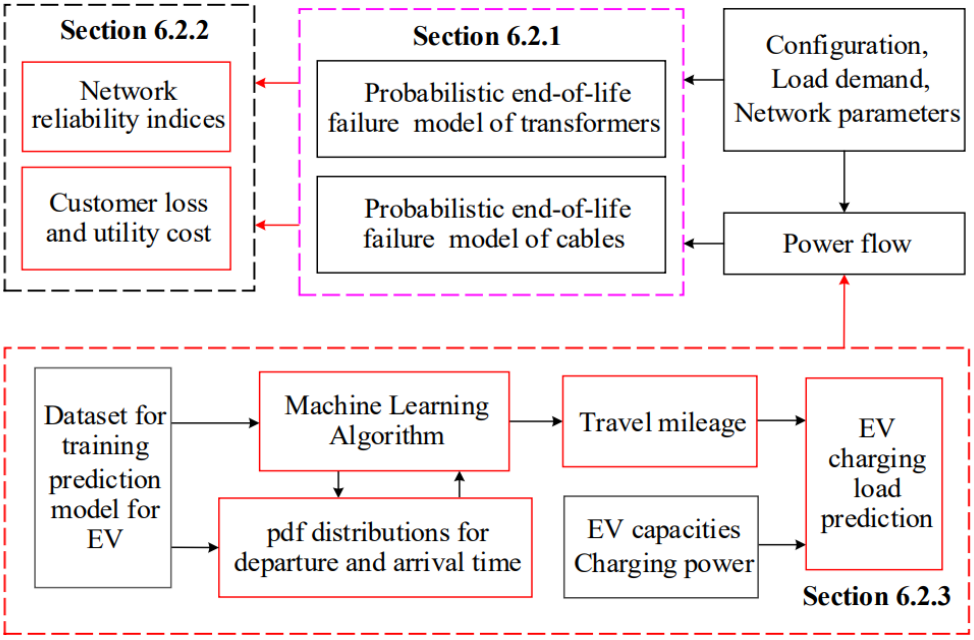

Fig. 6.1 Flowchart of the procedures.

6.2.1 Probabilistic Model of End-of-life Failure

6.2.1.1 End-of-life failure probability estimation

End-of-life failure is the conditional probability that a failure will occur within a period (e.g., 1 year) after the device has survived for a specified time, i.e., it indicates the likelihood that a component will go from a survival state to a failure state [119]. The end-of-life failure probability p of a device in the interval $(T_0, T_0 + t)$ is

$$p(t) = \frac{R(T_0) - R(T_0 + t)}{R(T_0)} \tag{6.1}$$

where $R(T_0)$ and $R(T_0 + t)$ are the survivor function at T_0 and $T_0 + t$. Model (6.1) assumes time as the only factor affecting end-of-life failure and does not explicitly represent other factors affecting the aging process, such as load. This chapter focuses on the impact of increasing loading due to EV integration on the failure probability.

Since loading variation causes varying temperature and aging speed, reducing the resolution of the estimation period results in improved accuracy of the probabilistic model of the end-of-life failure. Assuming n intervals from T_0 to $T_0 + t$, we denote the failure probabilities at the different intervals as $p(\Delta t), \dots, p(j\Delta t), \dots, p(n\Delta t)$, where

$$p(j\Delta t) = \frac{R(T_0 + (j-1)\Delta t) - R[T_0 + j\Delta t]}{R[T_0 + (j-1)\Delta t]} \tag{6.2}$$

The end-of-life failure probability in $(T_0, T_0 + t)$ is expressed as,

$$p(t) = p(\Delta t) + \cdots + p(j\Delta t) + \cdots + p(n\Delta t) \tag{6.3}$$

i.e.,

$$p(t) = \sum_{j=1}^{n} \left(1 - \frac{R[T_0 + j\Delta t]}{R[T_0 + (j-1)\Delta t]}\right) \tag{6.4}$$

For evaluating the end-of-life failure probability, R needs to be determined. The LoL at each interval is not always proportional to time duration Δt due to loading fluctuations. Incorporating the assessment of LoL in (6.4) is essential for the end-of-life failure probability evaluation, considering the EV integration.

As shown in [261], the Arrhenius-Weibull-distribution based end-of-life failure probabilities of transformer (p_T) and cable lines (p_L) is expressed as

$$p_T = \sum_{\mathrm{i}} \left\{1 - \exp\left[\left(\frac{\mathrm{T}_0 + \sum_{\mathrm{j}=1}^{\mathrm{i}-1} RAS_{\mathrm{j}}^{\mathrm{T}} \Delta \mathrm{t}}{L(\theta_r^T)}\right)^{\beta_T} - \left(\frac{\mathrm{T}_0 + \sum_{\mathrm{j}=1}^{\mathrm{i}} RAS_{\mathrm{j}}^{\mathrm{T}} \Delta \mathrm{t}}{L(\theta_r^T)}\right)^{\beta_T}\right]\right\} \tag{6.5}$$

$$p_L = \sum_{\mathrm{i}} \left\{1 - \exp\left[\left(\frac{\mathrm{T}_0 + \sum_{\mathrm{j}=1}^{\mathrm{i}-1} RAS_{\mathrm{j}}^{\mathrm{L}} \Delta \mathrm{t}}{L(\theta_r^L)}\right)^{\beta_L} - \left(\frac{\mathrm{T}_0 + \sum_{\mathrm{j}=1}^{\mathrm{i}} RAS_{\mathrm{j}}^{\mathrm{L}} \Delta \mathrm{t}}{L(\theta_r^L)}\right)^{\beta_L}\right]\right\} \tag{6.6}$$

where T_0 is the survival hours with respect to nominal lifespan, $L(\theta_r^T)$ and $L(\theta_r^L)$ are nominal lifespans when the hot-spot temperature is θ_r^T and θ_r^L for transformers and cable lines, respectively, β_T and β_L are the shape parameters of Arrhenius-Weill

distributions for transformers and cable lines, RAS_j^T and RAS_j^L are the relative aging speed (RAS) of transformers and cable lines at the *j*-th interval.

6.2.1.2 Yearly loss-of-life due to integration of EV

Clustering the yearly load into typical days reduces the complexity and computational time required to assess the annual failure probability. The estimation of the LoL and failure probability for a whole year can be calculated by combining the results obtained for the typical days. LoL and failure probability (p) for a year resulting from EV integration are defined as

$$LoL_{EV} = \sum_{l=1}^{n_{cl}} \left[\sum_{j=1}^{24} \left(RAS_j^{EV} - RAS_j \right) \times \Delta t \right] \times p_l^{clu} \times 365 \tag{6.7}$$

$$p = \sum_{l=1}^{n_{cl}} p_l^f \times p_l^{clu} \times 365 \tag{6.8}$$

where LoL_{EV} is the LOL due to the integration of EV, n_{cl} is the number of clusters, RAS_j^{EV} and RAS_j are the RAS of equipment at the *j*-th interval with and without EV integration, p_l^{clu} is the probability of cluster *l*, p_l^f is the end-of-life failure probability of equipment during the *l*-th clustered day.

6.2.2 Reliability Indices, Customer Loss, and Utility Cost

The reliability evaluation of a power system provides the reliability indices of networks/buses from the knowledge of the fault and repair parameters of the components parameters [262][263]: such as annual failure rate (repairable failure, λ/year), outage duration and repair duration [264], generally given as constant values. End-of-life failure is not commonly considered in reliability indices, e.g., system average interruption duration index (SAIDI), system average interruption frequency index (SAIFI), and expected energy not supplied (ENS) [130][139][153][155][156][172][241]. Indeed, since the end-of-life occurs only once during the whole lifetime of a component and is represented as a failure probability, it is not appropriate to integrate the end-of-life failure in SAIDI and SAIFI. Therefore, this subsection only deals with the inclusion of the end-of-life failure in the estimation of ENS, customer loss and utility cost.

6.2.2.1 Reliability indices

The reliability of network operation depends on the topology and the reliability of lines and transformers. High end-of-life failure probabilities of devices result in low reliability and higher unavailability. Usually, when a failure (random or end-of-life failure) occurs, the faulted component is disconnected by fault protection relays. Maintenance personnel are dispatched to repair or replace the component. According to [130], the vector of node unavailability ($\boldsymbol{U_{node}}$) triggered by end-of-life failure can be calculated by considering the yearly failure probabilities of lines ($\boldsymbol{p_L}$), failure probabilities of transformers ($\boldsymbol{p_{ST}}, \boldsymbol{p_{DT}}$), and the configuration of protection relays and circuit breakers, and expressed as

$$\boldsymbol{U_{node}} = \boldsymbol{RC} \times (\boldsymbol{d_L^e} \circ \boldsymbol{p_L}) + \boldsymbol{SC} \times (\boldsymbol{s_L^e} \circ \boldsymbol{p_L}) + \boldsymbol{d_{DT}^e} \circ \boldsymbol{p_{DT}} + \boldsymbol{d_{ST}^e} \circ \boldsymbol{p_{ST}} \tag{6.9}$$

where $\circ$ is the Hadamard product; $\boldsymbol{RC}$ is the repair coefficient matrix, representing the nodes affected by an outage of a branch when a replacement happens; $\boldsymbol{SC}$ is the switching coefficient matrix, which indicates the nodes with outage time equal to the expected branch switching times. $\boldsymbol{p_L} = [p_{L,1}, \dots, p_{L,n}]$ is the vector of yearly end-of-life failure probability for lines; $\boldsymbol{P_{DT}} = [p_{DT,1}, \dots, p_{DT,n}]$ is the vector of end-of-life failure probability for distribution transformers; $\boldsymbol{p_{ST}} = [p_{ST}, \dots, p_{ST}]$, vector of end-of-life failure probability for substation transformer; $\boldsymbol{d_L^e} = [d_{L,1}^e, \dots, d_{L,n}^e]$ is the expected replacement duration vector for lines; $\boldsymbol{s_L^e} = [s_{L,1}^e, \dots, s_{L,n}^e]$ is the expected switching duration vector; $\boldsymbol{d_{DT}^e} = [d_{DT,1}^e, \dots, d_{DT,n}^e]$ is the expected replacement duration vector for distribution transformers; $\boldsymbol{d_{ST}^e} = [d_{ST}^e, \dots, d_{ST}^e]$ is the expected replacement duration vector for the substation transformer.

The vector of expected ENS (in kWh) for each node due to end-of-life failure on transformers and lines is calculated by multiplying node unavailability with the average load $\widetilde{\boldsymbol{P}}$ (in kW).

$$\boldsymbol{ENS} = \boldsymbol{U_{node}} \circ \widetilde{\boldsymbol{P}} \tag{6.10}$$

6.2.2.2 Customer loss and power utility cost

Value of customer reliability VCR represents the willingness of customers to pay for a reliable electricity supply. VCR values are used by planners, asset owners, and regulators in balancing the cost of electricity with its value for various customers [265]. VCR values also help market operators, to find an economic balance between network cost and reliability. In the proposed procedure, VCR values, considering the type and proportion of loads, quantify the financial loss for customers due to lack of electricity. Total customer loss CL for a year due to end-of-life failure is expressed as

$$CL = \sum_{i=1}^{n} ENS_i \times VCR_i \tag{6.11}$$

where n is the number of buses; ENS_i and VCR_i are the ENS and VCR at bus i.

When an end-of-life failure happens in the network, the power utility needs to purchase new equipment and replace the damaged one. Assuming the cost for replacement of the *i*-th cable line, *i*-th distribution transformer and substation transformer are C_i^L, C_i^{DT} and C^{ST}, the yearly utility cost (UC) for managing end-of-life failure is

$$UC = \sum_{i=1}^{n}\left(C_i^L \times p_{L,i} + C_i^{DT} \times p_{DT,i}\right) + C^{ST} \times p_{ST} \tag{6.12}$$

6.2.3 Prediction Model of EV Charging Load

Travel open data of the National Household Travel Survey (NHTS) 2017 [266] is used to explore the driving patterns of drivers: the probability distribution functions (pdfs) of departure time and arrival time are derived, and a ML model is trained using the NHTS data. According to the specific characteristics of the test case, departure times and arrival times of each EV are generated by using pdfs and are provided as input to the pre-trained ML model to predict the daily travel distance. Considering the complete and uncoordinated home charging of EVs, the load demand and charging hours of each EV are estimated, as described below.

6.2.3.1 Distributions of departure time and arrival time

Travel distance is dependent on departure time, arrival time, the number of tours, and types of tours [260]. Departure time and arrival time are the essential factors for estimating travel mileage [267][268]. Therefore, probability distribution functions pdfs of departure time and arrival time need to be assessed. By analyzing the travel data, pdfs of the departure time and arrival time of vehicles fit normal distributions:

$$f_{dep}(t) = \frac{1}{\sigma_{dep}\sqrt{2\pi}} e^{-\left(t-\mu_{dep}\right)^2/2\sigma_{dep}^2}, 0 < t < 24 \quad (6.13)$$

where μ_{dep}= 9.21, and σ_{dep} = 3.04.

$$f_{arr}(t) = \frac{1}{\sigma_{arr}\sqrt{2\pi}} e^{-(t-\mu_{arr})^2/2\sigma_{arr}^2}, 0 < t < 24 \quad (6.14)$$

where μ_{arr} = 16.43, and σ_{arr}= 3.52.

6.2.3.2 Travel mileage representation using ML

ML models are popular tools commonly used in prediction and classification tasks. A multi-layer perceptron model (MLP) [269], with multiple hidden layers, is used to estimate travel mileages for all EVs. MLP is one type of ANN method. When the architecture contains multiple hidden layers, it can be classified as a Deep Learning [270] approach. The connections between the hidden layers and the nodes of MLP can identify the relationship between inputs and output [269][271][272] and predict with high accuracy.

MLP has been widely employed in the field of speech recognition, adaptive control systems, communication, robotics [273], localization and detection [274][275], fault classification [276], medical diagnosis [277], climate forecast [278] etc. The connections between the hidden layers and the nodes of MLP can identify the relationship between inputs and output [271][272]. A typical structure of the MLP with 2 outputs is depicted in Fig. 6.2, where the neurons are represented by circular nodes.

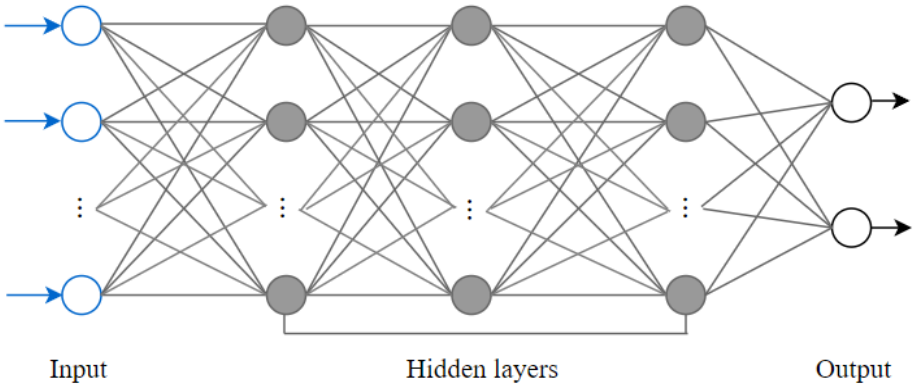

Fig. 6.2 Typical structure of MLP algorithm [277].

The Scikit-learn Python library is used to implement the MLP-based EV travel distance estimation according to the NHTS data. The input information includes the number, type, travel distance, departure time and arrival time of each trip, and the output is the total daily travel mileage of each EV.

Multiple MLP architectures were tested and the one with the best performance comprises 3 hidden layers with 100,100 and 50 nodes each. The activation function for each layer is 'RELU'. The optimizer is 'ADAM'. The MLP was trained using 100 epochs, and a batch size of 5 was used for training. For the accurate modelling of the users' behaviour and aligning with the practical experience, travel mileages exceeding 250 miles were removed from the original dataset. 80% of this reduced dataset was used for training and the remaining 20% for testing. The trained model is used to predict the travel milage using newly generated data according to the characteristics of the considered test cases.

To summarize, the ML algorithm is the following.

Algorithm: MLP method to predict the travel mileage

Input: 80% of the reduced dataset is for training, the rest of 20% is for testing, validation dataset generated by using the normal distributions of the original dataset

Output: Predicted mileage value for each input

1. Initialize

a. weight vector as W

b. minimization approach as MSE

c. optimization approach as ADAM

d. standardization as Standard Scaler

e. activation function as RELU

---

2. Apply Standard Scaler to the reduced dataset

3. While the error did not converge **do**

4. Train the MLP using W, MSE, ADAM, and RELU

5. End while

6. Use the trained model to predict travel mileage for each input of the validation dataset.

Evaluation indices of the MLP model are the correlation coefficient R2, mean squared error MSE, and mean absolute error MAE. The correlation coefficient determines the co-relationship or association between the variables. The higher R2, the higher the accuracy (a value equal to 1 indicates a perfect fit). Lower values of MSE and MAE indicate better prediction. The implemented MLP model provided perfect test accuracy with approximately 1.0000, 0.0035, and 0.0124 for R2, MSE, and MAE, respectively, yielding a very low error rate. Fig. 6.3 depicts the regression analysis between the mileage predicted by the MLP model and the actual mileage extracted from the dataset.

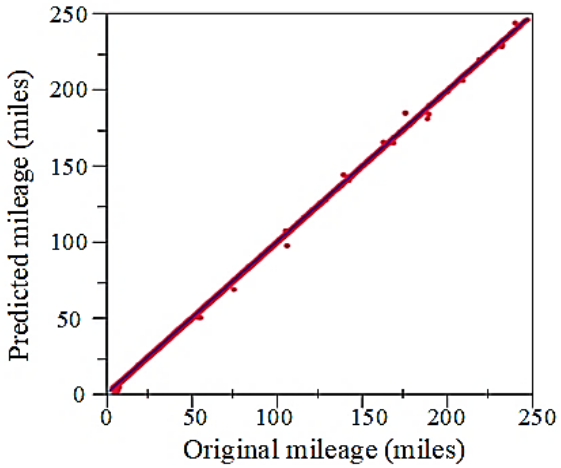

Fig. 6.3 Predicted mileage vs. actual mileage.

6.2.3.3 State-of-charge and expected EV charging load

According to [267][268], with the knowledge of the daily travel mileage (d) for each EV provided by the MLP model, state-of-charge level SoC and energy need to be charged E_{req} can be calculated by

$$SoC = \frac{D_N - \omega \cdot d}{D_N} \tag{6.15}$$

$$E_{req} = (1 - SoC) \cdot C_N \tag{6.16}$$

where ω shows the type of EV, D_N and C_N are the rated travel mileage and rated capacity. In the considered test cases, all the EVs are assumed to be battery electric vehicles (BEVs) and charged at rated power (i.e., the charging time is the ratio between the energy required and rated power). No smart charging/discharging algorithm is considered in this chapter. EV penetration ρ is defined as

$$\rho = \frac{N_{EV}}{N_{cust}} \times 100\% \tag{6.17}$$

where N_{EV} is the number of EVs, and N_{cust} is the number of customer houses. For instance, each house has two EVs on average when ρ is 200%. Uniform EV penetrations for all the nodes, between 0% to 200%, are considered in Section 6.3. In summary, the detailed procedures for the aggregated EV charging load estimation are shown in Fig. 6.4.

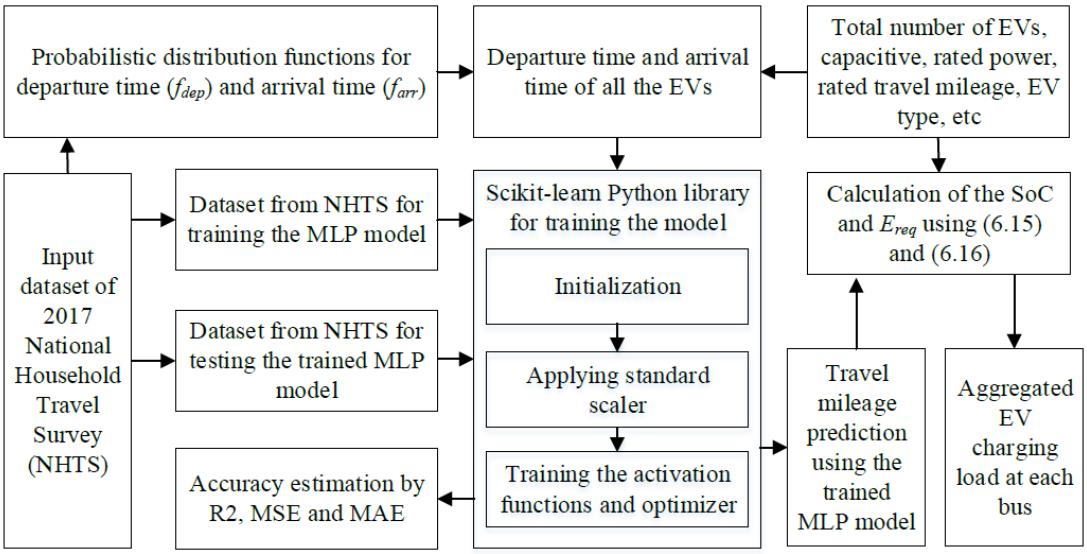

Fig. 6.4 Detailed procedures for EV charging load estimation.

Compared with other EV load estimation methodologies, the proposed method is based on the realistic dataset (2017 NHTS by the Department of Transportation of the United States) with a considerable size of data. Moreover, the original dataset has been modified to better align with the practical experience of EV users. The proposed MLP model can capture the driving behaviours of drivers with high accuracy in the estimation results. The mature Python library is available for training the model and more factors (e.g., diversity of trips,) can be easily integrated into the model to better study the driving patterns of EV owners.

6.3 Test Cases and Load Profile

6.3.1 Test Cases

Two test cases are considered: Case 1 uses a simple 5-bus network [241], and Case 2 is based on the IEEE 123-bus distribution test system [279], which shows the feasibility of the proposed method in a complex network. The detailed application of the method is described for Case1, while the reliability indices only are presented for Case 2. Test network configurations, the parameters of transformers and lines, and the clustered load profiles are described in this section.

(1) Case 1: 5-bus network

The 5-bus network is shown in Fig. 6.5, which includes 1 slack bus, 5 nodes, and 5 cables. A substation transformer (ST) is located at the slack bus. Distribution transformers (DT) are connected to the other buses. There is 1 circuit breaker at branch 1, a manual switch at branch 3, and two fuses at branches 4 and 5. Table 6.1 shows the number of customers, rated active power (P), and weighted VCR values at each bus [28]. DT sizes are 250, 200, 300, 150 and 150 kW for transformers from 1 to 5, respectively, assuming a unitary power factor for simplicity. The model parameters of transformers and cable lines are adapted from [118][120][261].

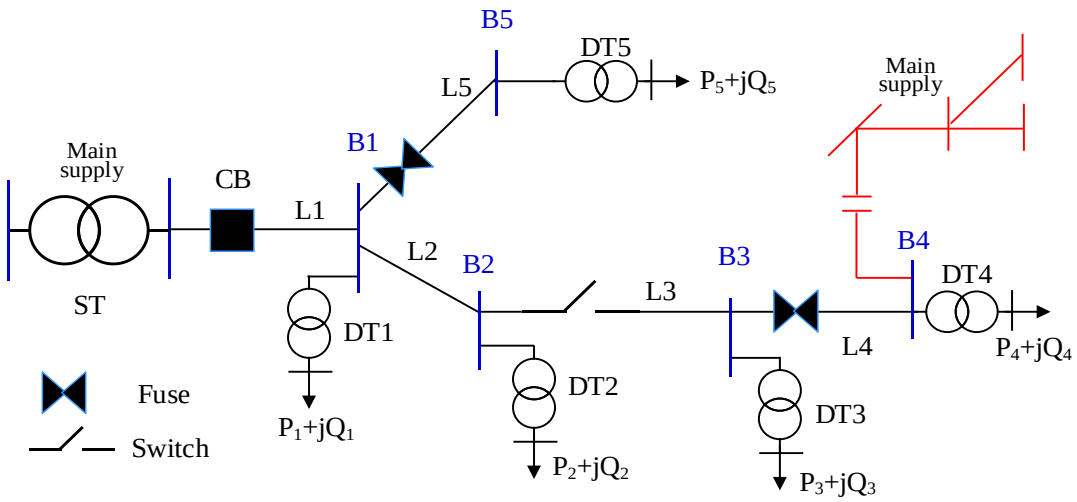

Fig. 6.5 Sample 5-bus network configuration [241].

Table 6.1 Bus Data of the test system

Parameter	Bus 1	Bus 2	Bus 3	Bus 4	Bus 5
No. of customer	50	40	60	30	30
Load P (kW)	200	160	240	120	120
VCR (AUD/kWh)	37.21	36.38	38.46	25.95	25.95

Table 6.2 Replacement Duration and Tripping Time

d^{L} (h)	d^{DT} (h)	d^{ST}(h)	s^{L} (h)
20	20	30	0.5

The lifespan for transformers is 180,000 hours for a rated temperature θ_r^T of 110 ºC, and the nominal lifespan for lines is 175,200 hours operating with a rated temperature θ_r^L of 80 ºC. Table 6.2 shows the replacement hours of ST and DT transformers and lines (i.e. d_{ST}, d_{DT}, and d_L, respectively) and the tripping time of protecting devices (i.e., s_L). Table 6.3 explains the power utility cost for replacing cable lines and transformers, considering the equipment and installation costs [280].

Table 6.3 Replacement Cost for Cables and Transformers

No.	1	2	3	4	5
L (kAUD)	66	132	98	102	186
DT (kAUD)	70	70	76	70	70
ST (kAUD)	200	—	—	—	—

Using the EV prediction model described in Section 6.2.3, the EV charging load profile at nodes 1 and 5 for Case 1 is shown in Fig. 6.8, supposing the nominal capacity, charging power, and travel mileage are 40 kWh, 10 kW, and 120 miles, respectively.

(2) Case 2: IEEE 123-bus network

The considered IEEE 123-bus network configuration contains 12 switches and 1 voltage regulator, as shown in Fig. 6.6. The switches are located at branches 121, 18, 25, 47, 72, 77, 87, 108, 115, 116, 117, and 118 (branch number is defined as the number of the corresponding ending bus). Every node has the same load variation profile, and every cable has the same current-carrying capacity at the reference ambient temperature, according to [279].

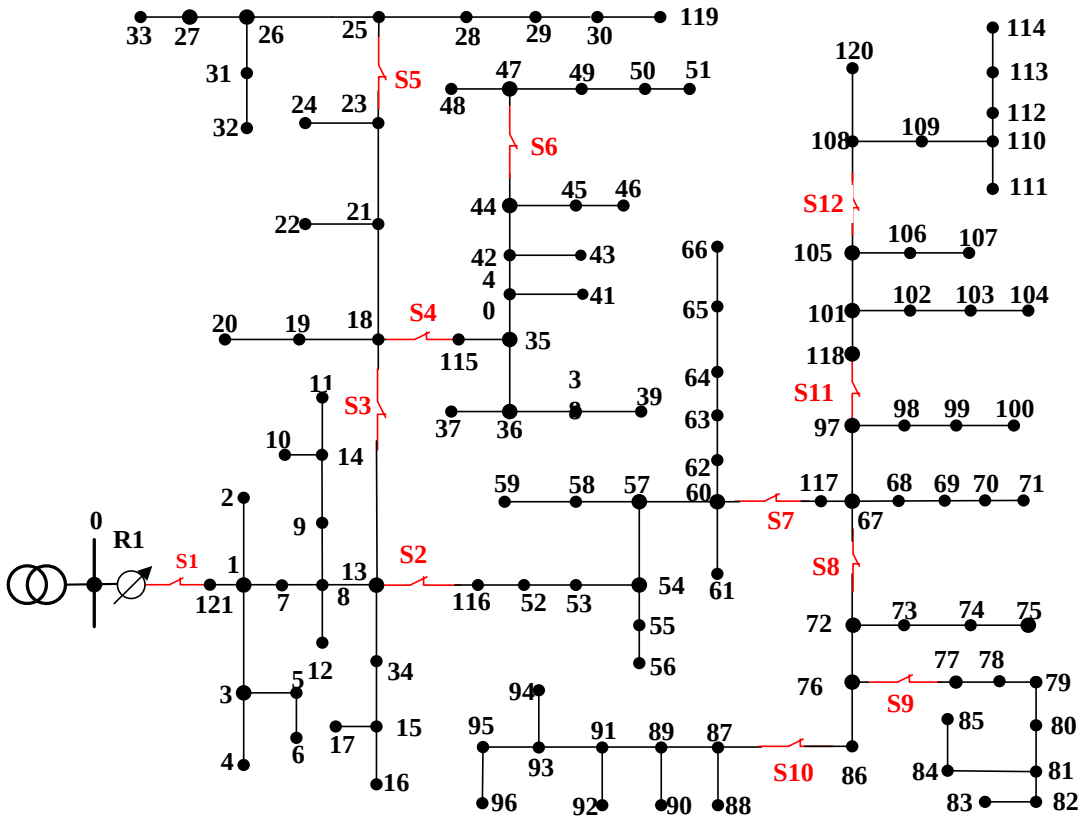

Fig. 6.6 Modified IEEE 123-bus network configuration.

6.3.2 Load Profile and EV Charging Load

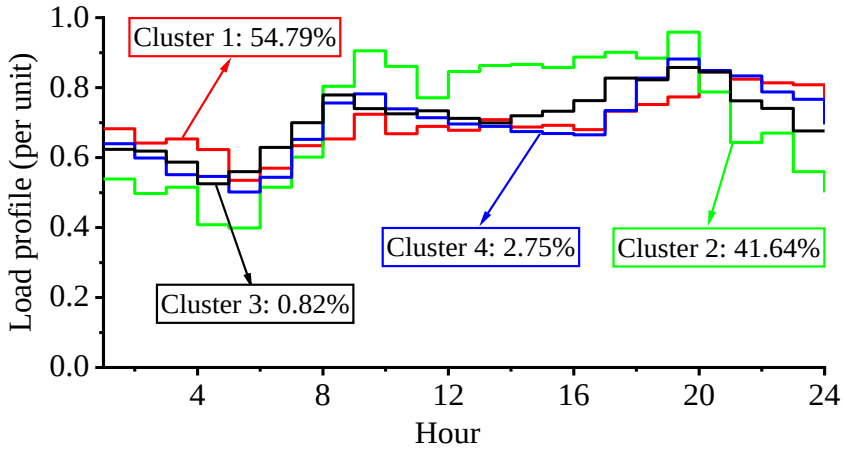

Fig. 6.7 Load profile for Case 1 and Case 2 without EV [231].

Fig. 6.7 shows the clustered load profile (4 typical days) without EV integration for a year from [231]. It contains four clusters with probabilities of 54.79%, 41.64%, 0.82%

and 2.75%, respectively. Using the EV prediction model described in Section 6.2, the EV charging load profile at nodes 1 and 5 for Case 1 is shown in Fig. 6.8, supposing the nominal capacity, charging power, and travel mileage are 40 kWh, 10 kW, and 120 miles, respectively. The EV charging load profile for Case 2 is obtained with the same procedure.

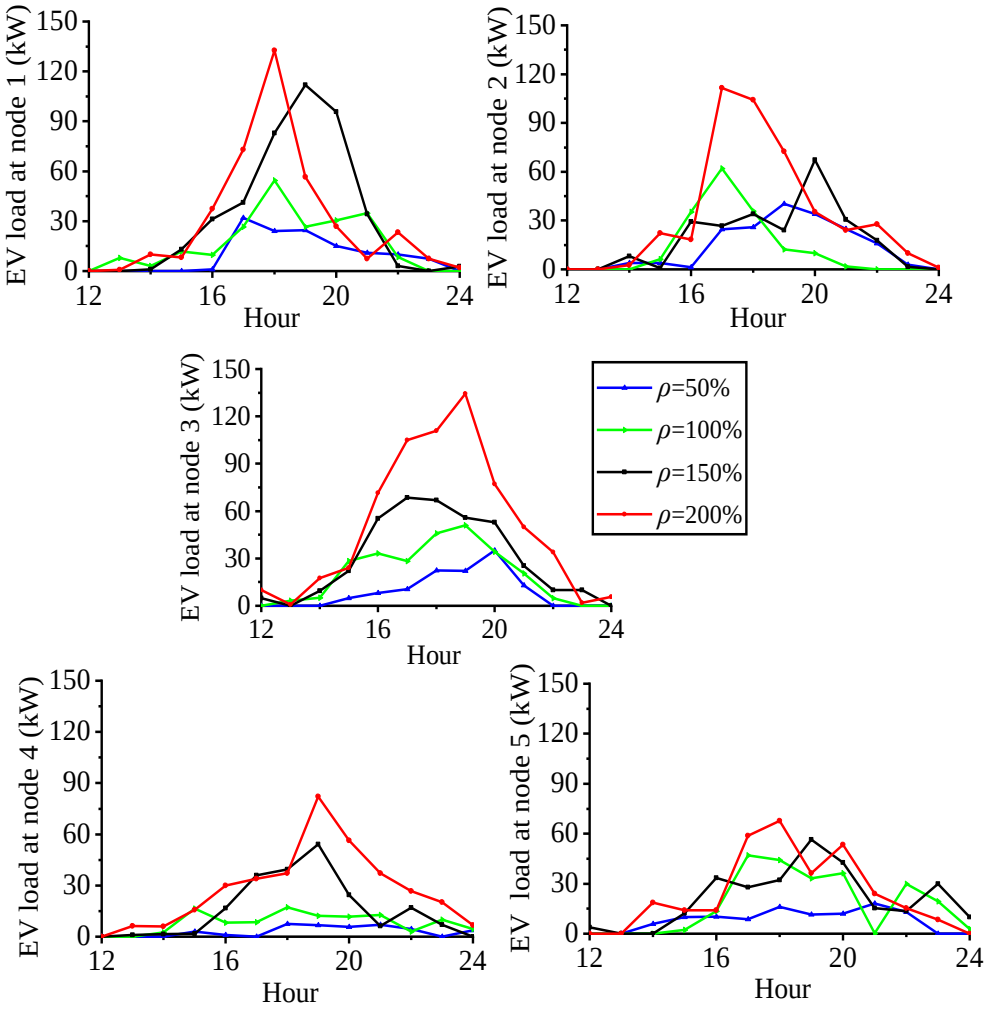

Fig. 6.8 Example EV charging load profile for Case 1.

6.4 Simulation Results

6.4.1 Simulation Results of Case 1

For Case 1, this section compares the results of end-of-life failure probabilities calculated by using the method and the traditional method. Detailed results, including end-of-life failure and network reliability indices, are presented and discussed.

6.4.1.1 Comparison of traditional method and method in [261]

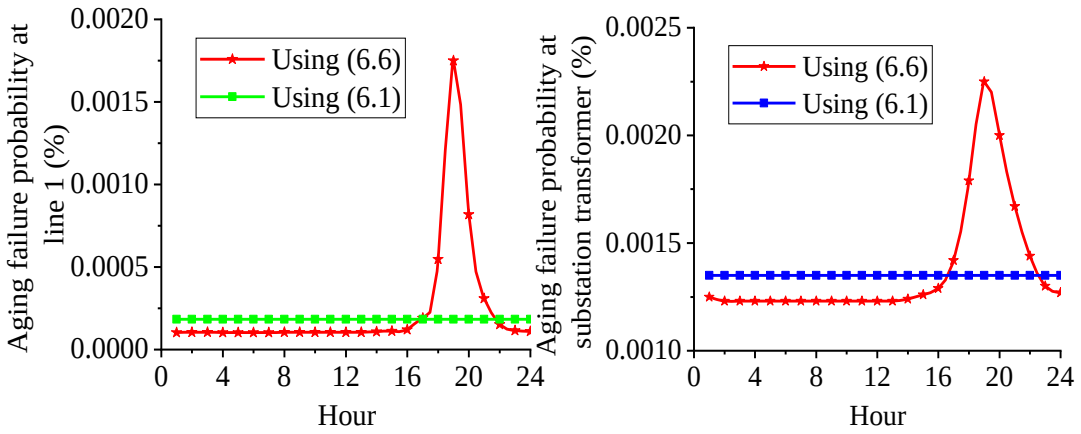

Fig. 6.9 End-of-life failure probabilities on line 1 and substation transformer.

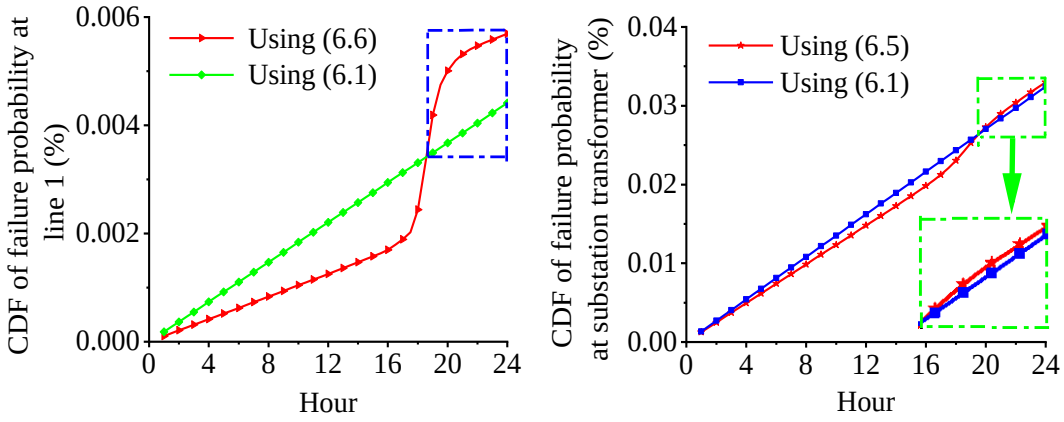

Fig. 6.10 CDF of end-of-life failure probabilities on line 1 and substation transformer.

The simulation results of a single day using (6.1) are compared with the results using (6.5) and (6.6) for aging failure probability and CDF of failure probability, respectively, as shown in Fig. 6.9 and Fig. 6.10. To calculate the end-of-life failure probability using (6.1), we need to determine the R and the predicted lifespan of a component. Assuming the average temperatures are 55.8℃ and 45℃ for line 1 and substation transformer, then the end-of-life failure probabilities and CDF are evaluated. Equation (6.1) presents an almost constant failure probability at each interval as the variation of the aging speeds is not considered for line and transformer. The load peak occurs from 17.00-21.00, and failure probability is expected to be higher during this period.

6.4.1.2 Loss-of-life and end-of-life failure probability

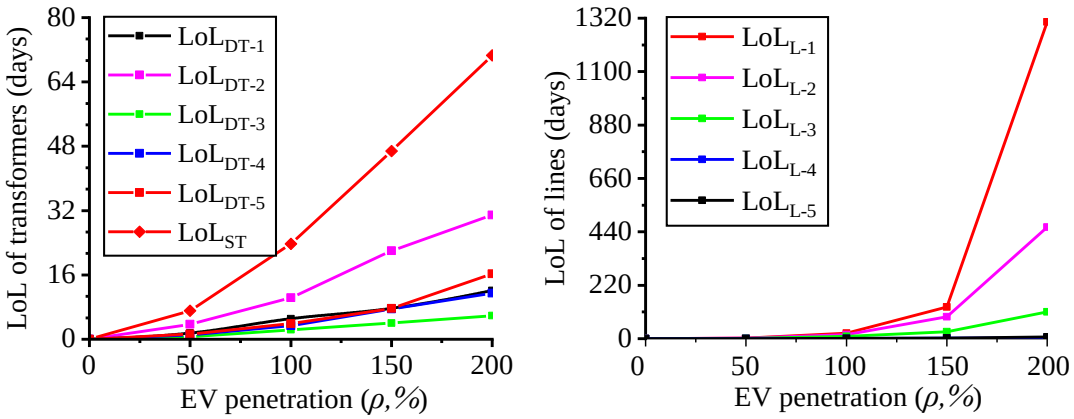

Fig. 6.11 Yearly LoL of transformers and lines due to different EV penetrations.

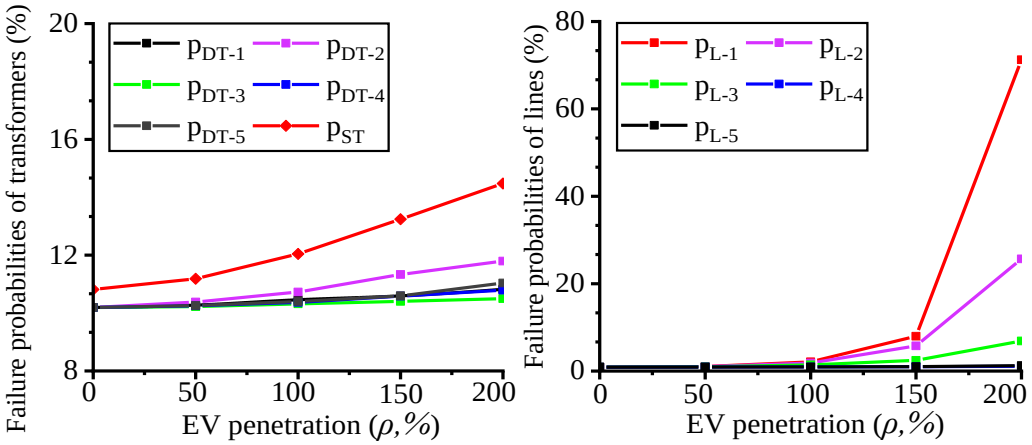

Fig. 6.12 Yearly end-of-life failure probability of transformers and cable lines.

The LoL and end-of-life failure probabilities of transformers and lines with growing EV penetration are shown in Figs 6.11 and 6.12, with T_0 = 165000 hours indicating the relative functional age (in hours) with respect to the rated lifespan. The results show that increasing EV penetration has growing impacts on the substation transformer, particularly for line 1 and line 2. The maximum LoL of the substation transformer and line 1 are expected to reach 70.6 and 1304.5 days when EV penetration is 200%. The failure probabilities on the substation transformer, line 1 and line 2 for a year are 14.5%, 71.3%, and 25.7% with 200% EV penetration, respectively. Equipment capacities also impact failure probabilities: the larger capacity, the lower failure probability.

6.4.1.3 Expected ENS, customer loss and utility cost

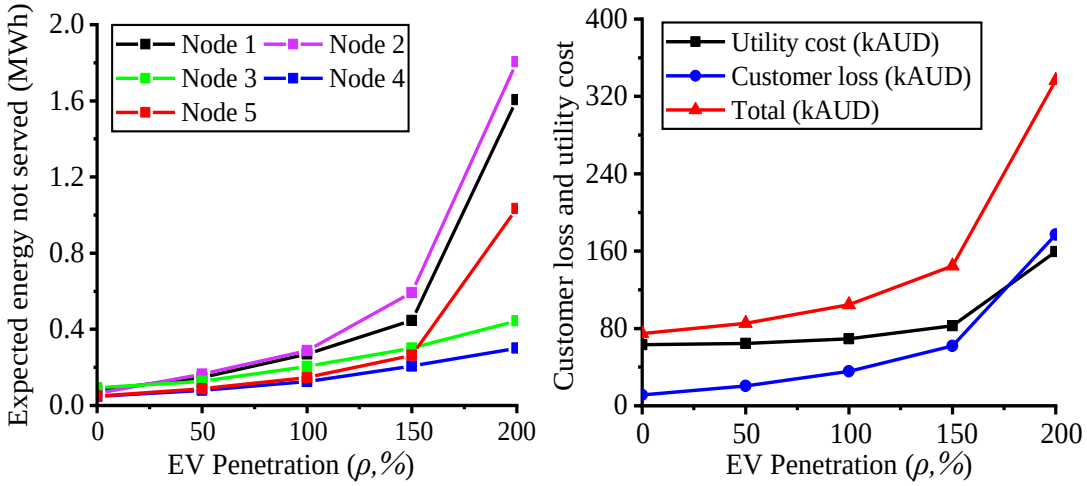

Fig. 6.13 Yearly expected ENS, CL and UC using the proposed method.

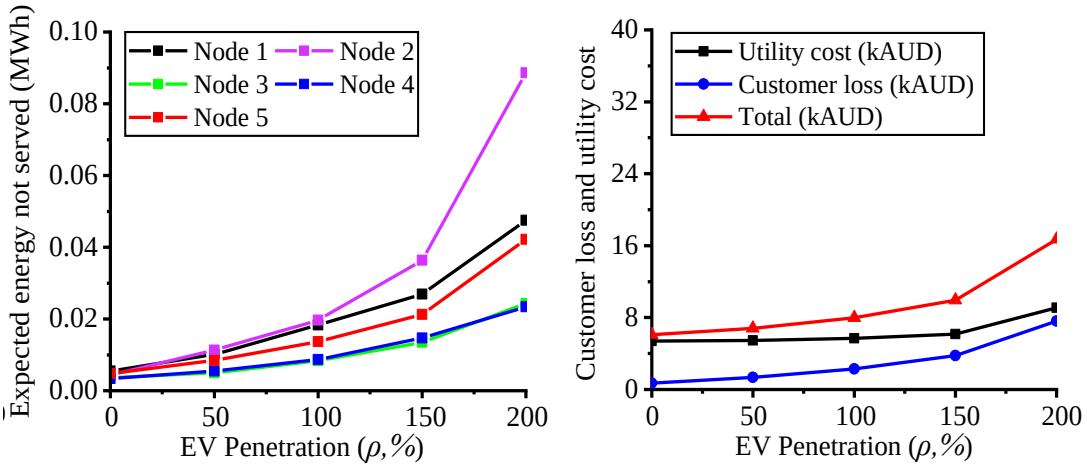

Fig. 6.14 Yearly expected ENS, CL and UC using the traditional method.

Assuming again T_0 = 165000 hours, Fig. 6.13 shows both the expected ENS and the customer loss at each bus, as well as the utility cost due to end-of-life failures. The results show that buses 1 and 2 have the highest unavailability, expected ENS, and customer loss. Although bus 3 has the maximum load, the reliability is also dependent on the network topology and configuration of tripping devices. As expected, all the indices increase with growing EV penetration. For example, total customer loss and utility cost due to end-of-life failure with 200% EV penetration is 159.3 kAUD and 177.2 kAUD, respectively.

For comparison, Fig. 6.14 shows the values of reliability indices obtained by the traditional method, based on the failure probabilities on cable lines and transformer

using (6.1) and survivor function based on Arrhenius-Weibull distribution and the resolution. In the results of Fig. 6.13, the impact of EV integration on end-of-life failure is only partially represented, as the loading enhancement due to EV charging during peak hours is not accurately considered.

6.4.1.4 Impacts of survival hour

According to (6.5)-(6.6), T_0 influences the failure probability to a great extent. Generally, T_0 depends on load history, maintenance history, and equipment status. The influence of T_0 on end-of-life failure probabilities for transformers and cable lines of Case 1 with 200% EV penetration are shown in Fig. 6.15. As expected, failure probabilities increase as T_0 grows.

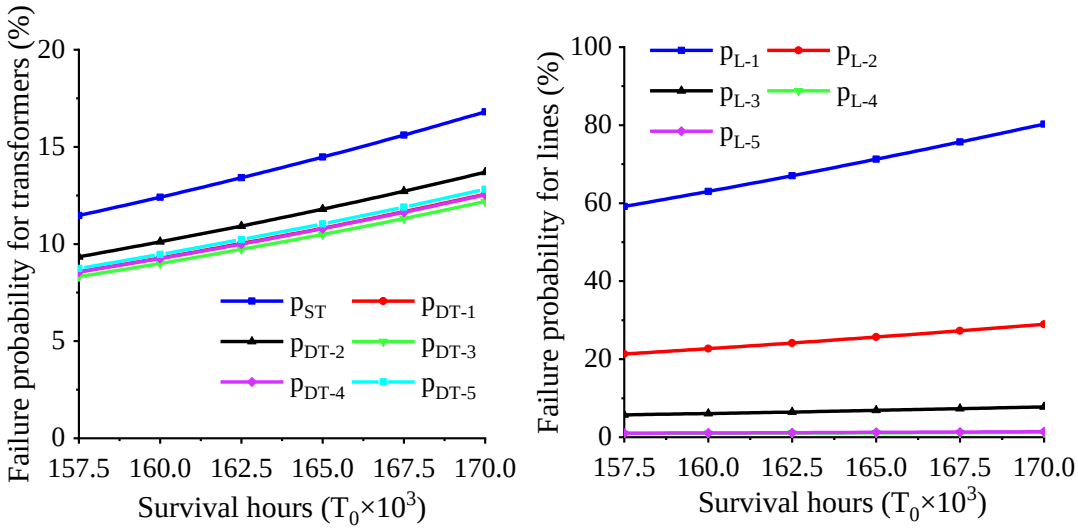

Fig. 6.15 End-of-life failure probabilities of transformers and cable lines.

Tables 6.4-6.6 present the yearly unavailability, expected ENS, customer loss and utility cost, assuming different values of T_0 and EV penetration is equal to 200%. Simulation results confirm that longer T_0 values result in lower reliability and higher customer losses. Long T_0 means the equipment comes closer to its end of life, therefore, the end-of-life failure probability is high.

The results show that the unavailability at buses 1, 2, and 5 is higher compared with buses 3 and 4, reaching 30 hours from 22 hours when T_0 is 157,500 hours. The total expected ENS increases from 4.25 MWh to 5.91 MWh, and total customer loss and

utility cost is reaching 384 kAUD when T_0 grows from 157,500 hours to 170,000 hours.

Table 6.4 Unavailability for a Year

Unavailability (hours)	T_0: Survival hour (10^3 hours)					
	157.5	160	162.5	165	167.5	170
Bus 1	21.28	22.75	24.3	25.93	27.64	29.44
Bus 2	21.44	22.92	24.48	26.12	27.85	29.66
Bus 3	6.65	7.17	7.72	8.30	8.92	9.58
Bus 4	6.88	7.41	7.98	8.58	9.22	9.89
Bus 5	21.52	23.01	24.58	26.22	27.95	29.77

Table 6.5 Expected ENS for a Year

ENS (MWh)	T_0: Survival hour (10^3 hours)					
	157.5	160	162.5	165	167.5	170
Bus 1	1.32	1.41	1.50	1.61	1.71	1.82
Bus 2	1.48	1.58	1.69	1.81	1.92	2.05
Bus 3	0.36	0.39	0.41	0.45	0.48	0.51
Bus 4	0.24	0.26	0.28	0.30	0.32	0.35
Bus 5	0.85	0.91	0.97	1.03	1.10	1.17
Total	4.25	4.54	4.86	5.19	5.54	5.91

Table 6.6 Customer Loss and Utility Cost for a Year

Parameter (k AUD)	T_0: Survival hour (10^3 hours)					
	157.5	160	162.5	165	167.5	170
CL	145	155	166	177	189	202
UC	130	139	149	159	170	182
Total	275	294	315	336	359	384

6.4.2 Integrated Impact from EV Penetration and Survival Hour

This section presents the yearly end-of-life failure probabilities of distribution transformers and lines, node unavailability, expected ENS, and customer loss considering the integrated impact of different EV penetration and survival hours. Fig. 6.16 and Fig. 6.17 show the yearly failure probability of the substation transformer, distribution transformers and cables. Increasing the penetration of EVs and growing

T_0 have heavier impacts on the failure probabilities on the substation transformer, distribution transformer 2 and line 1.

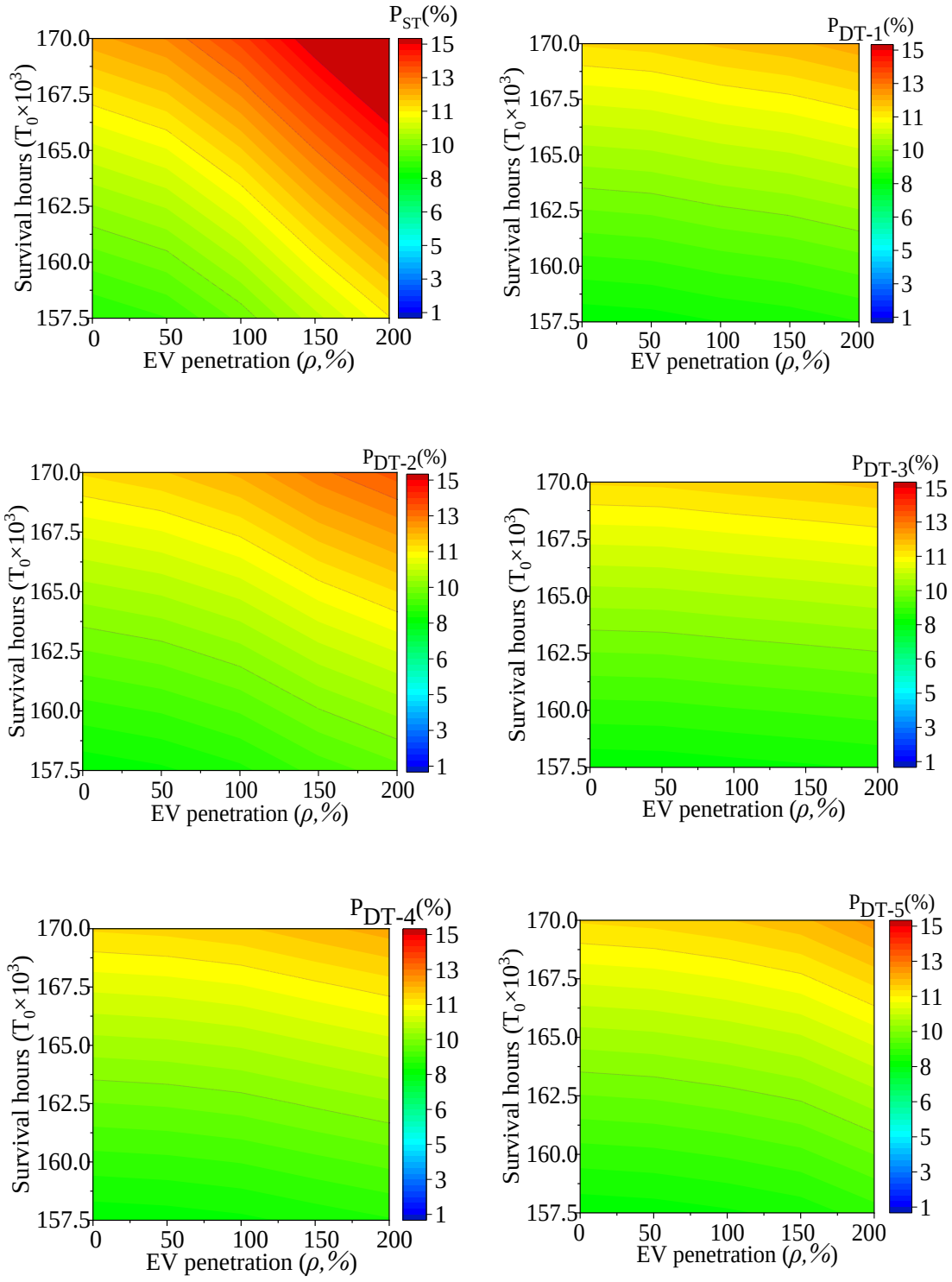

Fig. 6.16 Yearly failure probability of substation and distribution transformers.

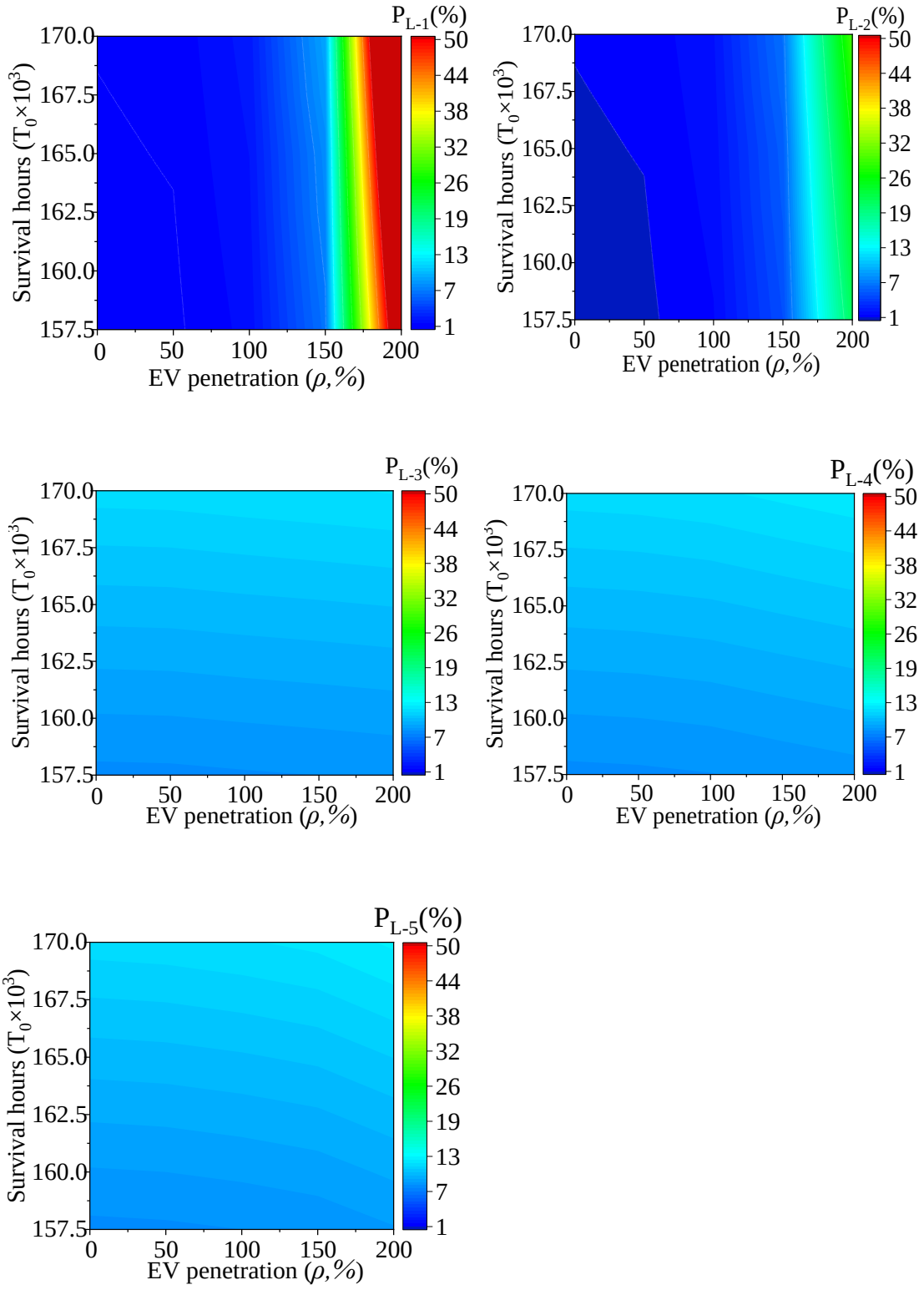

Fig. 6.17 Yearly failure probability of lines 1-5.

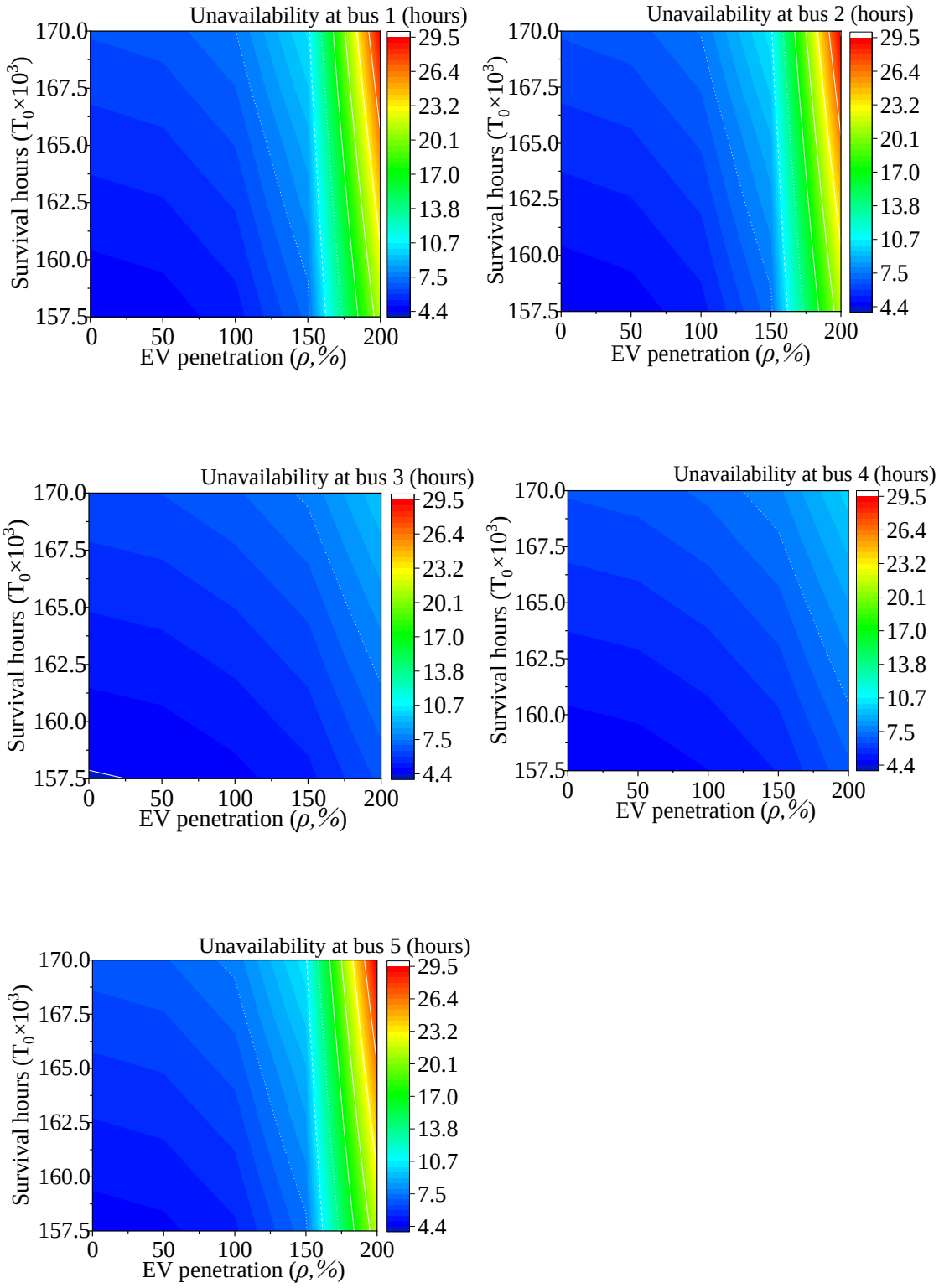

Fig. 6.18 Yearly unavailability at buses 1-5.

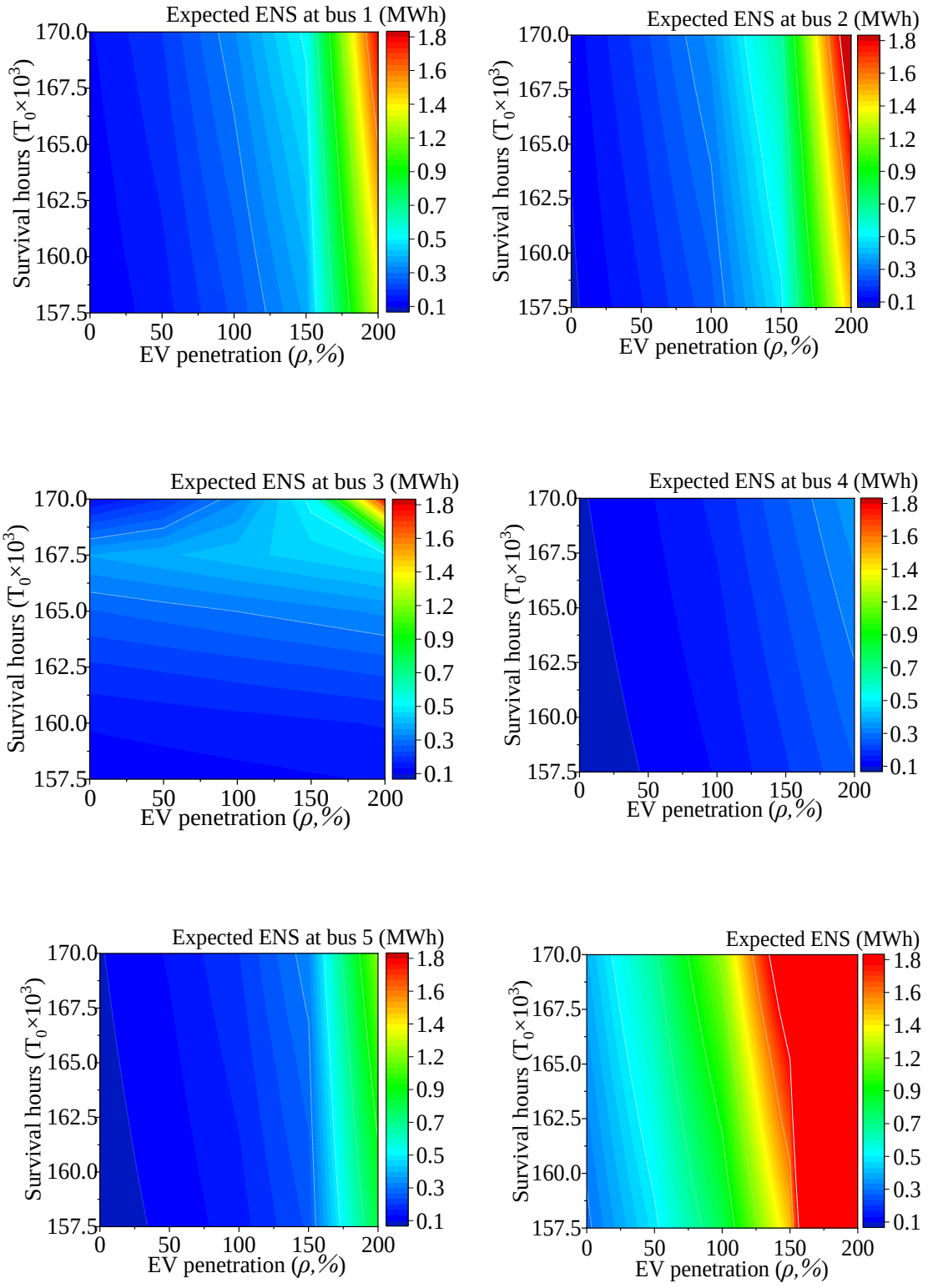

Fig. 6.19 Yearly expected ENS at buses 1-5 and the whole network.

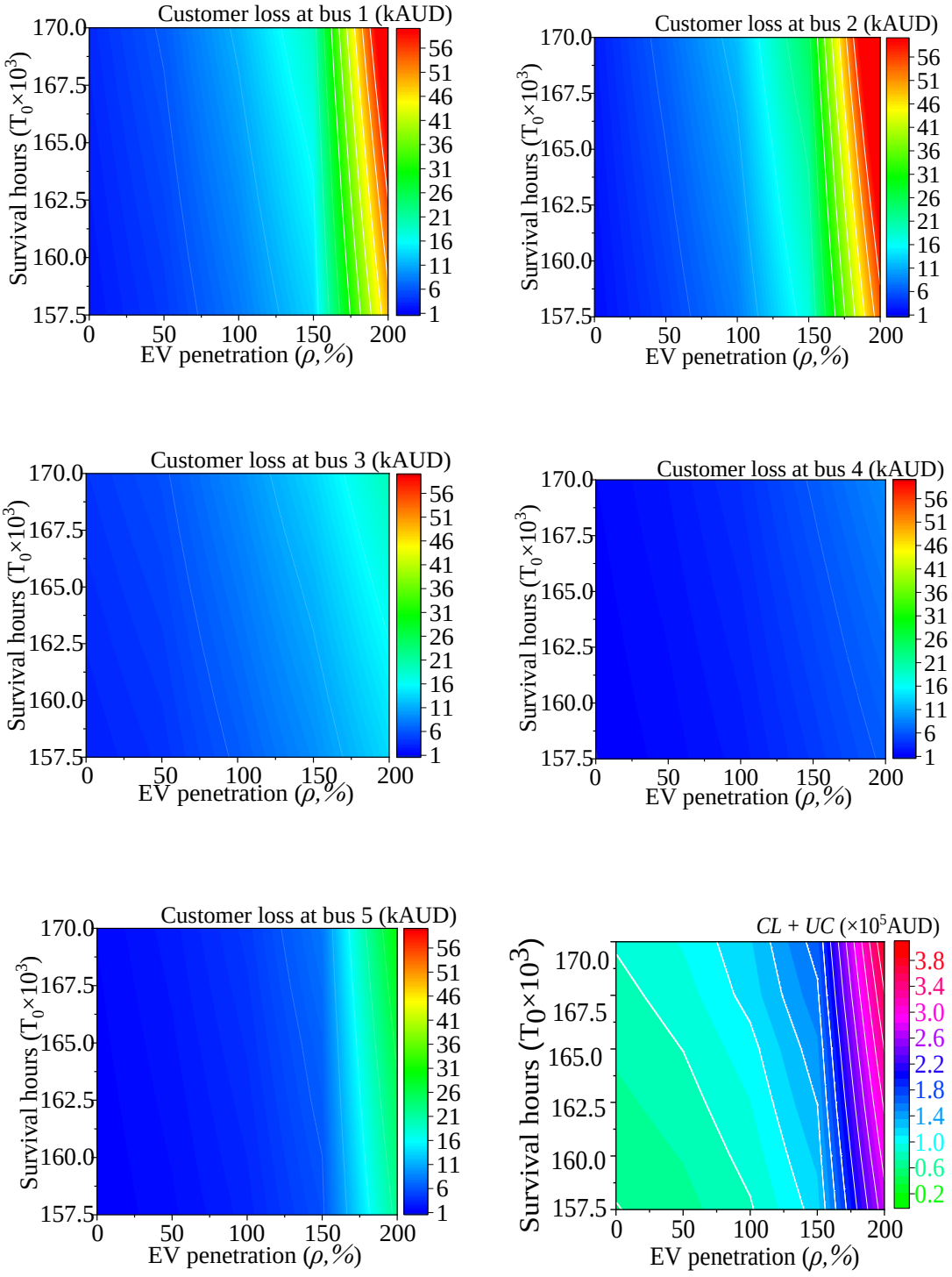

Fig. 6.20 Yearly customer loss at buses 1-5 and the whole network.

Fig. 6.18 explains the yearly unavailability of buses 1-5. Due to the network configuration and locations of the tripping devices, buses 1, 2 and 5 have higher

unavailability compared with buses 3 and 4. Fig. 6.19 and Fig. 6.20 are the yearly expected ENS and customer losses at different buses considering different EV penetrations and T_0. Notably, the expected ENS and total customer loss of the whole network are also presented. As expected, failure probabilities increase as EV penetration or T_0 increase, as well as ENS and customer loss.

6.4.3 Simulation Results of Case 2

This Section presents network reliability indices considering different EV penetration on IEEE 123-bus distribution test feeders. Fig. 6.21 shows the unavailability and expected ENS at each node when the EV penetration varies from 0% to 200%. Although network configuration and average load influence the values of these indices, the reliability is always decreasing when EV penetration values increase, as expected. It is worth mentioning that lower ENS with 100% EV penetration compared with 50% at bus 65 is due to separate EV data used for different penetrations, e.g., the estimated EV load is 53 kW and 30 kW with 50% and 100% penetration.

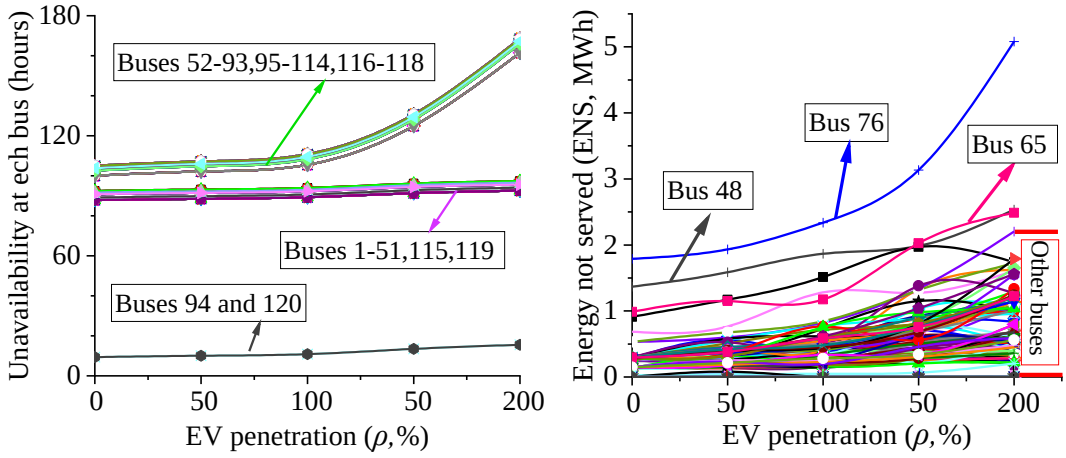

Fig. 6.21 Unavailability and ENS of each bus with different EV penetrations.

Fig. 6.22 shows the reliability indices and the impacts of EV penetration and survival hours for Case 2. The average unavailability, total expected ENS and total customer loss are considered the reliability indices. The EV penetration shows a nonlinear positive correlation with the reliability indices. Similarly, all the reliability indices increase with longer survival hours. The simulations validate the accuracy and effectiveness of the proposed end-of-life failure probabilistic models in the reliability calculation of a complex network.

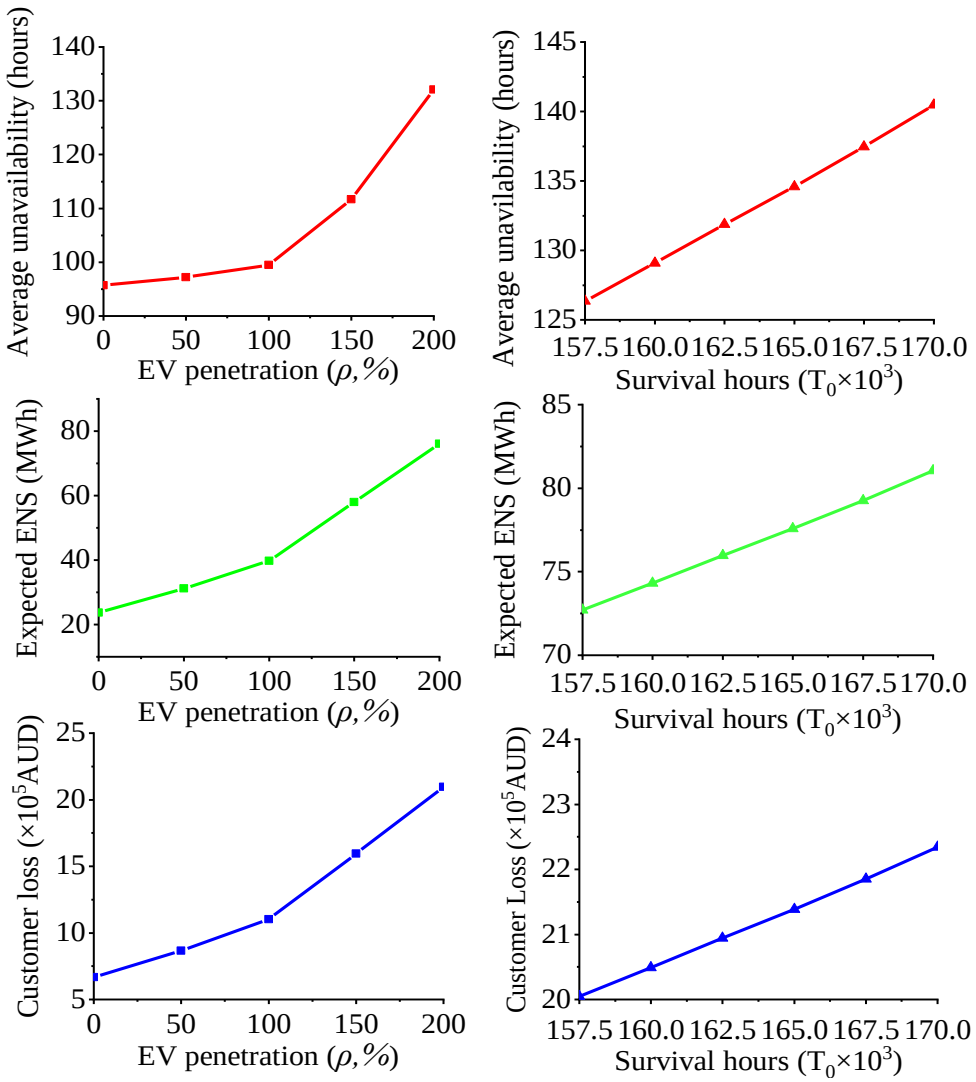

Fig. 6.22 Network reliability indices for Case 2.

6.5 Summary

To quantify the impact of significant EV charging load in distribution networks, this paper presents the end-of-life failure models of transformer and line that include relative aging speed and real-time loss-of-load into Arrhenius-Weibull distribution-based models. An accurate machine learning model of EV charging load is developed and used to generate realistic load demand due to the EV charging process. Network reliability indices due to end-of-life failure are calculated and the costs associated with energy not supplied for customers and equipment replacement for utility are obtained for two case studies.

The comparison between the results obtained using the proposed approach and the

traditional one shows that the proposed method is suitable for an accurate quantification of EV penetration impact. Results show that increasing the penetration of EVs aggravates the aging process and LoL, leading to higher end-of-life failure probabilities on transformers and cable lines. Thus, high EV penetration results in lower system reliability and higher cost for managing end-of-life failures. Moreover, higher survival hours have a similar impact on the probability of end-of-life failure and system reliability.

The proposed method is also useful for estimating residual lives and vulnerabilities of transformers and lines, thus providing valuable information for network planning and update, regulation, and investment decisions.

Chapter 7 An Optimization Procedure for Reliability Improvement and Cost Reduction Assessment Achievable through EV Smart Charging[5]

There is a general concern that increasing penetration of electric vehicles (EVs) will result in higher aging failure probability of equipment and lower network reliability. Also, the electricity costs may increase, due to the exacerbation of peak load led by unmodified EV fast charging. This chapter proposes a linear optimization model for the assessment of the benefits of EV smart charging on network reliability improvement and electricity cost reduction. The proposed optimization model aims at minimizing the loss of load due to aging failures and the power utility costs for repairing failures due to aging, other than the costs associated with EV charging. The approach adopts a piecewise linear model for the probabilistic representation of aging failures and a machine learning algorithm to represent the EV charging load. The total costs related to aging failure under three scenarios with/without EV smart charging are compared.

7.1 Introduction

Power utilities need to maintain a certain level of reliability for the electrical energy supply in distribution networks and with reasonable costs [177]. Aging failures of equipment are typically the main reason for low reliability and poor power quality

[5] This chapter is based on the paper J. Zhao, A. Arefi, A. Borghetti, and G. Ledwich, , "An Optimization Procedure for Reliability Improvement and Cost Reduction Assessment Achievable through EV Smart Charging" under preparation for submission.

[281].

The wide use of electric vehicles (EVs) is seen as a major contribution to sustainable global development [149]. However, higher loading by the increasing penetration of EVs may weaken system reliability, if adequate procedures are not applied to limit the impact of EV charging and discharging [282]. Effective reliability evaluation and reliability optimization strategy are essential tasks for power system operators and planners in the presence of extended integration of EVs. Additionally, the exacerbation of the peak period led by random EV charging results in higher payments from power utilities to wholesale electricity markets due to price fluctuation.

Reliability is defined as the probability of providing adequate electricity to the load with decent power quality in the planned time [155] and is normally described by the values of specific indices. The widely used indices for the reliability level are: system average interruption duration (SAIDI), system average interruption frequency (SAIFI), expected energy not supplied (EENS), loss of load probability (LOLP), customer interruption frequency (CIF), and customer interruption duration (CID) [139][156][170][283]. The reliability improvement methods can be divided as direct and indirect according to the objective functions of the regulating schemes: direct methods [152][158][181] try to maximize the system reliability, indirect methods [159][160][161] aim at improving network operation and performance by reducing power loss and enhancing voltage magnitude and balance.

From the perspective of investment by power utilities, reliability enhancement methods can also be classified into three groups: cost-free methods (flexibility-based), non-cost-free methods (technical method), and hybrid methods. Typical cost-free methods balance power supply and demand during contingencies by scheduling load and generation, including distributed generation (DG), demand response (DR), and smart EV charging/discharging. Within this framework, the impact of DG on network reliability is analyzed in [284] and a trade-off is determined between reliability and costs to achieve the maximum reliability level during contingencies. A load control algorithm by smart EV charging/discharging and DR is proposed in [166][285] to relieve peak loads and, therefore, improve system reliability. Non-cost-free methods involve investments in purchasing and/or operation of specific devices, such as protective devices (recloser, circuit breaker and fuse), switches, and tie lines to improve the network reconfiguration after a fault, and DSTATCOM [241][280].

Hybrid methods employ include both non-cost-free and cost-free countermeasures. For instance, in [189], the combination of DG and cross-connections is used to optimize system reliability.

Given the significant impact on system reliability, as analyzed in [283][160][286], and the expected increasing penetration of EVs, smart charging of EVs needs to be prioritized. Previous studies compare the reliability indices of LOLP and EENS with uncontrolled charging and smart charging [204], propose a time allocation of home charging and public charging [285], quantify the maximum permissible EV load that a system can tolerate without reliability degradation [111][287], propose bidirectional control strategies for EV charging stations [288], or focus on the optimal allocation of EV charging station [6][289]. Car parks with a large number of EVs are considered a backup energy source to support the grid in the event of feeder failure or feeder component failure [167].

To the best of our knowledge, only sudden failures (repairable failure), either represented by a constant failure probability or by using Monte-Carlo simulations, have been considered so far. Aging failures of cables and transformers due to degradation of insulation materials are in general overlooked, although lead to a considerable loss for the customers [119][290]. The uncontrolled home charging of EVs may heavily exacerbates the evening peak load [268]. As shown in [281] the increasing loading due to high EV penetrations shortens the lifespan of equipment and increases network unavailability.

This chapter focuses on the effects of aging failures due to the increasing integration of EVs. The EV charging demand is represented by the prediction of travel distance using a machine learning algorithm. An optimization procedure is proposed for the assessment of the effects of EV smart charging on system reliability enhancement. The proposed optimization is formulated as a mixed-integer quadratically-constrained programming (MIQCP) model that is solved by Gurobi 9.1. The model includes a piecewise linear representation of aging failure probabilities of transformers and cables. The objective function is given by the customer loss and the power utility total cost, including the costs associated with aging failures, power loss and EV charging. The main constraints of the optimization problem are associated with the power flow model, EV charging, and the proposed piecewise linear model for aging failure estimation.

The structure of the procedure is illustrated in Fig. 7.1.

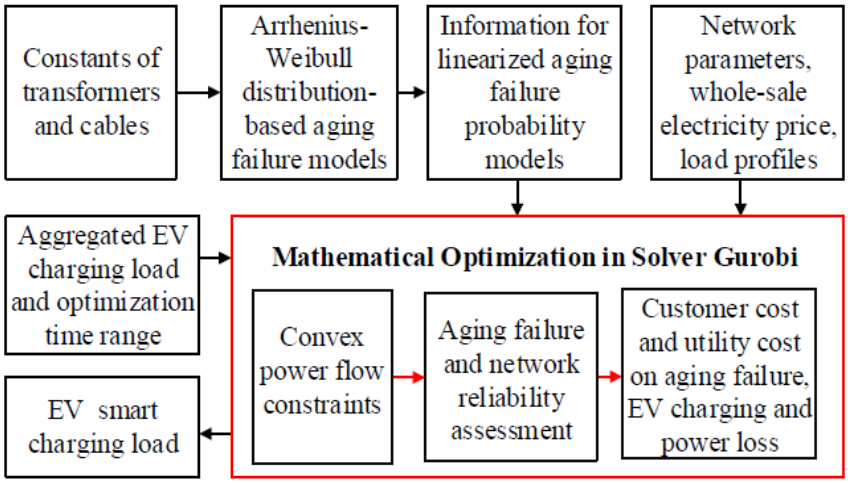

Fig. 7.1 Framework of the proposed reliability optimization model.

This chapter is structured as follows. Section 7.2 presents the formulation of the optimization problem. Section 7.3 describes the test network, normal load demand, EV profiles, and the aging failure probability model. Section 7.4 presents and analyses the simulation results. Section 7.5 summarizes and concludes the whole chapter.

7.2 Problem Formulation

Considering *N* (with index *i*) as the set of feeder buses (the customers at each bus are aggregated, as well as their EVs, and $i = N + 1$ indicates the substation transformer) and *Ts* (with index *j*) as the set of time slots in the optimization horizon, the variables of the model are grouped as follows

$$\boldsymbol{\pi_1} = \left\{E_{ij}, E_{ij}^{req}, P_{ij}^{EV}, P_{ij}^{max} \mid \forall\, i \in N, \forall\, j \in T_s\right\} \tag{7.1}$$

$$\boldsymbol{\pi_2} = \left\{P_{ij}, Q_{ij}, V_{ij}, B_{ij} \mid \forall\, i \in N, \forall\, j \in T_s\right\} \tag{7.2}$$

$$\boldsymbol{\pi_3} = \left\{\lambda_{ije}^{L}, p_{ije}^{L}, p_i^{L} \mid \forall\, i \in N, \forall\, j \in T_s, \forall\, e \in N_s^{L}\right\} \tag{7.3}$$

$$\boldsymbol{\pi_4} = \left\{\lambda_{ije}^{T}, p_{ije}^{T}, p_i^{T} \mid \forall\, i \in N+1, \forall j \in T_s, \forall\, e \in N_s^{T}\right\} \tag{7.4}$$

where,

$\boldsymbol{\pi_1}$ are the variables for EV charging at each bus (E_{ij} is the current energy level, E_{ij}^{req} is the required energy for being fully charged, P_{ij}^{EV} is the charging power, and P_{ij}^{max} is the maximum charging power considering the number of EVs connected to the

charging stations);

$\boldsymbol{\pi_2}$ are the optimal power flow variables (active power flow P_{ij}, reactive power flow Q_{ij}, bus voltage square magnitude V_{ij} and branch current square magnitude B_{ij});

$\boldsymbol{\pi_3}$ are the variables of the piecewise linear model of cable aging failure probability (λ_{ije}^{L} is the binary variable of the *e*-th segment, p_{ije}^{L} represents the failure probability at *e*-th segment, and p_i^L is the failure probability of *i*-th cable over a day);

$\boldsymbol{\pi_4}$ are the variables of the aging failure probability piecewise linear models of distribution transformers and the substation transformer (λ_{ije}^{T} is the binary variables of *e*-th segment, p_{ije}^{T} represents the failure probability at *e*-th segment, p_i^T is the failure probability of *i*-th transformer).

The considered time horizon is one year. For simplicity, the base load demand (without EV charging) for a year is clustered as load demands for three typical days. The duration of each time slot is 1 hour. The following subsections describe various parts of the model, the procedure for the calculation of the inputs, and the solution approach.

7.2.1 Objective Function

The objective function includes the customer cost (*CC*) due to aging failures, the utility cost (*UC*) for the replacement of damaged equipment, the EV charging cost (*EVC*) of EVs, and the cost associated with power loss costs (*PLC*):

$$\min F = CC + UC + EVC + PLC \tag{7.5}$$

CC considers the aging failure probabilities of lines p_k^L, distribution transformers p_i^{DT} and substation transformer p^{ST}. Considering the post-fault reconfiguration of tripping devices (e.g., circuit breaker, switches), the unavailability at bus *i* (U_i^{AF}) is defined by

$$U_i^{AF} = U_i^L + U_i^T \tag{7.6}$$

$$U_i^L = \sum_{k=1}^{N} RC_{ik} \cdot d_k^L \cdot p_k^L + \sum_{k=1}^{N} SC_{ik} \cdot s_k^L \cdot p_k^L \tag{7.7}$$

$$U_i^T = d_i^{DT} \cdot p_i^{DT} + d^{ST} \cdot p^{ST} \tag{7.8}$$

where RC_{ik} and SC_{ik} are the *ik*-th entries of the replacement coefficient matrix and the switching coefficient matrix, respectively [241]. d_k^L, d_i^{DT} and d^{ST} are the durations for

replacing *k*-th line, *i*-th distribution transformer and substation transformer. s_k^L is the switching duration of *k*-th line. The expected energy not supplied at bus *i* is calculated by multiplying unavailability to the average power $\tilde{P}_i$

$$EENS_i^{AF} = U_i^{AF} \cdot \tilde{P}_i \tag{7.9}$$

We integrate the value of customer reliability (VCR) and EENS to estimate the customer cost due to aging failures on equipment.

$$CC(\boldsymbol{\pi_2}, \boldsymbol{\pi_3}, \boldsymbol{\pi_4}) = \sum_{i=1}^{N} \left(ENS_i^{AF} \cdot VCR_i \right) \tag{7.10}$$

The calculation of the aggregate VCR values, considering different locational load components, is described in Section 7.3. To calculate *UC*, the cost of purchasing new equipment and replacing the damaged ones is combined with each device's aging failure probabilities.

$$UC(\boldsymbol{\pi_2}, \boldsymbol{\pi_3}, \boldsymbol{\pi_4}) = \sum_{i=1}^{N} (C_i^L \cdot p_i^L + C_i^{DT} \cdot p_i^{DT}) + C^{ST} \cdot p^{ST} \tag{7.11}$$

where C_i^L, C_i^{DT} and C^{ST} are the total replacement costs for *i*-th cable, *i*-th distribution transformer and the substation transformer. The charging cost for EVs for utilities is

$$EVC(\boldsymbol{\pi_1}, \boldsymbol{\pi_2}) = \sum_{i=1}^{N} \sum_{j=1}^{T_s} w_j \cdot P_{ij}^{EV} \cdot \Delta t \tag{7.12}$$

where w_j is the wholesale electricity price at *j*-th interval; P_{ij}^{EV} is the charging power of EVs on the bus *i* at *j*-th interval, Δt is the duration of one interval (1 hour). *PLC* is defined as

$$PLC(\boldsymbol{\pi_1}, \boldsymbol{\pi_2}) = \sum_{i=1}^{N} \sum_{j=1}^{T_s} w_j \cdot P_{loss} \cdot \Delta t \tag{7.13}$$

where P_{loss} is the power loss of the whole feeder.

7.2.2 Constraints

The constraints are associated with the network operational limits, EV load and charging power, and the piecewise linearization of failure probabilities in cables and transformers.

7.2.2.1 Probabilistic aging failure constraints

We use subscripts/superscripts T and L to differentiate the parameters and variables for transformers and cable lines, respectively. Failure probabilities (p_T, p_L) of transformers and lines are related to their loadings, temperatures, and functional age (T_0). T_0 is determined by historical operations, maintenance conditions and actual operational statuses [119]. Higher loading increases the temperature and accelerates relative aging speed (RAS^L, RAS^T, for lines and transformers, respectively) and loss-of-life. T_s is the total number of time slots for aging failure estimation. As described in [281], the mathematical expressions of aging failure probabilities on cable and transformer can be expressed as

$$p_L = \sum_{j=1}^{T_s} \left\{ 1 - \left[\left(\frac{T_0 + \sum_k^{j-1} RAS_k^L \Delta t}{L(\theta_r^L)} \right)^{\beta_L} - \left(\frac{T_0 + \sum_k^{j} RAS_k^L \Delta t}{L(\theta_r^L)} \right)^{\beta_L} \right] \right\} \tag{7.14}$$

$$p_T = \sum_{j=1}^{T_s} \left\{ 1 - \left[\left(\frac{T_0 + \sum_k^{j-1} RAS_k^T \Delta t}{L(\theta_r^T)} \right)^{\beta_T} - \left(\frac{T_0 + \sum_k^{j} RAS_k^T \Delta t}{L(\theta_r^T)} \right)^{\beta_T} \right] \right\} \tag{7.15}$$

where $L(\theta_r^L)$ and $L(\theta_r^T)$ are the rated lifespans of insulated cable and transformer under the rated operating temperatures θ_r^L and θ_r^T. β_L and β_T are the shape parameters of Arrhenius-Weibull distributions for line and transformer, respectively. Due to the non-linear characteristic of the aging failure probability equations, a piece-wisely linearized is adopted:

$$p = \begin{cases} s_1 \cdot \left(k - k_1^{ini}\right) + p_1^{ini} & k_1^{ini} < k < k_2^{ini} \\ s_2 \cdot \left(k - k_2^{ini}\right) + p_2^{ini} & k_2^{ini} < k < k_3^{ini} \\ \vdots & \vdots \\ s_{N_s-1} \cdot \left(k - k_{N_s-1}^{ini}\right) + p_{N_s-1}^{ini} & k_{N_s-1}^{ini} < k < k_{N_s}^{ini} \end{cases} \tag{7.16}$$

where k_e^{ini} is the initial location of the breakpoint and p_e^{ini} is the initial failure probability of e-th segment. It needs to mention that the ending location of the breakpoint of (e-1)-th segment k_{e-1}^{end} is equals to the initial location of the breakpoint of the e-th segment k_e^{ini}. The so-called big-M formulation is adopted to represent the aging failure probabilities on cables and transformers:

$$\sum_{e=1}^{N_s} \lambda_{ije} \leq 1 \tag{7.17}$$

$$k_{e_0}^{end} - k_{ij} \leq M \cdot \sum_{e=1}^{e_0} \lambda_{ije} \quad \forall\, e_0 \in \{1, \ldots, N_s\} \tag{7.18}$$

$$k_{e_0}^{end} - k_{ij} \geq -M \cdot \sum_{e=1}^{e_0} \lambda_{ije} \quad \forall\, e_0 \in \{1, \dots, N_s\} \tag{7.19}$$

$$p_{ije} \leq s_e \cdot \left(k_{ij} - \lambda_{ije} \cdot k_e^{ini}\right) + p_e^{ini} \tag{7.20}$$

$$p_{ije} \geq s_e \cdot \left(k_{ij} - \lambda_{ije} \cdot k_e^{ini}\right) + p_e^{ini} - M \cdot \left(1 - \lambda_{ije}\right) \tag{7.21}$$

$$p_{ije} \leq M \cdot \lambda_{ije} \tag{7.22}$$

$$p_{ije} \geq 0 \tag{7.23}$$

$$p_i = \sum_{j=1}^{T_s} \sum_{e=1}^{N_s} p_{ije} \tag{7.24}$$

where λ_{ije} is the binary variable; k_e^{ini} and k_e^{end} are values of the initial and ending breakpoint of the *e*-th segment; p_e^{ini} and s_e are the initial failure probability and slop of *e*-th segment; p_{ije} is the failure probabilities of the *e*-th segment on *i*-th equipment at the *j*-th interval, p_i is the aging failure probability at *i*-th equipment; and M is a big number (e.g., 1000); k_{ij} is the actual load in per unit for *i*-th transformer and temperature for *i*-th cable at *j*-th interval.

Constraints (7.17)-(7.19) are applied to determine the specific segment utilized according to the value of k_{ij}. Constraints (7.20)-(7.23) define the failure probability at each segment. Assuming $\lambda_{ije} = 0$, to meet the constraints (7.22)-(7.23), $p_{ije} = 0$; otherwise, constraints (20)-(21) are equivalent to:

$$p_{ije} = s_e \cdot \left(k_{ij} - \lambda_{ije} \cdot k_e^{ini}\right) + p_e^{ini} \tag{7.25}$$

The total failure probability p_i is defined in (7.24) by the summation of all the failure probabilities during all intervals.

The accuracy of the linearization is dictated by the number of segments. The higher number of segments leads to high accuracy but increases the solution time. A Python library named pwlf [291] is used to find the global best breakpoint locations of all segments based on the least squares fit when the number of line segments is provided. The aging failure probabilities of transformers when load varied from 0 p.u. to 2.0 p.u. by 0.001 are calculated using (7.14). These values are the inputs of the pwlf library-based procedure that finds the optimal breakpoints ($k_e^{T,ini}/k_e^{T,end}$), slopes (s^T) and initial failure probability ($p^{T,ini}$) for each segment. Comparing the failure probabilities using linearized equations and original model, the result illustrates good performance of piecewise linearization method when the number of segments is 10. The comparison

between the original aging failure model and the linearized model on transformers is shown in Fig. 7.2, and the sum-of-square error is 1.91 10^{-10}.

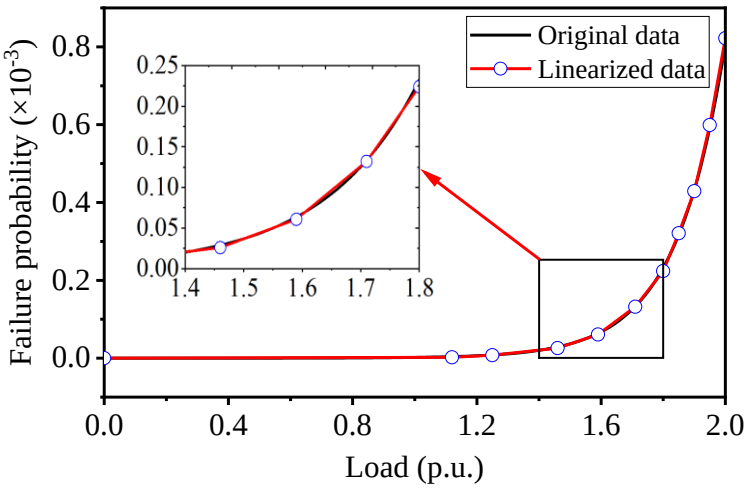

Fig. 7.2 Original data and linearized data for aging failure probability on transformers.

A similar procedure is adopted to linearize the aging failure probability of cables based on the temperature. According to [117], the temperature is dependent on the branch current from power flow calculation and its specifications, such as square current-carry capacity (B_Z), ambient reference temperature (θ_0), ambient temperature (θ_a), and thermal time constant (τ), shown in (7.26).

$$k_j^L = (\theta_r^L - \theta_0)\frac{B_j}{B_Z}\left(1 - e^{\frac{-\Delta t}{\tau}}\right) + \left(k_{j-1}^L - \theta_0\right)\frac{B_{j-1}}{B_Z}e^{\frac{-\Delta t}{\tau}} + \theta_a \qquad (7.26)$$

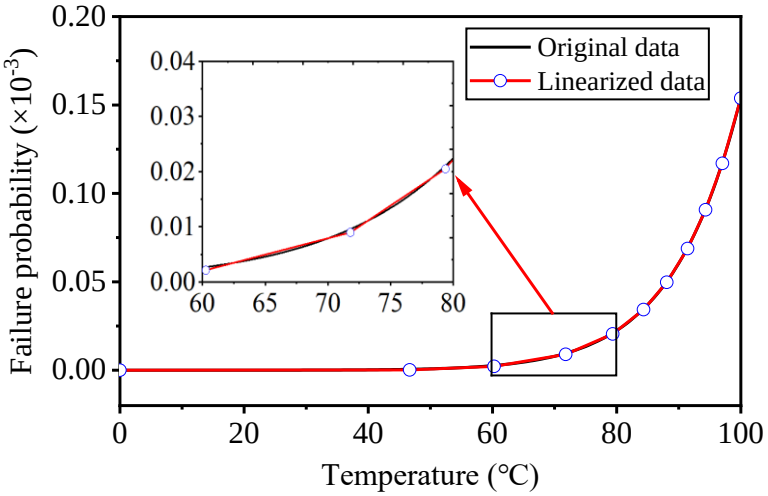

Fig. 7.3 Original data and linearized data for aging failure probability on cables.

We assume that the input is the temperature (varied from 0°C to 100°C) and the output

is the aging failure probability for the piecewise linearization. Original aging failure probabilities of lines are obtained using (7.15), the optimal breakpoints ($k_e^{L,ini}/k_e^{L,end}$), slope (s^L) and initial failure probability ($p^{L,ini}$) are found with pwlf from the result obtained. The comparison between the original aging failure model and the linearized model for cable is shown in Fig. 7.3 with 10 segments. The sum-of-square error is 8.42 10^{-12}.

Table 7.1 shows the information of each segment for the calculation of aging failure probabilities assuming the loss of life of historical operation are 170,000 and 165,000 hours for transformers and cables. The initial load/temperature ($k^{T,ini}$, $k^{L,ini}$) of e-th segment is the ending load/temperature ($k^{T,end}, k^{L,end}$) of (e-1)-th segment. The R2 values are 99.995% and 99.997%. The standard errors are in the interval [2.09 10^{-7}, 4.16 10^{-5}] and [2.35 10^{-7}, 4.71 10^{-5}] for each segment of aging failure probabilities of transformers and cables, respectively.

Table 7.1 Information of Piecewise Linearization for Transformers and Cables

No.	Transformer			Cable		
	$p^{ST,ini}$	s^{ST}	$k^{T,ini}$ (p. u.)	$p^{L,ini}$	s^L	$k^{L,ini}$ (°C)
1	9.07e-9	2.61e-6	0.00	1.40e-9	2.89e-9	0.00
2	2.20e-6	4.02e-5	1.12	1.36e-7	1.14e-7	46.67
3	7.60e-6	9.01e-5	1.25	2.14e-6	5.84e-7	60.27
4	2.59e-5	2.59e-4	1.46	8.97e-6	1.55e-6	71.79
5	6.08e-5	5.77e-4	1.59	2.05e-5	2.78e-6	79.37
6	1.32e-4	1.12e-3	1.71	3.43e-5	4.13e-6	84.34
7	2.24e-4	1.71e-3	1.80	4.97e-5	5.70e-6	88.07
8	3.21e-4	2.32e-3	1.85	6.88e-5	7.57e-6	91.43
9	4.29e-4	3.16e-3	1.90	9.07e-5	9.61e-6	94.33
10	5.99e-4	4.46e-3	1.95	1.17e-4	1.24e-5	97.03

7.2.2.2 EV load prediction and constraints

A multi-layer perceptron model (MLP) predicts the travel mileages of EVs in the test system. The typical MLP model is structured by an input layer, multiple hidden layers, and an output layer. The mathematical relationship between the input layer (***X***) and output layer (***O***) of an MLP with one hidden layer (***H***) is expressed as [292]

$$\boldsymbol{H} = f(\boldsymbol{\mu}_h \boldsymbol{X}^T + \boldsymbol{\sigma}_h) \tag{7.27}$$

$$\boldsymbol{O} = g(\boldsymbol{\mu}_o \boldsymbol{H}^T + \boldsymbol{\sigma}_o) \tag{7.28}$$

where $\boldsymbol{\mu}_h$, $\boldsymbol{\sigma}_h$ and f donate the weights, biases, and activation functions of the hidden layers; $\boldsymbol{\mu}_o$, $\boldsymbol{\sigma}_o$ and g are the weights, biases, and activation functions for the output layer.

The open data from the 2017 National Household Travel Survey (NHTS) [266] is utilized to study EV owners' driving behaviour and train the MLP model. For a better representation of practical experience, EVs with travel distances larger than 250 mileage have been removed from the original dataset. 80% of the modified NHTS dataset is utilized for training the MLP model with 100 epochs and a batch size of 5 by using the Scikit-learn Python library. The rest of the 20% is for testing the evaluation accuracy by using the correlation coefficient R2, mean squared error MSE and mean absolute error MAE. The best performance of MLP architecture contains 3 hidden layers and 50 nodes with approximately 1.0000, 0.0035 and 0.0124 for R2, MSE, and MAE.

According to the modified NHTS data, the probabilistic distribution functions of departure time (f_{dep}) and arrival time (f_{arr}) of vehicles have been shaped as normal distributions in Chapter 6, as shown in (6.13) and (6.14).

These normal distributions are used to generate the EV arrival time vector ($\boldsymbol{T_i^{arr}}$) and departure time vector ($\boldsymbol{T_i^{dep}}$), given the number of EVs in the test system. The time range for optimizing the aggregated EV charging load is between the earliest arrival time and earliest departure time for simplicity, shown in Fig. 7.4. Since the time horizon for an interval is 1 hour, floor and ceiling functions are utilized to assign the arrival times and departure times of all EVs to the corresponding intervals.

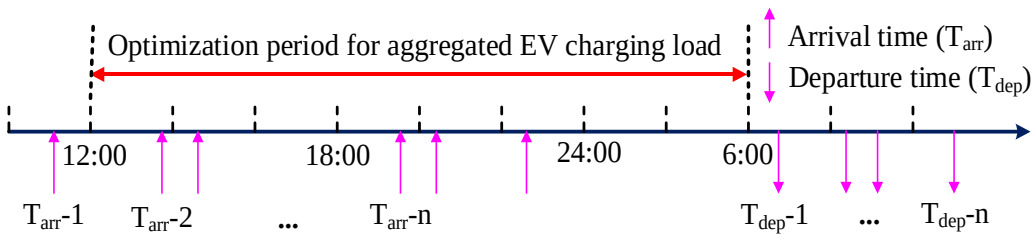

Fig. 7.4 Aggregated EV charging load optimization time range.

The newly generated vectors of $\boldsymbol{T_i^{arr}}$ and $\boldsymbol{T_i^{dep}}$ are then input to the pre-trained MLP

model to predict the EV travel mileage vector ($\boldsymbol{d^e}$). Combining the travel mileage and the EV battery data (i.e., rated charging power and capacity) the state-of-charge (SoC) level, initially stored energy (E_{il}^{ini}) and required energy ($E_{il}^{req,ini}$) of l-th EV connected to the i-th bus is calculated by (7.29)-(7.31).

$$SoC_{il} = \frac{D_{il}^r - \omega_{il} \cdot d_{il}^e}{D_{il}^r} \tag{7.29}$$

$$E_{il}^{ini} = SoC_{il} \cdot C_{il}^r \tag{7.30}$$

$$E_{il}^{req,ini} = (1 - SoC_{il}) \cdot C_{il}^r \tag{7.31}$$

where $D_{il}^r, \omega_{il}, d_{il}^e$ and C_{il}^r are the rated travel mileage, type (e.g., full electric or hybrid), expected travel mileage and the rated capacity of *l*-th EV on *i*-th bus. These parameters need to be categorized in time sequence before reading by the optimization algorithm. The EV penetration (φ) is defined as the ratio of the total number of EVs to the total number of houses.

To generate the optimized EV load at each bus, the following constraints are considered. Constraints (7.32)-(7.33) define the limit of charging power. The maximum charging power of bus *i* at the *j*-th interval (P_{ij}^{max}) are furtherly confined by (7.37). η_{ij}^a is the average charging efficiency. $P_{ij}^{r,c}$ is the rated charging power of EV on the *i*-th bus at *j*-th interval. Constraint (7.34) explains that all the EVs need to be fully charged before any journey on the next day, and $E_{ij}^{req,ini}$ is the initial required energy from EVs at bus *i* after arriving homes. Equivalent constraints (7.35) and (7.36) are utilized to calculate the energy required and energy stored by EVs on *i*-th bus at *j*-th interval.

$$P_{ij}^{EV} \geq 0 \tag{7.32}$$

$$\eta_{ij}^a \cdot P_{ij}^{EV} \leq P_{ij}^{max} \tag{7.33}$$

$$\sum_{j=1}^{T_s} E_{ij}^{req,ini} = \sum_{j=1}^{T_s} \eta_{ij}^a \cdot P_{ij}^{EV} \cdot \Delta t \tag{7.34}$$

$$E_{ij}^{req} = E_{ij-1}^{req} + E_{ij}^{req,ini} - \eta_{ij}^a \cdot P_{ij}^{EV} \cdot \Delta t \tag{7.35}$$

$$E_{ij} = E_{ij-1} + E_{ij}^{ini} + \eta_{ij}^a \cdot P_{ij}^{EV} \cdot \Delta t \tag{7.36}$$

$$P_{ij}^{max} = \begin{cases} P_{ij}^{c,r} & E_{ij}^{req} \geq P_{ij}^{c,r} \cdot \Delta t \\ E_{ij}^{req}/\Delta t & E_{ij}^{req} < P_{ij}^{c,r} \cdot \Delta t \end{cases} \tag{7.37}$$

7.2.2.3 Power flow constraints

The power flow calculation in the optimization model is based on the DistFlow model presented in [293][294] for radial networks, illustrated in Fig. 7.5 which represents a branch of the feeder with the load at the receiving end. Assumptions: the voltage at the substation (bus 0) is fixed and equal to 1 pu, and the network has a radial configuration so that the number of the buses is equal to the number of branches (each branch is identified by the number of the receiving-end bus), the network is balanced, and the single line representation is adopted, line charging currents are neglected.

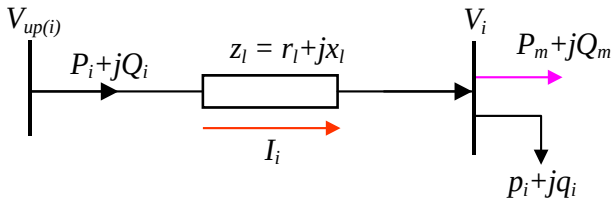

Fig. 7.5 Illustration of the simplified power flow line model (from [295]).

The formulation of the model is

$$P_i = p_i + r_i B_i + \sum_k A_{ik} P_k \tag{7.38}$$

$$Q_i = q_i + xB_i + \sum_k A_{ik} Q_k \tag{7.39}$$

$$V_i = V_{up(i)} - 2(r_i P_i + x_i Q_i) + (r_i^2 + x_i^2) B_i \tag{7.40}$$

$$P_i^2 + Q_i^2 - V_{up(i)} B_i \leq 0 \tag{7.41}$$

$$V_i \geq 0 \tag{7.42}$$

$$B_i \geq 0 \tag{7.43}$$

$$V_i^{min} \leq V_i \leq V_i^{max} \tag{7.44}$$

$$B_i \leq B_i^{max} \tag{7.45}$$

$$P_{loss} = \sum_{i=1}^{N} r_i \cdot B_i \tag{7.46}$$

where P_i, Q_i, V_i, and B_i are the active power flow at the sending end of the branch, reactive power flow at the sending end of the branch, the bus voltage square magnitude, and the branch current square magnitude of i-th branch/bus. $V_{up(i)}$ is the square voltage at the sending bus of branch i. P_m and Q_m are the total active power and reactive power of branch/branches connected by bus i directly, which are calculated

by the oriented graph matrix A. A_{ik} is the *ik*-th entry of A, it equals 1 when *i*-th bus is the sending bus of *k*-th branch, 0 for otherwise. p_i and q_i are the active power and reactive power drawn from bus *i*. r_i and x_i are the resistance and reactance of branch *i*. V_i^{min} and V_i^{max} are the lower bound and upper bound for square voltage (e.g., 0.9025 pu and 1.1025 pu), and B_i^{max} is the upper bound for square current at branch *i* (e.g., 2 times of square of rated current).

Constraints (7.38)-(7.43) are power flow equations [296]. Constraints (7.44)-(7.45) limit the voltage and current. Constraint (7.46) calculates the power loss of the network. At the end of the optimization, the procedure verifies that the relaxed constrained (7.41) reaches the equality condition.

7.2.3 Solution Approach

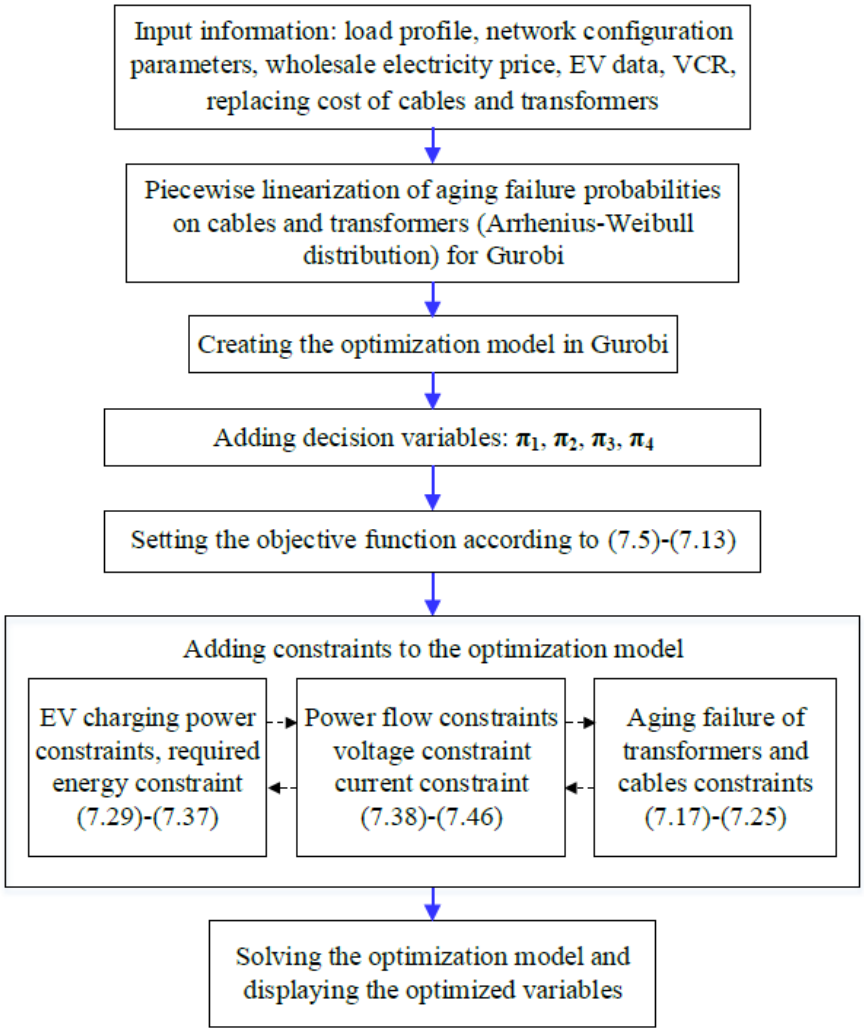

Fig. 7.6 Flowchart of the solution approach.

The procedure is illustrated in Fig. 7.6. The input is the pre-determined parameters, such as network parameters, EV parameters, information of piecewise segments for the failure model of transformers and cables, electricity retail price, and load profile. The MIQCP model includes adding the decision variables, the objective function according to the simulation scenario, equipment aging failure probabilities constraints, EV charging representation, the power flow model and the current and voltage limits. Finally, the proposed MIQCP model is solved by Gurobi 9.1. As the output of the solver is shown as a vector integrated by all the optimized variables, the results, e.g., optimized loads and failure probabilities, need to be assigned separately. All the input parameters are described in Section 7.3.

7.3 Simulation Cases and Load Profile

7.3.1 Simulation Network

A 5-bus network shown in Fig. 6.5 is utilized to illustrate the feasibility of the proposed method. Bus 0 is slacked bus with a fixed voltage (1.0 pu) on the substation transformer (ST). Distribution transformers (DTs) are connected by all the buses, and all the branches (Ls) are named by their receiving-end bus numbers. Besides, the circuit breaker is placed at branch 1, a manual switch is installed at branch 3, and two fuses are located at branches 4 and 5. The number of houses, rated active power (P) and weighted VCR vales at each bus are shown in Table 6.1. The distribution transformer capacity is assumed as 240 kW at 1.0 power factor for simplifying the calculations. Parameters of transformers and cables are adapted from [118],[281]. The nominal lifespan for transformers and cables are 180,000 and 175,200 hours under the rated temperatures of 110 ºC and 80 ºC, respectively. The replacement times of the substation transformer (r^{ST}), distribution transformers (r^{DT}), lines (r^{L}) and the tripping time (s^{L}) of protecting devices are 30 hours, 20 hours, 20 hours and 0.5 hour, separately. The current-carrying capacities at the reference ambient temperatures (θ_{a0}) for cable lines are 300A, 150A, 100A, 50A, 50A. The power utility costs for replacing cable lines and transformers taking the equipment cost and installation cost are shown in Table 6.3.

7.3.2 Simulation Base Load Profile and Electricity Price

Fig. 7.8 shows the clustered load profile (3 typical days) without EV integration for a year, adapted from [231]. The probability of each clustered day is 31%, 17% and 52%, respectively. The corresponding wholesale electricity prices for each typical day are also shown in Fig. 7.8.

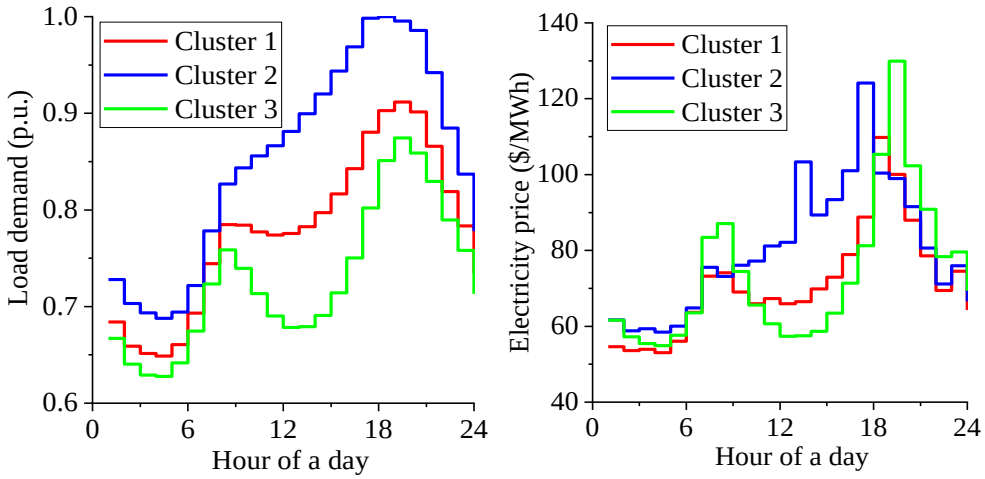

Fig. 7.8 Load profile without EV and wholesale electricity price.

7.3.3 EV Load Profile

The type of EV is indicated by the value of ω_{il}, such as $\omega_{il} = 1$ for full electrical EV (FEV). For simplicity, we assume all the EVs are of the same type. The rated travel mileage is 120, the rated capacity is 40 kWh, charging power is 10 kW, assuming a 200% EV penetration (i.e., every house has two EVs) in the test system. Departure times and arrival times are input into the pre-trained MLP model to predict the travel mileage of each EV. Then, SoC, the energy left and needed by each EV can be calculated by (7.27)-(7.29). After collecting those data, the aggregated information of each bus is summarized.

Fig. 7.9 shows the EV charging load profile with fast charging mode at buses 1-5 with 200% penetration. Fast charging starts when customers arrive at their homes. It is worth mentioning that the load demand from EV charging is dependent not only on the number of EVs but also on the travel distance. Therefore, even if buses 4 and 5 feed users with the same number of EVs, the average EV charging load is larger at bus

4 than at bus 5 due to longer travel distances.

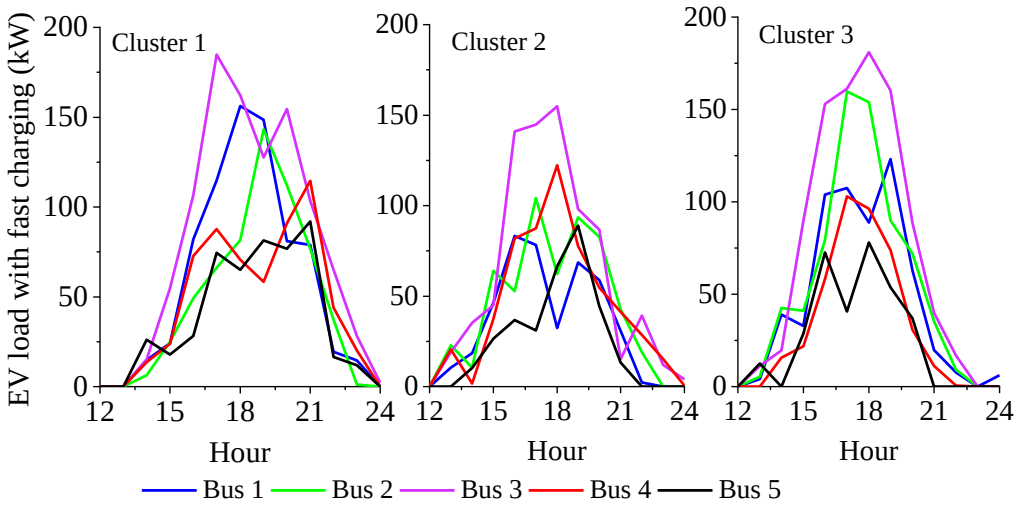

Fig. 7.9 EV charging load profile (ρ=200%) with fast charging mode.

It should be noticed that 200% EV penetration is considered for the scenario when EVs and EV smart chargers are popularized worldwide. With the global net zero targets for carbon dioxide emissions, growing environmental awareness, and governmental incentive policies on EV purchasing to facilitate the transition from traditional fossil fuel to green energy, EVs are gaining extreme interest globally. The home-used EV smart charger with real-time communication with the Distribution System Operator (DSO) makes EV smart charging possible. Meanwhile, as EV charging load is assumed as controllable load, with low EV penetration, the impact of smart charging on reliability improvement and cost reduction may not be significant.

7.3.4 Test Cases

Three cases are tested in the simulation: Case 1 simulates the aging failure-related and power utilities cost to the wholesale market for EV charging load and power loss under fast charging mode; Case 2 analyzes the aging failure-related cost and utility payment with the objective of minimizing the sum of charging costs and power loss costs, i.e., *EVC* + *PLC* of (7.5); Case 3 investigates network reliability, customer loss and power utility cost for the minimization of the total cost function *F* defined in (7.5).

7.4 Simulation Results and Analysis

This section compares the results of integrated load, aging failure probabilities of transformers and cables, customer loss due to aging failures, utility cost for managing aging failure, and utility payment on the wholesale market for EV charging load and power loss.

7.4.1 Total Load Including EV Charging for Different Cases

The simulation results of total loads including optimized EV charging demands with different objective functions are compared with fast charging for 3 clusters, separately. Figs. 7.10, 7.12, and 7.14 show the base load and electricity prices for clusters 1-3 from 1.00 pm to 6.00 am without EV charging load. The peak load generally occurs from 17.00 to 21.00 with higher electricity prices.

Figs. 7.11, 7.13, and 7.15 show the total loads including EV charging demands at ST and each bus of different cases for clusters 1-3. For case 1 (EV fast charging mode), the load peak is exacerbated when the electricity price is high. For case 2 (minimization of utility cost to feed EV load and power loss), the EV charging load is shifted to the period when the electricity price is low. For case 3 (minimization of the total costs including reliability), the load demands at ST and each bus have the minimum fluctuations.

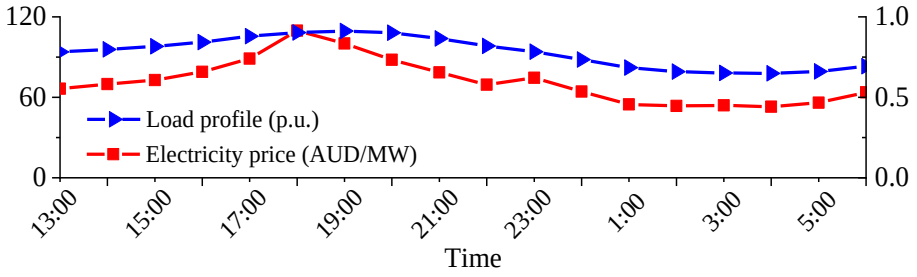

Fig. 7.10 Load profile and electricity price for cluster 1.

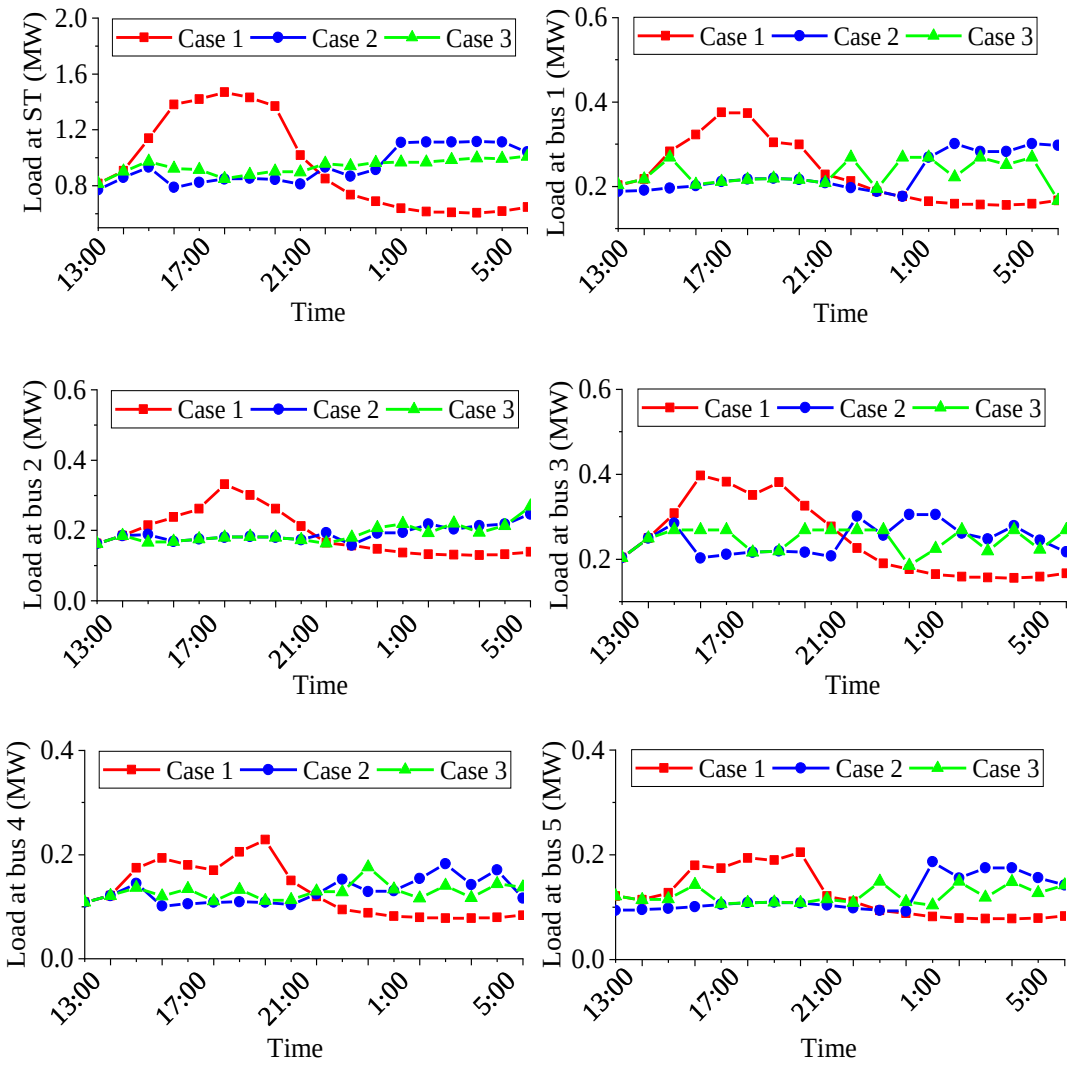

Fig. 7.11 Comparison of load demand at ST and buses for cases 1-3 of cluster 1.

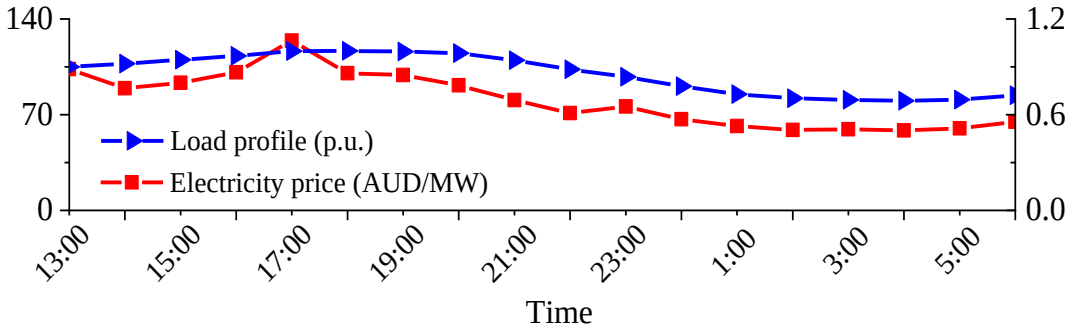

Fig. 7.12 Load profile and electricity price for cluster 2.

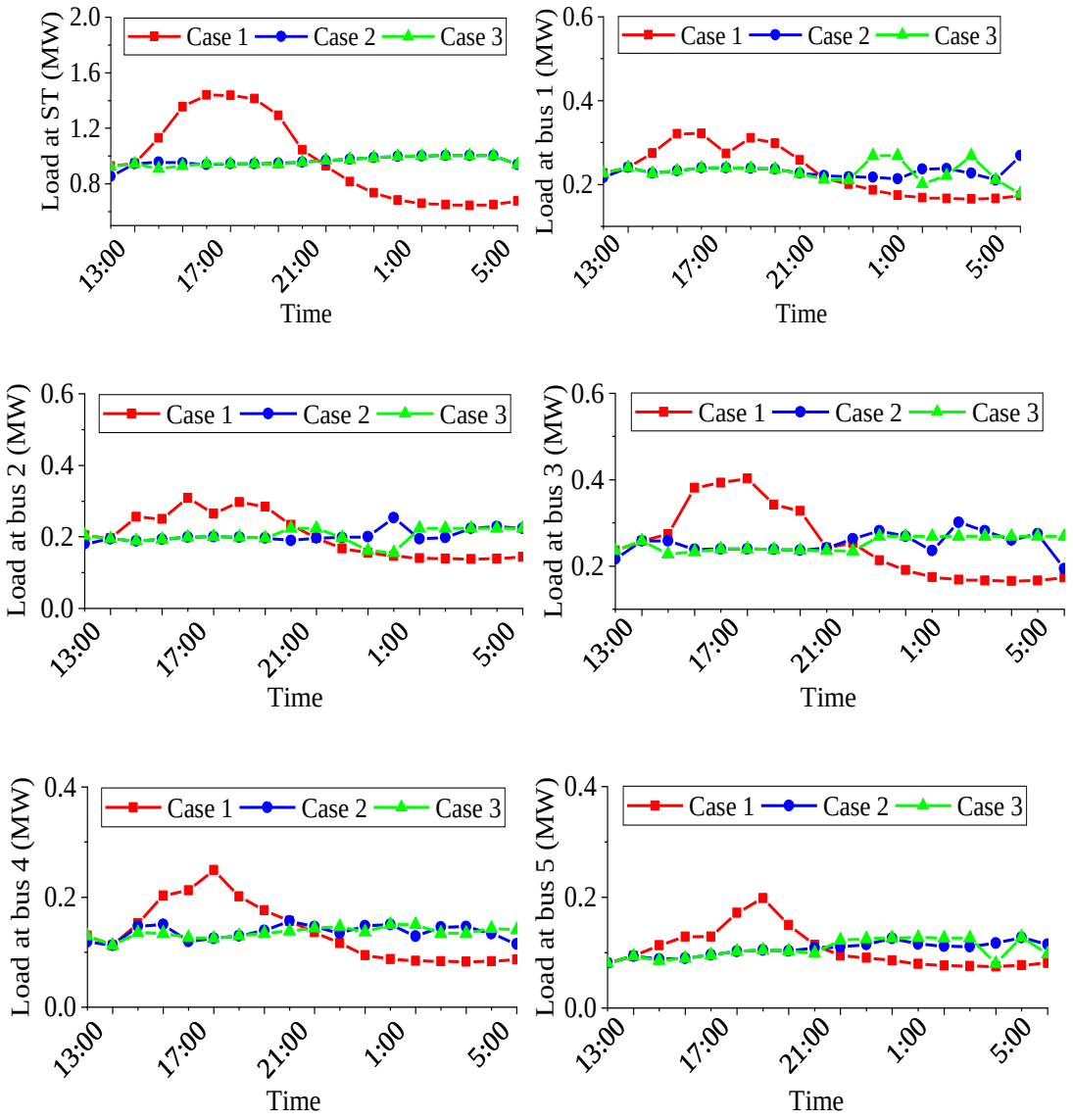

Fig. 7.13 Comparison of load demand at ST and buses for cases 1-3 of cluster 2.

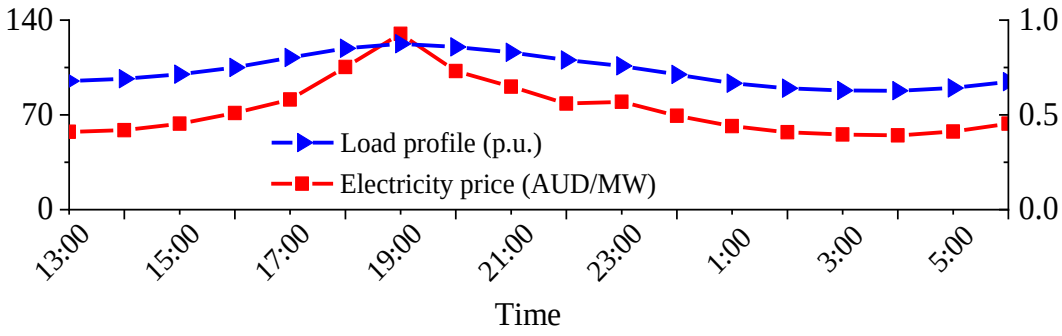

Fig. 7.14 Load profile and electricity price for cluster 3.

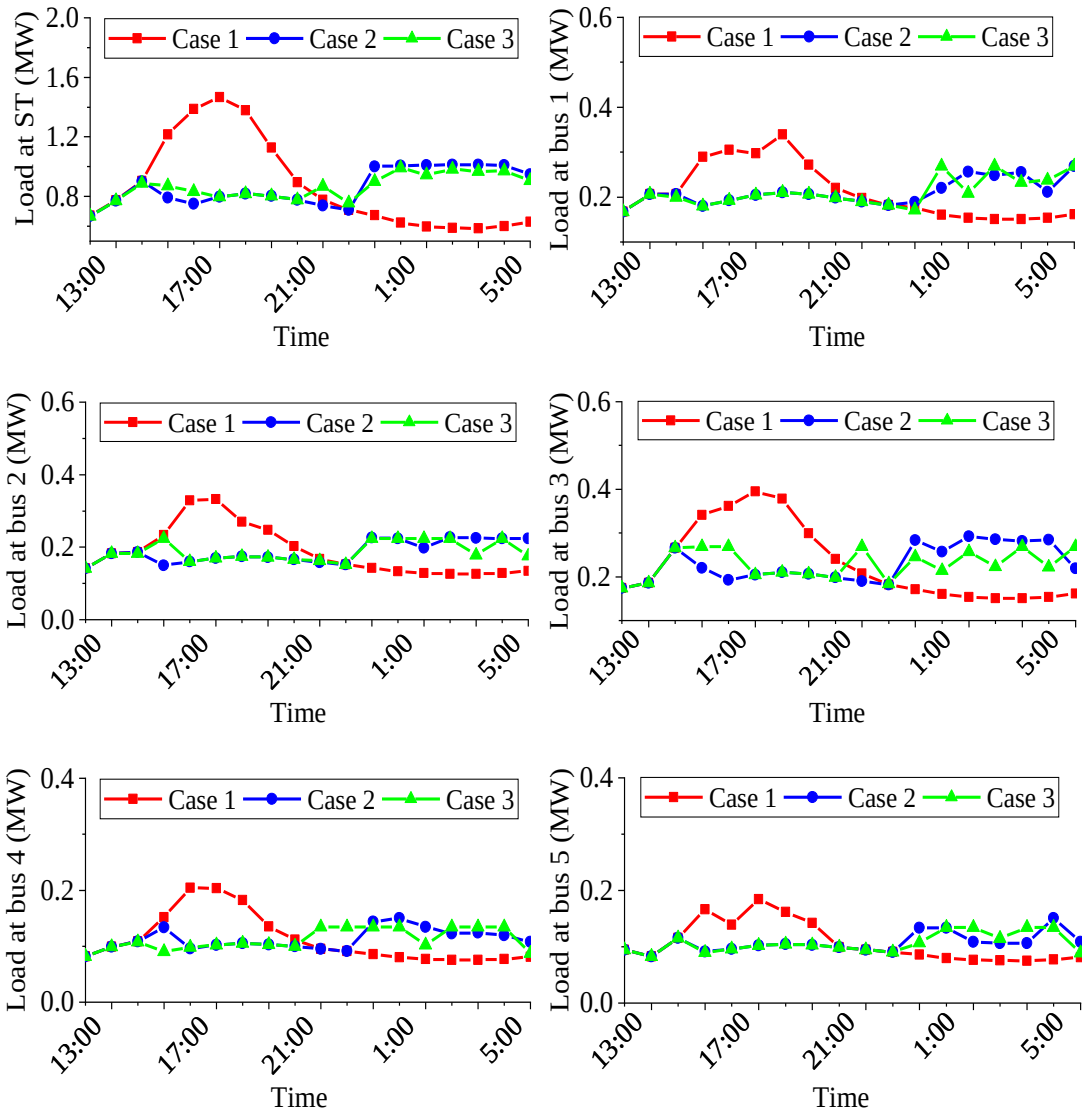

Fig. 7.15 Comparison of load demand at ST and buses for cases 1-3 of cluster 3.

7.4.2 Aging Failure Probability

This sub-section presents yearly aging failure probabilities of cables and transformers for the considered 3 cases. Aging failure probability is affected by temperature and power flow. For case 1, all the cable lines and transformers have the highest aging failures due to high aging speeds at peak hours as shown in Table 7.2. The aging failure probability of cable 1 is 100% indicating the termination of its life within one year. For cable line 2, the failure probability is higher than 50%. Cable lines show similar aging failure probabilities for Case 2 and Case 3 since the minimization of the electricity payments reduces the loading fluctuations. As shown in Table 7.3, the aging failure probabilities of ST and DTs are largely reduced in Cases 2 and 3 compared with

Case 1. As expected, all transformers have the lowest failure probability, which also depends on the transformer's capacity, in Case 3.

Table 7.2 Yearly Aging Failure Probability of Cables Lines

Line	1	2	3	4	5
Case 1	100%	63.694 %	5.762%	0.075%	0.070%
Case 2	6.890%	7.094%	0.338%	0.072%	0.071%
Case 3	7.307%	2.145%	0.410%	0.074%	0.073%

Table 7.3 Yearly Aging Failure Probability of DT and ST

DT	1	2	3	4	5	ST
Case 1	3.747%	6.294%	10.03%	16.51%	4.483%	3.089%
Case 2	1.067%	1.552%	2.163%	1.733%	1.447%	1.401%
Case 3	0.905%	0.938%	0.979%	0.956%	0.911%	1.348%

7.4.3 Reliability Indices and Total Cost

Tables 7.4 and 7.5 show the probabilistic network reliability indices, including yearly bus unavailability and EENS, for the considered three cases. For Case 1, the highest unavailability is at bus 5 followed by bus 2 and bus 1. The maximum EENS occurs at bus 1. Compared to Case 1, with average unavailability (denoted as Ave.) of 23.024 hours, the average unavailability in Case 2 and Case 3 is 2.383 and 1.785 hours. Moreover, the average EENS are 2850.7, 298.4 and 228.11 kWh in Cases 1-3.

Table 7.4 Yearly Bus Unavailability (U)

U (hour/yr)	1	2	3	4	5	Ave.
Case 1	34.44	34.95	4.904	6.215	34.61	23.02
Case 2	3.481	3.443	0.813	0.765	3.411	2.383
Case 3	2.478	2.484	0.730	0.740	2.494	1.785

Table 7.5 Yearly Expected Energy Not Supplied (EENS)

EENS (kWh/yr)	1	2	3	4	5	Ave.
Case 1	5291.2	4295.6	903.98	572.86	3189.6	2850.7
Case 2	533.13	421.73	151.95	71.824	313.36	298.40
Case 3	389.96	312.80	132.20	68.13	235.46	228.11

Table 7.6 Yearly Total Cost

Cost (kAUD)	EVC	PLC	UC	CC	Total
Case 1	107.97	12.71	191.46	458.57	797.71
Case 2	70.67	8.64	16.79	42.11	138.21
Case 3	73.45	8.70	13.63	33.6	129.38

The values of *EVC*, *PLC*, *UC*, and *CC* in a year are presented in Table 7.8 and Fig. 7.6. The total cost is 797.71, 138.2 and 129.38 kAUD for Cases 1, 2, and 3, respectively. The total cost declines significantly with the use of smart charging algorithms. Compared with Case 2, in Case 3 *EVC* and *CC* increase, whilst *UC* and *CC* decrease. Fig. 7.16 shows the values of total cost function F defined in (5) in the different cases. With EV charging load optimization, there is a yearly cost reduction of 659.5 kAUD (case 2) and 668.3 kAUD (case3) with respect to the fast-charging condition (case 1).

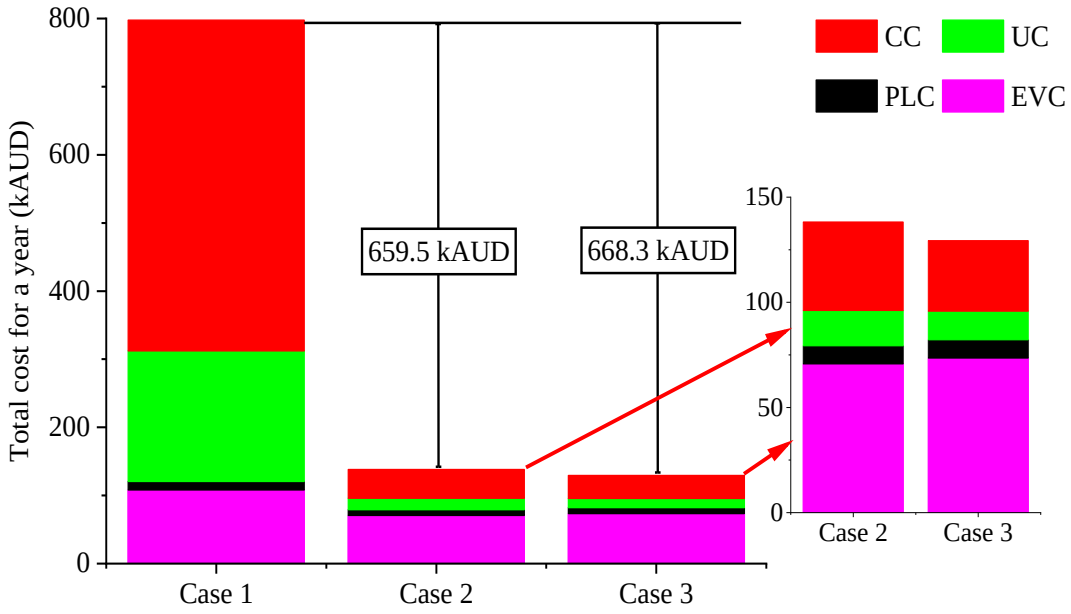

Fig. 7.16 Total cost comparison without and with optimization.

7.5 Summary

The paper illustrates the effectiveness of the proposed optimization procedure for assessing network reliability improvement and utility cost reduction that can be obtained by optimizing the EV charging load. The optimization procedure is a MIQCP

model including the linearized aging failure models for transformers and cable lines, EV charging constraints and power flow calculation.

The results show that network reliability is significantly influenced by the high probability of equipment aging failure due to the absence of EV smart charging, resulting in increased power utility costs and customer loss. With the adoption of a smart EV charging algorithm, aging failure probabilities in transformers and cables are reduced, and network reliability is greatly improved. The best improvement of network reliability is obtained by applying a smart charging strategy that minimalizes the total cost of customer loss and utilities (denoted as Case 3 in the paper). The presented optimization procedures can be extended by considering EV smart discharging and network reconfiguration.

Chapter 8 Conclusions and Future Work

This chapter explains the main findings of this thesis. Based on the research assumptions and findings, the recommendations for further studies are also summarized for future researchers.

8.1 Conclusions

In terms of congestion study, this thesis first characterizes the congestion and CM in PV generation and EV charging stations in distribution networks. Simulation results show that violation of current limits and voltage limits are the main reasons for congestion, and effective control of PV units and EV charging stations can play an essential role in the mitigation of congestion. Furtherly, spatial indices and temporal indices of thermal and voltage violations are proposed to indicate the level and seriousness of a congestion event. Spatial indices are maximum, average and cumulative values of violations, and temporal indices are the duration, rate and continuity of a congestion event. Two aggregate indices are also proposed to represent thermal congestion and voltage congestion by combining spatial indices and temporal indices. Moreover, indices to indicate the aggregated customers' contributions to congested areas are introduced to suggest the effective flexibility that needs to be given priority in managing congestion. With limited flexibilities in a distribution network, priority needs to be given to the customers with higher contribution indices in responding to the CM scheme.

As a long-term CM scheme, aged transformers and wires need to be distinguished and replaced to enhance the transmission capability and avoid future congestion. Network reliability is also closely associated with aging failures of transformers and lines. This thesis estimates the probabilistic aging failure on transformers and cables based on the Arrhenius-Weibull distribution considering actual operating time and temperature

under different load conditions. The impact of different EV penetrations on failure probabilities and LoL of transformers and cable lines are quantified. The simulation results illustrate the effectiveness of the probabilistic aging failure model in obtaining the vulnerability of specific components and justify the feasibility of the smart charging/discharging of EVs in reducing aging failures. Reliability assessment is also important in network planning and regulation in the presence of large-scale EV penetration. Network reliability, represented by node unavailability and expected ENS, is estimated by taking aging failure, network topology and post-failure reconfiguration into consideration. Customer reliability and power utility costs for replacing aged equipment are also calculated.

To better simulate the EV charging load, an accurate prediction of the EV charging load based on ML is adopted to generate the charging profile of EVs. Then, reliability and total cost due to aging failure considering the integrated impacts from different penetrations of EV and survival hours are simulated. Finally, a linear optimization of EV charging is developed to improve network reliability and reduce the cost of customers and power utilities in radial distribution networks. By effective regulation of EV charging load, aging failure probabilities and electricity payments to the wholesale market are minimized, thus maximizing the network reliability. Significantly, piece-wise linearization of the non-linear aging failure model simplifies the whole model and accelerates the calculation speed. The objective function includes aging failure cost, power loss, and the charging cost for EV charging load. The total cost is reduced by 668,300 AUD compared with the total cost without EV charging load optimization.

The main findings of this thesis are as follows:

- Congestion in active distribution is characterized as thermal violation and voltage violation. Congestion areas are enlarged considering voltage violations and coordinated control of PV and EV charging stations can effectively mitigate congestion.
- Calculation of the proposed congestion indices, including spatial indices, temporal indices and aggregated indices, can detect the vulnerable areas for congestion events based on load forecast and provide detailed information on congested branches and nodes. Power utilities can draw a congestion map, identify the

vulnerable areas according to the congestion level, and regulate short-term and long-term CM procedures in a distribution network.

- The proposed customer contribution indices are useful in finding the customers that have better performance over others in response to CM procedures and helping to build a fairer flexibility market for rewarding the participants.
- The Arrhenius-Weibull distribution-based model integrates the changing aging rate due to load demand fluctuations in estimating probabilistic aging failures and residual lives of transformers and cables. Higher penetration of EV aggravates the aging speed and LoL of components without proper coordination.
- Increasing EV penetration reduces network reliability and thus leads to higher customer loss and power utility costs. Higher survival hours result in a higher aging failure probability of transformers and cables, thus leading to low network reliability. The proposed method provides valuable information for network planning, regulation, and investment decisions.
- A MIQCP model has been developed to analyze the effectiveness of EV smart charging in improving network reliability and reducing the cost of customers and power utilities. With EV smart charging algorithm, total cost consists of customer loss, power utility cost, power loss and charging cost are reduced largely due to lower aging failure probability and improved network reliability.

8.2 Future Work

This thesis focuses on congestion level quantification and network reliability assessment considering the probabilistic aging failure of transformers and cables in distribution networks integrated by extensive penetration of PV generation and EVs. Based on the findings of this study, the following aspects can be further researched in the future:

- The proposed spatial, temporal and aggregated indices for quantifying congestion levels can be integrated with the studies on optimal reconfiguration, network expansion and investment planning. Considering the customer contribution indices in managing congestion and reliability issues, a fair local electricity market can be built for better participation of active customers in DR schemes.

- An evaluation model of survival hours with respect to nominal lifespan needs to be proposed based on each component's operating history and datasheet to improve the accuracy in the estimation of probabilistic aging failure of equipment. In the main chapters related to aging failure estimation, the survival hours are assumed to be a specific value without considering the history data of load flow, temperature, humidity, altitude, etc. The accuracy of aging failure estimation can be further improved by increasing load flow resolutions.
- With continuously increasing loading and penetration of DGs, the reliability issue by equipment aging failure is also becoming more severe in more expansive areas, such as transmission networks. The proposed reliability assessment method can evaluate the reliability of a larger region.
- A better and more realistic representation of EV charging strategies for load prediction, e.g., combining decentralized charging and centralized charging, needs to be furtherly studied in network reliability analysis. Given the benefit of V2G technology, the smart discharging of EVs can be integrated into the proposed linear reliability optimization model. When utilizing the V2G model, the inconvenience brought to customers needs to be addressed appropriately.
- DG and network reconfiguration can be included in the proposed MIQCP model of EV smart charging to relieve thermal stress on the equipment, strengthen network reliability, and achieve the optimal regulation of network flexibilities and protection devices. Moreover, as the most common reason for low network reliability, random failure can be integrated into the MIQCP model for reliability enhancement. The reliability optimization model can also interact with distribution network planning for determining the investment in equipment, such as switches, tie lines, and ESS.

Bibliography

[1] T. U. Solanke, P. K. Khatua, V. K. Ramachandaramurthy, J. Y. Yong, and K. M. Tan, "Control and management of a multilevel electric vehicles infrastructure integrated with distributed resources: A comprehensive review," *Renew. Sustain. Energy Rev.*, vol. 144, no. June 2020, p. 111020, 2021, doi: 10.1016/j.rser.2021.111020.

[2] H. M. Abdullah, A. Gastli, and L. Ben-Brahim, "Reinforcement Learning Based EV Charging Management Systems-A Review," *IEEE Access*, vol. 9, pp. 41506–41531, 2021, doi: 10.1109/ACCESS.2021.3064354.

[3] F. Gonzalez Venegas, M. Petit, and Y. Perez, "Active integration of electric vehicles into distribution grids: Barriers and frameworks for flexibility services," *Renew. Sustain. Energy Rev.*, vol. 145, no. March, 2021, doi: 10.1016/j.rser.2021.111060.

[4] J. Hu, X. Liu, M. Shahidehpour, and S. Xia, "Optimal operation of energy hubs with large-scale distributed energy resources for distribution network congestion management," *IEEE Trans. Sustain. Energy*, vol. 12, no. 3, pp. 1755–1765, 2021, doi: 10.1109/TSTE.2021.3064375.

[5] C. Edmunds *et al.*, "Congestion management with aggregated delivery of flexibility using distributed energy resources," *6th IEEE Int. Energy Conf. ENERGYCon 2020*, pp. 616–620, 2020, doi: 10.1109/ENERGYCon48941.2020.9236550.

[6] M. S. Alam and S. Ali Arefifar, "Optimal Allocation of EV Charging Stations in Distribution Systems Considering Discharging Economy and System Reliability," *IEEE Int. Conf. Electro Inf. Technol.*, vol. 2021-May, pp. 355–362, 2021, doi: 10.1109/EIT51626.2021.9491926.

[7] A. Pillay, S. Prabhakar Karthikeyan, and D. P. Kothari, "Congestion management in power systems - A review," *Int. J. Electr. Power Energy Syst.*, vol. 70, pp. 83–90, 2015, doi: 10.1016/j.ijepes.2015.01.022.

[8] P. Xue *et al.*, “Impact of Large-Scale Mobile Electric Vehicle Charging in Smart Grids: A Reliability Perspective,” *Front. Energy Res.*, vol. 9, 2021, doi: 10.3389/fenrg.2021.688034.

[9] D. S. Kirschen, “Demand-side view of electricity markets,” *IEEE Trans. Power Syst.*, vol. 18, no. 2, pp. 520–527, 2003, doi: 10.1109/TPWRS.2003.810692.

[10] A. K. Yadav, S. K. Srivastava, and A. Narain, “A Review on Congestion Management in Power System,” *Int. Conf. Electr. Electron. Eng. ICE3 2020*, pp. 359–364, 2020, doi: 10.1109/ICE348803.2020.9122988.

[11] M. M. Gajjala and A. Ahmad, “A survey on recent advances in transmission congestion management,” *Int. Rev. Appl. Sci. Eng.*, vol. 13, no. 1, pp. 29–41, 2021, doi: 10.1556/1848.2021.00286.

[12] L. Duchesne, E. Karangelos, and L. Wehenkel, “Recent Developments in Machine Learning for Energy Systems Reliability Management,” *Proc. IEEE*, vol. 108, no. 9, pp. 1656–1676, 2020, doi: 10.1109/JPROC.2020.2988715.

[13] A. K. Singh and S. K. Parida, “Congestion management with distributed generation and its impact on electricity market,” *Int. J. Electr. Power Energy Syst.*, vol. 48, no. 1, pp. 39–47, 2013, doi: 10.1016/j.ijepes.2012.11.025.

[14] J. Giraldez and D. Heap, “Overview of microgrids in a market environment,” *IEEE Green Technol. Conf.*, vol. 2015-July, pp. 36–43, 2015, doi: 10.1109/GREENTECH.2015.40.

[15] F. Bernáth and P. Mastný, “Distributed generation and voltage control in distribution network,” *Proc. 2014 15th Int. Sci. Conf. Electr. Power Eng. EPE 2014*, pp. 143–148, 2014, doi: 10.1109/EPE.2014.6839491.

[16] A. Singla, K. Singh, and V. K. Yadav, “Transmission congestion management in deregulated environment: A bibliographical survey,” *Int. Conf. Recent Adv. Innov. Eng. ICRAIE 2014*, 2014, doi: 10.1109/ICRAIE.2014.6909268.

[17] A. C. Tellidou and A. G. Bakirtzis, “Demand response in electricity markets,” *2009 15th Int. Conf. Intell. Syst. Appl. to Power Syst. ISAP ’09*, pp. 1–5, 2009, doi: 10.1109/ISAP.2009.5352855.

[18] N. Karthikeyan, B. R. Pokhrel, J. R. Pillai, B. Bak-Jensen, and K. H. B. Frederiksen, “Demand response in low voltage distribution networks with high PV penetration,” *2017 52nd Int. Univ. Power Eng. Conf. UPEC 2017*, vol. 2017-Janua, pp. 1–6, 2017, doi: 10.1109/UPEC.2017.8232014.

[19] S. Bahramirad, A. Khodaei, and R. Masiello, “Distribution Markets,” *IEEE Power Energy Mag.*, vol. 14, no. 2, pp. 102–106, 2016, doi: 10.1109/MPE.2016.2543121.

[20] J. Di, T. Chen, and Y. Hou, “Review of transmission network planning in market environment,” *Asia-Pacific Power Energy Eng. Conf. APPEEC*, 2013, doi: 10.1109/APPEEC.2013.6837126.

[21] T. Dronne, F. Roques, and M. Saguan, “Local flexibility markets for distribution network congestion-management in center-western Europe: which design for which needs ?” *Energies*, vol. 14:4113, 2021. https://doi.org/10.3390/en14144113.

[22] Q. Zhou, L. Tesfatsion, and C. C. Liu, “Short-term congestion forecasting in wholesale power markets,” *IEEE Trans. Power Syst.*, vol. 26, no. 4, pp. 2185–2196, 2011, doi: 10.1109/TPWRS.2011.2123118.

[23] D. T. Phan and S. Ghosh, “Predicting and mitigating congestion for an electric power system under load and renewable uncertainty,” *Proc. Am. Control Conf.*, vol. 2016-July, pp. 6791–6796, 2016, doi: 10.1109/ACC.2016.7526741.

[24] L. Min, S. T. Lee, P. Zhang, V. Rose, and J. Cole, “Short-term probabilistic transmission congestion forecasting,” *3rd Int. Conf. Deregul. Restruct. Power Technol. DRPT 2008*, no. April, pp. 764–770, 2008, doi: 10.1109/DRPT.2008.4523508.

[25] G. Zhang, B. Zhang, H. Sun, and W. Wu, “Ultra-short term probabilistic forecast of transmission congestion dynamics considering wind power integration,” *Dianli Xitong Zidonghua/Automation Electr. Power Syst.*, vol. 34, no. 13, pp. 1–6, 2010.

[26] A. Srivastava *et al.*, “Development of a DSO support tool for congestion forecast,” *IET Gener. Transm. Distrib.*, vol. 15, no. 23, pp. 3345–3359, 2021, doi: 10.1049/gtd2.12266.

[27] A. Gensler, B. Sick, and S. Vogt, “A review of deterministic error scores and normalization techniques for power forecasting algorithms,” *2016 IEEE Symp. Ser. Comput. Intell. SSCI 2016*, 2017, doi: 10.1109/SSCI.2016.7849848.

[28] B. Mohan and M. V. Ramesh, “Optimal dg placement under standard market design using GA,” *Proc. - ICETEEEM 2012, Int. Conf. Emerg. Trends Electr. Eng. Energy Manag.*, pp. 148–153, 2012, doi:

10.1109/ICETEEEM.2012.6494460.

[29] M. Khanabadi, Y. Fu, and C. Liu, “Decentralized transmission line switching for congestion management of interconnected power systems,” *IEEE Trans. Power Syst.*, vol. 33, no. 6, pp. 5902–5912, 2018, doi: 10.1109/TPWRS.2018.2838046.

[30] J. Zhang, S. Member, and A. Yokoyama, “Optimal power flow control for congestion management by interline power flow controller (IPFC),” *2006 International Conference on Power System Technology*, 2006, pp. 1-6, doi: 10.1109/ICPST.2006.321421.

[31] Y. T. Yoon, S. G. Raikar, and M. D. Ilic, “Congestion Management for Large Electric Power Systems Congestion Management for Large Electric Power Systems,” *6th Internaltional Conference on Probablistic Methods Applied to Power Systems*, no. 114, September 2000.

[32] A. Vengadesan and E. Engineering, “Transmission Congestion Management Through Optimal Placement and Sizing of Tcsc Devices in a Deregulated Power Network,” vol. 11, no. 8, pp. 697–713, 2020.

[33] H. Y. Yamin and S. M. Shahidehpour, “Transmission congestion and voltage profile management coordination in competitive electricity markets,” *Int. J. Electr. Power Energy Syst.*, vol. 25, no. 10, pp. 849–861, 2003, doi: 10.1016/S0142-0615(03)00070-X.

[34] Y. R. Sood and R. Singh, “Optimal model of congestion management in deregulated environment of power sector with promotion of renewable energy sources,” *Renew. Energy*, vol. 35, no. 8, pp. 1828–1836, 2010, doi: 10.1016/j.renene.2010.01.002.

[35] J. Bertsch, S. Hagspiel, and L. Just, “Congestion management in power systems: long-term modeling framework and large-scale application,” *Institute of Energy Economics at the University of Cologne (EWI)*, no. 15/03, 2015. http://hdl.handle.net/10419/121258.

[36] S. A. Hosseini, N. Amjady, M. Shafie-khah, and J. P. S. Catalão, “A new multi-objective solution approach to solve transmission congestion management problem of energy markets,” *Appl. Energy*, vol. 165, pp. 462–471, 2016, doi: 10.1016/j.apenergy.2015.12.101.

[37] S. Chanana and A. Kumar, “Power flow contribution factors based congestion management with real and reactive power bids in competitive electricity

markets," *2007 IEEE Power Eng. Soc. Gen. Meet. PES*, 2007, doi: 10.1109/PES.2007.385561.

[38] S. Gope, A. K. Goswami, P. K. Tiwari, and S. Deb, "Rescheduling of real power for congestion management with integration of pumped storage hydro unit using firefly algorithm," *Int. J. Electr. Power Energy Syst.*, vol. 83, pp. 434–442, 2016, doi: 10.1016/j.ijepes.2016.04.048.

[39] K. Paul, P. Dalapati, and N. Kumar, "Optimal Rescheduling of Generators to Alleviate Congestion in Transmission System: A Novel Modified Whale Optimization Approach," *Arab. J. Sci. Eng.*, 2021, doi: 10.1007/s13369-021-06136-y.

[40] S. Saravanabalaji, R. Krishnathevar, H. Thilagar S, and D. Durairaj, "A novel approach for congestion management using improved differential evolution algorithm," *Int. Trans. Electr. Energy Syst.*, vol. 28, no. 10, pp. 1–19, 2018, doi: 10.1002/etep.2614.

[41] B. K. Sarkar, A. De, and A. Chakrabarti, "Impact of Distributed Generation for congestion relief in power networks," *2012 1st Int. Conf. Power Energy NERIST, ICPEN 2012 - Proc.*, 2012, doi: 10.1109/ICPEN.2012.6492324.

[42] M. Sarwar and A. S. Siddiqui, "Congestion management in deregulated electricity market using distributed generation," *12th IEEE Int. Conf. Electron. Energy, Environ. Commun. Comput. Control (E3-C3), INDICON 2015*, no. 1, pp. 11–15, 2016, doi: 10.1109/INDICON.2015.7443618.

[43] M. Gitizadeh and M. Kalantar, "A new approach for congestion management via optimal location of FACTS devices in deregulated power systems," *3rd Int. Conf. Deregul. Restruct. Power Technol. DRPT 2008*, no. April, pp. 1592–1597, 2008, doi: 10.1109/DRPT.2008.4523659.

[44] Y. Tang, B. Ma, and Y. Li, "A new congestion management method considering voltage stability under electric market," 2008 Third International Conference on Electric Utility Deregulation and Restructuring and Power Technologies, 2008, pp. 567-571, doi: 10.1109/DRPT.2008.4523470.

[45] V. Gaonkar, R. B. Nanannavar, and Manjunatha, "Power system congestion management using sensitivity analysis and particle swarm optimization," *2017 Int. Conf. Energy, Commun. Data Anal. Soft Comput. ICECDS 2017*, pp. 1268–1271, 2018, doi: 10.1109/ICECDS.2017.8389646.

[46] J. P. Varghese, S. Ashok, and S. Kumaravel, "Optimal siting and sizing of

DGs for congestion relief in transmission lines," *Asia-Pacific Power Energy Eng. Conf. APPEEC*, vol. 2017-Novem, pp. 1–6, 2018, doi: 10.1109/APPEEC.2017.8309005.

[47] A. S. Bouhouras, G. C. Christoforidis, C. Parisses, and D. P. Labridis, "Reducing network congestion in distribution networks with high DG penetration via network reconfiguration," *Int. Conf. Eur. Energy Mark. EEM*, pp. 1–5, 2014, doi: 10.1109/EEM.2014.6861255.

[48] M. Pantoš, "Market-based congestion management in electric power systems with exploitation of aggregators," *Int. J. Electr. Power Energy Syst.*, vol. 121, no. March, 2020, doi: 10.1016/j.ijepes.2020.106101.

[49] S. T. Suganthi and D. Devaraj, "An improved teaching learning–based optimization algorithm for congestion management with the integration of solar photovoltaic system," *Meas. Control (United Kingdom)*, vol. 53, no. 7–8, pp. 1231–1237, 2020, doi: 10.1177/0020294020914930.

[50] K. Mwanza and Y. Shi, "Congestion Management: Redispatch and Application of FACTS," Dessertation, 2006.

[51] A. Narain, S. K. Srivastava, and S. N. Singh, "Congestion management approaches in restructured power system: Key issues and challenges," *Electr. J.*, vol. 33, no. 3, p. 106715, 2020, doi: 10.1016/j.tej.2020.106715.

[52] J. Verboomen, G. Papaefthymiou, W. L. Kling, and L. Van Der Sluis, "Use of phase shift transformers for minimising congestion Risk," Proceedings of the 10th International Conference on Probablistic Methods Applied to Power Systems, 2008, pp. 1-6. https://ieeexplore.ieee.org/abstract/document/4912673.

[53] A. N. M. M. Haque, D. S. Shafiullah, P. H. Nguyen, and F. W. Bliek, "Real-time congestion management in active distribution network based on dynamic thermal overloading cost," *19th Power Syst. Comput. Conf. PSCC 2016*, 2016, doi: 10.1109/PSCC.2016.7540985.

[54] G. De Carne, M. Liserre, K. Christakou, and M. Paolone, "Integrated voltage control and line congestion management in Active Distribution Networks by means of smart transformers," *IEEE Int. Symp. Ind. Electron.*, pp. 2613–2619, 2014, doi: 10.1109/ISIE.2014.6865032.

[55] K. Vijayakumar, "Optimal Location of FACTS Devices for Congestion Management in Deregulated Power Systems," *Int. J. Comput. Appl.*, vol. 16,

no. 6, pp. 29–37, 2011, doi: 10.5120/2015-1833.

[56] R. Surya, N. Janarthanan, and S. Balamurugan, “A novel technique for congestion management in transmission system by real power flow control,” *2017 Int. Conf. Intell. Comput. Instrum. Control Technol. ICICICT 2017*, vol. 2018-Janua, pp. 1349–1354, 2018, doi: 10.1109/ICICICT1.2017.8342766.

[57] V. P. Rajderkar and V. K. Chandrakar, “Comparison of series FACTS devices via optimal location in a power system for congestion management,” *Asia-Pacific Power Energy Eng. Conf. APPEEC*, pp. 0–4, 2009, doi: 10.1109/APPEEC.2009.4918227.

[58] T. Nireekshana, J. Bhavani, Y. Venu, and B. Phanisaikrishna, “Power Transmission Congestion Management by TCSC Using PSO,” *Proc. 4th Int. Conf. Comput. Methodol. Commun. ICCMC 2020*, no. Iccmc, pp. 491–497, 2020, doi: 10.1109/ICCMC48092.2020.ICCMC-00092.

[59] T. T. Nguyen and F. Mohammadi, “Optimal placement of TCSC for congestion management and power loss reduction using multi-objective genetic algorithm,” *Sustain.*, vol. 12, no. 7, pp. 1–15, 2020, doi: 10.3390/su12072813.

[60] A. Bagheri, A. Rabiee, S. Galvani, and F. Fallahi, “Congestion management through optimal allocation of facts devices using digsilent-based dpso algorithm-a real case study,” *J. Oper. Autom. Power Eng.*, vol. 8, no. 2, pp. 97–115, 2020, doi: 10.22098/joape.2019.6094.1462.

[61] J. G. Singh, S. N. Singh, and S. C. Srivastava, “Congestion management by using FACTS controller in power system,” *IEEE Reg. 10 Humanit. Technol. Conf. 2016, R10-HTC 2016 - Proc.*, pp. 4–10, 2017, doi: 10.1109/R10-HTC.2016.7906793.

[62] R. Retnamony and I. J. Raglend, “Congestion Management is to enhance the transient stability in a deregulated power system using FACTS devices,” *2015 Int. Conf. Control Instrum. Commun. Comput. Technol. ICCICCT 2015*, pp. 744–752, 2016, doi: 10.1109/ICCICCT.2015.7475379.

[63] M. H. Shariatkhah, M. R. Haghifam, and A. Arefi, “Load profile based determination of distribution feeder configuration by dynamic programming,” *2011 IEEE PES Trondheim PowerTech Power Technol. a Sustain. Soc. POWERTECH 2011*, pp. 1–6, 2011, doi: 10.1109/PTC.2011.6019329.

[64] R. Guguloth and T. K. S. Kumar, “LMP calculation and OPF based congestion

management in deregulated power systems," *ELEKTRO 2016 - 11th Int. Conf. Proc.*, pp. 299–304, 2016, doi: 10.1109/ELEKTRO.2016.7512085.

[65] S. Huang, Q. Wu, S. S. Oren, R. Li, and Z. Liu, "Distribution Locational Marginal Pricing Through Quadratic Programming for Congestion Management in Distribution Networks," *IEEE Trans. Power Syst.*, vol. 30, no. 4, pp. 2170–2178, 2015, doi: 10.1109/TPWRS.2014.2359977.

[66] P. Holmberg and E. Lazarczyk, "Congestion mangement in electricity networks: nodal, zonal and discriminatory pricing," Research Institute of Industrial Economics (IFN), no. 915, 2012. http://hdl.handle.net/10419/81489.

[67] S. Balamurugan, S. R. Shree, and K. R. M. V. Chandrakala, "Congestion management for multi area deregulated power system using price area concept," *Proc. 2017 IEEE Int. Conf. Technol. Adv. Power Energy Explor. Energy Solut. an Intell. Power Grid, TAP Energy 2017*, pp. 1–6, 2018, doi: 10.1109/TAPENERGY.2017.8397304.

[68] R. Hennig, M. Jonker, S. Tindemans, and L. De Vries, "Capacity Subscription Tariffs for Electricity Distribution Networks: Design Choices and Congestion Management," *Int. Conf. Eur. Energy Mark. EEM*, vol. 2020-Septe, 2020, doi: 10.1109/EEM49802.2020.9221994.

[69] S. Paraskar, D. K. Singh, and P. C. Tapre, "Lion algorithm for generation rescheduling based congestion management in deregulated power system," *2017 Int. Conf. Energy, Commun. Data Anal. Soft Comput. ICECDS 2017*, no. Cm, pp. 401–412, 2018, doi: 10.1109/ICECDS.2017.8390195.

[70] S. Bhattacharya, B. R. Kuanr, A. Routray, and A. Dash, "Transmission congestion management in restructured power system by rescheduling of generators using TLBO," *Proc. - 2017 IEEE Int. Conf. Electr. Instrum. Commun. Eng. ICEICE 2017*, vol. 2017-Decem, pp. 1–7, 2017, doi: 10.1109/ICEICE.2017.8191937.

[71] G. Yesuratnam and M. Pushpa, "Congestion management for security oriented power system operation using generation rescheduling," *2010 IEEE 11th Int. Conf. Probabilistic Methods Appl. to Power Syst. PMAPS 2010*, pp. 287–292, 2010, doi: 10.1109/PMAPS.2010.5528719.

[72] J. Srivastava and N. K. Yadav, "Rescheduling-based congestion management by metaheuristic algorithm: Hybridizing lion and moth search models," *Int. J. Numer. Model. Electron. Networks, Devices Fields*, no. August, pp. 1–18,

2021, doi: 10.1002/jnm.2952.

[73] M. U. Bashir, W. U. H. Paul, M. Ahmad, D. Ali, and M. S. Ali, “An Efficient Hybrid TLBO-PSO Approach for Congestion Management Employing Real Power Generation Rescheduling,” *Smart Grid Renew. Energy*, vol. 12, no. 08, pp. 113–135, 2021, doi: 10.4236/sgre.2021.128008.

[74] S. T. Suganthi, D. Devaraj, S. H. Thilagar, and K. Ramar, “Optimal generator rescheduling with distributed slack bus model for congestion management using improved teaching learning based optimization algorithm,” *Sadhana - Acad. Proc. Eng. Sci.*, vol. 43, no. 11, pp. 1–11, 2018, doi: 10.1007/s12046-018-0941-8.

[75] I. Kalogeropoulos and H. Sarimveis, “Predictive control algorithms for congestion management in electric power distribution grids,” *Appl. Math. Model.*, vol. 77, pp. 635–651, 2020, doi: 10.1016/j.apm.2019.07.034.

[76] F. Sossan and M. Marinelli, “An auto tuning substation peak shaving controller for congestion management using flexible demand,” *Proc. Univ. Power Eng. Conf.*, pp. 2–6, 2013, doi: 10.1109/UPEC.2013.6714963.

[77] C. M. Affonso and L. C. P. d. Silva, “Potential benefits of implementing load management to improve power system security,” *Int. J. Electr. Power Energy Syst.*, vol. 32, no. 6, pp. 704–710, 2010, doi: 10.1016/j.ijepes.2010.01.004.

[78] F. Shen, Q. Wu, S. Huang, X. Chen, H. Liu, and Y. Xu, “Two-tier demand response with flexible demand swap and transactive control for real-time congestion management in distribution networks,” *Int. J. Electr. Power Energy Syst.*, vol. 114, no. June 2019, p. 105399, 2020, doi: 10.1016/j.ijepes.2019.105399.

[79] O. Agbonaye, P. Keatley, Y. Huang, M. B. Mustafa, and N. Hewitt, “Design, valuation and comparison of demand response strategies for congestion management,” *Energies*, vol. 13, no. 22, 2020, doi: 10.3390/en13226085.

[80] R. Fonteijn, P. H. Nguyen, J. Morren, and J. G. Slootweg, “Demonstrating a generic four-step approach for applying flexibility for congestion management in daily operation,” *Sustain. Energy, Grids Networks*, vol. 23, p. 100378, 2020, doi: 10.1016/j.segan.2020.100378.

[81] S. Fattaheian-Dehkordi, M. Tavakkoli, A. Abbaspour, M. Fotuhi-Firuzabad, and M. Lehtonen, “An Incentive-Based Mechanism to Alleviate Active Power Congestion in a Multi-Agent Distribution System,” *IEEE Trans. Smart Grid*,

vol. 12, no. 3, pp. 1978–1988, 2021, doi: 10.1109/TSG.2020.3037560.

[82] D. A. Contreras, S. Muller, and K. Rudion, “Congestion Management Using Aggregated Flexibility at the TSO-DSO Interface,” *2021 IEEE Madrid PowerTech, PowerTech 2021 - Conf. Proc.*, pp. 1–6, 2021, doi: 10.1109/PowerTech46648.2021.9494793.

[83] S. Deb *et al.*, “Charging Coordination of Plug-In Electric Vehicle for Congestion Management in Distribution System Integrated with Renewable Energy Sources,” *IEEE Trans. Ind. Appl.*, vol. 56, no. 5, pp. 5452–5462, 2020, doi: 10.1109/TIA.2020.3010897.

[84] S, Deb, A. K. Goswami, R. L. Chetri, and R. Roy, “Distribution system congestion management by charging coordination of plug-in electric vehicle,” *2020 3rd International Conference on Energy, Power and Environment: Towards Clean Energy Technologies*, 2021, pp. 1-6, doi: 10.1109/ICEPE50861.2021.9404380.

[85] A. Al Zishan, M. M. Haji, and O. Ardakanian, “Adaptive Congestion Control for Electric Vehicle Charging in the Smart Grid,” *IEEE Trans. Smart Grid*, vol. 12, no. 3, pp. 2439–2449, 2021, doi: 10.1109/TSG.2021.3051032.

[86] M. Verhoog, N. Brinkel, and T. Alskaif, “Congestion management in LV grids using static and dynamic EV smart charging,” *SEST 2020 - 3rd Int. Conf. Smart Energy Syst. Technol.*, 2020, doi: 10.1109/SEST48500.2020.9203191.

[87] B. S. K. Patnam and N. M. Pindoriya, “DLMP Calculation and Congestion Minimization with EV Aggregator Loading in a Distribution Network Using Bilevel Program,” *IEEE Syst. J.*, vol. 15, no. 2, pp. 1835–1846, 2021, doi: 10.1109/JSYST.2020.2997189.

[88] E. S. Rigas and K. S. Tsompanidis, “Algorithms to Manage Congestion in Large-Scale Mobility-on-Demand Schemes that Use Electric Vehicles,” *SN Comput. Sci.*, vol. 2, no. 4, pp. 1–15, 2021, doi: 10.1007/s42979-021-00685-7.

[89] S. M. Hosseini, R. Carli, G. Cavone, and M. Dotoli, “Distributed control of electric vehicle fleets considering grid congestion and battery degradation,” *Internet Technol. Lett.*, vol. 3, no. 3, pp. 1–6, 2020, doi: 10.1002/itl2.161.

[90] M. Khanabadi, M. Doostizadeh, A. Esmaeilian, and M. Mohseninezhad, “Transmission congestion management through optimal distributed generation’s sizing and placement,” *2011 10th Int. Conf. Environ. Electr. Eng. EEEIC.EU 2011 - Conf. Proc.*, pp. 39–42, 2011, doi:

10.1109/EEEIC.2011.5874788.

[91] P. K. Masaud, Tarek Medalel, Mistry, Ronak Deepak, Sen, “Placement of large-scale utility-owned wind distributed generation based on probabilistic forecasting of line congestion,” 2017, pp. 979–986, doi: 10.1049/iet-rpg.2016.0944.

[92] M. Afkousi-Paqaleh, A. R. Noory, A. Abbaspour, and M. Rashidinejad, “Transmission congestion management using distributed generation considering load uncertainty,” *Asia-Pacific Power Energy Eng. Conf. APPEEC*, pp. 0–3, 2010, doi: 10.1109/APPEEC.2010.5449393.

[93] S. W. Alnaser and L. F. Ochoa, “Hybrid controller of energy storage and renewable DG for congestion management,” *IEEE Power Energy Soc. Gen. Meet.*, pp. 1–8, 2012, doi: 10.1109/PESGM.2012.6345393.

[94] M. Dashtdar, M. Najafi, and M. Esmaeilbeig, “Reducing LMP and resolving the congestion of the lines based on placement and optimal size of DG in the power network using the GA-GSF algorithm,” *Electr. Eng.*, vol. 103, no. 2, pp. 1279–1306, 2021, doi: 10.1007/s00202-020-01142-z.

[95] K. Spiliotis, S. Claeys, A. R. Gutierrez, and J. Driesen, “Utilizing local energy storage for congestion management and investment deferral in distribution networks,” *Int. Conf. Eur. Energy Mark. EEM*, vol. 2016-July, pp. 0–4, 2016, doi: 10.1109/EEM.2016.7521198.

[96] H. Labrini, A. Gad, R. A. Elshatshat, and M. M. A. Salama, “Dynamic graph based DG allocation for congestion mitigation in radial distribution networks,” *IEEE Power Energy Soc. Gen. Meet.*, vol. 2015-Septe, 2015, doi: 10.1109/PESGM.2015.7286611.

[97] E. Amicarelli, T. Q. Tran, and S. Bacha, “Flexibility service market for active congestion management of distribution networks using flexible energy resources of microgrids,” *2017 IEEE PES Innov. Smart Grid Technol. Conf. Eur. ISGT-Europe 2017 - Proc.*, vol. 2018-Janua, pp. 1–6, 2017, doi: 10.1109/ISGTEurope.2017.8260198.

[98] A. Yousefi, T. T. Nguyen, H. Zareipour, and O. P. Malik, “Congestion management using demand response and FACTS devices,” *Int. J. Electr. Power Energy Syst.*, vol. 37, no. 1, pp. 78–85, 2012, doi: 10.1016/j.ijepes.2011.12.008.

[99] A. Kumar and C. Sekhar, “DSM based congestion management in pool

electricity markets with FACTS devices," *Energy Procedia*, vol. 14, pp. 94–100, 2012, doi: 10.1016/j.egypro.2011.12.901.

[100] E. Shayesteh, M. P. Moghaddam, M. Ieee, and S. Taherynejhad, "Response Programs in Power Market," no. Cm, 2008. E. Shayesteh, M. Parsa Moghaddam, S. Taherynejhad and M. K. Sheikh-EL-Eslami, "Congestion Management using Demand Response programs in power market, " *2008 IEEE Power and Energy Society General Meeting - Conversion and Delivery of Electrical Energy in the 21st Century*, 2008, pp. 1-8, doi: 10.1109/PES.2008.4596877.

[101] V. Veerapandiyan, R. Kalaivani, and T. Mariammal, "Transmission system restructuring and optimal placement of DG for congestion management," *Proc. IEEE Int. Conf. Innov. Electr. Electron. Instrum. Media Technol. ICIEEIMT 2017*, vol. 2017-Janua, no. 978, pp. 239–249, 2017, doi: 10.1109/ICIEEIMT.2017.8116843.

[102] H. Doagou-Mojarrad, H. Rezaie, and H. Razmi, "Probabilistic integrated framework for AC/DC transmission congestion management considering system expansion, demand response, and renewable energy sources and load uncertainties," *Int. Trans. Electr. Energy Syst.*, no. August, pp. 1–23, 2021, doi: 10.1002/2050-7038.13168.

[103] S. K. Behera and N. K. Mohanty, "Congestion management using thyristor controlled series compensator employing Improved Grey Wolf Optimization technique," *Int. J. Electr. Eng. Educ.*, vol. 58, no. 2, pp. 179–199, 2021, doi: 10.1177/0020720918822730.

[104] F. Shen, Q. Wu, X. Jin, M. Zhang, S. Teimourzadeh, and O. B. Tor, "Coordination of dynamic tariff and scheduled reprofiling product for day-ahead congestion management of distribution networks," *Int. J. Electr. Power Energy Syst.*, vol. 135, no. October 2020, p. 107612, 2022, doi: 10.1016/j.ijepes.2021.107612.

[105] P. Du, Z. Chen, Z. Zhang, and Q. Zhao, "A Congestion Mitigation Model of Transmission Network Considering the Participation of Distribution Companies in Power Market," vol. 51, no. 4, 2021.

[106] S. B. Aruna, S. G. Fernandez, and S. G. Fernandez, "A Comprehensive Review on the Modern Power System Reliability Assessment," in *International Journal of Renewable Energy Research*, vol. 11, no. 4, 2021.

https://www.ijrer.org/ijrer/index.php/ijrer/article/view/12480/pdf.

[107] K. Qiu, “Reliability evaluation of power distribution systems considering electric vehicles and distributed,” Dissertation, 2020. Available: http://www.diva-portal.org/smash/record.jsf?pid=diva2%3A1507259.

[108] S. Peyghami, P. Palensky, and F. Blaabjerg, “An Overview on the Reliability of Modern Power Electronic Based Power Systems,” *IEEE Open J. Power Electron.*, vol. 1, no. March, pp. 34–50, 2020, doi: 10.1109/ojpel.2020.2973926.

[109] R. de Oliveira and C. L. T. Borges, “Influence of photovoltaic generation model and time resolution on the reliability evaluation of distribution systems,” *Int. J. Energy Res.*, vol. 45, no. 1, pp. 864–878, 2021, doi: 10.1002/er.5971.

[110] C. X. Wu, C. Y. Chung, F. S. Wen, and D. Y. Du, “Reliability/cost evaluation with pev and wind generation system,” *IEEE Trans. Sustain. Energy*, vol. 5, no. 1, pp. 273–281, 2014, doi: 10.1109/TSTE.2013.2281515.

[111] M. D. Kamruzzaman and M. Benidris, “Reliability-Based Metrics to Quantify the Maximum Permissible Load Demand of Electric Vehicles,” *IEEE Trans. Ind. Appl.*, vol. 55, no. 4, pp. 3365–3375, 2019, doi: 10.1109/TIA.2019.2914877.

[112] J. Dong *et al.*, “Integrating Transactive Energy into Reliability Evaluation for a Self-healing Distribution System with Microgrid,” *IEEE Trans. Sustain. Energy*, vol. 13, no. 1, pp. 122–134, 2021, doi: 10.1109/TSTE.2021.3105125.

[113] S. Argade, V. Aravinthan, and W. Jewell, “Probabilistic modeling of EV charging and its impact on distribution transformer loss of life,” *2012 IEEE Int. Electr. Veh. Conf. IEVC 2012*, pp. 1–8, 2012, doi: 10.1109/IEVC.2012.6183209.

[114] Q. Gong, S. Midlam-Mohler, V. Marano, and G. Rizzoni, “Distribution of PEV charging resources to balance transformer life and customer satisfaction,” *2012 IEEE Int. Electr. Veh. Conf. IEVC 2012*, pp. 1–7, 2012, doi: 10.1109/IEVC.2012.6183201.

[115] M. H. Mobarak and J. Bauman, “Vehicle-Directed Smart Charging Strategies to Mitigate the Effect of Long-Range EV Charging on Distribution Transformer Aging,” *IEEE Trans. Transp. Electrif.*, vol. 5, no. 4, pp. 1097–1111, 2019, doi: 10.1109/TTE.2019.2946063.

[116] M. Buhari, V. Levi, and S. K. E. Awadallah, “Modelling of ageing distribution cable for replacement planning,” *IEEE Trans. Power Syst.*, vol. 31, no. 5, pp. 3996–4004, 2016, doi: 10.1109/TPWRS.2015.2499269.

[117] G. Parise, L. Martirano, L. Parise, L. Gugliermetti, and F. Nardecchia, “A life loss tool for an optimal management in the operation of insulated LV power cables,” *IEEE Trans. Ind. Appl.*, vol. 55, no. 1, pp. 167–173, 2019, doi: 10.1109/TIA.2018.2866982.

[118] H. Turker, S. Bacha, D. Chatroux, and A. Hably, “Low-voltage transformer loss-of-life assessments for a high penetration of plug-in hybrid electric vehicles (PHEVs),” *IEEE Trans. Power Deliv.*, vol. 27, no. 3, pp. 1323–1331, 2012, doi: 10.1109/TPWRD.2012.2193423.

[119] W. Li, “Incorporating aging failures in power system reliability evaluation,” *IEEE Trans. Power Syst.*, vol. 17, no. 3, pp. 918–923, 2002, doi: 10.1109/TPWRS.2002.800989.

[120] S. K. E. Awadallah, J. V. Milanovic, and P. N. Jarman, “The influence of modeling transformer age related failures on system reliability,” *IEEE Trans. Power Syst.*, vol. 30, no. 2, pp. 970–979, 2015, doi: 10.1109/TPWRS.2014.2331103.

[121] X. Qi, Z. Ji, H. Wu, J. Zhang, and L. Wang, “Short-Term Reliability Assessment of Generating Systems Considering Demand Response Reliability,” *IEEE Access*, vol. 8, pp. 74371–74384, 2020, doi: 10.1109/ACCESS.2020.2988620.

[122] S. Shafiq, U. Bin Irshad, M. Al-Muhaini, S. Z. Djokic, and U. Akram, “Reliability Evaluation of Composite Power Systems: Evaluating the Impact of Full and Plug-in Hybrid Electric Vehicles,” *IEEE Access*, vol. 8, pp. 114305–114314, 2020, doi: 10.1109/ACCESS.2020.3003369.

[123] M. Kamruzzaman and M. Benidris, “Modeling of Electric Vehicles as Movable Loads in Composite System Reliability Assessment,” *IEEE Power Energy Soc. Gen. Meet.*, vol. 2018-Augus, 2018, doi: 10.1109/PESGM.2018.8585742.

[124] S. Guner and A. Ozdemir, “Impacts of feeder failure statistics on EV-supported distribution system reliability improvement,” *2019 IEEE Milan PowerTech, PowerTech 2019*, 2019, doi: 10.1109/PTC.2019.8810582.

[125] A. Alam *et al.*, “Optimal Placement of Reclosers in a Radial Distribution

System for Reliability Improvement," pp. 1–16, 2021.

[126] R. Sireesha, C. Srinivasa Rao, and M. Vijay Kumar, "Graph theory based transformation of existing Distribution network into clusters of multiple micro-grids for reliability enhancement," *Mater. Today Proc.*, no. xxxx, 2021, doi: 10.1016/j.matpr.2021.07.067.

[127] D. Hu, L. Sun, and M. Ding, "Integrated planning of active distribution network and DG integration in clusters considering a novel formulation for reliability assessment," *CSEE J. Power Energy Syst.*, vol. PP, no. 99, 2019, doi: 10.17775/CSEEJPES.2020.00150.

[128] P. Bayat, H. Afrakhte, and P. Bayat, "Reliability-oriented operation of distribution networks with multi-microgrids considering peer-to-peer energy sharing," *Sustain. Energy, Grids Networks*, vol. 28, p. 100530, 2021, doi: 10.1016/j.segan.2021.100530.

[129] S. Khan, S. Henein, and H. Brunner, "Optimal energy interruption planning and generation re-dispatch for improving reliability during contingencies," *2020 IEEE Power Energy Soc. Innov. Smart Grid Technol. Conf. ISGT 2020*, 2020, doi: 10.1109/ISGT45199.2020.9087713.

[130] M. Jooshaki *et al.*, "Linear Formulations for Topology-Variable-Based Distribution System Reliability Assessment Considering Switching Interruptions," *IEEE Trans. Smart Grid*, vol. 11, no. 5, pp. 4032–4043, 2020, doi: 10.1109/TSG.2020.2991661.

[131] H. Lee, B. O, S. Kim, and S. Kim, "V2G strategy for improvement of distribution network reliability considering time space network of EVs," in *Energies*, vol. 13, 4415, 2020. https://doi.org/10.3390/en13174415.

[132] S. Biswal, N. K. Sharma, and S. R. Samantaray, "Reliability-Based Cost Optimization in Power Distribution Systems Incorporating Distributed Generations and Capacitors," *Electr. Power Components Syst.*, pp. 1–14, 2021, doi: 10.1080/15325008.2021.2011489.

[133] A. Escalera, B. Hayes, and M. Prodanović, "A survey of reliability assessment techniques for modern distribution networks," *Renew. Sustain. Energy Rev.*, vol. 91, no. September 2017, pp. 344–357, 2018, doi: 10.1016/j.rser.2018.02.031.

[134] S. Kumar, R. K. Saket, D. K. Dheer, J. B. Holm-Nielsen, and P. Sanjeevikumar, "Reliability enhancement of electrical power system including

impacts of renewable energy sources: A comprehensive review," *IET Gener. Transm. Distrib.*, vol. 14, no. 10, pp. 1799–1815, 2020, doi: 10.1049/iet-gtd.2019.1402.

[135] R. H. A. Zubo, G. Mokryani, H. S. Rajamani, J. Aghaei, T. Niknam, and P. Pillai, "Operation and planning of distribution networks with integration of renewable distributed generators considering uncertainties: A review," *Renew. Sustain. Energy Rev.*, vol. 72, pp. 1177–1198, 2017, doi: 10.1016/j.rser.2016.10.036.

[136] H. Farzin, M. Moeini-Aghtaie, and M. Fotuhi-Firuzabad, "Reliability Studies of Distribution Systems Integrated with Electric Vehicles under Battery-Exchange Mode," *IEEE Trans. Power Deliv.*, vol. 31, no. 6, pp. 2473–2482, 2016, doi: 10.1109/TPWRD.2015.2497219.

[137] A. Tabares, G. Munoz-Delgado, J. F. Franco, J. M. Arroyo, and J. Contreras, "An Enhanced Algebraic Approach for the Analytical Reliability Assessment of Distribution Systems," *IEEE Trans. Power Syst.*, vol. 34, no. 4, pp. 2870–2879, 2019, doi: 10.1109/TPWRS.2019.2892507.

[138] W. C. Yeh, Y. C. Lin, Y. Y. Chung, and M. Chih, "A particle swarm optimization approach based on monte carlo simulation for solving the complex network reliability problem," *IEEE Trans. Reliab.*, vol. 59, no. 1, pp. 212–221, 2010, doi: 10.1109/TR.2009.2035796.

[139] Z. Li, W. Wu, B. Zhang, and X. Tai, "Analytical Reliability Assessment Method for Complex Distribution Networks Considering Post-Fault Network Reconfiguration," *IEEE Trans. Power Syst.*, vol. 35, no. 2, pp. 1457–1467, 2020, doi: 10.1109/TPWRS.2019.2936543.

[140] J. L. López-Prado, J. I. Vélez, and G. A. Garcia-Llinás, "Reliability evaluation in distribution networks with microgrids: Review and classification of the literature," *Energies*, vol. 13, no. 23, pp. 1–31, 2020, doi: 10.3390/en13236189.

[141] Z. Xu, H. Liu, H. Sun, S. Ge, and C. Wang, "Power supply capability evaluation of distribution systems with distributed generations under differentiated reliability constraints," *Int. J. Electr. Power Energy Syst.*, vol. 134, no. January 2021, p. 107344, 2022, doi: 10.1016/j.ijepes.2021.107344.

[142] H. Bai, S. Miao, P. Zhang, and Z. Bai, "Reliability evaluation of a distribution network with microgrid based on a combined power generation system,"

Energies, vol. 8, no. 2, pp. 1216–1241, 2015, doi: 10.3390/en8021216.

[143] N. Bhusal, M. Gautam, and M. Benidris, "Sizing of movable energy resources for service restoration and reliability enhancement," *IEEE Power Energy Soc. Gen. Meet.*, vol. 2020-Augus, pp. 21–25, 2020, doi: 10.1109/PESGM41954.2020.9281558.

[144] M. Memari, A. Karimi, and H. Hashemi-Dezaki, "Reliability evaluation of smart grid using various classic and metaheuristic clustering algorithms considering system uncertainties," *Int. Trans. Electr. Energy Syst.*, vol. 31, no. 6, pp. 1–28, 2021, doi: 10.1002/2050-7038.12902.

[145] S. Peyghami, F. Blaabjerg, and P. Palensky, "Incorporating Power Electronic Converters Reliability into Modern Power System Reliability Analysis," *IEEE J. Emerg. Sel. Top. Power Electron.*, vol. 9, no. 2, pp. 1668–1681, 2021, doi: 10.1109/JESTPE.2020.2967216.

[146] Q. Dong, J. Dong, L. Zhu, P. Kritprajun, and et al, "Impact of Self-healing Control on Reliability Evaluation in Distribution System with Microgrid," *2021 IEEE PES Innovative Smart Grid Technologies Europe (ISGT Europe)*, 2021, pp. 1–5, doi: 10.1109/ISGTEurope52324.2021.9640207.

[147] G. Munoz-Delgado, J. Contreras, and J. M. Arroyo, "Reliability Assessment for Distribution Optimization Models: A Non-Simulation-Based Linear Programming Approach," *IEEE Trans. Smart Grid*, vol. 9, no. 4, pp. 3048–3059, 2018, doi: 10.1109/TSG.2016.2624898.

[148] D. Božič and M. Pantoš, "Impact of electric-drive vehicles on power system reliability," *Energy*, vol. 83. pp. 511–520, 2015, doi: 10.1016/j.energy.2015.02.055.

[149] S. Cheng, Z. Wei, D. Shang, Z. Zhao, and H. Chen, "Charging Load Prediction and Distribution Network Reliability Evaluation Considering Electric Vehicles' Spatial-Temporal Transfer Randomness," *IEEE Access*, vol. 8, pp. 124084–124096, 2020, doi: 10.1109/ACCESS.2020.3006093.

[150] N. Z. Xu and C. Y. Chung, "Reliability evaluation of distribution systems including vehicle-to-home and vehicle-to-grid," *IEEE Trans. Power Syst.*, vol. 31, no. 1, pp. 759–768, 2016, doi: 10.1109/TPWRS.2015.2396524.

[151] L. Cheng, Y. Chang, J. Lin, and C. Singh, "Vehicle Integration Using Battery Exchange Mode," *IEEE Trans. Sustain. Energy*, vol. 4, no. 4, pp. 1034–1042, 2013.

[152] H. Farzin, M. Fotuhi-Firuzabad, and M. Moeini-Aghtaie, “Reliability Studies of Modern Distribution Systems Integrated With Renewable Generation and Parking Lots,” *IEEE Trans. Sustain. Energy*, vol. 8, no. 1, pp. 431–440, 2017, doi: 10.1109/TSTE.2016.2598365.

[153] K. R. Timalsena, P. Piya, and R. Karki, “A Novel Methodology to Incorporate Circuit Breaker Active Failure in Reliability Evaluation of Electrical Distribution Networks,” *IEEE Trans. Power Syst.*, vol. 36, no. 2, pp. 1013–1022, 2021, doi: 10.1109/TPWRS.2020.3010529.

[154] J. Kozyra, Z. Łukasik, A. Kuśmińska-Fijałkowska, and P. Kaszuba, “The impact of selected variants of remote control on power supply reliability indexes of distribution networks,” *Electr. Eng.*, no. 0123456789, 2021, doi: 10.1007/s00202-021-01383-6.

[155] M. R. Tur, “Reliability assessment of distribution power system when considering energy storage configuration technique,” *IEEE Access*, vol. 8, pp. 77962–77971, 2020, doi: 10.1109/ACCESS.2020.2990345.

[156] H. Shan, Y. Sun, W. Zhang, A. Kudreyko, and L. Ren, “Reliability Analysis of Power Distribution Network Based on PSO-DBN,” *IEEE Access*, vol. 8, pp. 224884–224894, 2020, doi: 10.1109/ACCESS.2020.3007776.

[157] R. S. Pinto, C. Unsihuay-Vila, and F. H. Tabarro, “Reliability-constrained robust expansion planning of active distribution networks,” *IET Gener. Transm. Distrib.*, vol. 16, no. 1, pp. 27–40, 2022, doi: 10.1049/gtd2.12263.

[158] A. M. Hariri, M. A. Hejazi, and H. Hashemi-Dezaki, “Reliability optimization of smart grid based on optimal allocation of protective devices, distributed energy resources, and electric vehicle/plug-in hybrid electric vehicle charging stations,” *J. Power Sources*, vol. 436, no. July, p. 226824, 2019, doi: 10.1016/j.jpowsour.2019.226824.

[159] A. Noori, Y. Zhang, N. Nouri, and M. Hajivand, “Multi-Objective Optimal Placement and Sizing of Distribution Static Compensator in Radial Distribution Networks with Variable Residential, Commercial and Industrial Demands Considering Reliability,” *IEEE Access*, vol. 9, pp. 46911–46926, 2021, doi: 10.1109/ACCESS.2021.3065883.

[160] W. Sun, F. Neumann, and G. P. Harrison, “Robust Scheduling of Electric Vehicle Charging in LV Distribution Networks under Uncertainty,” *IEEE Trans. Ind. Appl.*, vol. 56, no. 5, pp. 5785–5795, 2020, doi:

10.1109/TIA.2020.2983906.

[161] M. Naguib, W. A. Omran, and H. E. A. Talaat, “Performance Enhancement of Distribution Systems via Distribution Network Reconfiguration and Distributed Generator Allocation Considering Uncertain Environment | SGEPRI Journals & Magazine | IEEE Xplore,” vol. XX, no. Xx, pp. 1–9, doi: 10.35833/MPCE.2020.000333.

[162] K. Zou, G. Mohy-ud-din, A. P. Agalgaonkar, K. M. Muttaqi, and S. Perera, “Distribution system restoration with renewable resources for reliaiblity improvement under system uncertainties,” in *IEEE Transactions on Industrial Electronics*, vol. 67, no. 10, pp. 8438–8449, 2020, doi: 10.1109/TIE.2019.2947807.

[163] F. J. Ruiz-Rodriguez, M. Gomez-Gonzalez, and F. Jurado, “Reliability optimization of an electric power system by biomass fuelled gas engine,” *Int. J. Electr. Power Energy Syst.*, vol. 61, pp. 81–89, 2014, doi: 10.1016/j.ijepes.2014.03.019.

[164] K. Qian, C. Zhou, and Y. Yuan, “Impacts of high penetration level of fully electric vehicles charging loads on the thermal ageing of power transformers,” in Electrical Power and Energy Systems, vol.65, pp.102-112, 2015, doi: https://doi.org/10.1016/j.ijepes.2014.09.040.

[165] Q. Gong, S. Midlam-Mohler, E. Serra, V. Marano, and G. Rizzoni, “PEV charging control considering transformer life and experimental validation of a 25 kVA distribution transformer,” *IEEE Trans. Smart Grid*, vol. 6, no. 2, pp. 648–656, 2015, doi: 10.1109/TSG.2014.2365452.

[166] O. Sadeghian, M. Nazari-Heris, M. Abapour, S. S. Taheri, and K. Zare, “Improving reliability of distribution networks using plug-in electric vehicles and demand response,” *J. Mod. Power Syst. Clean Energy*, vol. 7, no. 5, pp. 1189–1199, 2019, doi: 10.1007/s40565-019-0523-8.

[167] S. Guner and A. Ozdemir, “Reliability improvement of distribution system considering EV parking lots,” *Electr. Power Syst. Res.*, vol. 185, no. May, p. 106353, 2020, doi: 10.1016/j.epsr.2020.106353.

[168] V. Y. Lyubchenko, A. F. Iskhakov, and D. A. Pavlyuchenko, “Reclosers optimal allocation for improving the distribution network reliability,” *Proc. - 2021 Int. Conf. Ind. Eng. Appl. Manuf. ICIEAM 2021*, pp. 13–18, 2021, doi: 10.1109/ICIEAM51226.2021.9446330.

[169] A. Banerjee, S. Chattopadhyay, M. Gavrilas, and G. Grigoras, “Optimization and estimation of reliability indices and cost of power distribution system of an urban area by a noble fuzzy-hybrid algorithm,” in *Applied Soft Computing Journal*, vol. 102, 2021. doi: https://doi.org/10.1016/j.asoc.2021.107078.

[170] M. Jooshaki, S. Karimi-Arpanahi, M. Lehtonen, R. J. Millar, and M. Fotuhi-Firuzabad, “Electricity distribution system switch optimization under incentive reliability scheme,” *IEEE Access*, vol. 8, pp. 93455–93463, 2020, doi: 10.1109/ACCESS.2020.2995374.

[171] J. R. Bezerra, G. C. Barroso, R. P. Saraiva Leão, and R. F. Sampaio, “Multiobjective Optimization Algorithm for Switch Placement in Radial Power Distribution Networks,” *IEEE Trans. Power Deliv.*, vol. 30, no. 2, pp. 545–552, 2015, doi: 10.1109/TPWRD.2014.2317173.

[172] Z. Li, W. Wu, X. Tai, and B. Zhang, “Optimization Model-Based Reliability Assessment for Distribution Networks Considering Detailed Placement of Circuit Breakers and Switches,” *IEEE Trans. Power Syst.*, vol. 35, no. 5, pp. 3991–4004, 2020, doi: 10.1109/TPWRS.2020.2981508.

[173] M. Jooshaki, S. Karimi-Arpanahi, M. Lehtonen, R. J. Millar, and M. Fotuhi-Firuzabad, “Reliability-Oriented Electricity Distribution System Switch and Tie Line Optimization,” *IEEE Access*, vol. 8, pp. 130967–130978, 2020, doi: 10.1109/ACCESS.2020.3009827.

[174] H. Karimi *et al.*, “Automated Distribution Networks Reliability Optimization in the Presence of DG Units Considering Probability Customer Interruption: A Practical Case Study,” *IEEE Access*, vol. 9, pp. 98490–98505, 2021, doi: 10.1109/ACCESS.2021.3096128.

[175] A. Heidari, Z. Y. Dong, D. Zhang, P. Siano, and J. Aghaei, “Mixed-integer nonlinear programming formulation for distribution networks reliability optimization,” *IEEE Trans. Ind. Informatics*, vol. 14, no. 5, pp. 1952–1961, 2018, doi: 10.1109/TII.2017.2773572.

[176] J. Jose and A. Kowli, “Optimal Augmentation of Distribution Networks for Improved Reliability,” *IEEE Syst. J.*, pp. 1–9, 2021, doi: 10.1109/JSYST.2021.3089716.

[177] R. C. Lotero and J. Contreras, “Distribution system planning with reliability,” *IEEE Trans. Power Deliv.*, vol. 26, no. 4, pp. 2552–2562, 2011, doi: 10.1109/TPWRD.2011.2167990.

[178] A. Kavousi-fard and T. Niknam, “Optimal Distribution Feeder Reconfiguration for Reliability Improvement Considering Uncertainty,” *IEEE Trans. Power Deliv.*, vol. 29, no. 3, pp. 1344–1353, 2014. doi: https://doi.org/10.1109/TPWRD.2013.2292951

[179] J. Jose and A. Kowli, “Path-Based Distribution Feeder Reconfiguration for Optimization of Losses and Reliability,” *IEEE Syst. J.*, vol. 14, no. 1, pp. 1417–1426, 2020, doi: 10.1109/JSYST.2019.2917536.

[180] N. G. Paterakis *et al.*, “Multi-Objective Reconfiguration of Radial Distribution Systems Using Reliability Indices,” *IEEE Trans. Power Syst.*, vol. 31, no. 2, pp. 1048–1062, 2016, doi: 10.1109/TPWRS.2015.2425801.

[181] P. Srividhya *et al.*, “Reliability improvement of radial distribution system by reconfiguration,” *Adv. Sci. Technol. Eng. Syst.*, vol. 5, no. 6, pp. 472–480, 2020, doi: 10.25046/aj050656.

[182] M. Razavi, H. Momeni, M. R. Haghifam, and S. Bolouki, “Multi-Objective Optimization of Distribution Networks Via Daily Reconguration,” *IEEE Trans. Power Deliv.*, vol. 8977, no. c, pp. 1–11, 2021, doi: 10.1109/TPWRD.2021.3070796.

[183] O. Kahouli, H. Alsaif, Y. Bouteraa, N. Ben Ali, and M. Chaabene, “Power system reconfiguration in distribution network for improving reliability using genetic algorithm and particle swarm optimization,” *Appl. Sci.*, vol. 11, no. 7, 2021, doi: 10.3390/app11073092.

[184] P. Lata and S. Vadhera, “TLBO-based approach to optimally place and sizing of energy storage system for reliability enhancement of radial distribution system,” *Int. Trans. Electr. Energy Syst.*, vol. 30, no. 5, pp. 1–20, 2020, doi: 10.1002/2050-7038.12334.

[185] X. Wu, S. Member, A. J. Conejo, and S. Mathew, “Optimal Siting of Batteries in Distribution Systems to Enhance Reliability,” vol. 36, no. 5, pp. 3118–3127, 2021. doi: 10.1109/TPWRD.2020.3034095.

[186] A. Azizivahed, E. Naderi, H. Narimani, M. Fathi, and M. R. Narimani, “A new bi-objective approach to energy management in distribution networks with energy storage systems,” *IEEE Trans. Sustain. Energy*, vol. 9, no. 1, pp. 56–64, 2018, doi: 10.1109/TSTE.2017.2714644.

[187] S. Junlakarn and M. Ilic, “Distribution system reliability options and utility liability,” *IEEE Trans. Smart Grid*, vol. 5, no. 5, pp. 2227–2234, 2014, doi:

10.1109/TSG.2014.2316021.

[188] F. M. Rodrigues, L. R. Araujo, S. Member, D. R. R. Penido, and S. Member, "A Method to Improve Distribution System Reliability Using Available Mobile Generators," in *IEEE System Journal*, vol. 15, no. 3, pp. 4635–4643, 2021, doi: 10.1109/JSYST.2020.3015154.

[189] I. Ziari, G. Ledwich, S. Member, A. Ghosh, and G. Platt, "Integrated Distribution Systems Planning to Improve Reliability Under Load Growth," in *IEEE Transactions on Power Delivery*, vol. 27, no. 2, pp. 757–765, 2012, doi: 10.1109/TPWRD.2011.2176964.

[190] A. Kavousi-fard, S. Member, M. A. Rostami, and S. Member, "Reliability-Oriented Reconfiguration of Vehicle-to-Grid Networks," in *IEEE Transactions on Industrial Informatics*, vol. 11, no. 3, pp. 682-691, June 2015, doi: 10.1109/TII.2015.2423093.

[191] A. Jafari, H. Ganjeh Ganjehlou, T. Khalili, and A. Bidram, "A fair electricity market strategy for energy management and reliability enhancement of islanded multi-microgrids," *Appl. Energy*, vol. 270, no. April, p. 115170, 2020, doi: 10.1016/j.apenergy.2020.115170.

[192] Z. Li, W. Wu, X. Tai, and B. Zhang, "A Reliability-Constrained Expansion Planning Model for Mesh Distribution Networks," *IEEE Trans. Power Syst.*, vol. 36, no. 2, pp. 948–960, 2021, doi: 10.1109/TPWRS.2020.3015061.

[193] D. Singh and K. S. Verma, "GA-based congestion management in deregulated power system using FACTS devices," *Proc. 2011 Int. Conf. Util. Exhib. Power Energy Syst. Issues Prospect. Asia, ICUE 2011*, pp. 1–6, 2012, doi: 10.1109/ICUEPES.2011.6497716.

[194] S. S. Reddy, M. S. Kumari, and M. Sydulu, "Congestion management in deregulated power system by optimal choice and allocation of FACTS controllers using multi-objective genetic algorithm," *2010 IEEE PES Transm. Distrib. Conf. Expo. Smart Solut. a Chang. World*, no. 2, 2010, doi: 10.1109/TDC.2010.5484520.

[195] F. H. Tavakoli, M. Hojjat, and M. H. Javidi, "Determining optimal location and capacity of DG units based on system uncertainties and optimal congestion management in transmission network," *2017 25th Iran. Conf. Electr. Eng. ICEE 2017*, pp. 1260–1265, 2017, doi: 10.1109/IranianCEE.2017.7985235.

[196] T. Bhattacharjee and A. K. Chakraborty, “Congestion management in a deregulated power system using NSGAII,” *2012 IEEE 5th Power India Conf. PICONF 2012*, no. Dm, 2012, doi: 10.1109/PowerI.2012.6479529.

[197] A. Prasanthi and T. K. Sindhu, “Optimal placement and rating of FACTS devices for congestion management in power system without and with wind energy integration,” *Proc. 2014 IEEE Int. Conf. Adv. Commun. Control Comput. Technol. ICACCCT 2014*, vol. 1, no. 978, pp. 224–229, 2015, doi: 10.1109/ICACCCT.2014.7019434.

[198] M. M. Esfahani, M. H. Cintuglu, O. A. Mohammed, “Optimal Real-time congestion management in power markets based on partical swarm optimization” *2017 IEEE Power & Energy Society General Meeting,* 2017, pp. 1-5, doi: 10.1109/PESGM.2017.8274117.

[199] M. H. Moradi and M. Abedini, “A combination of genetic algorithm and particle swarm optimization for optimal DG location and sizing in distribution systems,” *Int. J. Electr. Power Energy Syst.*, vol. 34, no. 1, pp. 66–74, 2012, doi: 10.1016/j.ijepes.2011.08.023.

[200] R. A. Hooshmand, M. J. Morshed, and M. Parastegari, “Congestion management by determining optimal location of series FACTS devices using hybrid bacterial foraging and Nelder-Mead algorithm,” *Appl. Soft Comput. J.*, vol. 28, pp. 57–68, 2015, doi: 10.1016/j.asoc.2014.11.032.

[201] S. Sachan and M. H. Amini, “Optimal allocation of EV charging spots along with capacitors in smart distribution network for congestion management,” *Int. Trans. Electr. Energy Syst.*, vol. 30, no. 9, pp. 1–14, 2020, doi: 10.1002/2050-7038.12507.

[202] A. Mohsenzadeh, C. Pang, and L. Yang, “Transmission congestion management considering EV parking lots and demand response programmes,” *Int. J. Ambient Energy*, vol. 42, no. 15, pp. 1727–1731, 2021, doi: 10.1080/01430750.2019.1614985.

[203] V. K. Prajapati and V. Mahajan, “Reliability assessment and congestion management of power system with energy storage system and uncertain renewable resources,” *Energy*, vol. 215, 2021, doi: 10.1016/j.energy.2020.119134.

[204] Y. Li, K. Xie, L. Wang, and Y. Xiang, “The impact of PHEVs charging and network topology optimization on bulk power system reliability,” *Electr.*

Power Syst. Res., vol. 163, no. May, pp. 85–97, 2018, doi: 10.1016/j.epsr.2018.06.002.

[205] N. I. Yusoff, A. A. M. Zin, and A. Bin Khairuddin, "Congestion management in power system: A review," *3rd Int. Conf. Power Gener. Syst. Renew. Energy Technol. PGSRET 2017*, vol. 2018-Janua, pp. 22–27, 2017, doi: 10.1109/PGSRET.2017.8251795.

[206] S. Phichaisawat, Y. H. Song, and G. A. Taylor, "Congestion management considering voltage security constraints," *PowerCon 2002 - 2002 Int. Conf. Power Syst. Technol. Proc.* , vol. 3, pp. 1819–1823, 2002, doi: 10.1109/ICPST.2002.1067845.

[207] F. Capitanescu and T. Van Cutsem, "A unified management of congestions due to voltage instability and thermal overload," *Electr. Power Syst. Res.*, vol. 77, no. 10, pp. 1274–1283, 2007, doi: 10.1016/j.epsr.2006.09.015.

[208] A. N. M. M. Haque, P. H. Nguyen, T. H. Vo, and F. W. Bliek, "Agent-based unified approach for thermal and voltage constraint management in LV distribution network," *Electr. Power Syst. Res.*, vol. 143, pp. 462–473, 2017, doi: 10.1016/j.epsr.2016.11.007.

[209] M. M. Rahman, A. Arefi, G. M. Shafiullah, and S. Hettiwatte, "Penetration maximisation of residential rooftop photovoltaic using demand response," *2016 Int. Conf. Smart Green Technol. Electr. Inf. Syst. Adv. Smart Green Technol. to Build Smart Soc. ICSGTEIS 2016 - Proc.*, no. October, pp. 21–26, 2017, doi: 10.1109/ICSGTEIS.2016.7885760.

[210] H. Pezeshki, A. Arefi, G. Ledwich, and P. Wolfs, "Probabilistic Voltage Management Using OLTC and dSTATCOM in Distribution Networks," *IEEE Trans. Power Deliv.*, vol. 33, no. 2, pp. 570–580, 2018, doi: 10.1109/TPWRD.2017.2718511.

[211] H. Emami and J. A. Sadri, "Congestion management of transmission lines in the market environment," *Int. Res. J. Appl. Basic Sci.*, vol. 3, no. S, pp. 2572–2580, 2012, [Online]. Available: www.irjabs.com.

[212] B. J. Kirby and J. W. Van Dyke, "Congestion management requirement, methods and performance indices," in Consortium for Electric Reliability Technology Solutions, June. 2002. Available: http://www.ntis.gov/support/ordernowabout.htm

[213] A. Ahmadian, M. Sedghi, and M. Aliakbar-Golkar, "Stochastic modeling of

Plug-in Electric Vehicles load demand in residential grids considering nonlinear battery charge characteristic," *20th Electr. Power Distrib. Conf. EPDC 2015*, no. April, pp. 22–26, 2015, doi: 10.1109/EPDC.2015.7330467.

[214] M. Mao, S. Zhang, L. Chang, and N. D. Hatziargyriou, "Schedulable capacity forecasting for electric vehicles based on big data analysis," *J. Mod. Power Syst. Clean Energy*, vol. 7, no. 6, pp. 1651–1662, 2019, doi: 10.1007/s40565-019-00573-3.

[215] A. Samimi, "Probabilistic day-ahead simultaneous active/reactive power management in active distribution systems," *J. Mod. Power Syst. Clean Energy*, vol. 7, no. 6, pp. 1596–1607, 2019, doi: 10.1007/s40565-019-0535-4.

[216] F. R. Badal, P. Das, S. K. Sarker, and S. K. Das, "A survey on control issues in renewable energy integration and microgrid," *Prot. Control Mod. Power Syst.*, vol. 4, no. 1, 2019, doi: 10.1186/s41601-019-0122-8.

[217] J. Zhao, A. Arefi, A. Borghetti, J. M. Delarestaghi, and G. M. Shafiullah, "Characterization of Congestion in Distribution Network Considering High Penetration of PV Generation and EVs," in *IEEE Power and Energy Society General Meeting*, 2019, vol. 2019-Augus, doi: 10.1109/PESGM40551.2019.8973859.

[218] S. Huang, Q. Wu, Z. Liu, and A. H. Nielsen, "Review of congestion management methods for distribution networks with high penetration of distributed energy resources," *IEEE PES Innov. Smart Grid Technol. Conf. Eur.*, vol. 2015-Janua, no. January, pp. 1–6, 2015, doi: 10.1109/ISGTEurope.2014.7028811.

[219] H. Sagha, G. Mokhtari, A. Arefi, G. Nourbakhsh, G. Ledwich, and A. Ghosh, "A New Approach to Improve PV Power Injection in LV Electrical Systems Using DVR," *IEEE Syst. J.*, vol. 12, no. 4, pp. 3324–3333, 2018, doi: 10.1109/JSYST.2017.2755075.

[220] K. Geschermann and A. Moser, "Evaluation of market-based flexibility provision for congestion management in distribution grids," *IEEE Power Energy Soc. Gen. Meet.*, vol. 2018-Janua, pp. 1–5, 2018, doi: 10.1109/PESGM.2017.8274215.

[221] A. Borghetti *et al.*, "Short-term scheduling and control of active distribution systems with high penetration of renewable resources," *IEEE Syst. J.*, vol. 4, no. 3, pp. 313–322, 2010, doi: 10.1109/JSYST.2010.2059171.

[222] E. Jonckheere, R. Banirazi, and E. Grippo, “Congestion managment for cost-effective power grid load balancing using FACTS and energy storage devices allocated via grid curvature means,” *Proc. Am. Control Conf.*, vol. 2019-July, pp. 3909–3915, 2019, doi: 10.23919/acc.2019.8814693.

[223] F. Zaeim-Kohan, H. Razmi, and H. Doagou-Mojarrad, “Multi-objective transmission congestion management considering demand response programs and generation rescheduling,” *Appl. Soft Comput. J.*, vol. 70, pp. 169–181, 2018, doi: 10.1016/j.asoc.2018.05.028.

[224] S. Huang, Q. Wu, M. Shahidehpour, and Z. Liu, “Dynamic power tariff for congestion management in distribution networks,” *IEEE Trans. Smart Grid*, vol. 10, no. 2, pp. 2148–2157, 2019, doi: 10.1109/TSG.2018.2790638.

[225] S. Huang and Q. Wu, “Dynamic Tariff-Subsidy Method for PV and V2G Congestion Management in Distribution Networks,” *IEEE Trans. Smart Grid*, vol. 10, no. 5, pp. 5851–5860, 2019, doi: 10.1109/tsg.2019.2892302.

[226] A. Hermann, J. Kazempour, S. Huang, and J. Ostergaard, “Congestion Management in Distribution Networks with Asymmetric Block Offers,” *IEEE Trans. Power Syst.*, vol. 34, no. 6, pp. 4382–4392, 2019, doi: 10.1109/TPWRS.2019.2912386.

[227] P. Chen, Z. Chen, and B. Bak-Jensen, “Probabilistic load flow: A review,” *3rd Int. Conf. Deregul. Restruct. Power Technol. DRPT 2008*, no. April, pp. 1586–1591, 2008, doi: 10.1109/DRPT.2008.4523658.

[228] T. Ghose, H. W. Pandey, and K. R. Gadham, “Risk assessment of microgrid aggregators considering demand response and uncertain renewable energy sources,” *J. Mod. Power Syst. Clean Energy*, vol. 7, no. 6, pp. 1619–1631, 2019, doi: 10.1007/s40565-019-0513-x.

[229] H. Liao and J. V. Milanovic, “Flexibility Exchange Strategy to Facilitate Congestion and Voltage Profile Management in Power Networks,” *IEEE Trans. Smart Grid*, vol. 10, no. 5, pp. 4786–4794, 2018, doi: 10.1109/TSG.2018.2868461.

[230] A. N. M. M. Haque, P. H. Nguyen, F. W. Bliek, and J. G. Slootweg, “Demand response for real-time congestion management incorporating dynamic thermal overloading cost,” *Sustain. Energy, Grids Networks*, vol. 10, pp. 65–74, 2017, doi: 10.1016/j.segan.2017.03.002.

[231] A. Narimani, G. Nourbakhsh, A. Arefi, G. F. Ledwich, and G. R. Walker,

"SAIDI constrained economic planning and utilization of central storage in rural distribution networks," *IEEE Syst. J.*, vol. 13, no. 1, pp. 842–853, 2019, doi: 10.1109/JSYST.2018.2852630.

[232] J. H. Teng, "A direct approach for distribution system load flow solutions," *IEEE Trans. Power Deliv.*, vol. 18, no. 3, pp. 882–887, 2003, doi: 10.1109/TPWRD.2003.813818.

[233] Distribution System Analysis Subcommittee, "IEEE 123 Node Test Feeder," *Power System Analysis, Computing and Economics Committee*, 1921.

[234] A. Forbes, "Customer-side voltage regulation to mitigate PV-induced power quality problems in radial distribution networks," Murdoch University, 2018.

[235] D. Fischer, A. Harbrecht, A. Surmann, and R. McKenna, "Electric vehicles' impacts on residential electric local profiles – A stochastic modelling approach considering socio-economic, behavioural and spatial factors," *Applied Energy*, vol. 233–234. pp. 644–658, 2019, doi: 10.1016/j.apenergy.2018.10.010.

[236] P. K. H. Dost, P. Spichartz, and C. Sourkounis, "Charging Behavior of Users Utilizing Battery Electric Vehicles and Extended Range Electric Vehicles Within the Scope of a Field Test," *IEEE Trans. Ind. Appl.*, vol. 54, no. 1, pp. 580–590, 2018, doi: 10.1109/TIA.2017.2758753.

[237] A. Akrami, M. Doostizadeh, and F. Aminifar, "Power system flexibility: an overview of emergence to evolution," *J. Mod. Power Syst. Clean Energy*, vol. 7, no. 5, pp. 987–1007, 2019, doi: 10.1007/s40565-019-0527-4.

[238] G. Tsaousoglou, P. Makris, and E. Varvarigos, "Electricity market policies for penalizing volatility and scheduling strategies: The value of aggregation, flexibility, and correlation," *Sustain. Energy, Grids Networks*, vol. 12, pp. 57–68, 2017, doi: 10.1016/j.segan.2017.09.004.

[239] E. T. Wondmagegnehu, J. Navarro, and P. J. Hernandez, "Bathtub shaped failure rates from mixtures: A practical point of view," *IEEE Trans. Reliab.*, vol. 54, no. 2, pp. 270–275, 2005, doi: 10.1109/TR.2005.847271.

[240] B. Behi, A. Baniasadi, A. Arefi, A. Gorjy, P. Jennings, and A. Pivrikas, "Cost – Benefit Analysis of a Virtual Power Plant Including Solar PV , Flow Battery , Heat Pump , Case Study," *Energies*, 2020.

[241] A. Arefi, G. Ledwich, G. Nourbakhsh, and B. Behi, "A Fast Adequacy Analysis for Radial Distribution Networks Considering Reconfiguration and

DGs," *IEEE Trans. Smart Grid*, vol. 11, no. 5, pp. 3896–3909, 2020, doi: 10.1109/TSG.2020.2977211.

[242] K. Kumar, B. G. Kumbhar, and S. Satsangi, "Assessment of Effect of Load Models on Loss-of-Life Calculation of a Transformer Using a Point Estimation Method," *Electr. Power Components Syst.*, vol. 46, no. 16–17, pp. 1808–1819, 2018, doi: 10.1080/15325008.2018.1511874.

[243] H. Pezeshki, P. J. Wolfs, and G. Ledwich, "Impact of high PV penetration on distribution transformer insulation life," *IEEE Trans. Power Deliv.*, vol. 29, no. 3, pp. 1212–1220, 2014, doi: 10.1109/TPWRD.2013.2287002.

[244] M. Dong and A. B. Nassif, "Combining modified weibull distribution models for power system reliability forecast," in *IEEE Transactions on Power Systems*, vol. 34, no. 2, pp. 1610–1619, March 2019, doi: 10.1109/TPWRS.2018.2877743.

[245] M. R. Sarker, D. J. Olsen, and M. A. Ortega-Vazquez, "Co-Optimization of Distribution Transformer Aging and Energy Arbitrage Using Electric Vehicles," *IEEE Trans. Smart Grid*, vol. 8, no. 6, pp. 2712–2722, 2017, doi: 10.1109/TSG.2016.2535354.

[246] S. J. Almalki and S. Nadarajah, "A new discrete modified weibull distribution," *IEEE Trans. Reliab.*, vol. 63, no. 1, pp. 68–80, 2014, doi: 10.1109/TR.2014.2299691.

[247] M. Buhari, V. Levi, and S. K. E. Awadallah, "Modelling of ageing distribution cable for replacement planning," *IEEE Trans. Power Syst.*, vol. 31, no. 5, pp. 3996–4004, 2016, doi: 10.1109/TPWRS.2015.2499269.

[248] D. Fischer, A. Harbrecht, A. Surmann, and R. McKenna, "Electric vehicles' impacts on residential electric local profiles – A stochastic modelling approach considering socio-economic, behavioural and spatial factors," *Applied Energy*, vol. 233–234. pp. 644–658, 2019, doi: 10.1016/j.apenergy.2018.10.010.

[249] D. E. Integration and G. Integration, "on behalf of the DEIP EV Data Availability Taskforce Distributed Energy Integration Program – Electric Vehicles Grid Integration Important notice," no. February, 2021.

[250] J. Zhao, A. Arefi, A. Borghetti, and G. Ledwich, "Indices of Congested Areas and Contributions of Customer to Congestions in Radial Distribution Networks," *J. Mod. Power Syst. Clean Energy*, vol. 67, 2021.

[251] Y. Dijoux and E. Idée, “Classes of virtual age models adapted to systems with a burn-in period,” *IEEE Trans. Reliab.*, vol. 62, no. 4, pp. 754–763, 2013, doi: 10.1109/TR.2013.2284731.

[252] S. Alshahrani, M. Khalid, and M. Almuhaini, “Electric vehicles beyond energy storage and modern power networks: Challenges and applications,” *IEEE Access*, vol. 7, pp. 99031–99064, 2019, doi: 10.1109/ACCESS.2019.2928639.

[253] X. Wang, C. Sun, R. Wang, and T. Wei, “Two-Stage Optimal Scheduling Strategy for Large-Scale Electric Vehicles,” *IEEE Access*, vol. 8, pp. 13821–13832, 2020, doi: 10.1109/aCCESS.2020.2966825.

[254] J. Su, T. T. Lie, and R. Zamora, “Modelling of large-scale electric vehicles charging demand: A New Zealand case study,” *Electric Power Systems Research*, vol. 167. pp. 171–182, 2019, doi: 10.1016/j.epsr.2018.10.030.

[255] H. Cai, Q. Chen, Z. Guan, and J. Huang, “Day-ahead optimal charging/discharging scheduling for electric vehicles in microgrids,” *Prot. Control Mod. Power Syst.*, vol. 3, no. 1, 2018, doi: 10.1186/s41601-018-0083-3.

[256] J. Brady and M. O’Mahony, “Modelling charging profiles of electric vehicles based on real-world electric vehicle charging data,” *Sustainable Cities and Society*, vol. 26. pp. 203–216, 2016, doi: 10.1016/j.scs.2016.06.014.

[257] A. Ul-Haq, C. Cecati, and E. El-Saadany, “Probabilistic modeling of electric vehicle charging pattern in a residential distribution network,” *Electric Power Systems Research*, vol. 157. pp. 126–133, 2018, doi: 10.1016/j.epsr.2017.12.005.

[258] J. Zhu *et al.*, “Electric vehicle charging load forecasting: A comparative study of deep learning approaches,” *Energies*, vol. 12, no. 14, pp. 1–19, 2019, doi: 10.3390/en12142692.

[259] D. Panahi, S. Deilami, M. A. S. Masoum, and S. M. Islam, “Forecasting plug-in electric vehicles load profile using artificial neural networks,” *2015 Australas. Univ. Power Eng. Conf. Challenges Futur. Grids, AUPEC 2015*, pp. 1–6, 2015, doi: 10.1109/AUPEC.2015.7324879.

[260] J. Tan and L. Wang, “Integration of plug-in hybrid electric vehicles into residential distribution grid based on two-layer intelligent optimization,” *IEEE Trans. Smart Grid*, vol. 5, no. 4, pp. 1774–1784, 2014, doi:

10.1109/TSG.2014.2313617.

[261] J. Zhao, A. Arefi, and A. Borghetti, “End-of-life Failure Probability Assessment Considering Electric Vehicle Integration,” no. 3, pp. 1–6, 2021, doi: 10.1109/aupec52110.2021.9597834.

[262] B. Hu, K. Xie, and H. M. Tai, “Inverse problem of power system reliability evaluation: Analytical model and solution method,” *IEEE Trans. Power Syst.*, vol. 33, no. 6, pp. 6569–6578, 2018, doi: 10.1109/TPWRS.2018.2839841.

[263] H. Kim and C. Singh, “Reliability modeling and simulation in power systems with aging characteristics,” *IEEE Trans. Power Syst.*, vol. 25, no. 1, pp. 21–28, 2010, doi: 10.1109/TPWRS.2009.2030269.

[264] S. Sharifinia, M. Rastegar, M. Allahbakhshi, and M. Fotuhi-Firuzabad, “Inverse Reliability Evaluation in Power Distribution Systems,” *IEEE Trans. Power Syst.*, vol. 35, no. 1, pp. 818–820, 2020, doi: 10.1109/TPWRS.2019.2952518.

[265] Australian Energy Regulator (AER), “Values of Customer Reliability-Consultation Update Paper,” April, 2019. Available: https://www.aer.gov.au/networks-pipelines/guidelines-schemes-models-reviews/values-of-customer-reliability/initiation#step-63906.

[266] Federal Highway Administration, U.S. Department of Transportation, “National Household Travel Survey,” 2017. [Online]. Available: http://nhts.ornl.gov.

[267] H. Jahangir *et al.*, “Charging demand of Plug-in Electric Vehicles: Forecasting travel behavior based on a novel Rough Artificial Neural Network approach,” *J. Clean. Prod.*, vol. 229, no. 2019, pp. 1029–1044, 2019, doi: 10.1016/j.jclepro.2019.04.345.

[268] A. Ahmadian, B. Mohammadi-Ivatloo, and A. Elkamel, “A Review on Plug-in Electric Vehicles: Introduction, Current Status, and Load Modeling Techniques,” *J. Mod. Power Syst. Clean Energy*, vol. 8, no. 3, pp. 412–425, 2020, doi: 10.35833/mpce.2018.000802.

[269] B. CM, *Neural networks for pattern recognition*. Oxford University Press, 1995.

[270] V.-E. Neagoe, A.-D. Ciotec, and G.-S. Cucu, “Deep Convolutional Neural Networks Versus Multilayer Perceptron for Financial Prediction,” pp. 201–206, 2018, doi: 10.1109/iccomm.2018.8484751.

[271] S. Baressi Šegota, D. Štifanić, K. Ohkura, and Z. Car, “Use of Artificial Neural Network for Estimation of Propeller Torque Values in a CODLAG Propulsion System,” *J. Marit. Transp. Sci.*, vol. 58, no. 1, pp. 25–38, 2020, doi: 10.18048/2020.58.02.

[272] M. J. Taud H., *Multiplayer perceptron (MLP) In: Geomatic Approaches for Modeling Land Change Scenarios*. Springer Berlin Heidelberg, 2018.

[273] A. Sadiq and N. Yahya, “Fractional Stochastic Gradient Descent Based Learning Algorithm For Multi-layer Perceptron Neural Networks,” *Int. Conf. Intell. Adv. Syst. Enhanc. Present a Sustain. Futur. ICIAS 2021*, pp. 0–3, 2021, doi: 10.1109/ICIAS49414.2021.9642687.

[274] Z. Sun, Y. Zhang, and Q. Ren, “A Reliable Localization Algorithm Based on Grid Coding and Multi-Layer Perceptron,” *IEEE Access*, vol. 8, pp. 60979–60989, 2020, doi: 10.1109/ACCESS.2020.2983739.

[275] S. Han, G. Kong, and S. Choi, “A Detection Scheme with TMR Estimation Based on Multi-Layer Perceptrons for Bit Patterned Media Recording,” vol. 55, no. 7, pp. 2019–2022, 2019, doi: 10.1109/TMAG.2018.2889875.

[276] R. Suresh, R. Shanmughasundaram, and R. S. Mohanrajan, “Model Based Fault Classification Method for Electric Vehicle Pertained Lithium-Ion Batteries Using Multi Layer Perceptron,” *Int. Conf. Emerg. Trends Inf. Technol. Eng. ic-ETITE 2020*, pp. 1–5, 2020, doi: 10.1109/ic-ETITE47903.2020.424.

[277] S. Wan, Y. Liang, Y. Zhang, and M. Guizani, “Deep Multi-Layer perceptron classifier for behavior analysis to estimate Parkinson’s disease severity using smartphones,” *IEEE Access*, vol. 6, pp. 36825–36833, 2018, doi: 10.1109/ACCESS.2018.2851382.

[278] M. Perceptron, “Short-term Rainfall Forecasting Using,” *IEEE Trans. Big Data*, vol. PP, no. XX, p. 1, 2018.

[279] Distribution System Analysis Subcommittee, “IEEE 123 node test feeder,” 2014. [Online]. Available: http://sites.ieee.org/pes-testfeeders/resources/123-bus Feeder.

[280] A. Arefi, A. Abeygunawardana, and G. Ledwich, “A new risk-managed planning of electric distribution network incorporating customer engagement and temporary solutions,” *IEEE Trans. Sustain. Energy*, vol. 7, no. 4, pp. 1646–1661, 2016, doi: 10.1109/TSTE.2016.2573290.

[281] J. Zhao, A. Arefi, and A. Borghetti, “End-of-life Failure Probability Assessment Considering Electric Vehicle Integration,” *2021 31st Australasian Universities Power Engineering Conference (AUPEC)*, 2021, pp. 1-6, doi: 10.1109/AUPEC52110.2021.9597834.

[282] D. Božič and M. Pantoš, “Impact of electric-drive vehicles on power system reliability,” *Energy*, vol. 83, pp. 511–520, 2015, doi: 10.1016/j.energy.2015.02.055.

[283] Q. Zhang, Y. Zhu, Z. Wang, Y. Su, and C. Li, “Reliability Assessment of Distribution Network and Electric Vehicle Considering Quasi-Dynamic Traffic Flow and Vehicle-to-Grid,” *IEEE Access*, vol. 7, pp. 131201–131213, 2019, doi: 10.1109/ACCESS.2019.2940294.

[284] P. Caramia, G. Carpinelli, and P. Verde, “Distribution Systems with Dispersed Generation,” *Power Qual. Indices Lib. Mark.*, vol. 28, no. 3, pp. 215–228, 2009, doi: 10.1002/9780470994405.ch5.

[285] X. Wang and R. Karki, “Exploiting PHEV to Augment Power System Reliability,” *IEEE Trans. Smart Grid*, vol. 8, no. 5, pp. 2100–2108, 2017, doi: 10.1109/TSG.2016.2515989.

[286] M. P. Anand, B. Bagen, and A. Rajapakse, “Probabilistic reliability evaluation of distribution systems considering the spatial and temporal distribution of electric vehicles,” *Int. J. Electr. Power Energy Syst.*, vol. 117, no. July 2019, p. 105609, 2020, doi: 10.1016/j.ijepes.2019.105609.

[287] M. D. Kamruzzaman and M. Benidris, “A reliability-constrained demand response-based method to increase the hosting capacity of power systems to electric vehicles,” *Int. J. Electr. Power Energy Syst.*, vol. 121, no. December 2019, p. 106046, 2020, doi: 10.1016/j.ijepes.2020.106046.

[288] K. Hou *et al.*, “A reliability assessment approach for integrated transportation and electrical power systems incorporating electric vehicles,” *IEEE Trans. Smart Grid*, vol. 9, no. 1, pp. 88–100, 2018, doi: 10.1109/TSG.2016.2545113.

[289] A. N. Archana and T. Rajeev, “A Novel Reliability Index Based Approach for EV Charging Station Allocation in Distribution System,” *IEEE Trans. Ind. Appl.*, vol. 57, no. 6, pp. 6385–6394, 2021, doi: 10.1109/TIA.2021.3109570.

[290] W. Li, “Evaluating mean life of power system equipment with limited end-of-life failure data,” *2005 IEEE Power Eng. Soc. Gen. Meet.*, vol. 3, no. 1, p. 2390, 2005, doi: 10.1109/pes.2005.1489084.

[291] C. F. Jekel and G. Venter, “pwlf : A Python Library for Fitting 1D Continuous Piecewise Linear Functions,” pp. 1–15, 2019.

[292] C. Huang *et al.*, “Day-ahead forecasting of hourly photovoltaic power based on robust multilayer perception,” *Sustain.*, vol. 10, no. 12, pp. 4–11, 2018, doi: 10.3390/su10124863.

[293] M. Farivar and S. H. Low, “Branch flow model: Relaxations and convexification-part i,” *IEEE Trans. Power Syst.*, vol. 28, no. 3, pp. 2554–2564, 2013, doi: 10.1109/TPWRS.2013.2255317.

[294] S. H. Low, “Convex relaxation of optimal power flow - Part i: Formulations and equivalence,” *IEEE Trans. Control Netw. Syst.*, vol. 1, no. 1, pp. 15–27, 2014, doi: 10.1109/TCNS.2014.2309732.

[295] M. Nick, R. Cherkaoui, J. Y. Le Boudec, and M. Paolone, “An Exact Convex Formulation of the Optimal Power Flow in Radial Distribution Networks Including Transverse Components,” *IEEE Trans. Automat. Contr.*, vol. 63, no. 3, pp. 682–697, 2018, doi: 10.1109/TAC.2017.2722100.

[296] J. Maleki Delarestaghi, A. Arefi, G. Ledwich, and A. Borghetti, “A distribution network planning model considering neighborhood energy trading,” *Electr. Power Syst. Res.*, vol. 191, no. September 2020, p. 106894, 2021, doi: 10.1016/j.epsr.2020.106894.